1-1-2014

Evaluation Of Presynaptic Dopamine Dynamics After: Toluene Inhalation Or Trkb Receptor Activation

Aaron Kwaku Apawu
Wayne State University,

EVALUATION OF PRESYNAPTIC DOPAMINE DYNAMICS AFTER: TOLUENE INHALATION OR TRKB RECEPTOR ACTIVATION

by

AARON KWAKU APAWU

DISSERTATION

Submitted to the Graduate School

of Wayne State University,

Detroit, Michigan

in partial fulfillment of the requirements

for the degree of

DOCTOR OF PHILOSOPHY

2014

MAJOR: CHEMISTRY (Analytical)

Approved by:

_____

Advisor Date

_____

_____

_____

DEDICATION

I dedicate this work to my late father James A. Apawu, my mum Gladys O. Apawu, my siblings David, Joel, and Emmanuel, my lovely wife Alvis and our two precious daughters Gladys and Danielle Apawu, my teachers and all whose love and guidance have enabled me to attain my present height in education.

ACKNOWLEDGMENTS

I would like to thank my advisor Dr. Tiffany Mathews for mentoring me during my graduate education at Wayne State University. Her advice, encouragement, and support together with the friendly atmosphere she created in her laboratory have contributed immensely to my graduate development. I would like to express my gratitude to her for believing in me. I would also like to express my appreciation to my collaborator and a member of my dissertation committee, Dr. Scott Bowen for allowing me to work in his laboratory and also for being available when I needed his help. Next, I express my gratitude to the rest of my dissertation committee, Dr. Tamara Hendrickson and Dr. Colin Poole for their counsel, comments, and insightful suggestions regarding my research. Your contributions have been very helpful in shaping my research.

I thank Dr. Parastoo Hashemi, and Dr. Francis Maina for their comments, advice, and help, the past members of the Mathew's laboratory, Dr. Kelly Bosse, Dr. Madiha Khalid, Dr. Johnna Birbeck, Stella, Christopher, Katie, Megan, Douglas, Michelle, and James for the help they provided me in diverse ways to enable me to come this far. My sincere thanks to my lab mate Brooke Newman for her assistance in my microdialysis and tissue content work. I'm also grateful to Sean Callan from Dr. Bowen's lab for helping me with my toluene project. To all my friends I say thank you for your friendship.

Last but not the least, I thank my parents for investing in my education, my brother David, my wife Alvis and our two daughters for all their sacrifices towards my graduate studies.

Above all, I express my heartfelt gratitude to God for the gift of life and for all the strides I have made in life.

CONTRIBUTIONS

Chapter 2: Materials and Methods

The toluene project was collaborative with Dr. Scott Bowen from the Department of Psychology at Wayne State University. This project spans chapters 3 through 5. All experiments in the toluene project were performed with outbred male Swiss-Webster mice, which required no in-house breeding, weaning, or genotyping.

The BDNF project described in chapter 6 involved genetically modified C57BL/6 mice; brain-derived neurotrophic factor (BDNF) heterozygote mice and their wildtype littermates. These mice required in-house breeding. Weaning and genotyping of mice was performed by Dr. Kelly Bosse and Brooke Newman with help from Dr. Johnna Birbeck, Christopher Rogalla, Michelle Colombo, and Stephanie Godden.

Chapter 3: Striatal Dopamine Dynamics in Mice Following Acute and Repeated Toluene Exposure

I performed all experiments in this chapter, which involved acute and 7 day repeated exposures of mice to toluene, locomotor activity measurements during toluene exposures, and slice fast scan cyclic voltammetry (FSCV). All behavior data analysis and graphing were done by Dr. Scott Bowen. I performed all FSCV data analysis and graphing. The results obtained from this work are in revision for publication in *Psychopharmacology*. I performed literature searches, writing of the manuscript, and corrections together with Dr. Scott Bowen and Dr. Tiffany Mathews.

Chapter 4: An In-depth Examination of Acute Toluene Exposure on the Striatal Dopamine System

The work in this chapter includes toluene exposure, slice FSCV, tissue content

analysis and *in vivo* microdialysis. I performed the acute exposure of mice to toluene and the locomotor activity measurements with assistance from Sean Callan from Dr. Bowen's laboratory in the Department of Psychology. I performed all tissue content analysis which involved taking mouse brain tissue, homogenizing tissue samples, analysis by high performance liquid chromatography (HPLC), and running of protein assays to normalize tissue content DA and its metabolites to tissue protein. I also performed all slice FSCV measurements.

In vivo microdialysis experiments involved construction of a toluene exposure chamber that allows toluene exposure, microdialysis sampling and locomotor activity measurements simultaneously. This chamber was built through a collaborative effort between Sean Callan and myself. I also performed microdialysis experiments with assistance from Sean Callan. The microdialysis experiment involved stereotaxic surgery, probe placement, microdialysis sample collection, and toluene exposure. I performed all microdialysis sample analysis by HPLC. All behavior data analysis was performed by Sean. I performed all neurochemical data analysis, graphing, literature searches, and wrote this chapter.

Chapter 5: An In-depth Examination of the Effect of Repeated Toluene Exposure on Striatal Dopamine System

I performed 7 day repeated exposures of mice to toluene with assistance from Sean Callan. Additionally, I performed all FSCV experiments and all tissue content analysis including protein assays. I performed microdialysis experiments with assistance from Sean Callan. I performed all HPLC analysis of microdialysis samples.

All behavior data analysis was performed by Sean. I performed all neurochemical data analysis, graphing, literature searches, and wrote this chapter.

Chapter 6: Probing the Ability of Presynaptic Tyrosine Kinase Receptors to Regulate Striatal Dopamine Dynamics

I performed FSCV experiments involving genistein, tyrphostin 23, 7,8-dihydroxy flavone (7,8-DHF) and the 7,8-DHF/K252a cocktail and analyzed and graphed the data. Dr. Francis Maina performed FSCV with BDNF, K252a, and the BDNF/K252a cocktail and analyzed and graphed the data. All electrochemical characterization of pharmacological agents was done by James Taylor with my assistance and supervision. The results obtained from this work were published in *ACS Chemical Neuroscience* (Apawu *et al*., 2013). I performed literature searches and wrote the manuscript and corrections together with Dr. Francis Maina and Dr. Tiffany Mathews.

TABLE OF CONTENTS

LIST OF TABLES

LIST OF FIGURES

ABBREVIATIONS

3-MT	3-methoxytyramine
7,8-DHF	7,8-dihydroxyflavone
5-HIAA	5-hydroxyindoleacetic acid
7-OH-DPAT	(±)-7-hydroxy-2-dipropylaminotetralin hydrobromide
AADC	L-aromatic amino acid decarboxylase
AC	adenylyl cyclase
aCSF	artificial cerebrospinal fluid
ADHD	attention deficit hyperactivity disorder
AMPA	alpha-amino-3-hydroxy-5-methyl-4-isoxazole propionic acid
BCA	bicinchoninic acid
BDNF	brain-derived neurotrophic factor
cAMP	cyclic adenosine monophosphate
CNS	central nervous system
COMT	catechol-*O*-methyltransferase
CPu	caudate putamen
CREB	cAMP response element binding protein
CV	cyclic voltammogram
DA	dopamine
DAT	dopamine transporter
DNA	2'-deoxyribonucleic acid
DOPAC	3,4-dihydroxyphenylacetic acid

EDTA	ethylenediaminetetraacetic acid
ERK	extracellular signal-regulated kinase
FSCV	fast scan cyclic voltammetry
GABA	gamma-aminobutyric acid
HPLC	high-performance liquid chromatography
HVA	homovanillic acid
IC_{50}	half maximal inhibitory concentration
IR	infrared
L-DOPA	L-3,4-dihydroxyphenylalanine
MAO	monoamine oxidase
MAPK	mitogen-activated protein kinase
nAChRs	nicotinic acetylcholine receptors
NAc	nucleus accumbens
NGF	nerve growth factor
NT	neurotrophin
NMDA	N-methyl-D-aspartate
p	pulse
p75	low-affinity nerve growth factor receptor
PCR	polymerase chain reaction
PI3K	phosphatidylinositol-3 kinase
PKC	protein kinase C
PLCγ	phospholipase C, γ

Ras	GTP binding protein
ROS	reactive oxygen
SEM	standard error of the mean
SHC	adaptor protein containing SH2 domain
SNc	substantia nigra pars compacta
TH	tyrosine hydroxylase
TrkA	tyrosine kinase receptor A
TrkB	tyrosine kinase receptor B
TrkC	tyrosine kinase receptor C
VMAT	vesicular monoamine transporter
V_{max}	maximum velocity
VTA	ventral tegmental area
WINCS	wireless instantaneous neurotransmitter concentration sensing
WT	wildtype

CHAPTER 1

Introduction and Overview

1.1 Fundamentals of neurochemistry

The brain communicates through specialized cells to execute a variety of functions. These specialized cells, called neurons, are estimated to number in the hundreds of billions in the brain.[2] Neurons differ in their structure, chemistry, location and connections depending on the specific task they perform in the central nervous system (CNS).[2] In general, a neuron consists of a cell body (also called a soma), which houses the nucleus as well as cytoplasmic organelles and is the site for most cellular processes including protein synthesis.[2, 3] Extending from the cell body is a single long structure called an axon, which terminates in multiple structures known as dendrites. The axon is responsible for conducting outgoing neuronal information in the form of an electrochemical signal to the nerve terminal to be propagated to another neuron. Dendrites receive incoming neuronal information during synaptic communication and transmit it to the cell body.

Neuronal communication involves both electrical and chemical processes. When a neuron is at rest, the inside of the cell is more negative than its surrounding. In this state, the neuron is described as being polarized, having a resting potential of -70 mV.[2] During neurotransmission, sodium (Na^+) channels located in the membrane open, allowing an influx of Na^+ ions into the cell causing the inside of the cell to become depolarized. During depolarization, an action potential is produced and propagated along the length of the axon. This process is described as neuronal firing. In response to depolarization, there is a spontaneous and transient opening of the potassium (K^+)

channels causing K^+ efflux to re-polarize the neuron. During the process of repolarization, the cell rebalances it's Na^+ and K^+ ions, here the cell is said to be in a refractory period where it cannot fire until it is back to its polarized state.[4] When the action potential reaches the axon terminal, it triggers neurotransmitter release into the synaptic space (a small gap 10-100 nm between two communicating neurons) in a process called exocytosis[5]. In the synaptic space, neurotransmitters act on specific receptors located on the post-synaptic terminal (dendrites) of the receiving neuron to propagate neuronal information. The neurotransmitters that remain in the synaptic space are metabolized or taken back to the presynaptic terminal to be re-packaged into vesicles. Examples of neurotransmitters include monoamines such as dopamine (DA), serotonin, norepinephrine, and histamine, or amino acids such as glutamate, gamma-aminobutyric acid (GABA), and glycine.

1.1.1 Biochemistry of the dopamine neurotransmitter

DA plays a crucial role in brain function. As a chemical messenger, DA is implicated in movement, learning, memory, cognition, and reward seeking behaviors.[2] Alterations or dysfunctions of the DA system have been linked to neurological diseases including attention deficit hyperactivity disorder (ADHD), Schizophrenia, Alzheimer's and Parkinson's diseases, and addiction.[2, 6]

Most DA neurons are localized in the midbrain. From here their fibers project into the forebrain and the striatum (Figure 1.1).[2, 7] The DA neurons located in the substantia nigra pars compacta (SNc) in the midbrain innervate the dorsal striatum (Caudate putamen; CPu) via the nigrostriatal pathway that is involved in learning and voluntary motor activity.[2, 8, 9] This pathway is known to be susceptible to neuronal death or

significant DA impairments during neurodegenerative disease like Parkinson's.[2, 10] The mesolimbic dopaminergic pathway involves projections of DA fibers from the ventral tegmental area (VTA) in the midbrain into the ventral striatum (nucleus accumbens; NAc) and the fibers from the olfactory tubercle into the amygdala, septum, and hippocampus.[2, 7] The mesolimbic pathway has been implicated in memory, addiction, and reward related behaviors.[2, 7, 11] The DA neurons in the VTA also innervate the cortex forming the mesocortical dopaminergic pathway which is involved in emotion, motivation, and cognition.[2] These VTA dopaminergic projections are together called the mesocorticolimbic system.[12, 13]

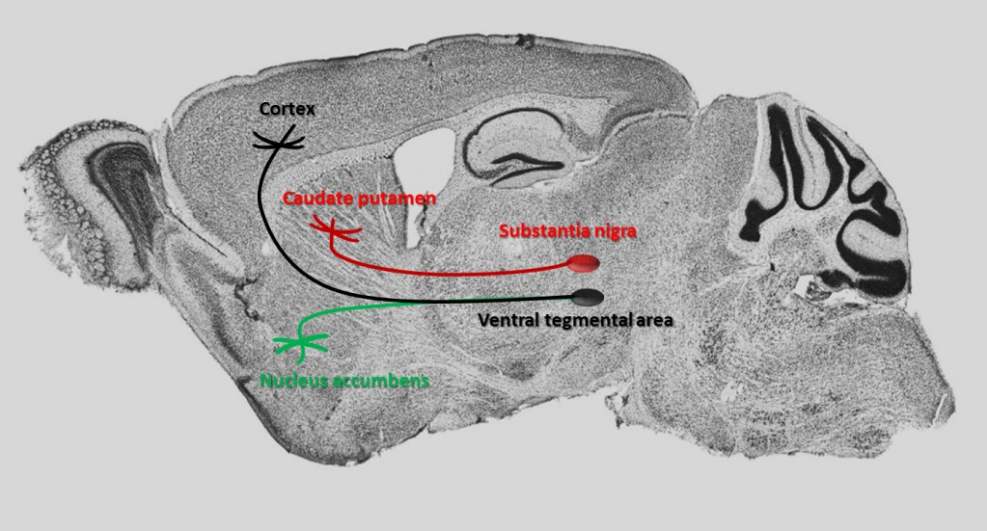

Figure 1.1: The main projections of dopamine (DA) cell bodies as shown in sagittal mouse brain slice. Projections have been color coded to distinguish the three main pathways. Red shows DA cell body projecting from the SNc to the CPu forming the nigrostriatal pathway. Black represents the projection from the VTA to the cortex in the mesocortical pathway. Green shows the mesolimbic pathway, which involves DA projections from the VTA into the NAc. This saggital mouse brain was adapted from Mouse Brain Atlas with permission from Elsevier.[1, 2]

DA is synthesized from L-tyrosine. During synthesis, which occurs in two main steps, L-tyrosine undergoes hydroxylation at its C3 carbon to produce L-3,4-dihydroxyphenylalanine (L-DOPA). This reaction is rate limiting and is catalyzed by tyrosine hydroxylase (TH) enzyme in the presence of Fe^{2+}, O_2, and tetrahydrobiopterin as cofactors. L-DOPA subsequently undergoes decarboxylation in the presence of L-aromatic amino acid decarboxylase (AADC) enzyme and pyridoxal phosphate cofactor to form DA (Figure 1.2). Following synthesis, DA is packaged into vesicles by vesicular monoamine transporter 2 (VMAT2), which protects vesicular DA from being metabolized by monoamine oxidase (MAO) until it is transported across the presynaptic terminal upon electrical stimuli. An action potential arriving at the axon terminal causes the vesicles to move to the nerve terminal to fuse with the cell membrane, releasing DA into the synaptic space. In the synaptic space, the primary role of DA is to activate specific DA post-synaptic receptors (located on the receiving neuron) to propagate the neuronal signal. There are two types of DA receptors: the DA D1-like receptors (sub-divided into the D1 and D5 receptors) and the DA D2-like receptors (sub-divided into the D2, D3, and D4 receptors). When DA D1-like receptors are activated, they increase cyclic adenosine monophosphate (cAMP) and neuronal activity through stimulation of adenylyl cyclase (AC). However, activation of DA D2-like receptors reduces cAMP levels and neuronal activity by inhibition of AC. Termination of the synaptic DA signal is achieved by: 1) the DA transporter (DAT) which takes DA back into the presynaptic terminal or, 2) DA is enzymatically degraded by MAO and catechol-*O*-methyl transferase (COMT) into its metabolites such as 3,4-dihydroxyphenylacetic acid (DOPAC), 3-methoxytryptamine (3-MT), and homovanillic acid (HVA) (Figures 1.3 and 1.4).[2, 3, 14]

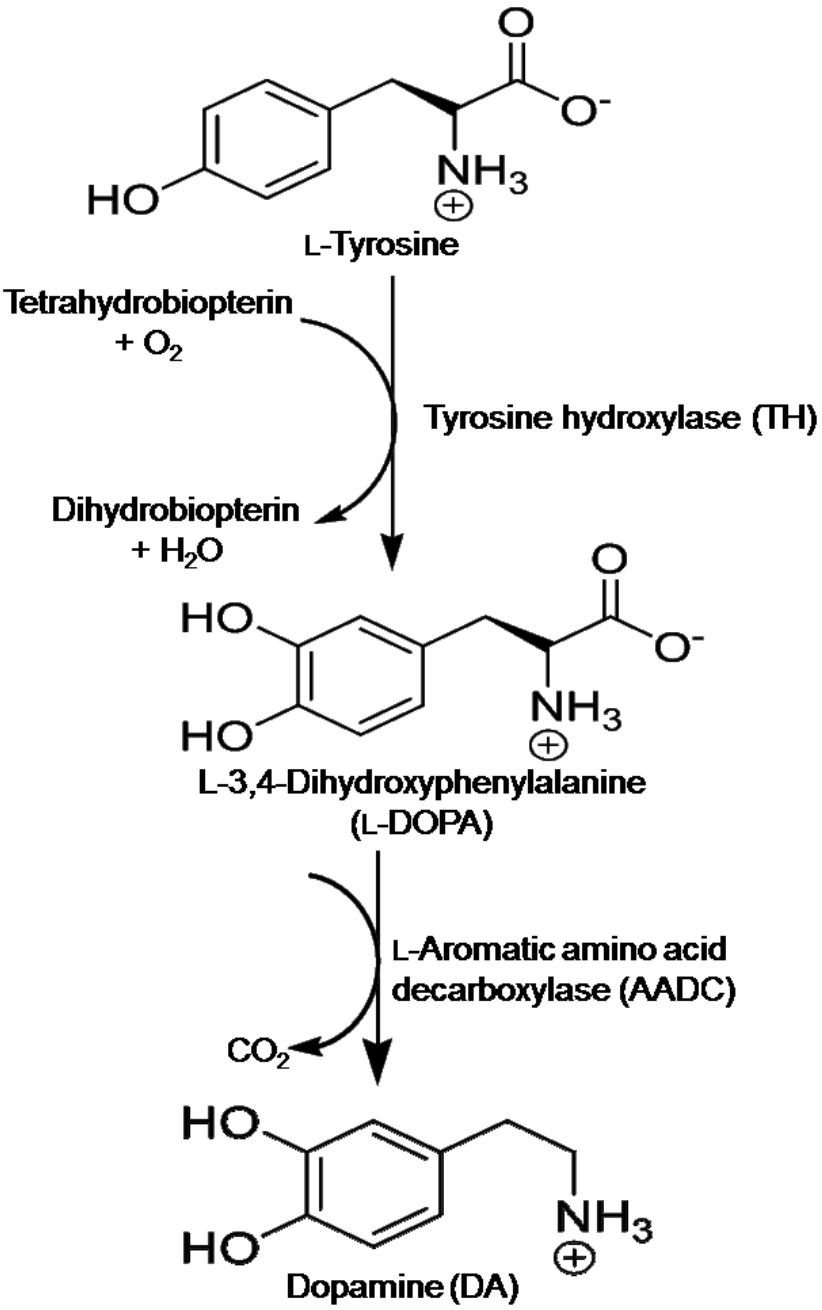

Figure 1.2: Biosynthesis of DA. TH catalyzes the conversion of L-Tyrosine to L-DOPA. The conversion of L-DOPA to DA is catalyzed by AADC.

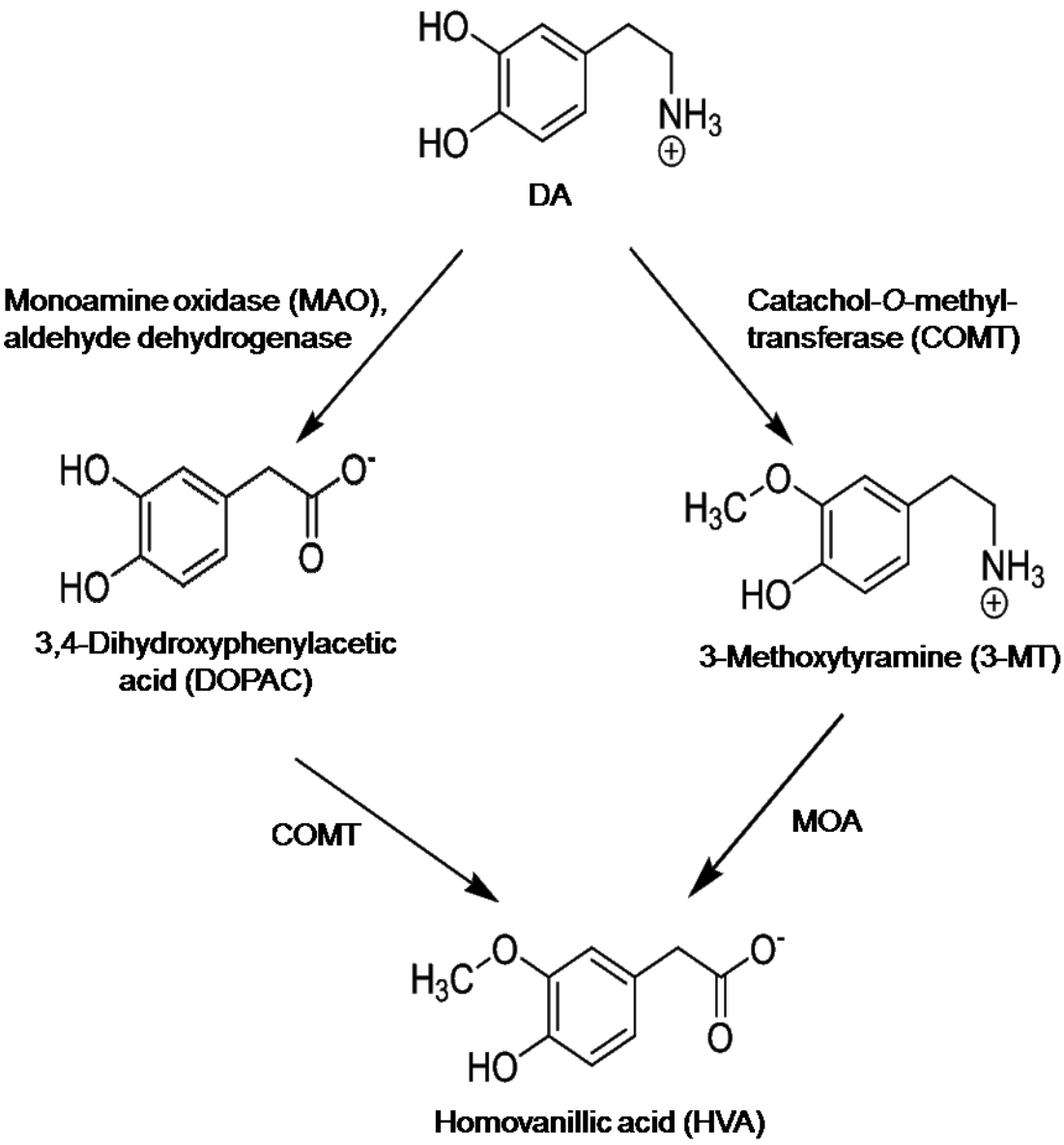

Figure 1.3: Pathway showing DA catabolism. This pathway involves conversion of DA by MAO to DOPAC which is subsequently converted to HVA by COMT. DA can also be converted into 3-MT in a reaction catalyzed by COMT and further broken down to HVA.

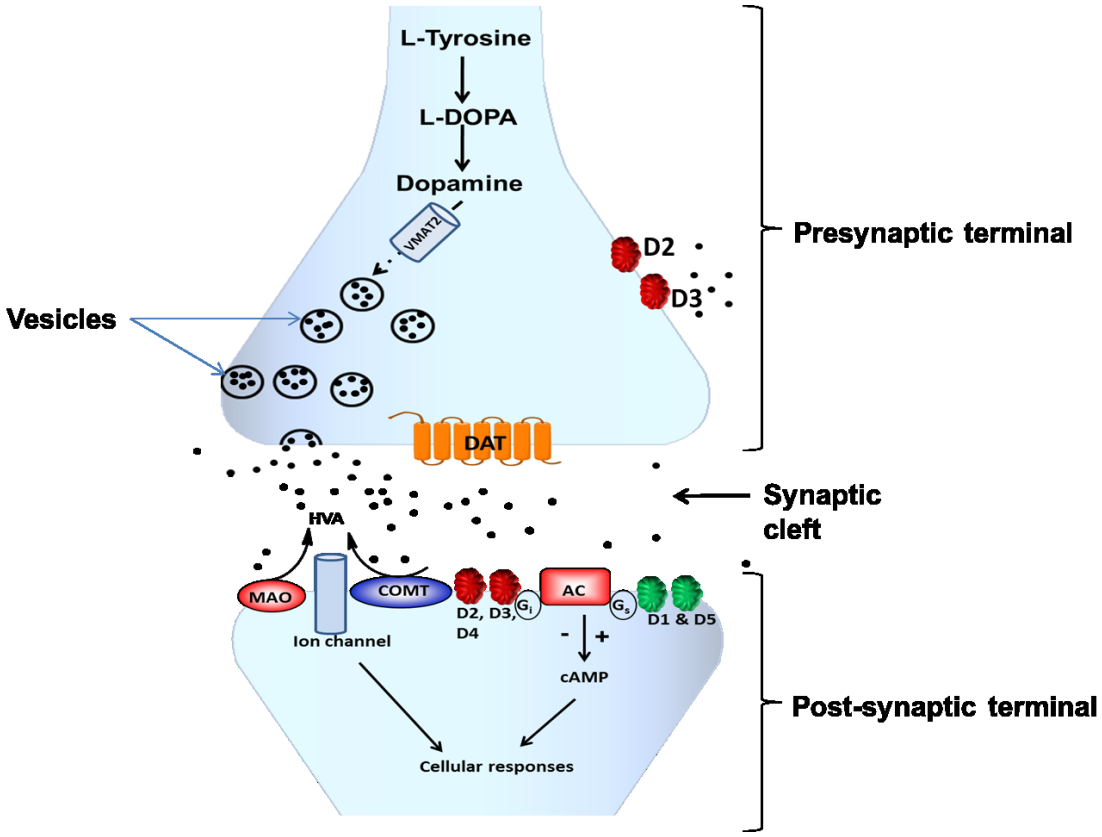

Figure 1.4: Schematic illustration of synaptic DA transmission. At the presynaptic terminal, synthesized DA is housed in vesicles. During neurotransmission, the arrival of an action potential at the presynaptic terminal triggers exocytotic release of DA into the synaptic cleft where it binds to DA receptors at the post-synaptic terminal of the receiving neuron to propagate neural information via secondary messengers. Definitions; G_i and G_s: inhibitory and stimulatory guanine nucleotide-binding proteins.

1.1.2 Brain derived neurotrophic factor (BDNF)

The DA system works in conjunction with many other neurotransmitters, neuromodulators and proteins within the brain. One key player in neuronal functions is a 27 kDa homodimeric protein, BDNF. BDNF belongs to a class of neurotrophins that include nerve growth factor (NGF), neurotrophin-3, (NT-3), and neurotrophin – 4/5 (NT-4/5).[15] BDNF exerts its effect through activation of high affinity tyrosine kinase receptor, TrkB (Figure 1.5). In addition, it binds to low affinity p75 receptors to form a complex that regulate Trk mediated signaling by influencing the TrK receptor conformation.[16-18] BDNF is synthesized in the cell body of neurons, packaged into vesicles and then transported to the nerve terminal for local secretion.[16] Following exocytotic release from the nerve terminal, BDNF in the extracellular milieu binds to the TrkB receptor causing receptor dimerization. This dimerization induces activation of kinases, which catalyze phosphorylation of the tyrosine residue of the receptor to provide binding sites for signaling proteins such as growth factor receptor-bound protein 2 (GBR2), adaptor protein containing SH2 domain (SHC), and son of sevenless (SOS).[15, 16] Subsequent activation of these signaling proteins via phosphorylation triggers numerous signaling cascades identified in three main pathways namely the phosphatidylinositol-3-kinase (PI3K), the Ras/mitogen activated protein kinase (MAPK), and phospholipase C, γ (PLCγ) pathways.[15, 16, 18] Activation of these pathways leads to various cellular events that modulate different neuronal functions including cell survival, neurogenesis, synaptic plasticity, synaptic transmission, and neurotransmitter release.[2, 19-21] Alteration in the level and function of BDNF has been implicated in neurological diseases including Parkinson's disease and drug addiction.[22-27]

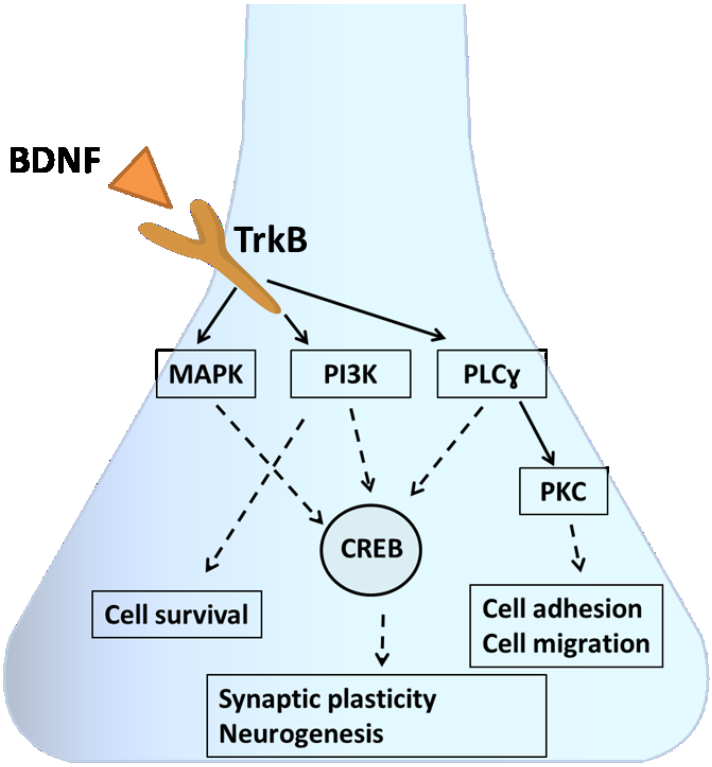

Figure 1.5: Schematic illustration of the action of brain derived neurotrophic factor (BDNF) through TrkB receptors. Activation of TrkB by BDNF triggers neuronal cascades that activate cAMP response element binding protein (CREB). The neuronal cascades involve phospholipase Cγ (PLCγ), the Ras/mitogen activated protein kinase (MAPK), and phosphatidylinositol-3-kinase (PI3K) pathways that leads to several functions including neuronal growth, differentiation, and synaptic plasticity.

1.2 Addictive drugs and the dopamine system

Drugs of abuse interfere with normal brain function causing neuroadaptations that can lead to drug addiction.[28] Drug addiction is a complex brain disorder that involves persistent and compulsive intake of drugs regardless of their destructive consequences.[29, 30] Examples of addictive drugs include amphetamine, nicotine, ethanol, cocaine, marijuana, opioids, and solvent inhalants.[31, 32] Each of these drugs is unique and may exert its effect through different neuronal substrates.[29, 33] However, one common property of addictive drugs is their action on the mesolimbic DA system, which is integral to the brain reward mechanism.[29] Addictive drugs activate the mesolimbic DA circuitry, which subsequently leads to elevation of extracellular DA levels in the terminal region, NAc.[11, 29, 34] These drug induced alterations in extracellular DA levels may be achieved through diverse mechanisms. For instance, ethanol increases DA neuron firing in the VTA through inhibition of N-methyl-D-aspartate (NMDA) receptors or activation of $GABA_A$ receptors.[31, 35] Nicotine, which mediates its actions through acetylcholine receptors, and opiates which act through opioid receptors, also indirectly increase DA neuron firing in the VTA.[31, 35] On the other hand, cocaine increases extracellular DA levels by directly acting on the DA transporter (DAT) to inhibit DA re-uptake, while amphetamine reverses the function of DAT to release DA from the terminal region of DA neurons.[11, 31] This common induced elevation in extracellular DA levels has been linked to the reinforcement effect of most drugs of abuse.[11] Meanwhile, solvent inhalants including volatile organic solvents like toluene have also been reported to influence the mesolimbic DA system; nonetheless, their mode of action is not well understood.[36-38] Taken together, although drugs of addiction involves several

neurotransmitters and affects multiple brain regions, the mesolimbic DA circuitry appears to be a common pathway where the actions of drugs of abuse converge.[29, 39]

1.3 Toluene abuse

1.3.1 Toluene as an inhalant

Toluene is a widely used industrial solvent produced mainly from petroleum and as a byproduct of the coke oven industry.[40] It is found in several consumable products such as paint, paint thinners, glue, degreasers, and adhesives.[41, 42] Aside from its conventional uses in these products, toluene is also abused as an inhalant for its euphoric effect. This form of drug abuse is administered by directly inhaling vapors from the products, inhaling concentrated vapor trapped in a bag or breathing from rags soaked in toluene containing products.[43, 44] Because solvents like toluene are legal, easily accessible, and inexpensive, younger populations are at increased risk for its use and abuse as inhalants.[41, 45] In the United States, a recent epidemiology report showed that, from 2002 to 2011, the number of first time inhalant users ranged between 719,000 to 877,000; while in 2012, a total of 584,000 people age 12 or older used inhalants for the first time, of which 62.5% were under the age of 18.[46]

Solvents like toluene are known to cause diminished mental and physical capabilities such as ataxia, dis-inhibition, dizziness, incoordination, lethargy, slowed reflexes, slowed thinking and movement, slurred speech, and memory loss.[47-51] There are also substantial reports that have shown that chronic inhalant use damages the liver, kidneys, and optic nerves, and leads to coma and death by respiratory depression.[41, 43, 52-54] Inhalant use by pregnant mothers can also cause complications during pregnancy and child birth.[55]

1.3.2 Behavioral and pharmacological effects of toluene

Toluene has similar neurobehavioral effects as other CNS depressants including alcohol.[37, 56] For example, toluene has reinforcing/rewarding effects. This consequence is evident in existing work that showed that mice will self-administer toluene intravenously.[57] In earlier work that was done by Weiss *et al.*, it was also demonstrated that monkeys would work to gain brief access to toluene vapor just as they would for amphetamine or opiates.[58] Furthermore, condition placed preference model has shown that rats and mice will spend more time in a chamber where they were previously paired with toluene than in one without toluene.[59-61] In addition to having reinforcing properties, tolerance to toluene inhalation has also been identified in animal models.[62-65] In early work reported by Himnan, toluene induced tolerance developed to locomotor behavior including ataxia and inhibition of rearing to repeated toluene exposure as measured in an open field.[64] In another study, monkeys, whose cognition functions were examined using delayed matching-to-sample behavior following repeated exposure to toluene, were noted to have developed tolerance to their response times for sample selection.[65] Other toluene induced neurobehavioral effects that have been reported include spontaneous motor activation, behavior sensitization, toluene dependence, discriminative stimulus effects, disruption in operant behavior, anticonvulsant effects, and synergistic effects with other drugs of abuse.[37, 56, 66-76] These data together with many more provide useful evidence that toluene abuse produces behavioral effects that are similar to many other drugs of abuse.[37, 56]

1.3.3 Neurochemical evidence of toluene's neural action

Though the exact mechanism underlining toluene's neural action is not well understood, existing reports have implicated a number of neurotransmitters in toluene's action. These neurotransmitters include GABA, glutamate, serotonin, glycine, and DA.[36, 37, 62, 77] For example, high-resolution magnetic resonance spectroscopy data showed that acute binge inhalation of 8000 or 12,000 ppm toluene reduced levels of GABA (12%) and glutamate (8%) in the hippocampus, as well as the index of glutamatergic tone (22%) in the dorsal anterior striatum of rat brains.[78] Cruz and co-workers used recombinant receptors expressed in *Xenopus* oocytes to examine the influence of toluene on NMDA receptors and found that a toluene dose of up to ~ 9 nM inhibited NMDA-mediated current in a rapid, reversible, and a dose dependent manner.[79] In addition, the extent of effect varied from one receptor sub-unit to another with the highest in NR1/2B (IC_{50} = 0.17 mM) followed by NR1/2A (IC_{50} = 1.4 mM) and then NR1/2C (IC_{50} = 2.1 mM).[79] These results are consistent with the data obtained from a more recent study where acute treatment of primary cultures of rat hippocampal neurons with 0.1-10 nM toluene solutions inhibited NMDA-mediated currents (IC_{50} = 1.5 mM), while no effect on response induced by the non-NMDA-agonist kainic acid.[80] Meanwhile, four day treatments of the neurons to 1 mM toluene increased the whole cell response to exogenously applied NMDA, and reduced the GABA mediated response, but did not alter responses generated by kainic acid.[80] Chronic toluene treatment was increased the amplitude of synaptic NMDA currents but decreased GABA mediated current.[80] Furthermore, toluene potentiates the function of α1 glycine receptor subtypes in oocytes and mouse serotonin-3 receptor function, but inhibits

nicotinic acetylcholine receptors (nAChRs) in rodents.[77, 81, 82] There is also substantial evidence about toluene's influence on the DA system, particularly on the mesolimbic dopaminergic pathway. Riegel and his team showed that perfusion of toluene directly into the VTA of a rat's brain increased DA concentrations in both the VTA and the NAc.[36] Gerasimov *et al.* also demonstrated that acute inhalation of 3000 ppm toluene increased extracellular DA levels in the prefrontal cortex of freely moving rats.[71] Furthermore, acute exposure of rats to 11,500 ppm toluene potentiated transient neuronal firing in the VTA DA neurons while another study reporting that seven daily intraperitoneal injections of 600 mg/kg toluene elevated DA levels in the CPu and NAc.[83, 84]

Taken together, these data provide significant evidence that the abused solvent toluene alters brain chemistry through multiple mediators that have also been implicated in neuronal alterations induced by other drugs of abuse.[85-89]

1.4 Tools to evaluate neurochemical function

1.4.1 *In vivo* microdialysis

Microdialysis is an *in vivo* sampling technique that allows small molecules such as neurotransmitters and neuropeptide to be sampled from freely moving animals and analyzed using analytical tools. Microdialysis sampling is based on the principle of diffusion and size exclusion where small molecules migrate along a concentration gradient in to a probe and are collected and analyzed.[90] The microdialysis probe plays a central role in the sampling process. The probe consists of a semi-permeable membrane with specific molecular weight cut-off allowing only molecules within certain molecular weight range to be sampled (Figure 1.6). This feature of the probe provides a

means of selectivity for the sampling process. There are different probe designs, each of which is unique for sampling from a specific organ. For example, the concentric probe is rigid and is suitable for use in brain sampling.[91] Other types of microdialysis probes are linear, shunt, and flexible probes.[91]

Microdialysis has been widely used in animal research (usually rodents) to probe extracellular levels of neurotransmitters and their metabolites and how pharmacological agents influence them. When sampling from the brain, the microdialysis probe is inserted through a guide cannula, which is implanted in a brain region of interest during stereotaxic surgery. Samples from the extracellular matrix are collected by slowly and continuously perfusing artificial cerebrospinal fluid (aCSF) through the inlet of the probe. Perfusion of the buffer, which is similar in composition to the brain fluid but typically lacks the neurotransmitter(s) of interest, creates a concentration gradient that causes molecules to diffuse through the semi-permeable membrane of the probe. The neurotransmitters are collected from the outlet of the probe as dialysate samples (Figure 1.6). The flow rate of the perfusing buffer depends on factors such as desired sample volume, sample collection time, and the needed analytical sensitivity.[90] The semi-permeable membrane of the probe excludes large molecules like proteins from the dialysate samples. The samples collected can be analyzed with a variety of analytical techniques.

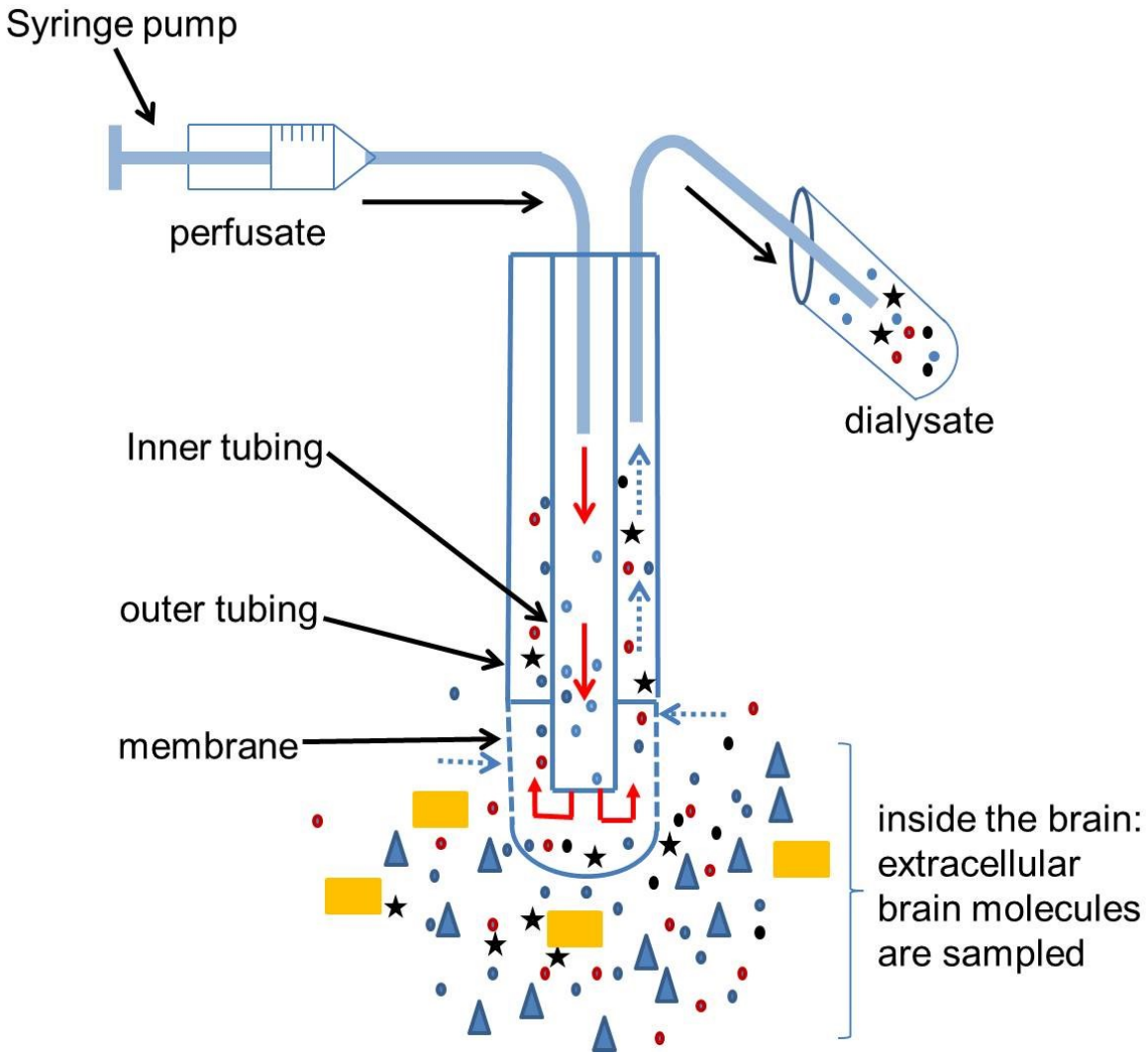

Figure 1.6: Microdialysis sampling through a semi-permeable membrane. Microdialysis probe consist of a semi-permeable membrane that allows selective sampling of small molecules. Shown here is a schematic of a concentric probe used for microdialysis sampling from the brain. It consists of inner and outer tubing. During sampling, dialysate buffer (perfusate) is pumped through the inner tubing to create concentration gradient between the brain tissue and the probe. Molecules diffuse along their concentration gradient and only small ones pass through the membrane into the outer tubing and are swept into a collection vial as dialysate samples.

1.4.1.1 Separation and detection of dialysate samples

Microdialysis samples are commonly analyzed using a separation technique with a detection method. The separation techniques used in microdialysis measurements include high performance liquid chromatography (HPLC) and capillary electrophoreses (CE).[92-95] Coupling microdialysis to these techniques allows the constituents of the dialysate samples to be separated and subsequently detected with a vast array of detection systems including mass spectrometers, fluorescence, and electrochemical detectors.[92, 94, 96] This combination allows microdialysis to be used to analyze multiple analytes simultaneously. HPLC has been widely used as a separation tool in microdialysis measurements because it is commercially available and does not involve complex instrumentation, making it easy to use. Although CE has higher mass sensitivity and better temporal resolution (in seconds) compared to HPLC (in minutes), advances have been made in miniaturizing HPLC columns (4 – 5 mm internal diameter) into microbore columns (0.3 – 1.0 mm internal diameter), which have led to improvements in temporal resolution and mass sensitivity of HPLC measurements.[92, 96-98] HPLC with electrochemical detection has been widely used to analyze monoamine neurotransmitters such serotonin and DA as well as their metabolites DOPAC, HVA, 3-MT, and 5-hydroxyindoleacetic acid (5-HIAA). In electrochemical detection, the analyte must be electroactive; therefore any other non-electroactive species are undetected. Since, electroactive species are oxidized and reduced at unique potentials, electrochemical detection provides high selectivity and is also known for its good sensitivity.[99] Examples of electrochemical detectors are amperometric detectors where approximately 10% of the analyte are oxidized or reduced, and coulometric detectors,

which have a flow through cell design making it possible for nearly a 100% of the analyte to be oxidized.[100] Since most amino acid neurotransmitters are not electroactive, they require pre-column derivatization to make them electroactive.[91, 99] Amino acid neurotransmitters have also been analyzed using HPLC with fluorescence detection and mass spectrometry. Mass spectrometry provides high selectivity and conclusive identification of analyte using their molecular masses.[91] Also, mass spectrometry allows analysis of small sample volumes containing low concentrations of analyte.[96] However, microdialysis samples are of high ionic strength that can cause clogging of the ionization source of the mass spectrometer creating high background noise and requires additional desalting procedures prior to analysis.[91]

Analysis of microdialysis samples can be done using an online or offline arrangement of the separation and detection set-ups. In an online set-up, microdialysis samples are directly transferred to a separation system that analyzes the samples as they are collected. This arrangement eliminates the problem of sample degradation and minimizes contamination due to sample handling.[90, 96] In the offline arrangement, samples are collected for later analysis. This procedure is susceptible to contamination due to handling and sample degradation. However, the offline arrangement has been used widely because most laboratories cannot afford the expensive instrumentation and expertise that go with the online analysis.[96]

1.4.1.2 Advantages and disadvantages of *in vivo* microdialysis

One advantage of microdialysis is its ability to measure basal extracellular levels of neurotransmitters and metabolites. In addition, the technique allows simultaneous analyses of multiple analytes. The main drawback of microdialysis is low spatial

resolution due to the relatively large size of the microdialysis probe (2 mm long, 240 µm diameter) compared to distinct brain regions, which can be < 0.5 mm^3.[96] Compared to the fast neuronal events (on a milliseconds time scale), microdialysis has poor temporal resolution. Thus, microdialysis is a less suitable choice for measurements of neurotransmitter release and uptake dynamics.

1.4.2 Fast scan cyclic voltammetry (FSCV)

FSCV belongs to a family of electroanalytical techniques that measures current generated by electroactive species in response to an applied potential at the surface of a working electrode. In FSCV, the applied potential is triangular in shape with parameters sufficient for the test chemical to undergo a redox reaction. Typically, the working electrode is held at a negative potential, ramped up to a positive potential, and then brought back down to the starting negative potential. These potentials are scanned with respect to a silver-silver chloride (Ag/AgCl) reference electrode (Figure 1.7). Unlike classic cyclic voltammetry, the waveform in FSCV is scanned at a faster rate (> 100 V/s) to improve sensitivity.[101, 102] The waveform takes approximately 10 ms to complete a cycle and is repeated several times (usually at 10 Hz) at 100 ms intervals. In the forward scan of the applied potential, electrons are transferred from the analyte to the electrode (oxidation) whereas the reverse scan causes electrons to move from the electrode to the analyte (reduction, Figure 1.7). The flow of electrical charge is measured as current, which is proportional to the concentration of the test chemical according to Faraday's law of electrolysis (Equation 1).

$$Q = nFN \qquad (1)$$

In this equation, Q is the total electric charge measured in Coulombs, n is the number of moles of electrons per molecule lost or gained, F is Faraday's constant, given as 9.649 x 10^4 Coulombs/mole, and N is the number of moles of analyte undergoing electrolysis. Where current (I) is given as a change in charge (Q) with respect to time (Equation 2).

$$I = dQ / dt \qquad (2)$$

In addition to the faradaic current, a large charging current is produced due to the fast scan rate and therefore the small change in current caused by the electrolysis of the analyte is obtained by background subtracting the charging current. This attribute makes FSCV useful in measuring only changes in current and not the absolute current.[101, 103] Nonetheless, its temporal resolution in milliseconds has made it a powerful tool to monitor the fast chemical events of several neurotransmitters in the brain.

The working electrode used in FSCV serves as a key component in the measurement. In brain measurements where FSCV is coupled to a microelectrode, high spatial resolution is achieved because the microelectrode, which is typically 7 μm in diameter and 50 – 200 μm in length allows measurements from discrete brain regions with minimal tissue damage.[104-106] The commonly used microelectrode consists of a carbon fiber encased in a glass capillary. Carbon fiber microelectrodes offer several advantages which include the fact that fabrication is easy and cheap, they are less susceptible to fouling when implanted in brain tissue, and permit the use of large potential windows.[101]

The data obtained from FSCV in brain measurements is in three different forms. One form is a plot of the Faradaic current as a function of the applied potential referred

to as cyclic voltammogram (Figure 1.8A). The cyclic voltammogram provides a unique 'fingerprint' of the analyte that is used for identification. Cyclic voltammograms are unique for a given electroactive species in terms of shape and oxidation and reduction potentials, providing selectivity for the FSCV technique. For molecules whose cyclic voltammograms may look identical, their identities can be further confirmed using pharmacological verification.[107, 108] The FSCV data can also be visualized in a 3-dimensional color plot of current (z-axis), time (x-axis) and applied potential (y-axis), where the oxidation and reduction currents are color coded respectively (Figure 1.8B). Finally, FSCV data can be represented as a current versus time trace, where the rising phase of the plot primarily represents release and the decay phase is the uptake of the neurotransmitter (Figure 1.8C).

With the above mentioned superiority over other available techniques, FSCV has been used extensively both *in vivo* (in free moving or anesthetized animals) and in brain slices to study the dynamics of many neurotransmitters including DA, serotonin, norepinephrine, epinephrine, histamine, adenosine, tyramine, and octopamine.[106, 109-114]

1.4.2.1 Slice fast scan cyclic voltammetry

A complete description of slice FSCV with instructional video can be found in: *Maina, F. K,* Khalid, M.,*Apawu, A. K,* and Mathews, T. A.* (2012) *J. Vis. Exp, 59, pii: 3464. doi: 10.3791/3464.*[106] **Co-first-authors.*

Slice FSCV is a useful tool to characterize the release and uptake profiles of many neurotransmitters including DA dynamics in rodent models. In this method, the test animal is euthanized and its brain is removed and sliced into coronal brain slices, which are equilibrated in continuously oxygenated aCSF buffer. Voltammetric

recordings are made from a coronal brain slice placed in a temperature controlled chamber that is continuously perfused with oxygenated aCSF buffer. During measurement, neurotransmitter release is evoked with a single (monophasic, 350 μA, 60 Hz, and 4 ms pulse width) or multiple electrical pulses delivered onto the brain slice through a bipolar stimulating electrode and the neurotransmitter release is measured at a working electrode, usually a carbon fiber microelectrode surface (Figure 1.7) as described above and also in Maina *et al.*[106]

Slice FSCV has numerous advantages, which include the ability to make measurements from different brain regions of the same coronal slice. Furthermore, in this method, probe placement is easier since no stereotaxic coordinates are needed. A working microelectrode and bipolar stimulating electrode are positioned on the brain slice by viewing through a microscope. The brain region of interest is located with the help of a rodent brain atlas and anatomical markings on the brain slice. With these aids, measurements can be made from sub-anatomical brain regions that are very close to each other. Slice FSCV allows test of pharmacological agents on neurotransmitter dynamics like *in vivo* measurements. Since multiple coronal brain slices (typically 400 μm) can be obtained from the same brain region, it is possible to do multiple pharmacological tests in a single animal using slice FSCV. Reproducibility of the pharmacological tests is also high since it is done in a system that is controlled by the experimenter. In addition, this method provides selectivity in probing autoreceptor functionality since measurements can be made from the presynaptic terminals without direct inputs from post-synaptic receptors.

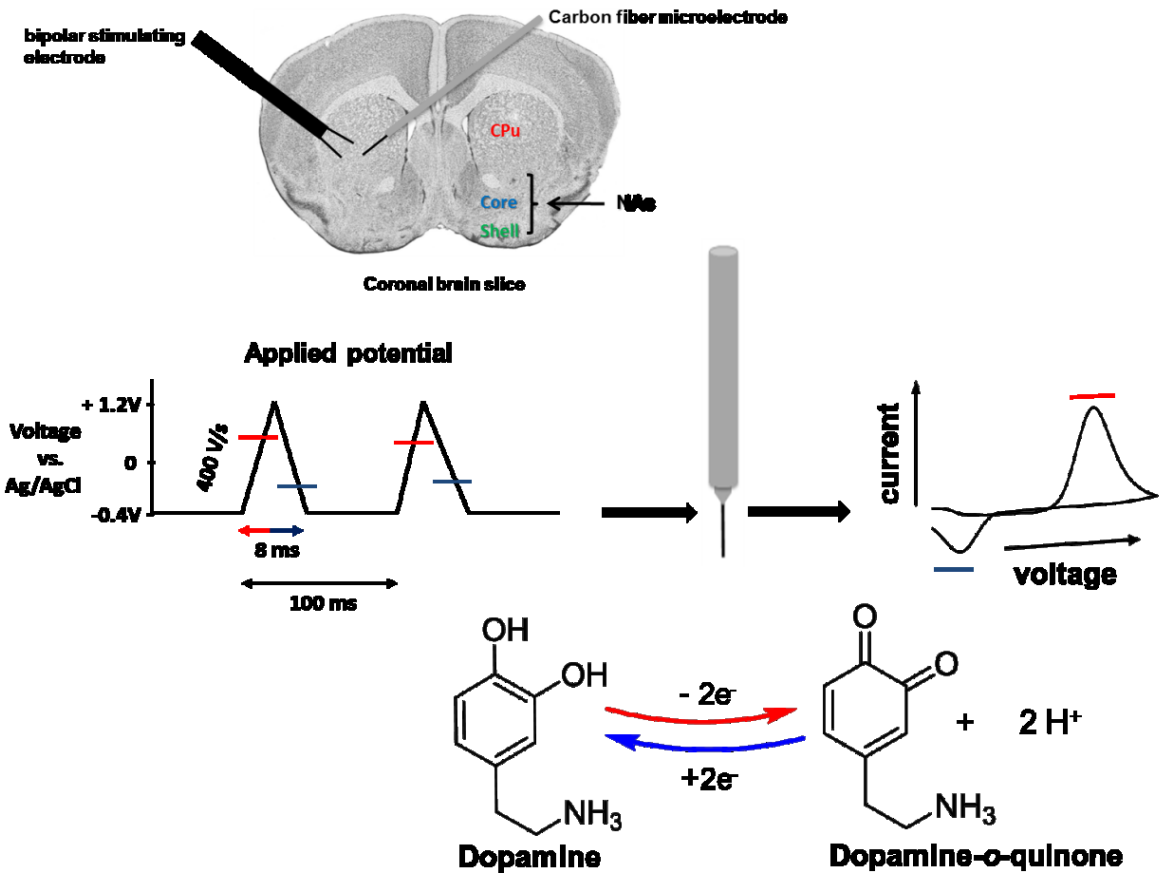

Figure 1.7: Slice fast scan cyclic voltammetric (FSCV) measurement of DA dynamics. In slice FSCV of DA, coronal brain slice (top panel) is electrically stimulated to evoke DA. The applied waveform at the microelectrode surface is scanned from -0.4 V to +1.2 V and back to -0.4 V. DA oxidized to form dopamine-*o*-quinone in the forward scan and in the reverse, dopamine-*o*-quinone is reduced back to DA. The redox reaction generates current measured and converted to concentration. The coronal brain slice was adapted from Mouse Brain Atlas with permission from Elsevier [1].

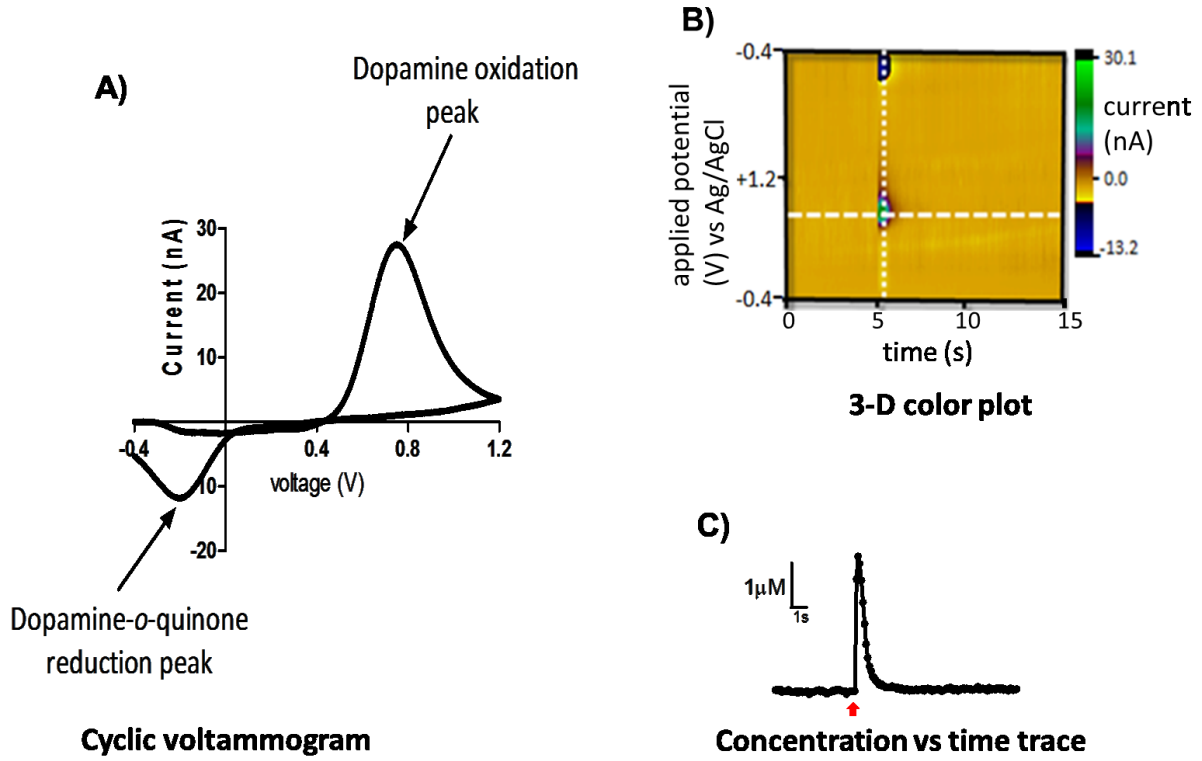

Figure 1.8: Representative FSCV data. Data obtained from FSCV experiments are expressed in three different plots A) A cyclic voltammogram (CV) provides information about the oxidation and reduction potentials of DA (~ 0.6 V and - 0.2 V respectively). These characteristic potentials together with the shape of the voltammogram can be used to identify DA. B) A 3-D color plot showing concentration (z-axis) versus applied potentials (y-axis) versus time (x-axis), where green and blue colors represent oxidation and reduction currents respectively. C) A plot of oxidation current versus time gives a concentration-time trace where the red arrow shows the point of electrical stimulation to evoke DA during measurement. The ascending phase of the concentration-time trace primarily denotes DA release whereas the descending phase shows DA uptake.

1.4.2.2 Advances in fast scan cyclic voltammetry

Overwhelming progress has been made in the use of FSCV in brain measurements. These advances span different aspects of FSCV including electrode fabrication, waveform modification, miniaturization of instrumentation, and clinical use. For example, the sensitivity of FSCV measurements has been improved significantly through modification of the carbon fiber microelectrode surface.[115, 116] Recent work by Hashemi and colleagues showed that electrodeposition of a cation exchange polymer called Nafion on a carbon fiber microelectrode surface increased the sensitivity of *in vivo* FSCV detection of serotonin in rats, which was hampered by fouling of the microelectrode surface by extracellular metabolites including 5-HIAA.[115] In a related study, coating the surface of a carbon microelectrode with a carbon nanotube (CNT)-Nafion mixture also significantly enhanced the sensitivity (~ 4 fold increase) of FSCV detection of adenosine in rat brain slices without altering temporal resolution.[116] Other electrode modifications include microelectrode arrays, which not only allow simultaneous FSCV measurements from multiple electrodes but also measurement of multiple molecules.[117, 118] Another addition to the field was the development of microelectrode that can be chronically implanted into the brain to make measurements over a long period of time. [104] This chronically implanted microelectrode, which was first reported by Clark *et al*., is useful in tracking neurotransmitter changes in behaving animals over time and can help to study the progression of neurological disorders including addiction.[104] The chronically implanted electrode consists of a carbon fiber encased in a fused silica with the fiber and silica interface insulated with two-component epoxy and the protruding fiber (7 μm in diameter and 150 – 200 μm in length) treated

with 2-propanol.[104] This microelectrode is biocompatible and can be used to monitor sub-second DA dynamics in rodents over 4 months with no significant tissue damage.[104, 119-121] In addition to microelectrode modifications, optimizing the wave form of the applied potential and the scan rate have also improved sensitivity of FSCV measurements.[102] These modifications have contributed to the use of FSCV to effectively measure a wide variety of electroactive species in the brain.[5, 102, 108, 115]

FSCV measurements have also been improved in the area of instrumentation. Currently, a wireless instantaneous neurotransmitter concentration sensing system (WINCS) has been developed that allows FSCV measurements to be made from behaving animals in an environment without restrictions from cables while transmitting neurochemical data remotely to an analysis system.[122-124] This technology reduces electrical noise interference and movement artifacts in the measurements.[122] The WINCS coupled to FSCV has been used to detect DA, histamine, adenosine, and serotonin in animal models and is now being fine-tuned to be used in humans to monitor neurochemicals in deep brain stimulation feedback.[111, 122-125]

1.4.3 Brain tissue content analysis of neurotransmitters

Brain tissue content analysis provides a means to assess intracellular levels of neurotransmitters and their metabolites in animal brain tissues. The method has been widely used to examine the intracellular levels and catabolism of most monoamines including DA in rodent models.[84, 94, 126, 127] It involves sacrificing animals (usually by cervical dislocation followed by decapitation) and then their brains are removed and dissected to obtain tissue from the region on interest. The use of cervical dislocation is preferred to other methods of euthanasia such as anesthesia or carbon dioxide

inhalation because it eliminates potential interference in the brain chemistry, since stress as a result of injection of an anesthetic or suffocation may alter the levels of brain chemicals.[128, 129] Brain tissues are frozen immediately after they are removed to ensure that the neurochemicals do not degrade. Prior to analysis, the tissues are homogenized in a strong acid (perchloric acid is commonly used) to extract neurochemicals from the tissue and then the samples are centrifuged. The supernatant is analyzed using a separation techniques coupled to a detector. HPLC with electrochemical detection has been widely used to analyze tissue samples.[84, 94, 126, 127] First, standards of the compound of interest are run individually to obtain their retention time to enable identification of analyte peaks. The samples are then run at appropriate attenuation. The analyte peaks obtained are integrated against calibration curves of their respective standards to obtain their concentration in the tissue samples. Since tissue content analysis uses free hand dissection, different sizes of tissues are taken from the regions of interest, it is important to normalize the analyte concentrations to the tissue weight or its protein content. Normalizing the analyte concentration to protein content of the tissue is advantageous as it minimizes problems associated with weighing wet tissue samples including loss of tissue and degrading neurochemicals if there is too much time delay.

Although tissue content analysis using HPLC does not have good temporal resolution as compared to a technique like FSCV, it has been useful to understand how intracellular neurotransmitter levels and metabolism are influenced by drugs of abuse, neurological disorders, and gene modification.[84, 94, 130, 131] Tissue content analysis has also be used to investigate the biosynthesis of DA, in which case the activity of TH (the rate limiting enzyme in biosynthesis of DA) is indirectly examined by inhibiting AADC

(the enzyme that catalyzes the decarboxylation of L-DOPA) and then measuring the accumulation of L-DOPA in tissue samples.[94, 127]

1.4.4 Behavioral testing in animal models

Behavioral assays used in animal models have provided useful clues to the neural mechanism underlining the action of most drugs of abuse. They have also been used to measure observable traits of genetically modified animals that are used as models for most neurological disorders.[132-135] The assays encompass simple locomotor activity measurements to more sophisticated behavioral paradigms such as condition placed preference and operant behavior.[59, 61, 68, 104, 136, 137] Locomotor activity has been widely used to characterize the neurobehavioral profile of most drugs of abuse. Such characterization is based on existing data that have linked induced locomotion to changes in the mesolimbic dopaminergic system. For example, direct injection of DA into the NAc stimulates rat's locomotor activity, while destroying DA neurons in the NAc with 6-hydroxydopamine decreases drug induced stimulated locomotor activity.[138-140] Thus, stimulation of locomotor activity is thought to correspond to increased extracellular DA levels in the NAc.[34, 141]

Locomotor activity testing involves putting an animal in an activity chamber or placing a whole cage of a singly housed animal into an activity set-up, depending on the goal of the experiment. The activity chamber or set-up is equipped with three sets of infrared (IR) emitter-detector arrays attached outside of the set-up, two of which are positioned in the x- and y-axis to measure the position and horizontal movement of the animal while the third pair is placed in the z-axis to measure the jumping and rearing activities of the animal. During data collection, the position and locomotor activity of the

animal is detected by interruption in the light beams emanating from the IR emitter to the detector. This interruption in the IR beam generates an analog signal that is recorded by automated activity software installed on a computer. The data obtained from this type of measurement include total distance traveled during the experiment, horizontal count, horizontal time, vertical count, vertical time, stereotypic count (repetitive movements) and stereotypic time. In testing the effect of pharmacological agent on locomotor behavior, the animals may be pre-treated or treated during measurement depending on the mode of the drug administration. For volatile solvents including toluene, a calculated amount of the solvent is introduced and volatilized in the activity chamber, which is made airtight (static system) or the vapor is continuously generated in a dynamic system. Locomotor activity is measured during the treatment.

1.5 Research objectives

Because dopaminergic innervations in the striatal region of the brain are involved in several neuronal functions and have been implicated in many neuronal disorders including drug addiction, understanding the DA dynamics in this terminal region is a crucial component of the attempt to decipher the mechanism underlining neuronal disorders.

The overarching objective of my research work is two-fold: 1) *To understand how the striatal DA system adapts to acute and chronic toluene inhalation*, and 2) *To understand how a trophic factor, brain derived neurotrophic factor (BDNF) modulates striatal DA release and uptake.*

1.5.1 Research objective 1: *To understand how the striatal DA system adapts to acute and chronic toluene inhalation: This project is a collaborative work with Dr. Scott Bowen*

from the Department of Psychology, Wayne State University. Part of this work is in revision for publication in Psychopharmacology.

Drug addiction involves substances such as amphetamine, cocaine, methamphetamine, and alcohol. However, one area that has received little attention is inhalant abuse, which is defined as the deliberate inhalation of volatile organic solvents in order to attain a euphoric feeling.[45] One of the most widely abused inhalants among the adolescent population is toluene.[142] The abused inhalant toluene has potent behavioral and neurochemical effects. Available evidence suggests that toluene inhalation alters DA neurotransmission in the brain.[36, 71] However, the exact mechanism underling toluene's effect on the DA system, particularly DA release and uptake dynamics, has remained elusive. The present study seeks to elucidate toluene's action on the striatal DA system by using behavioral testing and neurochemical measurements including techniques such as *in* vivo microdialysis, slice FSCV, and tissue content analysis.

The overall hypothesis of this work was that both acute and repeated toluene inhalation will alter DA release and uptake dynamics in the mesolimbic DA terminals. This hypothesis is based on existing behavioral data that has shown that toluene inhalation has a rewarding effect and can stimulate locomotor activity in rodent models.[58, 68, 74] Our hypothesis is also supported by neurochemical data that has shown that acute toluene inhalation can potentiate extracellular DA levels in the pre-frontal cortex and the NAc.[36, 71, 143]

1.5.2 Research objective 2: *To understand how a trophic factor; brain derived neurotrophic factor (BDNF), modulate striatal DA release and uptake. Portions of this*

work have been published in the manuscript by Aaron K. Apawu, Francis K. Maina, James Taylor, and Tiffany A. Mathews in ACS Chem Neurosci., 2013, 4(5): 895 – 905.

BDNF regulates growth, differentiation, and survival of neurons through activation of high affinity tyrosine kinase receptor, TrkB.[144-147]. There is also considerable evidence that suggests that BDNF modulates striatal DA function.[21, 148-150] From previous work in the Mathews laboratory, it was proposed that the reduction in BDNF expression is directly responsible for decrease in evoked-DA release, while the compensatory response to lifelong reductions in BDNF would lead to decreased DA transporter function.[94] Based on this work, we have hypothesized that BDNF modulates presynaptic DA dynamics in the striatum through activation of the TrkB receptor. Typically, molecular techniques have been used to probe the effect of TrkB receptor activation and the potential pathways through which BDNF may influence DA dynamics.[148, 149] However, the exact mechanism by which BDNF regulates presynaptic DA release and uptake processes remains elusive. The goal of the present work is to examine the ability of FSCV to measure the action of tyrosine kinase receptors on striatal DA dynamics and then characterize the involvement of presynaptic TrkB receptors in regulating striatal DA release and uptake processes. FSCV provides the unique ability to measure both DA release and uptake rate on a milliseconds time scale consistent with release and uptake events. The use of a carbon fiber microelectrode of ~ 7 microns in diameter ensures high spatial resolution with negligible tissue damage.

CHAPTER 2

Materials and Methods

The chapter expounds on the materials and methods used in all experiments reported in this dissertation. The methods discussed here include behavioral assays and neurochemical techniques used to understand brain function. Specific details of each technique are discussed in subsequent chapters. All experimental protocols and animal procedures used in this dissertation were approved by the Institutional Animal Care and Use Committee (IACUC) of Wayne State University.

2.1 Chemicals

Toluene (purity > 99.5%) was purchased from Fisher Scientific Co. (Fairlawn, NJ). Chemicals used to prepare artificial cerebrospinal fluid (aCSF) for voltammetry and *in vivo* microdialysis, and mobile phase for HPLC analysis were purchased from Fisher Scientific Co. (Fairlawn, NJ) and Sigma (St. Louis, MO). Pharmacological agents used in this work were purchased from specific vendors as follows: BDNF from PeproTech (Rocky Hill, NJ), 7,8-dihydroxyflavone, genistein, and tyrphostin 23 were from Tokyo Chemical Industry Co. Ltd. (Portland, OR) or EMD Chemicals, Inc. (Gibbstown, NJ), and K252a was from LC Laboratories (A Division of PKC Pharmaceuticals Inc., Woburn, MA).

2.2 Animal subjects

Adolescent outbred male Swiss-Webster mice (~ 4 week old) were used in the inhalant (toluene) abuse project. The choice of mouse strain was based on previous work that has demonstrated that Swiss-Webster mice have higher toluene induced locomotor activity than other mouse strains.[74] Swiss-Webster mice were purchased

from Harlan Breeding Laboratories (Haslett, MI) and housed in a vivarium at Wayne State University, which is certified by the Association for Assessment and Accreditation of Laboratory Animal Care (AAALAC). Mice were kept in groups of 10 - 12 animals per cage and had *ad libitum* access to Rodent Lab Diet 5001 (PMI, Nutrition International, Inc., Brentwood, MO), and water. The environment of the vivarium was temperature controlled (20 – 22 ^{o}C) with a 12-h light cycle (0600 – 1800 h).

The second project involved the use of genetically modified C57BL/6 mice, where mice had no mutation (wildtype), or one copy of the mutated brain-derived neurotrophic factor gene (heterozygote BDNF mice; $BDNF^{+/-}$). $BDNF^{+/-}$ and their wildtype littermates were purchased from Jackson Laboratories (Bar Harbor, ME) and breeding pairs were established. All neurochemical experiments were performed on offspring that were born and raised in-house. When mice were approximately 3 weeks of age, they were separated from their parents, ear-punched (for identification purposes), and less than 2 cm of their tail was taken to determine their genotype by using polymerase chain reaction (PCR) analysis of tail DNA. (For detailed procedure, see Bosse *et al., 2012).*[94]

2.3 Toluene exposure procedure

Toluene exposure was performed in static exposure chambers consisting of 26.5 liter cylindrical glass jars (diameter 28.5 cm; height 45 cm; total floor space = 638 cm^2) housed within a fume hood (Figure 2.1). Each chamber was equipped with a vapor diffuser with a fan attached to a Plexiglas^{TM} lid. On the day of exposure, a mouse was placed in the floor of a chamber approximately 50 cm from the vapor diffuser and allowed a 5 minute acclimation period; after which, a known concentration of toluene

(calculated using the ideal gas equation, simplified for room temperature[151]) was injected through an injection port onto filter paper in the vapor diffuser. The fan was then turned on to diffuse toluene within the chamber for a period of 30 minutes; after which the fan was turned off and the chamber was opened to allow the mouse a 30 minute period of no toluene vapor inhalation (recovery). For the air-control experiments, the same procedure was followed, but no toluene was injected into the chamber. Routinely, the concentration of toluene vapor in the chamber was confirmed and monitored using a single wavelength-monitoring infrared spectrometer (Miran 1A, Foxboro Analytical) to ensure that there were no leaks in the chamber. Mean concentrations of toluene were within 2% of nominal, approximately 2.5 minutes after toluene was injected into the exposure chamber it was within 2% of the desired concentrations throughout the 30-minute exposure period followed by rapid clearance when chamber was opened (Figure 2.2).

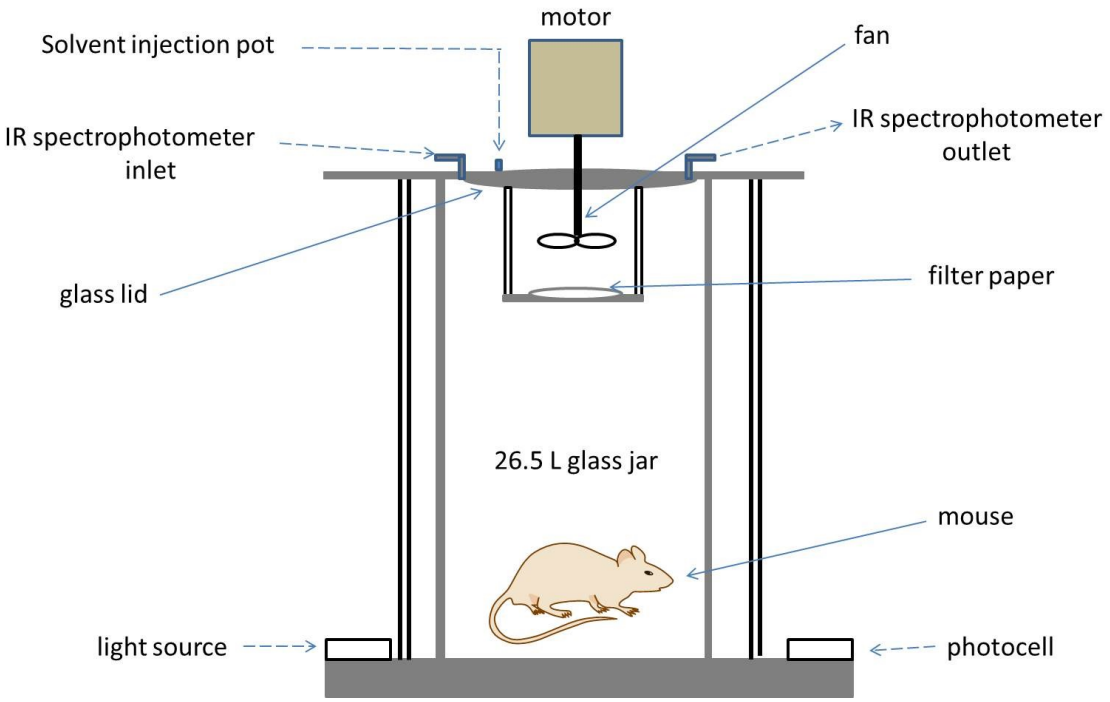

Figure 2.1: Schematic diagram of toluene exposure chamber.

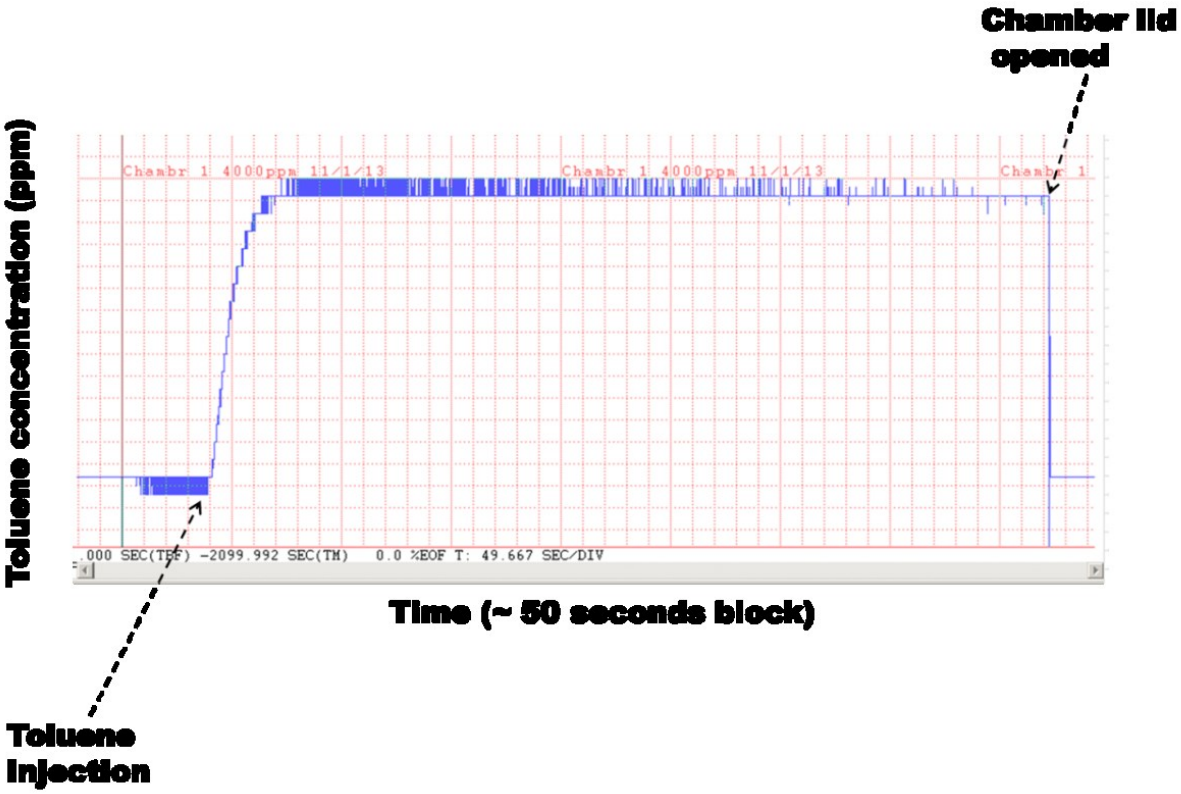

Figure 2.2: Representative infrared spectrograph of toluene vapor in toluene exposure chamber. Data was obtained during routine check for leaks in the chamber. Each block represents ~ 50 seconds. Following injection of a calculated volume of liquid toluene, the vapor diffused quickly to reach 4000 ppm concentration and remained within 2% of the desired concentrations throughout the exposure period. When the lid of the chamber was removed, toluene cleared quickly from the chamber. Infrared spectrograph was provided by Sean Callan from the Bowen lab.

2.4 Locomotor activity measurement

The toluene exposure set-up consisted of three pairs of 16-beam infrared (IR) emitter-detector arrays (Med Associates, St. Albans, VT) located outside of the chamber. Two of these (IR) emitter-detector arrays were positioned ~ 2.5 cm from the floor of the chamber at a right angle to each other in the x- and y-axes allowing the position and locomotion of the mouse to be detected and measured by the count of interruptions in the IR beams in the horizontal and vertical planes. The third pair of IR emitter-detector arrays were in the z-plane located ~ 7 cm from the floor of the chamber recorded jumps and rearing activities of the mouse. The interruptions in the IR beams generated analog signals recorded by automated activity software (Open Field Activity Software [SOF-811], Med Associates, St. Albans, VT) as locomotor activity. In this work, locomotor activity was defined as the sum of interruptions of the lower IR beams in the x- and y-axes.

2.5 Slice fast scan cyclic voltammetry (FSCV)

Slice FSCV was used to measure electrically evoked DA release and uptake dynamics in the striatum of mouse brain slices.

2.5.1 Brain slice preparation

Following asphyxiation, mice were decapitated and their brains were rapidly removed and immediately placed into chilled pre-oxygenated (95% O_2/5% CO_2) sucrose artificial cerebral spinal fluid (aCSF) for 10 minutes. The composition of the sucrose aCSF was 180 mM sucrose, 30 mM NaCl, 4.5 mM KCl, 1 mM $MgCl_2$, 26 mM $NaHCO_3$, 1.2 mM NaH_2PO_4, and 10 mM D-glucose, and pH = 7.4. The mouse brain was then sectioned into 400 µm thick coronal brain slices using a vibratome (Vibratome, St.

Louis, MO). Brain slices with the striatal complex consisting of the caudate putamen (CPu) and the nucleus accumbens (NAc) were immediately transferred into continuously oxygenated fresh aCSF (aCSF for voltammetric recordings consisting of 0.4 mM ascorbic acid, 126 mM NaCl, 2.5 mM KCl, 1.2 mM $MgCl_2$, 2.4 mM $CaCl_2$, 25 mM $NaHCO_3$, 1.2 mM NaH_2PO4, 11 mM D-glucose, and pH = 7.4) and were allowed to acclimate in the buffer for at least 1 hour before voltammetric recordings.

2.5.2 Electrode fabrication

Carbon fiber microelectrodes were made in-house by threading a single strand carbon fiber (Goodfellow Oakdale, PA) of diameter 7 μm into a 10 cm long glass capillary (dimensions o.d. 1.2 mm, i.d. 0.68 mm; A-M systems, Carlsborg, WA) using vacuum suction. The glass capillary was then pulled into two equal halves using an electrode puller (Model PE-21 with the following settings: main magnet = 90.7, sub-magnet = 23.2, and heater = 53.4; Narishige, Tokyo, Japan). There is a heating element at the center of the electrode puller, which heats the center of the glass capillary, stretching the glass capillary vertically until the magnetic force is the strongest, pulling the capillary into two discrete electrodes. The pulled halves of the glass capillary had ~ 4.4 mm glass taper which was tightly sealed around the glass-carbon fiber interface. The carbon fiber protruded centimeters beyond the end of the taper was placed under a microscope (Olympus, Tokyo, Japan) and trimmed using a scalpel to the length of 50 - 200 μm (Figure 2.2). The microelectrodes were stored at room temperature until they were required for experimental use. When ready, they were backfilled with 0.15 M potassium chloride and a lead wire (Squire Electronics Inc., Cornelius, OR) was inserted to establish electrical contact. Silver/silver chloride reference electrodes

(Ag/AgCl) were fabricated by coating a silver wire (250 µm in diameter; A-M Systems, Carlsborg, WA) with silver chloride by anodizing (+1 V) the wire in 1 M hydrochloric acid for 5 minutes.

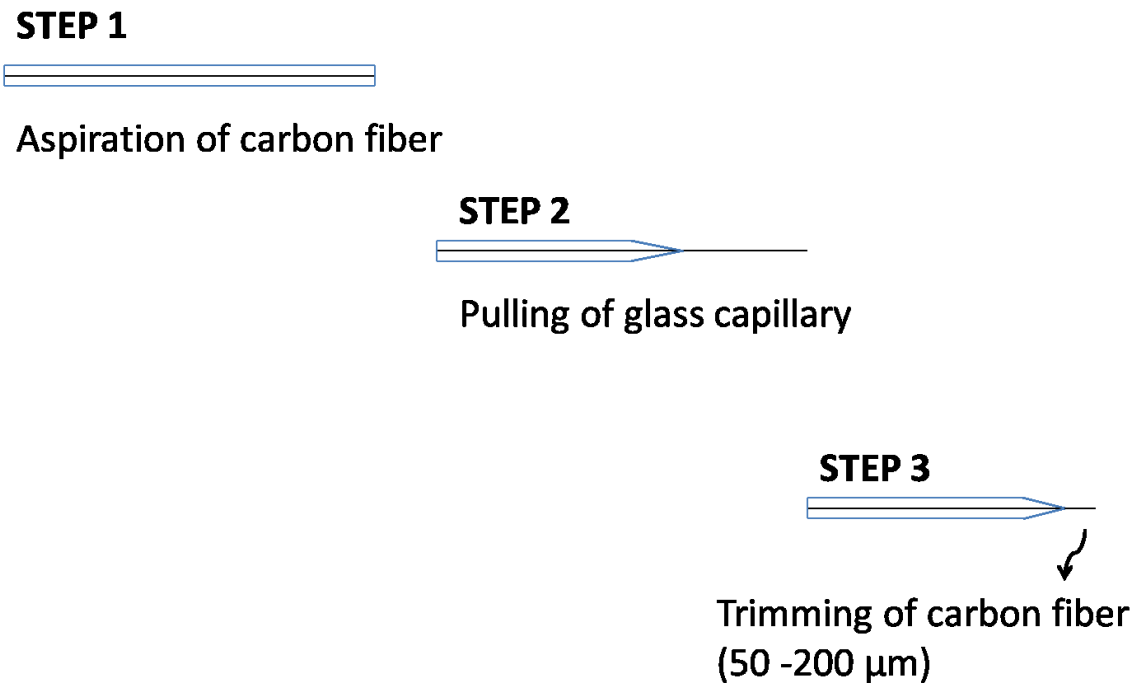

Figure 2.3: Stepwise illustration of carbon fiber microelectrode fabrication. Electrode fabrication was accomplished in three steps: aspiration of carbon fiber into glass capillary, pulling of glass capillary and trimming carbon fiber extending from glass capillary to a length of 50 – 200 µm.

2.5.3 Microelectrode calibration

Following fabrication, the carbon fiber microelectrode was calibrated using flow injection analysis to test for its viability and sensitivity. In this procedure, the microelectrode was lowered vertically into one of the three ports of a flow T-cell. This flow cell had the Ag/AgCl reference electrode sealed in it and one of the remaining two ports of the cell was connected to a syringe pump which continuously pumped modified aCSF (composition: 2.5 mM KCl, 126 mM NaCl, 1.2 mM NaH_2PO_4, 2.4 mM $CaCl_2$, 1.2 mM $MgCl_2$, and 25 mM $NaHCO_3$, and pH = 7.4) at a flow rate of 2 mL/min. The third port was connected to a syringe that would be used to deliver a 3 μM dopamine (DA) standard. During electrode calibration, 1 – 2 mL of the DA standard was manually injected into the stream of modified aCSF. DA was detected at the microelectrode surface when there was a rise in the current being measured. The calibration process was repeated at least three times and the average of the maximum current obtained in each injection was calculated by dividing the average current by the concentration of the DA standard (3 μM). Besides calibrating the microelectrodes before use, a post-calibration of the microelectrode was performed after data collection from a mouse brain. The post calibration factor obtained was used in determining the response factor of the electrode for all data analysis.

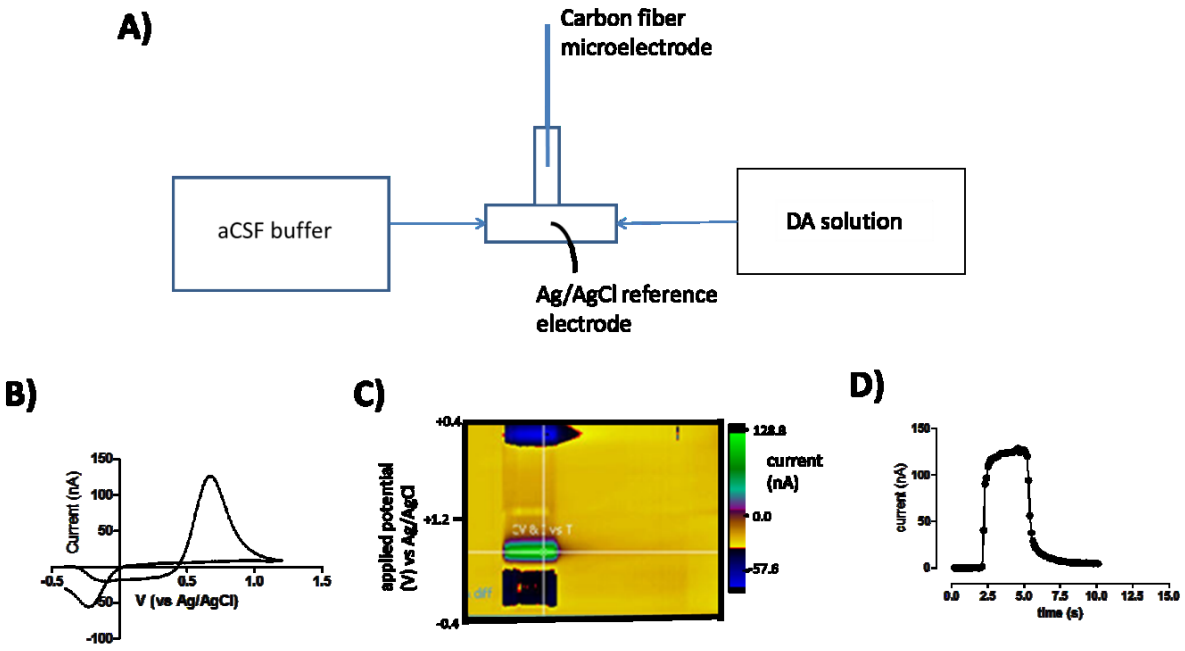

Figure 2.4: Flow injection analysis (FIA) set-up showing calibration of a microelectrode. The microelectrode is calibrated using FIA. **A)** FIA set-up consists of a flow T-cell connected to a Ag/AgCl reference electrode, a syringe pump continuously supplying aCSF, and a another syringe containing 3 µM DA standard. **B)** Background subtracted cyclic voltammogram of DA standard showing DA oxidation and reduction peaks that identifies DA. **C)** Representative 3-dimensional color plot of applied potential versus time versus current showing oxidation and reduction current of DA in green and blue colors respectively. **D)** Current versus time plot showing oxidation current (130 nA) generated from injection of 3 µM DA standard. Injection of DA standard is repeated 3 times and the average of the maximum current is divided by the concentration of the DA standard. The calibration factor in the representative data is 130/3 = 43 nA/µM.

2.5.4 FSCV data collection

Before voltammetric measurements were made, a recording chamber (Custom Scientific, Denver, CO) was continuously perfused with oxygenated aCSF (aCSF for voltammetric recordings) using a perfusion pump (Watson Marlow Limited, Falmouth, England) set at a flow rate of 1 mL/min. The temperature of the chamber was adjusted to 32 ^{o}C. The recording chamber where the slice would be placed had a submerged Ag/AgCl reference electrode. A brain slice was placed into the slice holder where it was submerged in aCSF. With the aid of a microscope, a bipolar tungsten stimulating electrode (Plastics One, Roanoke, VA) and the carbon fiber microelectrode were then lowered onto the brain surface in the striatum about 100 – 200 µm apart, while the microelectrode was placed ~ 75 µm deep into the slice. All three electrodes were connected to a head stage potentiostat (Dagan Corporation, Minneapolis, MN) and were controlled by TH software (ESA Inc., Chelmsford, MA). To evoke DA release, a single pulse electrical stimulation (monophasic, 350 µA, 60 Hz, and 4 ms pulse width) generated by a Neurolog® stimulator (Digitmeter, Hertfordshire, England) was delivered to the brain slice via the stimulating electrode. Evoked DA release was measured by applying a potential to the microelectrode surface in the form of a triangular waveform (- 0.4 V versus a Ag/AgCl reference electrode, ramped to + 1.2 V and then back to - 0.4 V) at a scan rate of 400 V/s. The DA response was measured by the electrode as current. A single stimulation was applied to the brain slice every 5 minutes, and DA recordings were measured for 15 seconds. When three successive DA release profiles were within 10% of each other with respect to current, then a stable baseline was considered and

these pre-drug measurements were used to determine maximum stimulated DA release and uptake.

2.5.5 FSCV data analysis

The DA release profiles were initially determined as current versus time, and by using the post calibration factor (a conversion factor), the current was converted into concentration. Once the results were in the form of concentration versus time, traces were analyzed using LabVIEW™ National Instruments software (Austin, TX), where each curve was fitted to a set of Michaelis-Menten based equations using nonlinear regression.[106, 110, 152-154] Stimulated DA release per electrical pulse ($[DA]_p$) and DA uptake kinetics expressed as maximum velocity of the DA transporter (V_{max}) were obtained by setting K_m (which represents the affinity of DA to its transporter) to a fixed value of a 160 nM, which allowed us to vary the $[DA]_p$ and V_{max}. The goodness of fit was determined by the coefficient of determination (R^2) parameter generated by the software (R^2 values > 0.8 were used).

2.6 *In vivo* microdialysis

In vivo microdialysis was used to measure extracellular DA level during toluene exposure. The microdialysis procedure involves stereotaxic surgery of a probe followed by sample collection and analysis of dialysate samples.

2.6.1 Stereotaxic surgery

Prior to stereotaxic surgery, mice were transported to the laboratory and weighed. Each mouse was placed into a chamber connected to isoflurane and oxygen until the mouse was anesthetized. The mouse was removed from the chamber and placed onto a heading pad (~ 37 °C) and covered with paper towels to maintain its body

temperature. Isoflurane was delivered through a nosepiece. Then the pre-operative preparation began. A small section of the animal's fur covering the skull was shaved. To protect the eyes from dehydration during the surgical procedure, sterile artificial tear lubricant ophthalmic ointment was carefully applied to the eyes. The shaved area above the skull was disinfected with betadine and 70% alcohol, and then a small incision was made. The exposed skull was cleaned with 10% hydrogen peroxide to dissolve the thin membrane covering the skull making Bregma visible. The mouse was placed into a mouse stereotaxic frame (David Kopf Instruments, Tujunga, CA) where the anesthesia plane was maintained by securing its nose to a tube connected to isoflurane and oxygen, where their flow rates were adjusted as needed. The head of the mouse was secured firmly on the frame using two non-puncture ear bars and a nose clamp so that the top of the mouse's skull was straight and stable. Bregma on the skull surface was located, since coordinates for finding brain regions of interest are referenced using Bregma. The coordinates used for the CPu were: anterior-posterior (AP) +0.80 mm, lateral (L) -1.3 mm, and ventral (V) -2.5 mm; and NAc: anterior-posterior (AP), +1.2 mm; lateral (L), -0.6 mm; ventral (V) -4.2 mm from Bregma, determined from a mouse brain atlas and empirically refined.[1] The coordinates for the CPu or the NAc were marked and an approximately 1 mm diameter burr hole was drilled in the skull for guide cannula placement. A second hole was drilled for a skull cap screw that does not require coordinates. A CMA/7 guide cannula (CMA microdialysis, Chelmsford, MA) was carefully lowered into the first hole. The guide cannula and the screw were firmly held in place on the skull by dental cement, which was also used to cover any exposed area of the skull. When the dental cement was dry, the mouse was taken from the stereotaxic

frame and placed on a heating pad covered with a paper towel in a recovery chamber. Following recovery from anesthesia (indicated by independent movement in the recovery chamber), the mouse was transferred to a microdialysis bucket furnished with bedding, food, and water.

2.6.2 Simultaneous collection of microdialysis samples and behavioral testing during toluene treatment

Mice were allowed three days to fully recover from surgery before any behavioral testing and dialysate samples were collected. Prior to sample collection, a dummy probe in the guide cannula was removed and a microdialysis probe (CMA/7, 2 mm long for CPu or 1 mm long for NAc, 240 µm diameter, 6 kDa molecular weight cut-off; CMA Microdialysis, Chelmsford, MA) was inserted into the guide cannula. To measure locomotor behavior and extracellular DA levels simultaneously, the mouse was placed in an experimental chamber (glass tank of dimensions: 41 cm length x 20.3 cm width x 25.5 cm height) housed in a fume hood. The chamber was modified to allow microdialysis sampling lines through a small hole in the lid. The chamber was equipped with IR emitter-detector arrays (Med Associates, St. Albans, VT) located outside of the chamber permitting locomotor activity of the mouse to be monitored during sample collection. ACSF (composition in mM: 147 NaCl, 3.5 KCl, 2 Na_2HPO_4, 1.0 $CaCl_2$, 1.2 $MgCl_2$, and pH 7.4) was perfused through the probe overnight at a flow rate of 0.4 µL/min. The next day at approximately 0900 h, the flow rate of the perfusing aCSF was increased to 1.1 µL/min (sampling from CPu) or 0.8 µL/min (sampling from NAc) for an equilibration time of 1 hour prior to baseline sample collection. Dialysate samples were collected in 15-minute fractions from the freely moving mouse before and during toluene

exposure, during recovery from toluene exposure, and post recovery. During the post recovery phase of dialysis collection, the regular aCSF was switched to a high K^+ concentration aCSF buffer (composition in mM: 60 KCl, 89 NaCl, 2.0 Na_2HPO_4, 1.0 $CaCl_2$; 1.2 $MgCl_2$; pH 7.4), and perfused through the microdialysis probe for 15 minutes, after which it was switched back to regular aCSF. The infusion of high K^+ aCSF directly into the striatum stimulates neurotransmitter release and enables evaluation of the resulting changes in extracellular DA levels in toluene exposed and air-control mice. Meanwhile, locomotor activity was simultaneously monitored by the count of interruptions in the IR beams attached to the outside of the chamber generating analog signal recorded by automated activity software (Open Field Activity Software). Toluene exposure was accomplished using a dynamic exposure system equipped with Praxair flow regulators, porter mass flow meters, and a Med PC interface that regulated the amount of toluene vapor administered. During toluene exposure, toluene vapor was generated by bubbling regulated amounts of air through toluene in a flask. The vapor was channeled through tubing, where it was diluted with controlled amounts of air to produce the desired concentration of toluene vapor (4000 ppm) that was perfused through the experimental chamber for 30 minutes (Figure 2.1). The settings on the dynamic system that produced the desired toluene concentration were obtained by adjusting the regulators while monitoring and measuring toluene concentration in the chamber prior to the experiment using a single wavelength-monitoring IR spectrometer. During the recovery phase or air-control experiment, the toluene bubbler was turned off to allow only air to perfuse through the chamber.

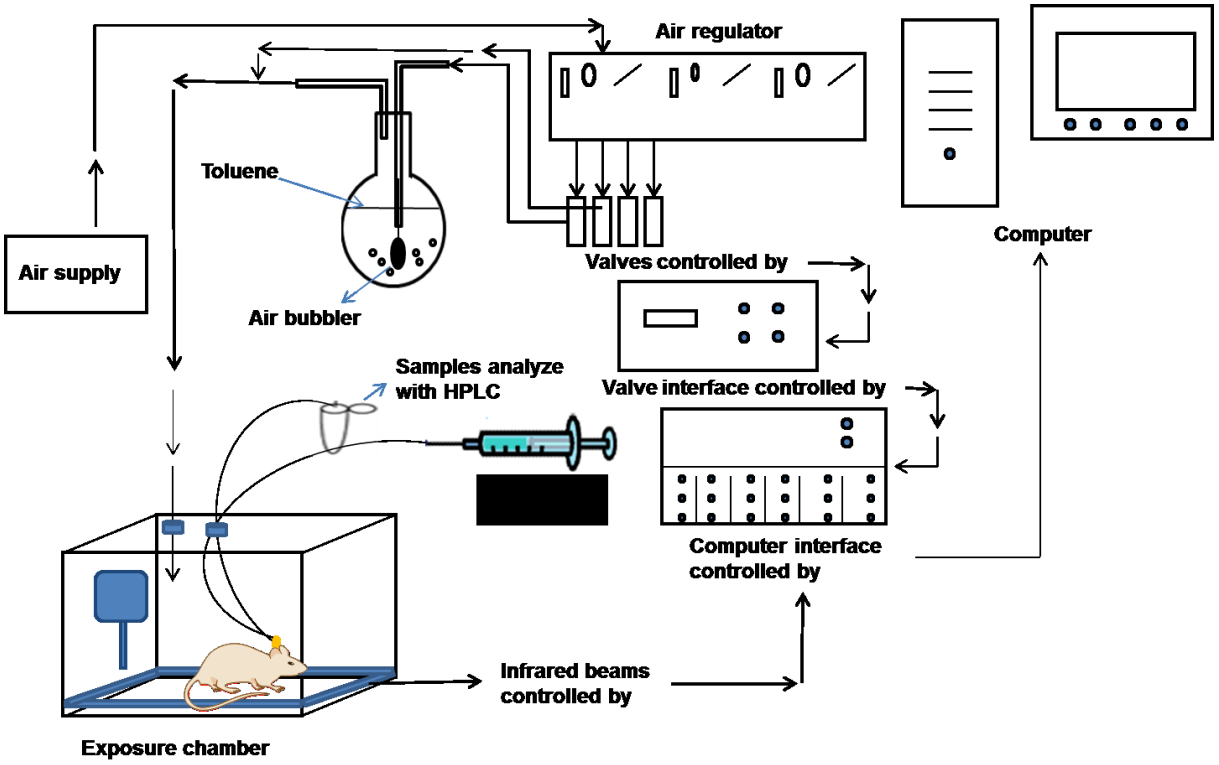

Figure 2.5 Dynamic toluene exposure set-up for simultaneous monitoring of locomotor activity and dialysate sample collection. By opening the first valve on the air regulator, air was bubbled through toluene in the flask to generate toluene vapor that was diluted with air in the tubing regulated by the second valve. The amount of toluene perfused into the chamber was controlled by Praxair flow regulators, porter mass flow meters, and a Med PC interface. Dialysate samples were collected from free moving mouse in the experimental chamber through perfusion of aCSF from the syringe through the microdialysis probe to sample small molecules such as neurotransmitters from the brain region of interest. Simultaneously, locomotor activity was monitored by the count of interruptions in the IR beams attached to the chamber that generate analog signal recorded by automated activity software on the computer.

2.6.3 Sample analysis using high performance liquid chromatography (HPLC)

All collected dialysate samples were stored in a -80 ^{o}C freezer and analyzed within two weeks of collection. HPLC with electrochemical detection was used to separate and analyze samples by manually injecting 20 µL of dialysate samples (CPu samples with 5 µL storage buffer consisting of 0.2 M perchloric acid, 0.2 µM ascorbic acid, and 0.2 µM EDTA) or 10 µL (samples from the NAc) into a 20 or 10 µL injection loop respectively. The mobile phase consisted of 75 mM NaH_2PO_4, 3 mM 1-octanesulfonic acid, 0.125 mM ethylenediaminetetraacetic acid (EDTA), 9% acetonitrile, 0.2 - 0.5% triethylamine, and pH = 3.0. The analytes were separated on a C_{18} column (Luna 100 x 3 mm, C_{18}, 2.6 µm column; Phenomenex, Torrance, CA) using an isocratic LC-20AD pump (Shimadzu, Columbia, MD) operated at a flow rate of 0.4 mL/min. DA was electrochemically detected using an ESA 5014B microdialysis cell (E1 = -150 mV; E2 = +220 mV; ESA Coulochem III) with an in-line ESA 5020 guard cell positioned before injection loop. The voltage of the guard cell was set at +350 mV. Separation and quantification of the analytes were controlled by LC Solutions Software (Shimadzu, Columbia, MD). DA standards were run after the experiment and DA's retention time was between 7 – 8 minutes. Integration and quantification of the DA peak area were performed against known concentrations of DA standards.

2.7 Histological verification of microdialysis probe placement

After microdialysis experiments, mice were sacrificed by CO_2 narcosis, decapitated, and their brains were removed. The brains were stored in 3.7% formaldehyde solution until used for histological verification. Briefly, brains were transferred into 2% dye and allowed to sit for about 18 hours. The brains were then

removed from the dye and rinsed 3 times each with 95% ethanol and water and were placed in 70% ethanol. Excess dye was washed off the brains by shaking in a 70% ethanol solution for 3 - 4 hours by affixing vials on a plate shaker. The solution was changed to a fresh 70% ethanol solution and allowed to shake overnight. The next day, the brains were rinsed with 95% ethanol solution by sitting them in the solution for 30 minutes, followed by water wash where they were not shaken for 45 minutes. The brains were wiped dry and fixed in 2% agarose solution (Agarose, type 1, Molecular Biology Grade, 15 - 30 °C). After the agarose solidified with the imbedded brain, the brains were sliced into 150 µm coronal slices with a vibratome until slices from the striatal complex containing the CPu and NAc were obtained. The slices were viewed under a microscope (Olympus SZX7) and photomicrographs of the track of the microdialysis probe in the striatum were taken.

2.8 Brain tissue content analysis of dopamine and its metabolites following toluene exposure

Following acute or repeated toluene inhalation, mice were sacrificed by cervical dislocation after which their brains were rapidly removed and placed on a petri dish covered with a paper towel soaked with ice cold aCSF (composition in mM: 147 NaCl, 3.5 KCl, 2 Na_2HPO_4, 1.0 $CaCl_2$, 1.2 $MgCl_2$, and pH 7.4). The mouse brains were dissected and tissues were quickly taken from the brain regions of interest (the CPu and NAc). The dissected regions of interest were placed in labeled tubes, which were immediately frozen in liquid nitrogen and stored at -80 °C. On the day of analysis samples were weighed and then prepared for homogenization by adding 200 µL (NAc samples) or 250 µL (CPu samples) 0.1 M $HClO_4$ to each sample. The samples were

then homogenized using a Misonix Microson^{TM} ultrasonic cell disruptor (continuous, 12 - 15 one second per pulse at 50% duty, 3 - 4 microtip setting; Misonix Incorporated, Farmingdale, NY). The homogenates were centrifuge at 12,000 rpm for 10 minutes in a refrigerated tabletop centrifuge (Eppendorf centrifuge 5424, Eppendorf AG, Hamburg, Germany) and aliquots of the supernatant were analyzed for DA and its metabolites; 3,4-dihydroxyphenylacetic acid (DOPAC), homovanillic acid (HVA), and 3-methoxytyramine (3-MT) using HPLC with an electrochemical detector. The HPLC and electrochemical settings for tissue content were the same as was previously reported in the microdialysis section (*see Section 2.6.3*). The results were analyzed by integration of peak areas against calibration curves obtained from standards of DA and its metabolites and expressed as nM concentration. The remaining supernatant of the samples were used for protein analysis, which involves colorimetric detection and quantification of total protein from the tissue sample. Bovine serum albumin (BSA) standards (20 µL) or the tissue content samples were diluted with 30 µL distilled water and then 1 mL bicinchoninic acid (BCA) working reagent (50:1, BCA Reagent A: BCA Reagent B) was added to each sample. The content of each tube was mixed well and incubated in a 37 °C for 30 minutes in an Isotemp 205 Water Bath (Fisher Scientific, Pittsburgh, PA). After incubation, the tubes were cooled to room temperature and 200 µL of their contents were pipetted into 96-well microplate and analyzed on a VersaMax ELISA Microplate Reader (Molecular Devices, Sunnyvale, CA) using SoftMax Pro software to obtained µg of protein in tissue. Tissue content DA and its metabolites were expressed as ng per mg protein.

2.9 Statistical data analysis

All behavioral (locomotor) data were analyzed with SPSS statistical software where data for acute toluene exposures was analyzed using a 3 x 10 repeated measures analysis of variance (ANOVA) with toluene treatment (0, 2000, and 4000 ppm) as the between subjects factor, and the 3-minute time blocks as the within-subjects factors. Locomotor data from the repeated toluene experiment were analyzed using a 3 x 7 x 10 repeated measures ANOVA with toluene treatment (0, 2000, and 4000 ppm) as the between subjects factor with days and 3-minute time blocks as the within-subjects factors. Significant main effects and interactions were determined using Tukey's post hoc contrasts and simple main effects analyses. Statistical analyses of all data from neurochemical measurements (slice SFCV, *in vivo* microdialysis, and tissue content analysis) were performed using GraphPad Prism Software (GraphPad Software Inc., San Diego, CA) and statistical significance determine by Student's t-test, one-way, or two-way ANOVA followed by appropriate post-hoc tests. All data were expressed as mean ± standard errors of the means (SEM) where differences were considered to be statistically significant when $P < 0.05$.

CHAPTER 3

Striatal Dopamine Dynamics in Mice Following Acute and Repeated Toluene Exposure

Adapted from:
Apawu, A. K., Mathews, T. A., Bowen, S. E., "Striatal Dopamine Dynamics in Mice Following Acute and Repeated Toluene Exposure", *in revision for Psychopharmacology.*

3.1 Introduction

Toluene is inhaled by individuals to achieve intoxication.[41, 43, 142] The repeated deep inhalation of solvents like toluene can result in effects similar to alcohol intoxication with diminished mental and physical capabilities.[41] While research on inhalants lags behind other drugs of abuse, the last decade has resulted in a significant increase in knowledge about inhalants' pharmacological properties and their effects.[37, 41, 51, 142] Preclinical models of acute inhalant exposure have shown an extensive range of neurobehavioral effects that are concentration-dependent, reversible, and occur at concentration levels which are much lower than those necessary to produce explicit toxicological signs.[37, 43, 56] A growing number of preclinical studies demonstrate that toluene influences a variety of neurotransmitter systems including, dopamine (DA), gamma-aminobutyric acid (GABA), and glutamate (see review[37]). Toluene, like other drugs of abuse, has been shown to elevate extracellular DA levels in the prefrontal cortex [71] and in the nucleus accumbens (NAc),[36, 143] which is consistent with toluene's reported rewarding effects. However, the neurochemical adaptions within the striatum following toluene exposure are not completely understood. Specifically, it is unclear

whether increases in extracellular DA levels are due to alterations in DA release and/or uptake mechanisms following toluene exposure.

The present experiments were designed to explore the neuro-adaptations of striatal DA release and uptake mechanisms using slice fast scan cyclic voltammetry (FSCV) following acute and repeated toluene inhalation. Toluene concentrations of 2000 and 4000 ppm were chosen because they are behaviorally stimulating.[74, 155-157] A major advantage of using FSCV to probe presynaptic DA dynamics is its high temporal resolution, which is on the order of milliseconds, and it provides the ability to differentiate DA release and uptake parameters.

3.2 Hypothesis

Based on acute toluene exposure as measured by microdialysis,[36, 71, 143] we hypothesized that, following acute toluene exposure, we would observe a dose-dependent increase DA release, while decreasing DA uptake in the striatum. Although there are no neurochemical measurements evaluating striatal DA after repeated toluene exposure, we hypothesized that following repeated toluene exposure (i.e., withdrawal), we would observe an opposite effect (as observed with other abused compounds[158, 159]) with a decrease in both DA release and uptake in the striatum.

3.3 Materials and Methods

The materials and methods used are as described in chapter 2, with, specific details provided here. Toluene vapor exposure and locomotor activity measurements were conducted using the procedure in sections 2.3 and 2.4, respectively. Briefly, after being weighed, mice were placed into an exposure chamber, given 5 minutes to acclimate, and then exposed to toluene or air vapors for 30 minutes during which time

locomotor activity was recorded. Chambers were opened to diffuse toluene vapors and locomotor activity was recorded for an additional 30 minutes recovery period. For each concentration of toluene (0, 2000, or 4000 ppm), the amount of toluene injected was calculated using the ideal gas equation, simplified for room temperature.[151] Mice were used in either an acute (single day) or repeated (7 days) toluene or air (control) exposure. Prior to slice FSCV measurements, brain slices were obtained approximately 45 minutes after acute toluene or 24 hours after repeated toluene exposure. Electrically stimulated DA release was evoked every 5 minutes using a single electrical pulse and the response was measured with a carbon fiber microelectrode. After stable release recordings (> 30 minutes), toluene was dissolved in increasing concentrations (0.01 – 10 mM) into oxygenated artificial cerebrospinal fluid (aCSF) and each concentration was perfused over the slice for 30 minutes during which DA release and uptake were measured. The peak oxidation current for DA was converted into concentration based on a post-calibration factor calculated by calibrating the microelectrode with 3 μM DA.

3.3.1 Data Analysis

Locomotor activity was analyzed with SPSS software. Acute toluene data were analyzed using a 3 x 10 repeated measures analysis of variance (ANOVA) with toluene treatment (0, 2000, and 4000 ppm) as the between-subjects factor, and the 3-minute time blocks as the within-subjects factors. Repeated toluene data were analyzed using a 3 x 7 x 10 repeated measures ANOVA with toluene treatment (0, 2000, and 4000 ppm) as the between-subjects factor, with days and the 3-minute time blocks as the within-subjects factors. An alpha level of $P < 0.05$ determined statistical significance. Tukey's *post hoc* contrasts and simple main effects analyses were used to determine

the significant main effects and interactions. Statistical analysis of voltammetry data was performed using GraphPad Prism Software. The criteria for statistical significance for DA release and uptake parameters were set to $P < 0.05$. Statistical significance was determined by one-way ANOVA with Dunnett's Multiple Comparison Test. All data are reported as mean ± standard errors of the means (SEM).

3.4 Results

3.4.1 Distance traveled during and following acute toluene exposure

As seen in Figures 3.1A and B, a significant main effect was observed for acute toluene exposure ($F_{2,53} = 12.25$, $P < 0.001$), time ($F_{9,477} = 2.01$, $P < 0.05$), as well as a significant time x toluene interaction ($F_{18,477} = 2.14$, $P < 0.01$). *Post hoc* analysis revealed that acute exposure to 2000 and 4000 ppm toluene significantly increased locomotor activity of mice across the 30 min exposure period as compared to the air-only controls ($P < 0.01$) with no significant differences between the 2000 and 4000 ppm concentrations.

Recovery from acute toluene exposure also resulted in concentration-dependent effects in locomotor activity (Figures 3.1A and C). Significant main effects were observed for toluene treatment ($F_{2,53} = 17.95$, $P < 0.001$), time ($F_{9,477} = 53.76$, $P < 0.001$), as well as a significant time x toluene interaction ($F_{18,477} = 8.20$, $P < 0.01$). *Post hoc* analysis revealed that previous exposure to both concentrations of toluene significantly increased locomotor activity of mice as compared to the air-only controls ($P < 0.01$), with activity decreasing significantly over 30 min to levels comparable to air-controls.

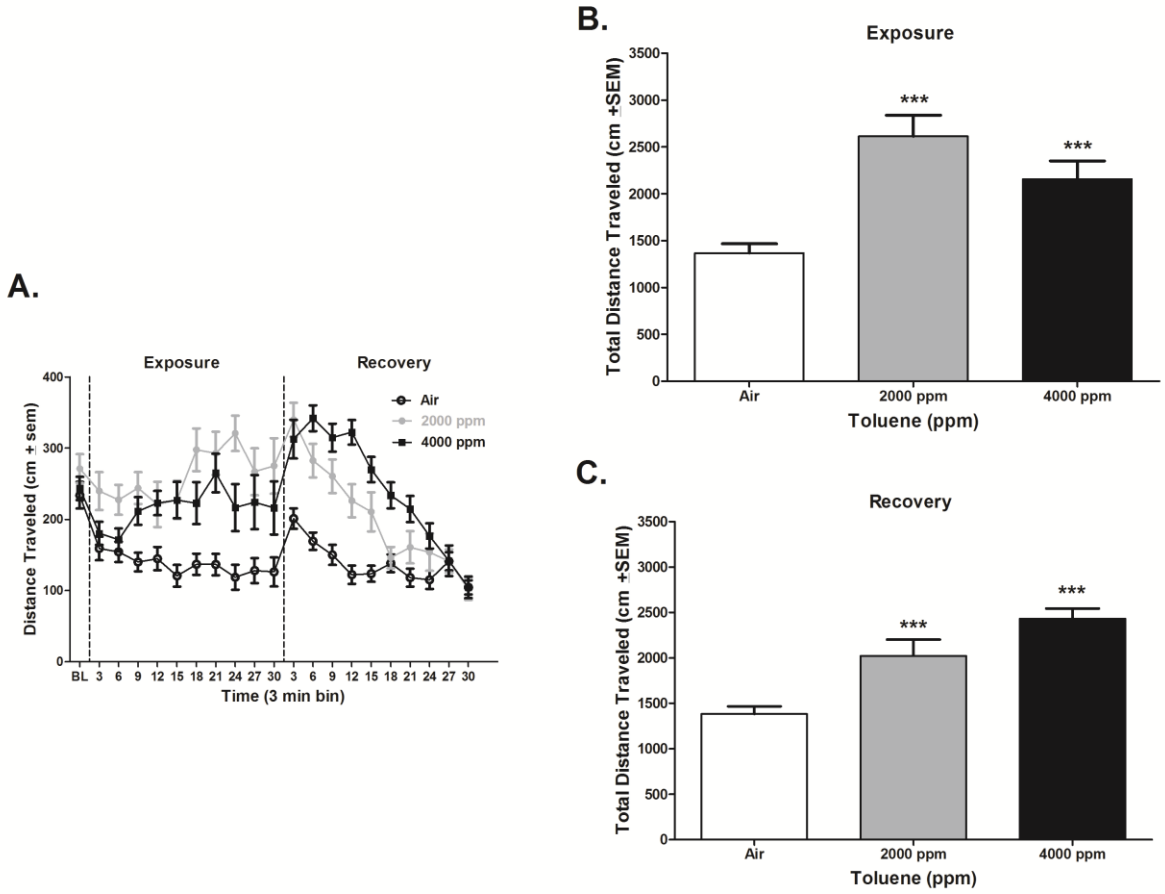

Figure 3.1: Locomotor activity during and after acute toluene exposure. A) A plot of distance traveled (cm ± SEM) versus time (3 minute bins) with three defined partitions, from left to right: 5 minute acclimation, 30 minute toluene exposure, and 30 minutes recovery period. **B)** Effect of acute toluene exposure on total distance traveled. **C)** Total distance traveled during recovery from acute toluene exposure. Statistical significance was determined using one-way ANOVA with Dunnett's Multiple Comparison Test. ****P* < 0.001 (air-control, n = 15; 2000 ppm, n = 15; 4000 ppm, n = 15).

3.4.2 Striatal dopamine release and uptake following acute toluene exposure

Striatal DA release and uptake (in caudate putamen (CPu), NAc core and shell) were compared between air-controls (Figure 3.2) and mice receiving acute toluene exposure (0, 2000, or 4000 ppm) followed by a 30-minute withdrawal period. Voltammetry data from control (air) mice had the highest stimulated DA release and DA uptake rates in the CPu, followed by the NAc core, then NAc shell, consistent with previously reported regional differences in DA release/uptake dynamics in the striatum[160-164]. One-way ANOVA with Dunnett's post test revealed that 45 minutes after acute exposure to 4000 ppm toluene produced significant elevation in electrically evoked DA release (Figure 3.2C) across the sub-anatomical brain regions in the striatum (CPu: $F_{2,134} = 3.80$; $P < 0.05$, NAc core: $F_{2,93} = 5.22$; $P < 0.01$, and NAc shell $F_{2,60} = 5.37$; $P < 0.05$) compared to control mice. Acute toluene (2000 and 4000 ppm) exposure had no effect on DA uptake rates across the striatal regions (Figure 2D, CPu: $F_{2,134} = 2.51$; $P > 0.05$; core: $F_{2,93} = 1.36$; $P > 0.05$, shell $F_{2,60} = 2.06$, $P > 0.05$).

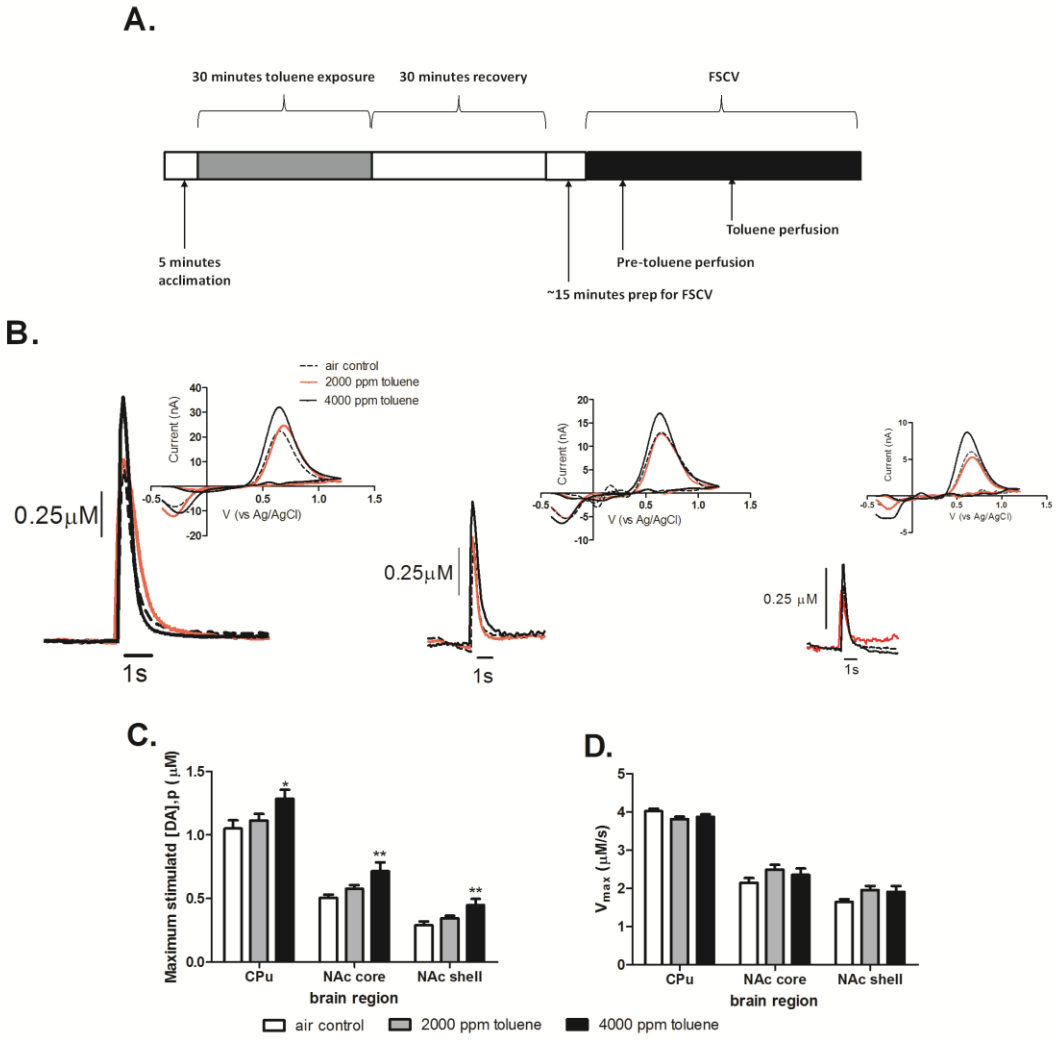

Figure 3.2: Acute toluene exposure increases electrically stimulated DA release with no effect on DA uptake. A) Toluene exposure and neurochemical protocol. Forty-five minutes after acute toluene exposure the brains were harvested and DA release and uptake dynamics were assessed in the striatum. B) Representative cyclic voltammograms (inset) and concentration versus time traces. **C)** Stimulated DA release after a single 30-minute exposure to 0, 2000, or 4000 ppm of toluene. **D)** DA uptake rates across sub-anatomical brain regions of the striatum. Data are expressed as means ± SEMs (n = 6-12/brain region). Statistical significance was determined by one-way ANOVA with Dunnett's Multiple Comparison Test; where *$P < 0.05$, **$P < 0.01$.

To determine if direct application of toluene on a brain slice influences DA release and uptake dynamics, cumulative concentrations (0.01, 0.03, 0.1, 0.3, 10 mM) of toluene were perfused over brain slices from either air-control or 4000 ppm toluene exposed animals. Electrically evoked DA release was measured every 5 minutes for 30 minutes for each dose of toluene. Both control and 4000 ppm toluene mice showed a decrease in electrically evoked DA when toluene was directly applied to the slice. However, acute toluene exposure (4000 ppm) shifted the dose response curve to the right compared to the control mice (Figure 3.3). The half maximal inhibitory concentration (IC_{50}) was significantly reduced (for toluene-exposed mice (IC_{50} not reported because plot is not sigmoidal) compared to control mice (174 ± 2 μM; Student's t-test, P = 0.01, n = 4-5/ treatment group), suggesting toluene exposed mice are less sensitive to the effects of toluene perfusion. Additionally, the decay side of the concentration versus time curve was evaluated, which showed that DA uptake was significantly reduced at concentrations equal to and greater than 0.03 and 0.10 mM in air- and toluene-treated mice, respectfully (Figure 3.4).

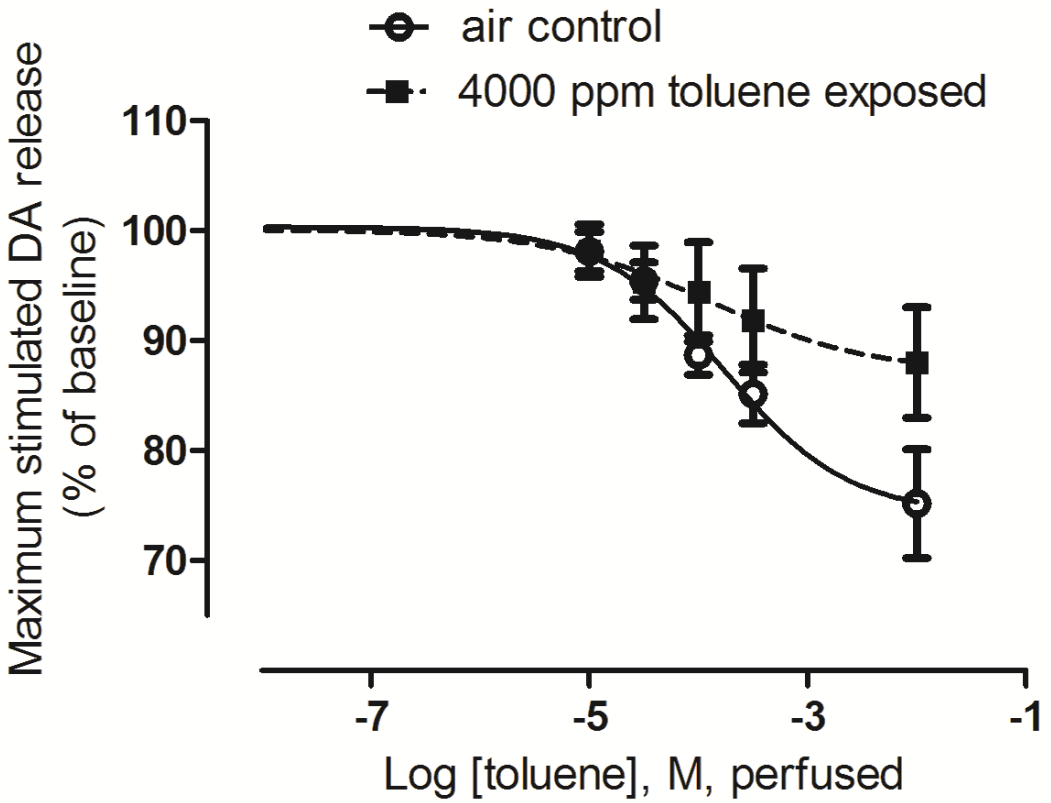

Figure 3.3: Right shift in toluene dose response curve after previous exposure to toluene. Electrically evoked DA release was assessed during perfusion of cumulative concentrations of toluene over the CPu. The shift in the dose-response curve to the right suggests that toluene exposed mice are less sensitive to direct application of toluene compared to air-controls. *P* = 0.01, n = 4-5/treatment group, Student's t-test.

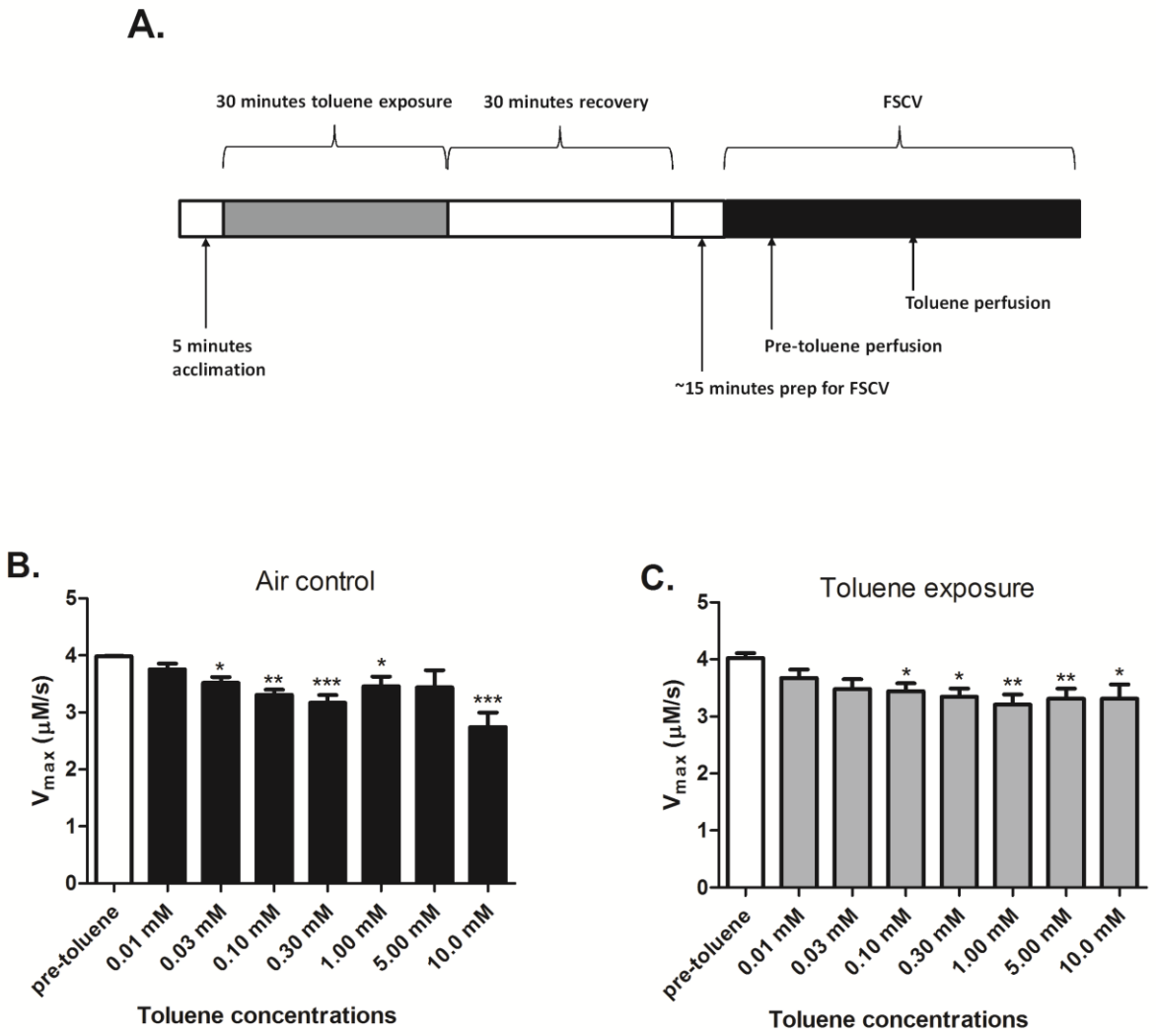

Figure 3.4: DA uptake during perfusion of cumulative concentrations of toluene over the CPu. A) Toluene exposure and neurochemical protocol. **B)** Effect of toluene perfusion on DA uptake was measured from air-control mice and **C)** from mice acutely exposed to 4000 ppm of toluene. Data are expressed as means ± SEMs (n = 4-5/treatment group). Statistical significance was determined by one-way ANOVA with Dunnett's Multiple Comparison Test; where ***P < 0.001, **P < 0.01, *P < 0.05, compared to air-control.

3.4.3 Distance traveled during and following repeated toluene exposure

As seen in the exposure panels of Figure 3.5, repeated toluene treatment had a significant main effect ($F_{2,43}$ = 3.37, P < 0.05). There was also a main effect for Day ($F_{6,258}$ = 7.69, P < 0.001), and a significant Day x Toluene treatment interaction ($F_{12,258}$ = 3.72, P < 0.001). Significant main effects were also observed for Time block ($F_{9,387}$ = 1.89, P = 0.05), and for the Time block x Toluene treatment interaction ($F_{18,387}$ = 1.61, P = 0.05). As shown in Figure 3.5E and F, repeated toluene treatment produced increases in locomotor activity across the exposure session and across days of exposure with 4000 ppm of toluene producing the greatest increases in activity (P < 0.05).

As seen in the recovery panels of Figure 3.5, recovery from repeated toluene treatment produced a concentration-dependent effect in locomotor activity with patterns of locomotor activity changing when toluene was cleared from the chamber. There was no main effect for Toluene treatment or for Day (P > 0.05). There was a significant Day x Toluene treatment interaction ($F_{12,258}$ = 2.82, P < 0.01). In general, activity decreased across exposure days with locomotor activity after the 4000 ppm toluene exposure producing the greatest decrease. A significant main effect was observed for Time block ($F_{9,387}$ = 45.27, P < 0.001) and for the Time block x Toluene treatment interaction ($F_{18,378}$ = 5.28, P < 0.001). During the recovery period, locomotor distance traveled decreased as the session progressed with toluene animals being more active initially and less active finally than their air-controls.

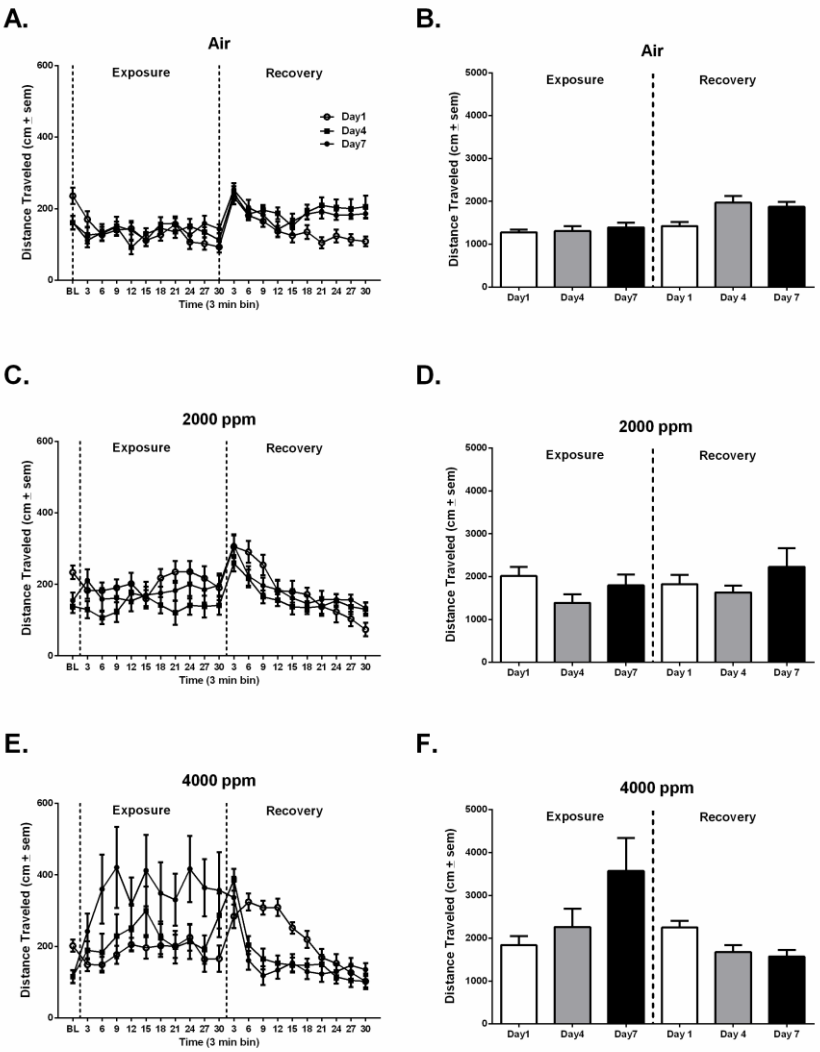

Figure 3.5: Locomotor activity during and after repeated toluene exposure. The effects of 0 (air-control), 2000, or 4000 ppm inhaled toluene on mouse locomotor activity**.** The left-most partition of each graph represents a 5 minute acclimation period, the middle partition represents 30 minute toluene exposure, with the right partition representing 30 minute post toluene exposure. The distance traveled by mice was measured during and after toluene exposure and analyzed using repeated measures ANOVA with toluene treatment (2000 or 4000 ppm) as the between subjects factor, and the 3 minute time blocks as the within-subjects factors. **A)** A plot of distance traveled (cm ± SEM) versus time (3 minute bin) for air-control. **B)** A plot of distance traveled (cm ± SEM) versus days of toluene exposure (days 1, 4, and 7 selected for simplicity). **C)** Distance traveled (cm ± SEM) versus time (3 minute bin) for 2000 ppm toluene treatment with corresponding **D)** distance versus day plot. **E)** A plot of distance traveled (cm ± SEM) versus time (3 minute bin) and **F)** distance-day plot for repeated 4000 ppm toluene treatment. Statistical significant main effects and interactions were determined by Tukey's post hoc contrasts and simple main effects analyses (air-control, n = 14; 2000 ppm, n = 16; 4000 ppm, n = 16).

3.4.4 Striatal dopamine dynamics after repeated toluene exposure

Electrically evoked DA release was measured in the three discrete sub-regions of the striatum 24 hours after 7 days of either 2000 or 4000 ppm of toluene exposure. Repeated toluene exposure following withdrawal had no effect on stimulated DA release ($F_{2,85}$ = 0.388, P > 0.05; Figure 3.6C) or DA uptake in the CPu in either 2000 or 4000 ppm toluene exposure when compared to control mice ($F_{2,85}$ = 0.265, P > 0.05; Figure 3.6D).

After repeated toluene exposure and a 24 hour withdrawal period, there was a significant decrease in electrically evoked DA release in the NAc core ($F_{2,67}$ = 15.4, P < 0.001, Figure 3.6C) and shell ($F_{2,54}$ = 13.9, P < 0.001, Figure 3.6C) compared to their air-controls. After seven days of repeated toluene exposure, electrically-stimulated DA release from the NAc core had an approximately 25% reduction in DA release in 2000 and 4000 ppm toluene exposed mice, (2000 ppm: 0.6 ± 0.03 μM; n = 9, 4000 ppm: 0.6 ± 0.04 μM; n = 6) compared to air-controls (0.8 ± 0.05 μM; n = 6, Figure 3.6C). In a similar manner, repeatedly exposed toluene-treated mice had an approximately 25 and 50% decrease in evoked DA release in the NAc shell of 2000 and 4000 ppm toluene exposed mice respectively (2000 ppm: 0.3 ± 0.02 μM; n = 7, 4000 ppm: 0.2 ± 0.03 μM; n = 4) compared to air-controls (0.4 ± 0.02 μM; n = 8, Figure 3.6C). An inherent advantage of using FSCV is its ability to resolve DA release and DA uptake. DA uptake rates from the NAc core and shell were not different after repeated toluene exposure following withdrawal compared to their air-controls (Core: $F_{2,67}$ = 0.932, P > 0.05, Shell: $F_{2,54}$ = 0.182, P >0.05, Figure 3.6D).

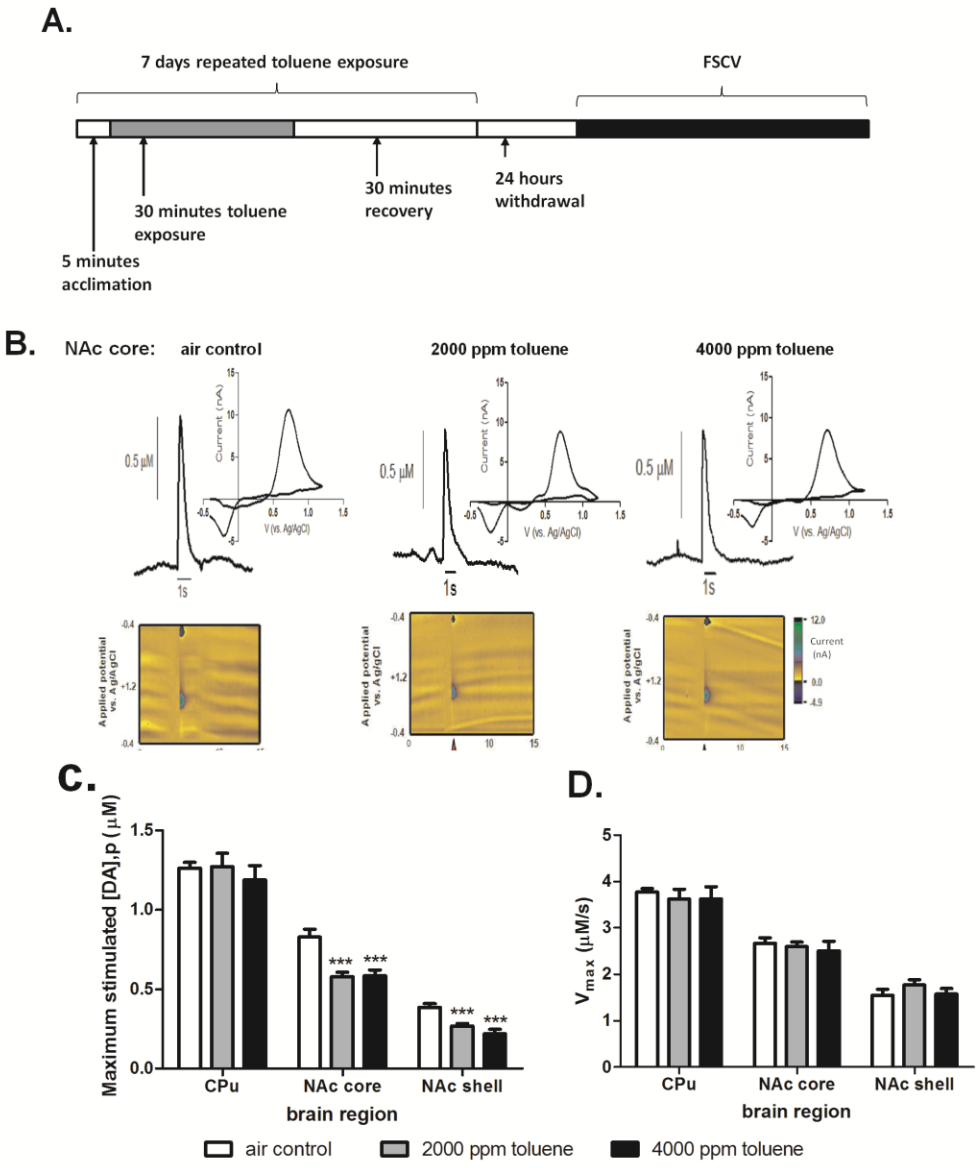

Figure 3.6: Repeated exposure to toluene attenuates electrically stimulated DA release but not uptake in the nucleus accumbens (NAc). A) Toluene exposure and neurochemical protocol. **B)** Representative cyclic voltammograms (inset) and concentration versus time traces for the measurements in the NAc core. Below the concentration versus time traces are corresponding color plots, where the x-axis represents time in seconds, the y-axis is the applied potential of the triangular waveform, and the current is shown in color. The triangle below the color plots indicates the point of electrical stimulation. **C)** Maximum electrically-evoked DA release from air-control, 2000, and 4000 ppm repeated toluene exposed mice across sub-anatomical brain regions in the striatum. **D)** DA uptake rates after repeated toluene treatment. Data are expressed as means ± SEMs (n = 4 -10/treatment group). Statistical significance was determined by one-way ANOVA with Dunnett's Multiple Comparison Test; where ***P < 0.001 compared to air-control.

3.5 Discussion

The present study was undertaken to evaequate the components of the striatal DA system following acute and repeated toluene exposure (2000 or 4000 ppm) by using slice FSCV, a technique with millisecond temporal resolution allowing for differentiation of DA release and uptake parameters. Previous studies have shown that acute and repeated toluene administrations alter locomotor activity as well as striatal DA dynamics.[36, 56, 68, 143] However, the neurochemical reports to date have focused mainly on how toluene influences striatal dopaminergic changes using microdialysis, which does not provide the temporal resolution to tease apart contributions from release and uptake. In the present study, slice voltammetry revealed that stimulated striatal DA release was potentiated after an acute exposure to 4000 ppm of toluene with no effect on striatal DA uptake. A single exposure to toluene resulted in a decreased sensitivity to increasing concentrations of toluene perfusion compared to their air-control. To better understand how the striatal complex adapts to the neurobiological changes of repeated toluene exposure, a 7-day toluene protocol followed by a 24 hour withdrawal period was evaluated. Unlike acute toluene exposure, repeated toluene exposure attenuated DA release in the NAc at all doses with no difference in DA uptake rates, while there were no differences in either DA release or uptake in the CPu. Together, these findings point to the ability of toluene to differentially regulate pre-synaptic DA release depending on the exposure and withdrawal length with no effect on DA uptake across the striatum.

Behaviorally, acute 30 min toluene exposure to either 2000 or 4000 ppm increased locomotor behavior above what was observed for air-control animals and these increases in activity were observed for approximately 30 min post exposure.

These results are similar to the increases in locomotor activity reported for acutely inhaled toluene and extend earlier work demonstrating dose-dependent increases in locomotor activity at concentrations between 500 to 5000 ppm with the largest increases occurring in the range of 2000 to 5000 ppm.[68, 156, 165, 166]

Neurochemically, this FSCV study provides important insight on how toluene influences DA release in acute and repeated toluene exposure models, while demonstrating toluene inhalation following withdrawal does not alter DA uptake in the striatum. After a single 4000 ppm toluene exposure there was significant potentiation in electrically-stimulated DA release across the sub-regions of the striatal complex, while there was no difference in DA uptake rates. Previous microdialysis studies suggested that the rise in extracellular DA levels was a reduction of DA uptake attributed to toluene.[143] A limitation of using microdialysis to interpret release and uptake parameters is that it does not have the temporal resolution to separate these components, but slice voltammetry does. Although our coronal slices contain only the striatal terminals and lacks input from the midbrain regions such as the ventral tegmental area and substantia nigra, toluene exposure prior to FSCV demonstrated significant potentiation in DA release even with a 30 min recovery period. Taken together, the FSCV results demonstrate the sensitivity of slice FSCV to measure these subtle but persistent DA changes after toluene inhalation followed by a 30 min recovery period. Finally, our slice voltammetric data suggests that acute toluene inhalation has no direct effect on DA uptake across the striatum.

Together, these results suggests that acute exposure to 4000 ppm toluene alters the DA release mechanism in the CPu, which was further supported by results acquired

after direct application of toluene over the slice. Unlike acute toluene exposed mice, air-treated mice had a significant decrease in electrically evoked DA when toluene was directly applied indicating that toluene itself has the ability to influence DA release. Despite these large concentrations (> 0.01 mM) of toluene, slice FSCV results suggest that toluene is interacting directly at the DA terminal; however, its target is unknown. The toluene dose-response curve is not like DA receptor agonist dose response curves[110, 167, 168], as it does not asymptotically approach zero at the highest concentrations of toluene perfusion. Instead the toluene dose response curves for both air- and toluene-treated animals asymptotically approaches 70% and 90%, respectively (an ~ 30% and ~ 10% reduction in stimulated DA release) suggesting that toluene may be acting upon non-dopaminergic receptors such as N-methyl-D-aspartate (NMDA) receptors, metabotropic glutamate receptor, or the nicotinic receptor, mediating this response (for review see Bowen *et al*. 2006 [37]). To determine which of these receptors may be responsible for the decrease in DA release, future experiments should evaluate antagonists of these receptors to determine if they can block the effects of direct application of toluene. Interestingly, when acute concentrations of toluene were directly applied to the slice, FSCV detected a decrease in DA uptake rates in air- and toluene treated mice (Figure 3.4). The main objective when applying toluene directly to brain slices was to evaluate DA release dynamics, even so we discovered that considerably high toluene concentrations had to be used to induce subtle but significant changes in the DA dose response curve. Thus, there appears to be a divergent effect on DA transport kinetics depending on the route of administration of toluene. For example, toluene inhalation followed by a 30 minute recovery phase does not influence DA

uptake rates, while direct application of toluene causes a significant decrease in DA uptake in both air- and toluene treated animals. Future studies, should further evaluate these route difference in administering toluene; in particular, evaluation of DA uptake immediately after toluene inhalation versus direct application. Overall, the acute toluene FSCV results demonstrate that either pretreatment with toluene inhalation or direct application of toluene leads to alterations in DA release, while only direct application of millimolar concentrations of toluene decreases DA uptake in the CPu.

As compared to acute exposures, repeated administrations of toluene (4000 ppm) over 7 days resulted in increased locomotor activity across days of exposure with marked decreases in electrically-stimulated DA release observed in the NAc core and shell 24 hrs after the last toluene exposure. The increases in locomotor activity with repeated exposure to 4000 ppm toluene in the present study are similar to previous reports for inhaled toluene and other abused solvents[64, 74, 157, 169, 170] and can be interpreted as sensitization to toluene. Previous studies have also reported development of sensitization after toluene was repeatedly administered intraperitoneally[38, 84, 171] or orally.[72] Conversely, examination of the recovery data (see Fig. 3.5E, right side) shows that animals returned to baseline levels more quickly as the days of repeated exposure continued, suggesting the development of tolerance to toluene's stimulating behavioral effects. These observed effects of toluene are similar to other investigations that have reported the emergence of tolerance after repeated exposure to several abused inhalants.[169, 172]

Using slice FSCV to evaluate 7-day toluene exposure followed by 1-day of withdrawal, our repeated toluene results showed no difference in DA uptake rates

throughout the striatal complex as observed for the acute toluene inhalation. Therefore, toluene's mechanism of action after a withdrawal period does not appear to be like other drugs of abuse (e.g., cocaine, methylphenidate, or amphetamines) that inhibit or reverse the direction of the DA transporter to elevate extracellular DA levels in the striatum. Instead, both the acute and repeated toluene inhalation following withdrawal resulted in altering stimulated DA release dynamics in the striatal terminal most likely through a heteroreceptor.

Repeated 2000 and 4000 ppm toluene exposure followed by 1-day of withdrawal induced a significant reduction in evoked-DA release in both the NAc core and shell, suggesting repeated exposure to toluene may be brain region specific since presynaptic DA release in the CPu remained unchanged after 7 days of repeated toluene exposure. This is the *first* FSCV study to evaluate DA dynamics after repeated toluene exposure following 1-day of withdrawal. Slice FSCV results demonstrated that repeated toluene exposure lead to specific dopaminergic changes in the NAc. The fact that this attenuation in stimulated DA release was not observed immediately after acute toluene exposure suggests that repeated exposure induces significant neurobiological changes (i.e., sensitization) in the NAc.

There are numerous reports on the acute effects of toluene on striatal dopaminergic dynamics, but relatively little neurochemical evidence of repeated exposure after a sub-chronic or chronic toluene protocol and even fewer following a withdrawal period. Few studies have evaluated the dopaminergic tone after repeated toluene exposure, and those that have used various doses and exposures of toluene. Long-term toluene (80 ppm and higher) exposure leads to an increase in DA D2 agonist

affinity in the CPu, but DA D2 expression is not different.[173] A tissue content study demonstrated that DA catabolism was decreased in the putamen of rats after sub-chronic toluene (40 ppm) exposure, which was attributed to a decreased DA degradation rate as the DA/DOPAC was elevated. Further, repeated toluene exposures in rats potentiated the extracellular DA response in the NAc to cocaine.[75] However, baseline DA levels in the NAc were not different between the repeated saline and toluene treated animals.[75] Our slice FSCV results would suggest that a decrease in stimulated DA release could possibly reflect lower amounts of DA in the terminal, which could lead to decreased extracellular DA levels in the striatum. However, since DA uptake is not altered it is possible that the change in DA release is not sufficient to influence extracellular DA levels. Although extracellular DA levels were not different in the microdialysis study by Beyer et al., this could be a result of the different experimental procedures: 1) toluene levels of 8000 ppm versus 2000 or 4000 ppm, 2) an intermittent repeated exposure (5 days with 2 days off followed by 5 days) versus 7 continuous days of repeated toluene exposure followed by 1 day of withdrawal, 3) species differences (rats versus mice), and/or 4) quantitative microdialysis was not used to evaluate basal DA levels. The attenuation in electrically-stimulated DA release in the NAc after repeated toluene exposure could be a result of a compensatory down regulation of the DA system; although further studies are required to verify this hypothesis. In order to have a more comprehensive understanding of striatal and accumbal effects of toluene, other neurotransmitter systems like GABA or glutamate should also be evaluated. Taking the acute and repeated toluene exposure followed by a withdrawal period together, our observations highlight the biphasic DA release

response to toluene exposure depending on whether it was acutely or repeatedly administered. These changes in striatal DA release are not a result of toluene interacting with the DA transporter, since our FSCV results showed no difference in DA uptake either after acute or repeated toluene exposure.

3.6 Conclusions

In summary, the present studies extend earlier work showing that acute and repeated exposure to toluene potentiates locomotor activity. Acutely, toluene exposure elevated stimulated DA release across the striatum, while repeated toluene inhalation followed by 1 day of withdrawal attenuated DA release in the NAc regions only. Whether toluene exposure is acute or repeated, DA uptake rates were not different across the striatum, suggesting that toluene has no effect on DA transporter kinetics. Furthermore, the toluene dose-response curve emphasizes that direct application of toluene to the slice augments both terminal DA release and DA uptake, albeit through what receptor sub-type toluene is influencing DA release is currently unknown.

CHAPTER 4

An In-depth Examination of Acute Toluene Exposure on Striatal Dopamine System

4.1 Introduction

The impact of toluene inhalation on the dopamine (DA) system has been of great interest due to the central role DA plays in addiction and reward seeking behaviors.[174-177] Since increases in dopaminergic neurotransmission, particularly at the mesolimbic terminal such as the nucleus accumbens (NAc) has been associated with the locomotor stimulatory effect of drugs of abuse,[141, 171] a number of studies have utilized behavioral assays together with neurochemical and/or physiological techniques to understand toluene's action in the DA terminal regions.[36, 71, 83, 171, 178] While the current behavioral and neurochemical/physiological data available suggest that toluene can alter DA neurotransmission, the neural mechanisms underlying toluene's action on the DA system are still not well understood.[36, 38, 83, 143, 166, 179] In our initial characterization of the behavior and neurochemical effect of toluene inhalation (Chapter 3), we showed that acute exposure to 2000 and 4000 ppm toluene increased locomotor activity of mice while, neurochemically, 4000 ppm toluene inhalation potentiated electrically stimulated DA release across the caudate putamen (CPu) and the NAc (Figure 3.2). These observations have led to numerous questions that need to be addressed in order to better understand how toluene interacts with the DA system.

One such question is "How does acute toluene exposure exert immediate effect on the DA dynamics, considering that neurochemical measurements were made after 30 minutes of withdrawal from the toluene treatment?" Because it was shown that the

behavioral effect of toluene significantly dropped to levels comparable to that of their air-control counterparts by the end of the 30 minutes of withdrawal (Figure 3.1A), it is possible that important details of toluene's immediate action on DA dynamics could be missed when fast scan cyclic voltammetry (FSCV) measurements were made afterwards. Thus, in the present chapter, FSCV measurements of DA release and uptake were taken following 30 minute of toluene treatment in order to examine the immediate action of toluene on the DA system.

Furthermore, our previous data (Chapter 3) begs the question of whether the alterations in DA release across the striatum were caused by inhibition of the presynaptic DA autoreceptors. Presynaptic DA autoreceptors consist of D2 and D3 receptor subtypes which are differentially expressed across the brain with the islands of Calleja having the highest density of the D3 receptors.[180] Across the striatal region of the brain, D3 receptors have higher density in the ventral striatum (NAc) than in the dorsal striatum (CPu).[181] Within the ventral striatum, D3 receptors are expressed more in the NAc shell than the core.[182-185] Meanwhile, the D2 receptors are expressed homogenously across the striatum.[184, 186] There are numerous reports in the literature that have implicated D2/D3 autoreceptors in the action of addictive drugs. For example, in both human and animal research, long term cocaine or nicotine use can increase D3 receptor density in the striatum and substantia nigra.[184, 187-190] Moreover, DA D2 receptor-deficient mice have demonstrated enhanced sensitivity to the rewarding effects of cocaine, while sub-chronic exposure to low (≥ 80 ppm) concentrations of toluene increases the affinity of D2 receptor agonist and DA receptor density.[191-193] Presynaptic autoreceptors play an integral role in regulating extracellular DA levels through

feedback inhibition, where activation of the receptors at the nerve terminal by locally released DA leads to inhibition of DA synthesis and further DA release.[182, 194-197] In the initial characterization of toluene's effect on DA dynamics, we observed impaired stimulated DA release in the NAc core and shell following repeated toluene exposure (Figure 3.6), which has led to the hypothesis that one potential target of abused toluene could be the presynaptic DA autoreceptors. It is possible that the observed decrease in DA release in the NAc core and shell could be a result of downward regulation of DA release mediated by DA autoreceptors in response to repeated toluene exposure. Since the attenuation in DA release was exclusive to the NAc, we expect that D3 autoreceptors, which are prominently expressed in the NAc, could be playing a major role in toluene's action. The implication of our hypothesis is that impairment of presynaptic DA autoreceptors may potentiate DA neuron excitability and DA release,[193] which could account for the increase in DA release across the striatum following acute exposure to 4000 ppm toluene (Figure 3.2C).

In the present work, slice FSCV and pharmacological testing with a potent DA D3 autoreceptor agonist, (±)-7-hydroxy-2-dipropylaminotetralin hydrobromide (7-OH-DPAT), was used to examine the functionality of presynaptic DA D3 autoreceptors in toluene exposed and air-control mice. The functionality of presynaptic D3 autoreceptors has been widely studied using 7-OH-DPAT.[181, 198, 199] An important advantage of using slice FSCV in this work is that it allowed us to selectively probe presynaptic autoreceptors without any contributions from the postsynaptic terminal. [200]

Another critical question this chapter seeks to address is, "Do the changes in DA release induced by acute toluene exposure lead to alterations in extracellular DA

levels"? To answer this question, we built a toluene exposure chamber that allowed dialysis samples and activity data to be collected simultaneously from a free-moving mouse during exposure to either toluene or air. This set-up allowed for evaluation of DA levels before toluene inhalation began, during and after exposure to see the direct effect of toluene on extracellular DA levels in the mouse striatal brain region.

Lastly, because preliminary data showed changes in DA release, another question that this chapter will address is whether these alterations are a result of alterations in DA synthesis and catabolism, which can be measured by evaluating DA tissue content. Herein, DA levels and its metabolites 3,4-dihydroxyphenylacetic acid (DOPAC), homovanillic acid (HVA), and 3-methoxytyramine (3-MT) were measured using tissue content analysis, which exclusively examined intracellular concentrations of neurotransmitters and their metabolites.

4.2 Materials and Methods

4.2.1 Toluene exposure and locomotor activity measurement

Acute toluene treatments before voltammetry and tissue content analysis used the same set-up described in Section 2.3 but without a recovery phase. Mice were exposed to 0 (air-control), 2000, or 4000 ppm of toluene vapor for 30 minutes, during which their locomotor activities were measured using infrared (IR) emitter-detector arrays attached to the chamber.

4.2.2 Slice fast scan cyclic voltammetry

Immediately after 30 minutes of toluene/air exposure, mice were sacrificed, and their brains were removed (< 10 minutes) and prepared for slice FSCV measurements using the procedure discussed in Section 2.5. To determine if the DA D3 autoreceptor

was influenced by toluene, cumulative doses (0.001, 0.01, 0.03, 0.1, 0.3, 1, and 10 μM) of DA D3 autoreceptor agonist, 7-OH-DPAT were perfused over brain slice following a stable DA signal. The effect on DA release and uptake was measured every 5 minutes for 30 minutes per dose of 7-OH-DPAT. DA was measured as current versus time traces that were converted into concentration using a post-calibration factor of microelectrode. The concentrations versus time plots were analyzed for DA kinetics (DA release and uptake) using non-linear fits based on Michaelis-Menten sets of equations.[106, 110, 152-154]

4.2.3 Brain tissue content analysis of dopamine and its metabolites

Following 30 minutes of toluene/air exposure, mice were sacrificed by cervical dislocation and their brains were quickly removed, dissected into discrete regions of interest, and prepared for tissue content using the same procedure outlined in section 2.8.

4.2.4 Simultaneous *in vivo* microdialysis and locomotor activity measurement

The procedure for simultaneous *in vivo* microdialysis and locomotor activity measurement was first described in section 2.6. A graphical depiction of the time-line for making the measurements in this acute toluene study is given in Figure 4.1.

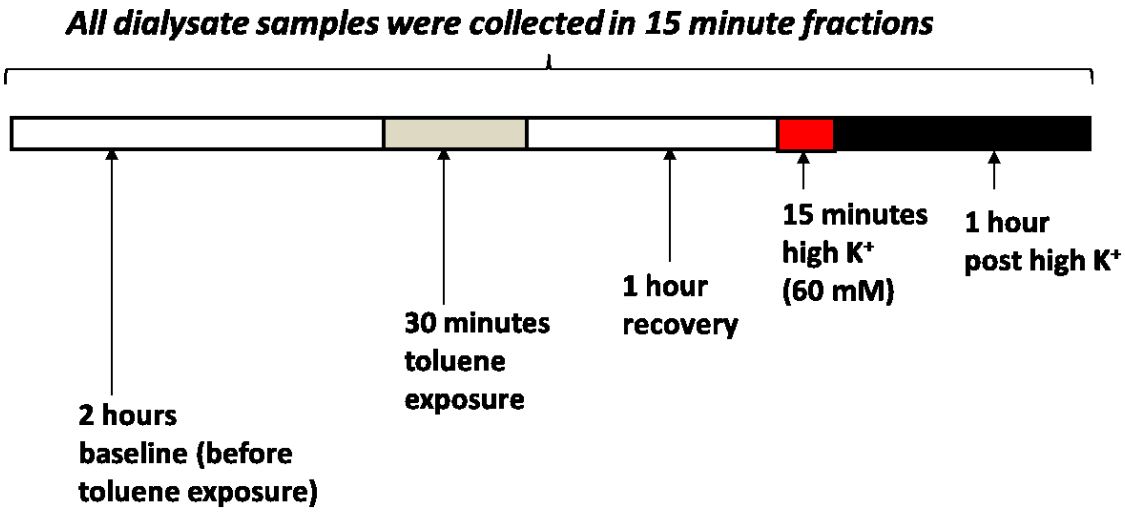

Figure 4.1: Graphical representation of the time-line for behavior and microdialysis data collection. The experiment was partitioned into the following sections: 2 hours of baseline, 30 minutes of toluene exposure, 1 hour recovery, 15 minutes of stimulated DA release with 60 mM high K^+ artificial cerebrospinal fluid (aCSF), and 1 hour post high K^+ aCSF. High K^+ concentration aCSF consist of (mM): 60 KCl, 89 NaCl, 2.0 Na_2HPO_4, 1.0 $CaCl_2$; 1.2 $MgCl_2$; pH 7.4). Dialysate samples were collected every 15 minutes throughout the experiment. Locomotor activity was monitored the entire time.

4.2.5 Data analysis

Statistical analyses of data from locomotor activity measurements and *in vivo* microdialysis were performed with repeated measures analysis of variance (ANOVA) using SPSS software and statistical significance was determined using Tukey's *post hoc* contrasts, simple main effects analyses, and Student t-test. Statistical analyses of FSCV and tissue content data were performed with one-way ANOVA followed by Dunnett's Multiple Comparison Test, and Student t-test using GraphPad Prism Software. Data were expressed as mean ± standard error of the mean (SEM) and statistical significance determined as $P < 0.05$.

4.3 Results

4.3.1 Distance traveled during acute toluene exposure

Locomotor activity before and during toluene exposure was measured and expressed as distance traveled in three minutes bins (Figure 4.2A), which is partitioned into two main panels. The first panel represents the distance traveled by mice during 5 minutes of acclimation (baseline) and the second panel shows distance traveled during 30 minutes of toluene exposure. Statistical analysis of this data was done using 3 x 10 repeated ANOVA with toluene treatment (0, 2000, and 4000 ppm) as the between subjects factor, and the 3-minute time blocks as the within-subjects factors. The result obtained showed a significant main effect of Time ($F_{5,140} = 5.82$, $P < 0.05$, n = 5-8/group) but not Time x Toluene interaction, even though the effect seems trending ($F_{10,140} = 1.75$, $P = 0.052$, n = 5-8/group). This result suggests that the locomotor activity of mice changes with time but is not dependent on toluene treatment. There was no effect of toluene dose ($F_{2,28} = 0.76$, $P = 0.48$, n = 5-8/group). The locomotor activity was also

condensed to the total distance traveled throughout the 30 minutes of toluene/air exposure (Figure 4.2B). One-way ANOVA analysis of the toluene treatment groups showed no effects of toluene treatment on locomotor activity ($F_{2,14}$ = 1.439, P = 0.26, n = 5-8/group). This lack of effect of acute toluene exposure on locomotor activity is not consistent with what we previously demonstrated in our initial behavior characterization (Figure 3.1) but we believe the disparity may be due to low statistical power in the present data.

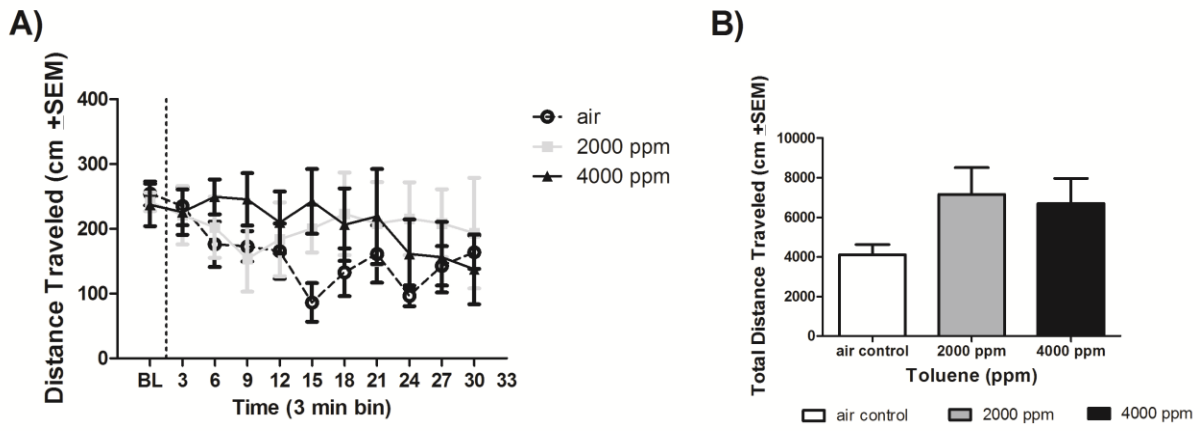

Figure 4.2: Effect of acute toluene exposure on locomotor activity of mice. A) Locomotor activity expressed as distance traveled versus time in 3 minutes bins. Before the dashed line is the activity during 5 minutes of acclimation and after the dashed line demonstrates activity during 30 minutes of toluene/air exposure. There was a significant main effect of time (P < 0.05) but no effect of toluene dose (P > 0.05) **B)** Total distance traveled versus toluene dose. Data as mean ± SEM, n = 5-8/group.

4.3.2 Dopamine release and uptake following acute toluene exposure

Slice FSCV was used to characterize the effect of acute toluene exposure on presynaptic DA dynamics in three sub-anatomical regions in the striatum of mouse the brain: the CPu, NAc core and shell. Mice were exposed to 30 minutes of air, 2000 or 4000 ppm toluene vapor and immediately afterwards (in less than 10 minutes) were sacrificed and their brains prepared for FSCV measurement. The measured electrically evoked DA release was expressed as maximum stimulated DA release per a single electrical pulse (μM) and DA uptake as maximum velocity of the DA transporter (V_{max} in μM/s). The DA measurements from the striatum of air-control mice showed the highest DA release and uptake in the CPu, followed by the NAc core and then the NAc shell. Statistical analysis of the data obtained using one way ANOVA showed a significant main effect of toluene treatment on DA release in all three sub-anatomical brain regions (CPu: $F_{2,48} = 6.27$; $P = 0.004$,; NAc core: $F_{2,42} = 8.36$, $P < 0.001$; NAc shell: $F_{2,39} = 10.36$, $P < 0.001$; Figure 4.3). Dunnett's Multiple Comparison Test between treatments revealed that, following acute exposure to 2000 ppm of toluene, DA release in both the CPu (1.70 ± 0.13 μM, n = 5) and the NAc core (0.66 ± 0.06 μM, n = 5) were not altered compared to their air-controls (CPu: 1.77 ± 0.14 μM, n = 6; NAc core: 0.49 ± 0.06 μM, n = 5, Figure 4.2). However, acute exposure to 2000 ppm toluene vapor did increase DA release in the shell (2000 ppm toluene: 0.53 ± 0.05 μM, n = 5; air-control: 0.26 ± 0.04 μM, n = 4; $P < 0.05$). Consistent with earlier observations (Figure 3.2), acute exposure to 4000 ppm toluene increased electrically evoked DA release in the three brain regions (CPu: 2.23 ± 0.10 μM, n = 7; NAc core: 0.95 ± 0.04 μM, n = 5 and NAc shell: 0.63 ± 0.07 μM, n = 5) as shown by current-time traces and background subtracted cyclic

voltammograms (Figure 4.3B). Similarly, DA uptake rates in the CPu and the core were not altered following toluene treatment compared to their air-controls (CPu: $F_{2,51} = 0.70$, $P = 0.50$; NAc core: $F_{2,42} = 0.78$, $P = 0.46$; one-way ANOVA, Figure 4.3E). Interestingly, only 2000 ppm toluene exposure elevated DA uptake in the NAc shell (2000 ppm: 2.22 ± 0.15 μM/s, n = 5; air-control: 1.31 ± 0.14 μM/s, n = 4; $P < 0.001$, Dunnett's Multiple Comparison Test).

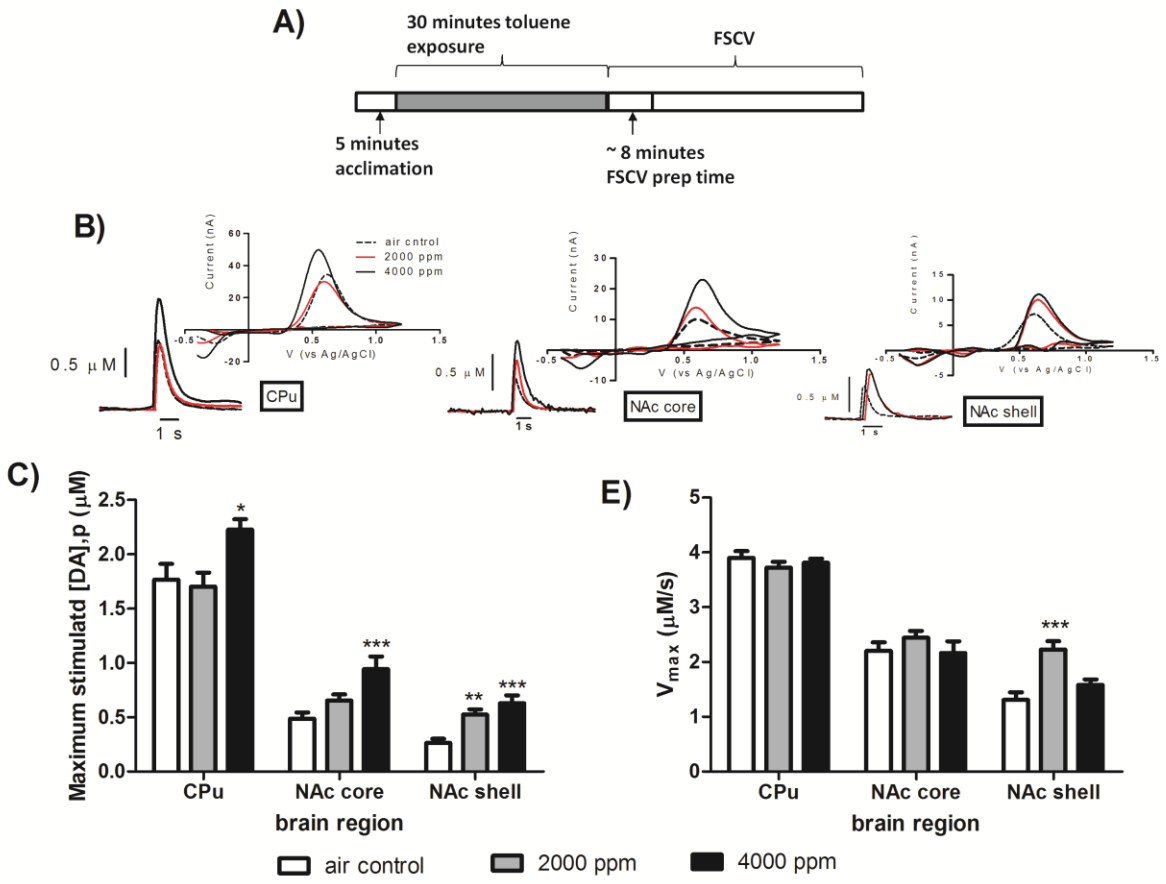

Figure 4.3: Effect of acute toluene exposure on DA release and uptake. A) Acute toluene exposure and FSCV experimental timeline which includes 5 minutes acclimation time, 30 minutes toluene exposure and ~ 8 minutes preparation before FSCV measurements. **B)** Effect of acute toluene exposure on electrically evoked DA release across the three striatal brain regions. **C)** DA uptake rates across the three striatal sub-regions following toluene exposure. Data expressed as mean ± SEM. Statistical significance was determined by one-way ANOVA with Dunnett's Multiple Comparison Test performed for each brain region (**P* < 0.05, ***P* < 0.01, ****P* < 0.001, n = 4 – 7/group).

4.3.3 Effect of acute toluene exposure on presynaptic D3 autoreceptors

Dose response curves showing the effect of 7-OH-DPAT on DA release were generated from mice exposed to 4000 ppm toluene and their air-control counterparts. The toluene dose (4000 ppm) was chosen because of its profound effect on DA release across all three sub-anatomical brain regions in the striatum (Figure 4.3). Dose response curves obtained in the CPu with 7-OH-DPAT following stable DA signal did not differ between air- and toluene-treated mice as shown by the overlap of the two curves. The IC_{50} value is defined as the concentration at which the maximum DA response was decreased by 50%. There was no difference between toluene treated mice and their air-controls when comparing IC_{50} values (air: IC_{50} = 70 ± 1 nM, toluene treated: IC_{50} = 32 ± 1 nM, P =1.00, n = 4-5/group, Student t-test, Figure 4.4A). The effect of cumulative doses of the DA D3 agonist was also evaluated on DA uptake kinetics between the two treatment groups. One-way ANOVA showed a significant effect of 7-OH-DPAT on DA uptake in both groups of mice (air-control: $F_{7,112}$ = 12.4, P < 0.0001, Figure 4.4B and toluene exposed: $F_{7,112}$ = 12.4, P < 0.0001, Figure 4.4C). Further statistical analysis of the DA uptake data with Dunnett's Multiple Comparison Tests revealed that perfusion of 0.1 μM 7-OH-DPAT attenuated DA uptake in only air-control mice.

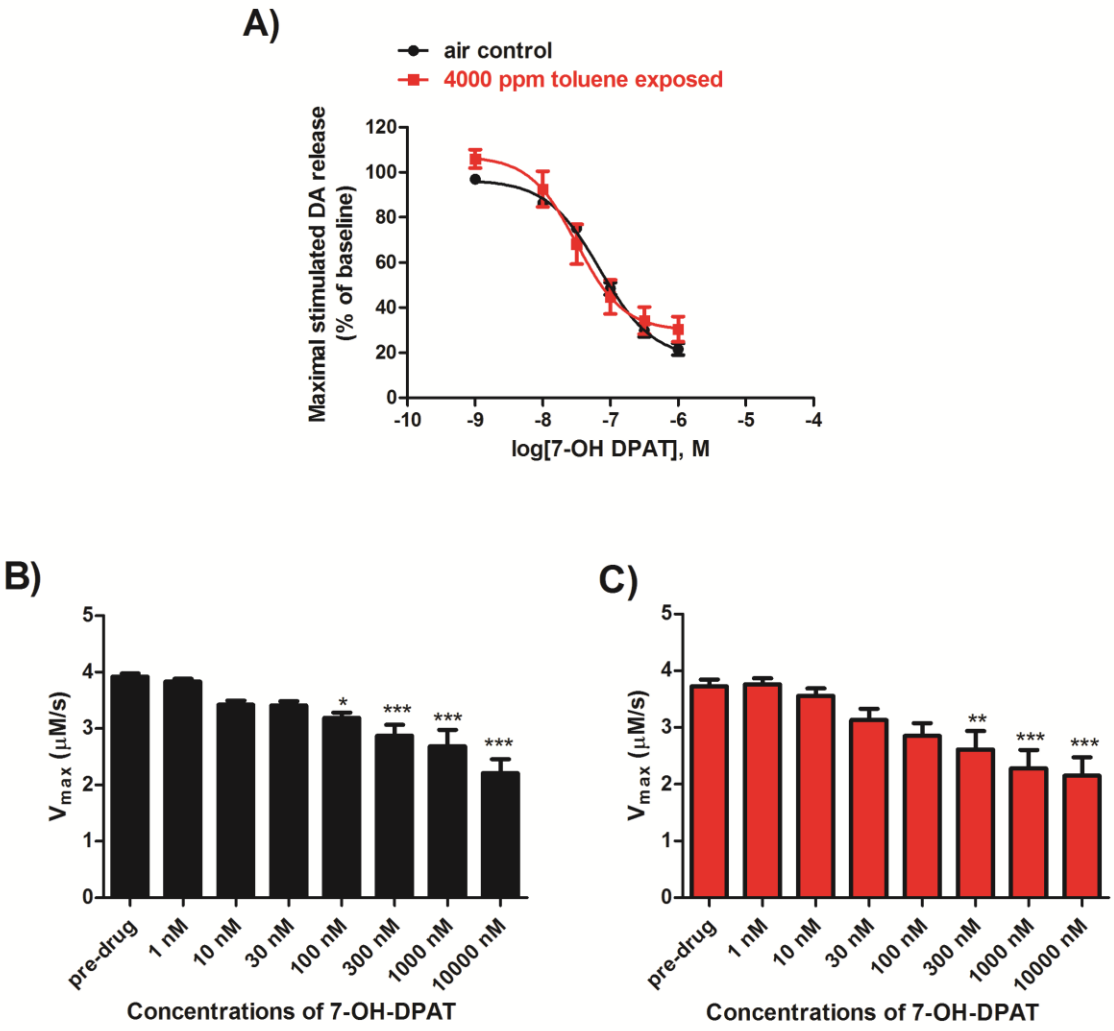

Figure 4.4: Effect of D3 agonist, 7-OH-DPAT on presynaptic DA release and uptake in the CPu of toluene exposed and air-control mice. **A)** Dose response curve showing the effect of cumulative doses (0.001 -10 µM) of 7-OH DPAT on DA release in toluene treated mice (IC_{50} = 32 ± 1 nM) and their air-controls (IC_{50} = 70 ± 1 nM). Statistical analysis was done with Student's t-test. **B)** The effect of 7-OH-DPAT on DA uptake in air-control mice, and **C)** in toluene exposed mice expressed as V_{max} (µM/s). Data was plotted as mean ± SEM. Statistical analysis performed with one-way ANOVA with Dunnett's Multiple Comparison Test. *P > 0.05, ***P > 0.001, n = 4-5/group).

4.3.4 Monitoring the effect of acute toluene exposure on locomotor behavior and extracellular dopamine levels in the CPu

The main advantage of monitoring locomotor behavior simultaneously with dialysate sample collection is that it will enable us to better understand how the behavior effects of toluene relate to alterations in the extracellular DA levels. In this experiment, the average distance traveled by mice during 5 main phases of microdialysis experiments were examined. These phases were 2 hours of baseline, 30 minutes toluene/air exposure, 1 hour recovery, 15 minutes high K^+ aCSF infusion, and 1 hour post-high K^+ aCSF infusion. To be able to compare the locomotor activities of each phase to the other and also be consistent with dialysis collection time, the data obtained have been expressed as average distance traveled per minute over the time course of 15 minutes. Statistical analysis of the results (Figure 4.5) using repeated measures analysis showed significant within-subject effect of time ($F_{3,25}$ = 6.96, P = 0.002) and a significant Time x Toluene interaction ($F_{3,25}$= 3.18, P = 0.04) from pre-toluene/air to recovery. These observations demonstrate that the locomotor activity of the mice was altered during the experiment and that the alteration was dependent on toluene treatment. Further statistical analysis using Student t-test revealed a significant increase in locomotor behavior during the second half (T2) of the exposure to 4000 ppm toluene (11.4 ± 3.4 cm/min) relative to their air-controls (1.42 ± 1.42 cm/min, P < 0.05, n = 5). Meanwhile, no significant differences in locomotor behavior were found between toluene and air-control mice during recovery phase through to post-high K^+ phase (Figure 4.5).

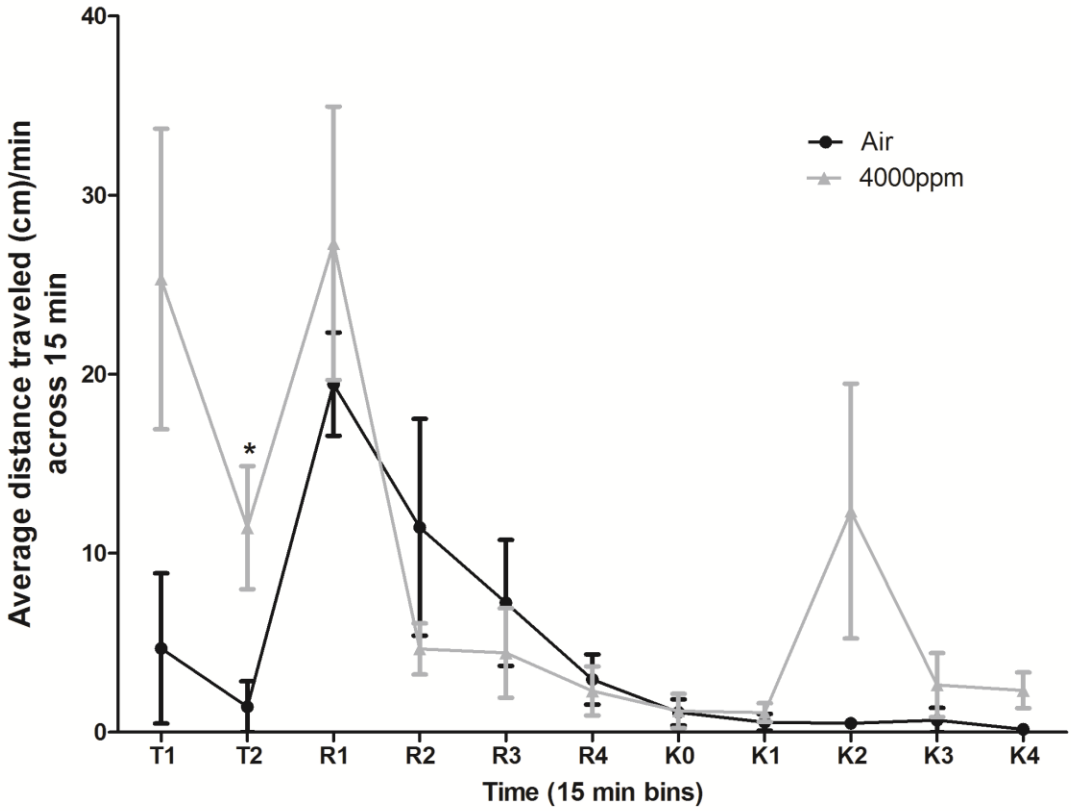

Figure 4.5: Effect of acute toluene exposure on locomotor behavior during dialysate sample collection. Locomotor activity was expressed in 15 minutes bins.T1-T2 represent the 30 minutes of toluene/air exposure; R1-R4 constitute the 1 hour recovery phase; K0 is 15 minutes of hight K^+ aCSF infusion; and K1-K4 denote post high K^+ aCSF perfusion. Data compares locomotor activity of 4000 ppm toluene exposed mice to their air-controls. Statistical analysis was performed with repeated measures ANOVA with toluene as the between subjects factor, and 15-minute time blocks as the within-subject factor. T1 and T2 in toluene and air-control mice were compared respectively using a Student t-test (*$P < 0.05$, n = 5-6).

The microdialysis set-up allowed sampling and further detection of extracellular DA levels using HPLC coupled to an electrochemical detector. Dialysis samples were collected every 15 minutes across the five experimental phases to examine the extracellular DA levels before, during, and after acute toluene exposure. The effect of acute toluene exposure on chemically stimulated DA release was measured using high K^+ concentration aCSF infusion method. The presence of high K^+ stimulates neurotransmitter release leading to increased extracellular levels of neurotransmitters like DA which can be measured by microdialysis. The extracellular DA levels collected during the 5 phases of the experiment are expressed as percentage of the baseline DA concentration in toluene exposed and air-control mice, respectively. These percentages were plotted against time in 15 minute bins. There was no effect from 4000 ppm toluene exposure on extracellular DA levels during or after toluene exposure. On the contrary, statistical analysis using a Student t-test (two tailed) showed that infusion of high K^+ aCSF caused a significant increase in extracellular DA level in mice that were exposed to toluene compared to their air-control counterpart ($t = 2.43$, $P < 0.05$, $df = 9$, Figure 4.6). This alteration in chemically stimulated DA release is congruent with what was observed using electrical stimulation in slice FSCV.

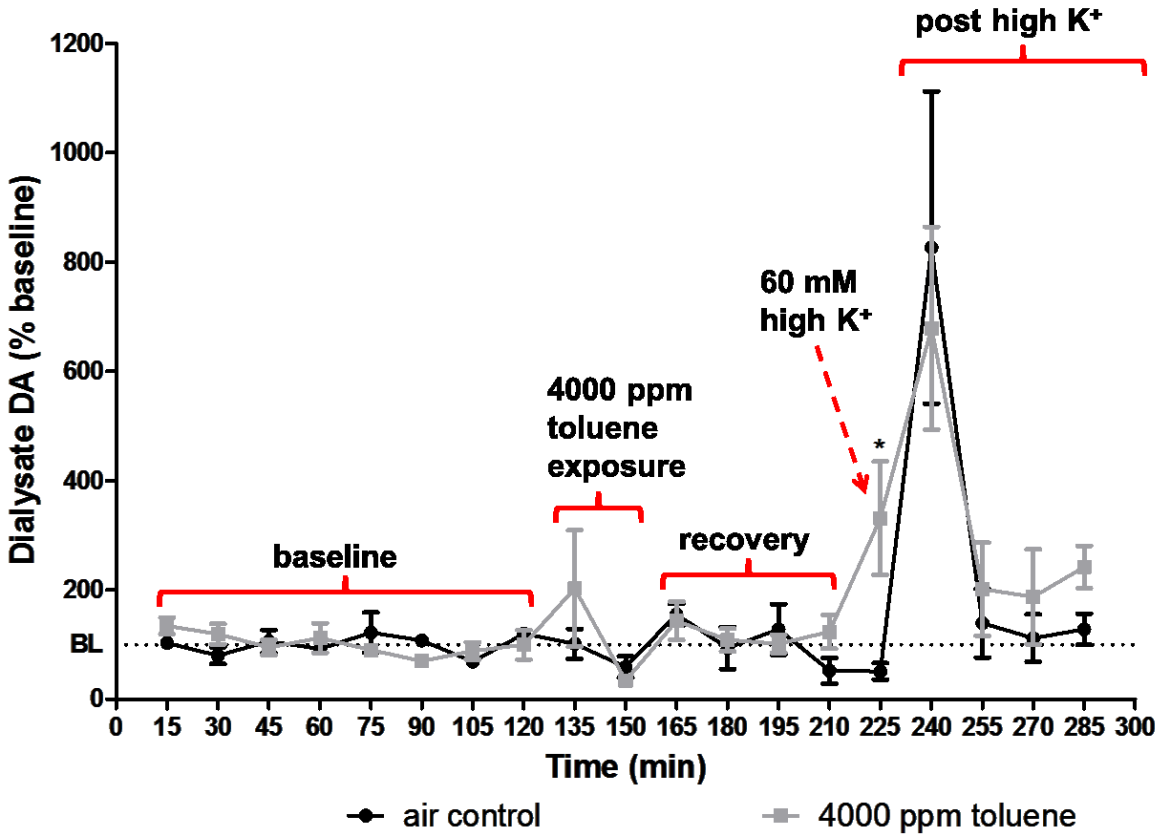

Figure 4.6: Effect of acute toluene exposure on extracellular DA levels. Dialysis sample collection was made every 15 minutes before (baseline), during (toluene/air), and after toluene inhalation. There was no effect of toluene exposure on extracellular DA levels in the CPu. However, prior toluene exposure to 4000 ppm alters high K^+-stimulated DA release (dashed red arrows). *P < 0.05, n = 5-6 (paired Student t-test).

4.3.5 Effect of acute toluene exposure on extracellular DA and catabolism

To determine if intracellular DA and it catabolism are direct targets of toluene's neural action in the CPu and NAc, tissue content of DA and its metabolites (DOPAC, HVA, and 3-MT) were measured in brain tissues obtained from mice acutely exposed to 4000 ppm toluene and their air-controls. Representative retention times for these analytes were 6.5, 8.3, 15.0 and 18.0 minutes for DOPAC, DA, HVA, and 3-MT, respectively (Figure 4.7). The tissue concentration of DA and its metabolites were analyzed against their respective standards and expressed as ng per µg of brain tissue protein. The DA tissue content and its metabolites measured from air-control mice were compared to that of the toluene exposed mice (Figure 4.8B and C). In the CPu, statistical comparison using a Student t-test showed no significant difference in DA tissue levels between the two groups of mice (air-control: 877 ± 105 ng/mg protein; toluene exposed mice: 1086 ± 72 ng/mg protein; t = 1.64, $P > 0.05$, df = 22). However, in the CPu, there was a significant reduction of DOPAC in toluene exposed mice compared to the air-control mice (air-control: 371 ± 44 ng/mg protein, toluene: 221 ± 17, t = 3.20, $P < 0.01$, df = 22, two tailed Student t-test). Meanwhile, the metabolites HVA and 3-MT levels in the CPu were not different between the air and toluene-exposed mice ($P > 0.05$). Similarly, there was a significant reduction in only DOPAC, but not DA, HVA or 3-MT, levels in the NAc following acute toluene exposure (DOPAC; air-control: 481 ± 76 ng/mg protein, toluene: 234 ± 30 ng/mg protein, t = 3.03, $P < 0.05$, df = 10, two tailed Student t-test). The interaction between DA and DOPAC was evaluated. The ratio of DA/DOPAC was significantly higher in the CPu of toluene exposed mice compared to the air-control littermates (air-control: 2.3 ± 0.2, toluene exposed: 5.1 ± 0.4, t = 6.78, $P <$

0.0001, df = 22, two tailed Student t-test) and in the NAc (air-control: 1.1 ± 0.03, toluene exposed: 2.2 ± 0.2, t = 4.55, $P < 0.01$, n = 6, two tailed Student t-test). Collectively, these observations suggest that acute toluene exposure influences DA catabolism, particularly the conversion of DA to DOPAC in the CPu and the NAc.

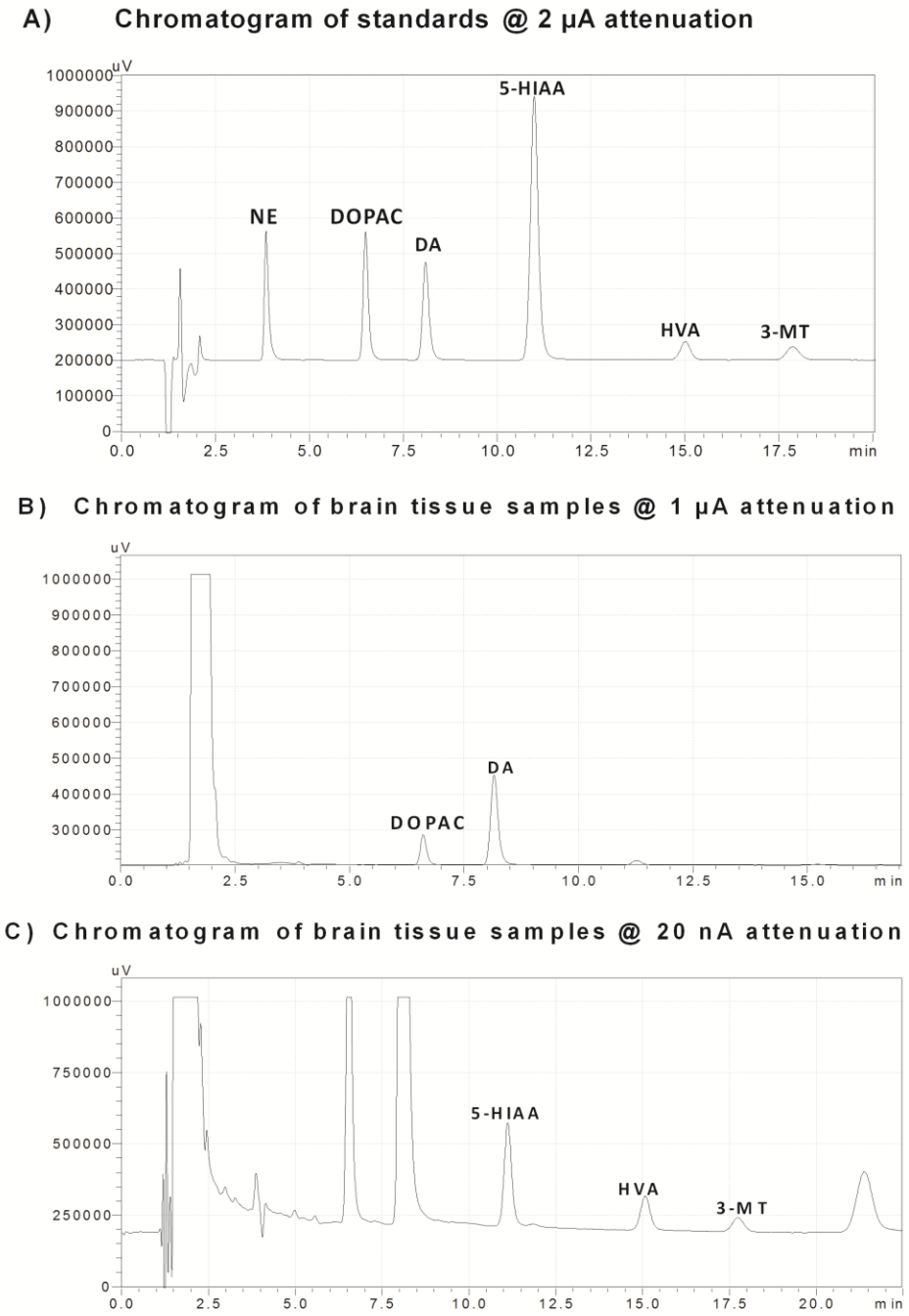

Figure 4.7: Representative chromatograms for neurotransmitters and metabolites. A) Chromatogram of standard solution containing norepinephrine (NE) , DOPAC, DA, 5-HIAA (5-hydroxyindoleacetic acid), HVA, and 3-MT run at 2 µA attenuation**. B)** Chromatogram of brain tissue sample run at 1 µA attenuation showing DA and DOPAC peaks**. C)** Chromatogram of brain tissue sample run at 20 nA attenuation showing peaks including 5-HIAA, HVA, 3-MT.

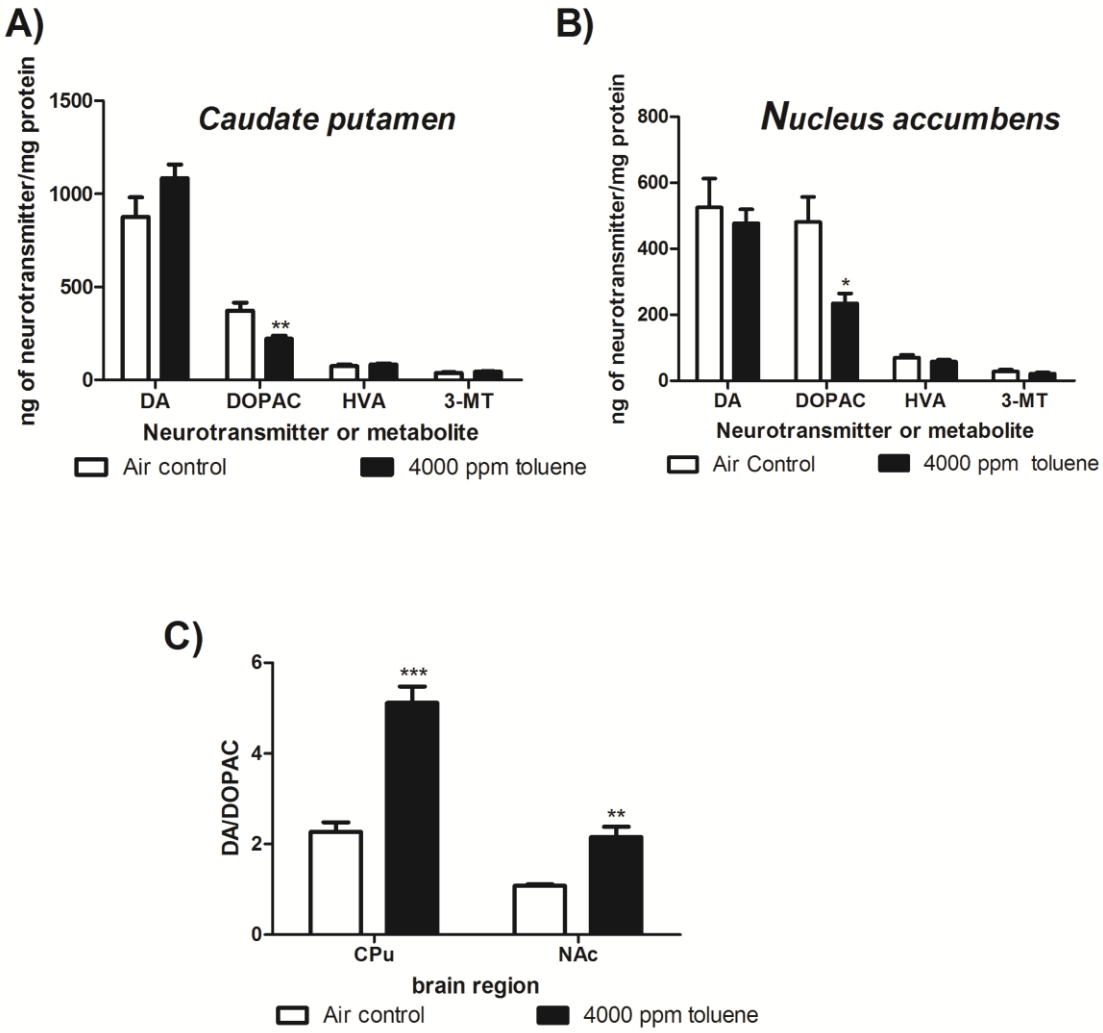

Figure 4.8: Effect of acute toluene exposure on tissue content DA and its metabolites. A-B) Average concentrations of DA, DOPAC, HVA, and 3-MT from CPu and NAc of mice previously exposed to 4000 ppm toluene vapor compared to their air-control littermates. **C)** Effect of acute toluene exposure on DA catabolism expressed as DA/DOPAC ratio for CPu and NAc. Data shown as mean ± SEM. Statistical significance determined using two tailed Student t-test (*P < 0.05, **P < 0.01, ***P < 0.001, n = 6).

4.4 Discussion

Previously, we have shown that acute toluene inhalation influences striatal DA by increasing DA release, but exerts no effect on DA uptake kinetics (Chapter 3). Our initial study suggested potential neural targets for toluene's action, which we decide to further examine in the present chapter. In the previous study, mice were allowed a 30-minute recovery period followed by another 15 minutes needed to obtain the brain slices; one of the concerns with this approach was that the 30-minute withdrawal period could be contributing to the changes observed in DA release. Therefore, the toluene treatment was modified to exclude the recovery phase so that FSCV measurements were made following toluene exposure (< 10 minutes). Consistent with previous findings (Chapter 3), the present data confirm that acute toluene inhalation potentiates DA release across the striatum of mouse brain. Since similar observations were made after the recovery phase of the toluene treatment in the earlier study (Chapter 3), collectively, our data suggest that acute toluene inhalation elevates stimulated DA release for at least 30 minutes after toluene exposure. Evidence about the persistent nature of alterations in the DA system induced by acute toluene exposure was demonstrated by Beckley *et al.* in their recent work where retrograde labeling and slice electrophysiology were used to examine the acute effect of toluene inhalation on the mesolimbic DA system.[201] They found that acute exposure of rats to 5700 ppm toluene increased excitatory synaptic strength of DA projections in the NAc with elevations persisting for up to 3 and 21 days in the NAc core and shell, respectively.[201] Our previous acute FSCV data (Chapter 3) compared with our present FSCV observation (Figure 4.3) further support the hypothesis that toluene induces long lasting alterations in the DA system.[84]

In the experiments presented in this chapter, mice exposed to 2000 ppm toluene without a recovery period, showed increase in both DA release and uptake dynamics only in the NAc shell. The sub-anatomical brain regions in the striatum differ in both their anatomy[182, 202-205] and function.[206-208] Within the NAc, the core is implicated in locomotor stimulatory effects of drugs, whereas the shell is noted for its involvement in emotions and motivation.[202, 203] From our FSCV data, inhalation of 2000 ppm toluene vapor altered both DA release and uptake in only the NAc shell, while a higher concentration (4000 ppm) potentiated DA release across all three sub-anatomical regions of the striatum but had no effect on DA uptake. Taken together, these FSCV data imply that toluene's action across the striatum may be dose and region dependent. A similar specificity was reported in the work done by Di Chiara and colleagues, where they demonstrated that intravenous injection of 1 mg/kg of cocaine increased extracellular DA levels in both the NAc core and shell, while a lower dose (0.5 mg/kg) selectively increased extracellular DA levels in the shell.[207] This kind of specificity is also consistent with the action of amphetamine and morphine on the DA system in the NAc.[207] Thus, from our FSCV results, it is likely that toluene may share similar neural sites(s) with other drugs of abuse.[82]

A common characteristic amongst drugs of abuse is that they elevate extracellular DA levels,[177] which is achieved by increasing DA neuronal firing (e.g. nicotine and opiate), inducing DA release from the DA terminal (e.g. amphetamine) or blocking DA uptake (e.g.cocaine).[31, 193] Using slice FSCV, our results demonstrate that acute inhalation of toluene increases striatal DA release; therefore, it is logical to expect the increase in DA release to lead to an increase in extracellular DA levels across the

CPu. However, our microdialysis results showed no difference in extracellular DA levels in the CPu during toluene inhalation, although locomotor activity was elevated over the same time period (Figure 4.5). These microdialysis results appear contrary to the work reported by Stengard *et al.,* where exposure to 1000 or 2000 ppm toluene vapor for two hours increased motor activity and extracellular DA levels in the striatum by 47% in rats.[143] However, when toluene was administered (800 mg/kg) intraperitoneally, motor activity was potentiated in rats, but extracellular levels of DA and its metabolites in the striatum were not altered.[209] These discrepancies in microdialysis results can be attributed to differences in the animal model being used (rat versus mouse), dose (high versus low), duration of treatment (brief versus extended), and the mode of toluene administration (injection versus inhalation). The toluene exposure model used in the present work was selected because it mimics brief and high doses of toluene that are thought to be observed by those who 'huff' in real life. Since acute toluene inhalation elicited similar effects across the CPu and the NAc, the CPu was chosen to examine the effect of acute toluene exposure on extracellular DA levels because it is a DA rich region in the striatum. By measuring locomotor activity and extracellular DA levels simultaneously, it was hoped that a correlation or a direct relationship would be observed between extracellular DA levels and locomotor behavior. Because there was no correlation between toluene induced locomotor activity and extracellular DA levels in the CPu, we believe that DA neurotransmission in the CPu may not be directly involved in locomotor stimulatory effects induced by acute toluene inhalation. Another possibility could be that toluene is directly influencing post-synaptic DA receptors or other

receptors through a mechanism that does not increase extracellular DA levels in the CPu as suggested by Kondo *et al.* [209]

To better understand if DA release mechanisms were altered after toluene inhalation, aCSF containing high K^+ concentration (60 mM) was infused directly through the microdialysis probe for 15 minutes. The presence of high K^+ causes depolarization of neurons and exocytosis, such that neurotransmitters are released into the synapse causing elevation in extracellular levels of neurotransmitters which can be measured by microdialysis. This procedure has been widely used in microdialysis experiments to probe the influence of drug treatment or gene alteration on DA release.[94, 126, 210] From our microdialysis data, the infusion of high K^+ aCSF led to a greater DA response in toluene exposed mice compared to their air-controls, confirming that acute toluene exposure elevates presynaptic DA release in the CPu, just as we observed with FSCV.

Hypothesis that has been put forth by numerous groups is that toluene induces DA release in the striatum could be mediated by presynaptic DA autoreceptors. In the present work, we asserted that this release could be mediated by presynaptic DA autoreceptors, possibly D3 mechanisms. To test this DA D3 autoreceptor hypothesis, slice FSCV was used to evaluate the DA D3 receptor in the CPu. When a cumulative dose response curve of DA D3 agonist, 7-OH-DPAT was obtained by perfusion of the agonist over the CPu, there was no difference in the IC_{50} values between the control and toluene-treated mice suggesting that there is no difference in the function or the sensitivity of the DA D3 receptors in the striatum. Thus, although slice FSCV data suggest that DA release is elevated in toluene treated mice, it does not appear to be mediated via the DA D3 receptors. This FSCV data does not rule out the possible

involvement of D2 autoreceptors in toluene's action. However, considering that acute toluene inhalation did not alter DA uptake or extracellular DA levels in the CPu, it is possible that the toluene induced elevation may not be mediated by DA autoreceptors.

Since DA release was altered in both slice FSCV and microdialysis experiments, it is possible that this alteration in DA release is due to the fact that there is more intracellular DA available for release. Examining brain tissue content, we could evaluate intracellular DA levels as well as its metabolites. Tissue content results from this study highlight that acute toluene inhalation had no effect on intracellular levels of DA, HVA, and 3-MT in both the CPu and the NAc. However, the intracellular concentration of DOPAC was decreased in both the CPu and NAc. The DA/DOPAC ratio was increased in the toluene exposed mice suggesting that the breakdown of DA into DOPAC is decreased in toluene-treated mice.

Collectively, since our data demonstrate that acute toluene inhalation alters presynaptic DA release but not DA uptake, D3 autoreceptors, extracellular DA levels, and DA synthesis in the CPu, it is most likely that some other neurotransmitter system such as glutamate or gamma-aminobutyric acid (GABA) that can influence presynaptic DA release could be mediating acute toluene's action on the DA system in the striatum.[37]

4.5 Conclusions

In summary, the present data show that acute toluene exposure increases stimulated DA release across the striatum. However, this increase in is not mediated by presynaptic DA D3 autoreceptors. Although stimulated DA release is elevated after acute toluene exposure, extracellular DA levels remain unchanged during toluene

inhalation. Despite no changes in extracellular DA levels in the CPu during toluene inhalation, locomotor activity was enhanced. Finally, intracellular DA levels were unaltered suggesting that the increase in stimulated DA release is not a result of excess DA accumulation in vesicles. The tissue content results do suggest that there are alterations in DA catabolism in both the CPu and NAc. Taken together, the results here suggest that acute toluene inhalation perturbs DA release in the CPu but most likely via an indirect mechanism since intracellular DA and uptake were unaltered after toluene inhalation.

CHAPTER 5

An In-depth Examination of the Effect of Repeated Toluene Exposure on Striatal Dopamine (DA) System

5.1 Introduction

Drug addiction is initiated by repeated drug administration, which leads to neuroadaptations in the brain reward pathway including the mesolimbic dopaminergic system.[176, 177] This suggests that understanding how long term toluene exposure affects the striatal DA system could provide clues to the underlining mechanisms of toluene abuse. Few reports exist that have shown the effect of chronic toluene exposure on the DA system.[84, 191, 211] In our initial characterization of the effect of toluene exposure on striatal DA dynamics, we showed that daily, intermittent toluene exposure for 7 days significantly altered DA release in only the nucleus accumbens (NAc), a region implicated in drug addiction[2]; but not the caudate putamen (CPu, Figure 3.6). One of the caveats of our original study was that we waited 24 hrs after the 7th toluene exposure to make neurochemical measurements; this delay was because we were trying to coordinate an appropriate time for FSCV measurements to be made. However, it was noted that neurochemical examination should be made immediately after the final exposure to better understand the effects of chronic toluene exposure. The present chapter examines the alterations that repeated toluene exposure induces immediately on the striatal DA system, particularly, the accumbal DA system, since our initial study highlighted that this region had the greatest alterations in DA dynamics. Based on our observations from Chapters 3 and 4, we hypothesized that, daily, intermittent toluene exposure for 7 days would dose-dependently decrease DA release in the NAc as a

result of compensatory response to chronic toluene inhalation. Furthermore, we expect an increase in the extracellular DA level in the NAc and a decrease in DA tissue content and it catabolism.

To determine if our hypothesis is valid, we will use slice fast scan cyclic voltammetry (FSCV) to evaluate the possible role of DA autoreceptors in the proposed compensatory response of the accumbal DA dynamics to chronic toluene exposure. We will also evaluate baseline extracellular DA levels in the NAc after daily, intermittent toluene exposure. To date there are no reports that have used this *exact protocol* to measure extracellular DA levels. We believe that our model closely mimics the brief but repeated toluene inhalation observed in toluene addiction. *In vivo* microdialysis will be used to measure extracellular DA levels, with simultaneous measurement of locomotor activity; this approach will allow us to understand how locomotor activity correlates with extracellular DA levels in the NAc. Finally, brain tissues will be analyzed to determine the effect of repeated toluene treatment on intracellular DA levels and its metabolites (3,4-dihydroxyphenylacetic acid, DOPAC; homovanillic acid, HVA; and 3-methoxytyramine, 3-MT). We expect tissue content analysis to shed light on toluene's influence on DA catabolism. Previous work by another group has shown that the region of the putamen in rats has decreased DA catabolism after sub-chronic exposure to 40 ppm toluene, an effect the authors attributed to decreased DA degradation as the DA/DOPAC ration was elevated.[212] By examining DA dynamics using slice voltammetry, *in vivo* microdialysis, and tissue content analysis, we anticipate developing a more comprehensive understanding about the impact toluene inhalation has on the striatal DA system.

5.2 Materials and Methods

5.2.1 Toluene exposure and locomotor activity measurements

Repeated toluene exposures before voltammetry and tissue content analysis were done using the same procedure described in section 2.3, where mice were allowed 5 minutes of acclimation, followed by 30 minutes of exposure to 0 (air-control), 2000, or 4000 ppm and then 30 minutes recovery. This toluene exposure procedure was performed each day for seven consecutive days. On day 7 the recovery phase was excluded and mice were sacrificed immediately after the 30 minutes of air/toluene exposure. Locomotor activity data were obtained during the acclimation, exposure and recovery phases (except day 7) of the procedure.

5.2.2 Slice fast scan cyclic voltammetry following repeated toluene exposure

After the 7th toluene exposure, mice were immediately sacrificed (no recovery phase) and their brains were prepared for slice FSCV measurements using the procedure discussed in section 2.5. To determine if repeated toluene exposure can influence presynaptic DA autoreceptors, DA dynamics in the NAc core were evaluated using a cumulative dose response curve of 7-OH-DPAT (1, 10, 30, 100 nM). FSCV measurements and analyses were performed using the procedure previously described in section 4.2.2.

5.2.3 Brain tissue content analysis of DA and its metabolites

After the 7th exposure to toluene/air, mice were sacrifice by cervical dislocation and their brains were rapidly removed, prepared, and analyzed for DA tissue content and its metabolites using the same procedure discussed in section 2.8.

5.2.4 *In vivo* microdialysis and locomotor activity measurement

Simultaneous *in vivo* microdialysis and locomotor activity measurements were made as described in section 2.6. The timeline for the repeated toluene/air exposure and microdialysis measurements is as shown in Figure 5.1.

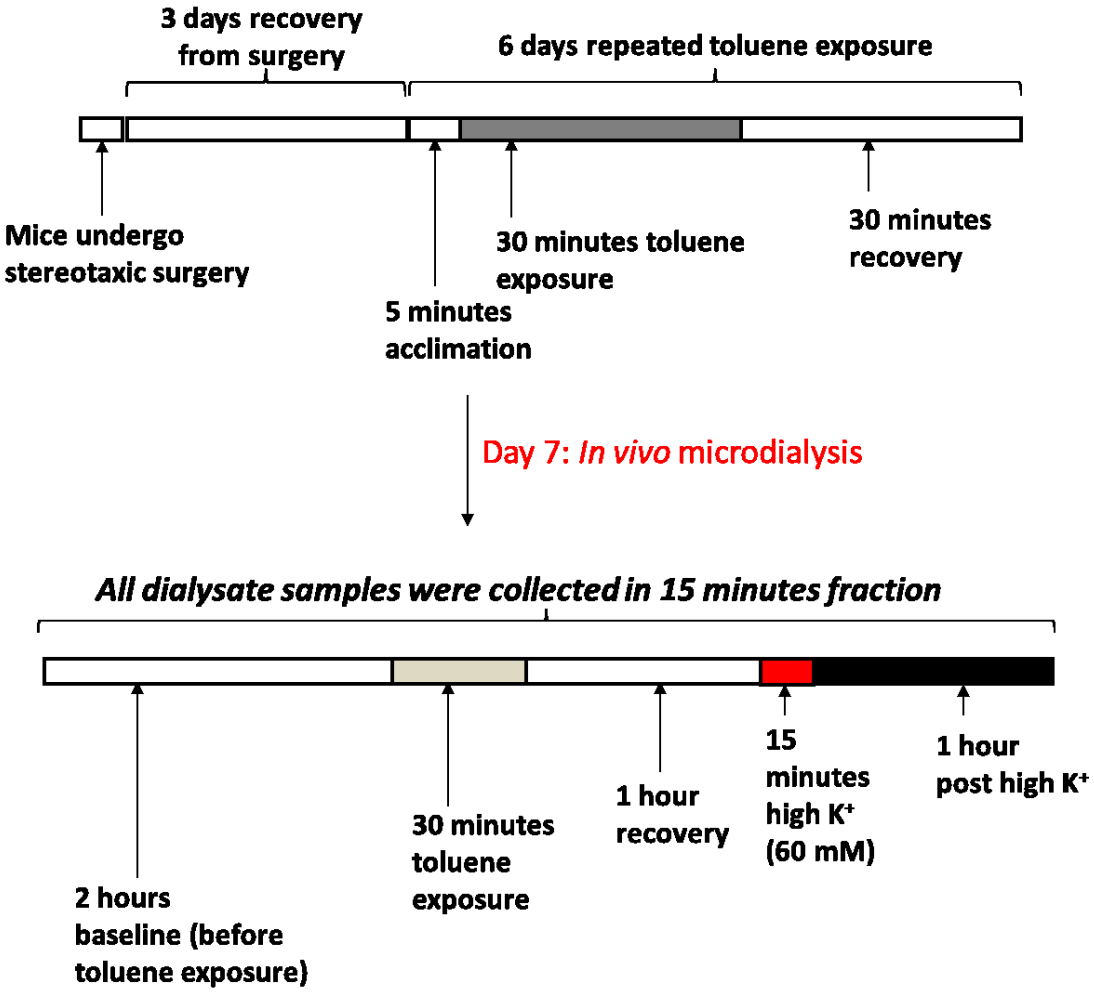

Figure 5.1: Timeline for repeated toluene/air exposure and microdialysis measurements.

5.2.5 Data analysis

Statistical analyses of data from locomotor activity measurements were performed with SPSS software using repeated measures analysis of variance (ANOVA) where toluene treatment (0, 2000, and 4000 ppm) was represented as the between subjects factor, with days and 3-minute time blocks as the within-subjects factors. Statistical significance was determined using Tukey's *post hoc* contrasts, simple main effects analyses, Dunnett's Multiple Comparison Test or Student t-test. Statistical analyses of FSCV and tissue content data were performed with GraphPad Prism Software using one-way ANOVA followed by Dunnett's Multiple Comparison Test or Student t-test. Data was expressed as mean ± standard error of the mean (SEM) and statistical significance determined as $P < 0.05$.

5.3 Results

5.3.1 Distance traveled during and following repeated toluene exposure

The effect of repeated toluene exposure on locomotor behavior was monitored within and across days of exposure. Statistical analyses of the results were performed using 3 x 7 x 10 repeated measures ANOVA with toluene treatment (0, 2000, and 4000 ppm) as the between subjects factor with days and 3-minute time blocks as the within-subjects factors revealed trends similar to those already established in Chapter 3 (Figure 3.5). However, some of these trends did not reach statistical significance presumably due to low statistical power. The specific results from this chapter demonstrate that the main effect of toluene treatment did not reach statistical significance ($F_{2,14} = 0.94$, $P = 0.42$). There was also no effect of Day ($F_{6,84} = 1.97$, $P = 0.08$) and Day x Toluene treatment interaction ($F_{12,84} = 3.10$, $P = 0.70$). However, there

was a significant main effect of time ($F_{9,126}$ = 0.75, P = 0.002) and a marginal Time x Toluene treatment interaction ($F_{18,126}$ = 1.67, P = 0.05). In all, the total distance traveled during 4000 ppm toluene treatment increased across days of treatment (P < 0.05; Dunnett's Multiple Comparison Test) as seen in Figure 5.2F. Recovery from repeated toluene treatment produced no main effect of Dose ($F_{2,14}$ = 2.80, P = 0.10) or Day ($F_{5,70}$ = 1.59, P = 0.18). However, there was a marginal effect of Day x Toluene treatment interaction ($F_{10,70}$ = 1.94, P = 0.05). Particularly for 4000 ppm toluene treatment, locomotor activity during recovery decreased across days of treatment. Dunnett's Multiple Comparison Test of the total distance traveled during recovery revealed a significant decrease in locomotor activity across days (P < 0.05, Figure 5.3F). Furthermore, a significant main effect was observed for Time block ($F_{9,126}$ = 20.6 , P < 0.001) and for the Time block x Toluene treatment interaction($F_{18,\ 126}$ = 5.52, P < 0.001) suggesting that the progressive decrease in locomotor activity during the recovery period was dependent on toluene treatment.

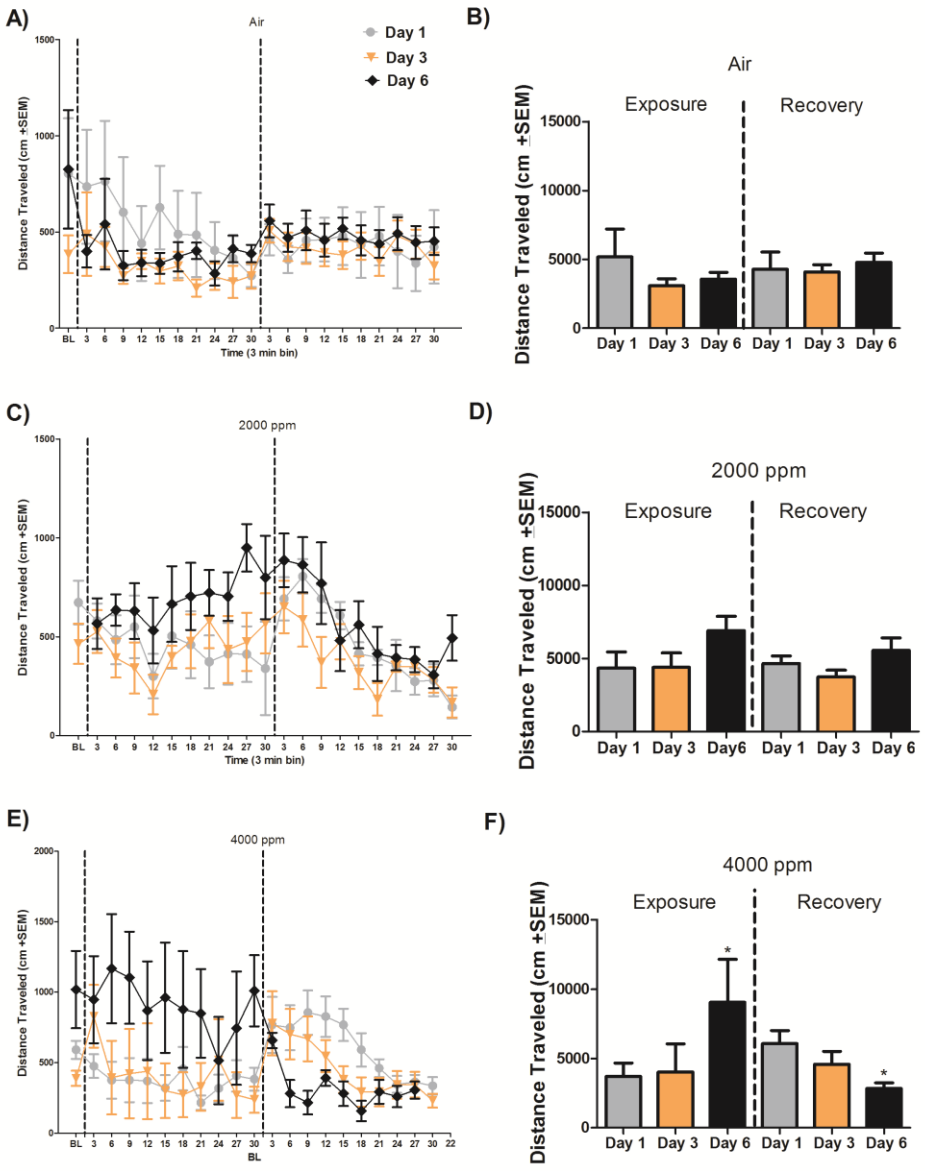

Figure 5.2: Locomotor activity during and after repeated toluene (0, 2000 or 4000 ppm) exposure. The left graphs represent locomotory activity, with the first 5 min acclimation, the middle section represents 30 minutes toluene exposure, and the right section shows 30 min post toluene exposure. **A)** A plot of distance traveled (cm ± SEM) versus time (3 minute bin) for air-control. **B)** A summation of distance traveled (cm ± SEM) versus days of toluene exposure. **C)** Distance traveled (cm ± SEM) versus time (3 minute bin) for 2000 ppm toluene treatment with corresponding **D)** A summation plot of distance versus day. **E)** A plot of distance traveled (cm ± SEM) versus time (3 minute bin) and **F)** A summation of distance versus day plot for repeated 4000 ppm toluene treatment. For all graphs, days 1, 3, and 6 were selected for simplicity. Statistical significant main effects and interactions were determined by Tukey's post hoc contrasts and simple main effects analyses. Significance between total distance traveled across days was also examined using Dunnett's Multiple comparison Test. **P* < 0.05 (air-control, n = 10; 2000 ppm, n = 5; 4000 ppm, n = 6).

5.3.2 DA release and uptake following repeated toluene exposure

Electrically stimulated DA release and uptake were measured across the CPu, NAc core, and NAc shell following the 7th toluene/air exposure (no recovery). The results obtained were expressed as maximum stimulated DA release in μM and DA uptake as maximum velocity of the DA transporter (V_{max}) in μM/s. Statistical analysis of these data (Figure 5.3) using one way-ANOVA across each brain region showed no significant main effect of repeated toluene exposure on DA release in the CPu ($F_{2,42}$ = 0.94, P = 0.40), which is consistent with previous observations (Figure 3.6C) where FSCV measurements were made 24 hours after the last toluene exposure. In the NAc, there was a significant main effect of repeated toluene exposure on DA release ($F_{2,72}$ = 10.64, P < 0.0001). Dunnett's Multiple Comparison tests revealed that both repeated exposures to 2000 and 4000 ppm toluene significantly decreased DA release in the NAc core (air: 0.79 ± 0.08 μM; 2000 ppm: 0.47 ± 0.04 μM; 4000 ppm: 0.50 ± 0.03 μM; P < 0.001). However, there was no main effect of repeated toluene exposure on DA release in the shell (air: 0.67 ± 0.04 μM; 2000 ppm: 0.53 ± 0.04 μM; 4000 ppm: 0.60 ± 0.08 μM; $F_{2,36}$ = 0.86, P = 0.43). These NAc core DA release results parallel the results obtained after a 24 hour recovery period. Taken together these results highlight that toluene has a significant impact on DA release in the core and that this alteration can still persist 24 hours after the toluene exposure.

With respect to DA uptake in the CPu, there was no difference between toluene-treated mice and their air-controls (air: 4.37 ± 0.11 μM/s; 2000 ppm: 4.67 ± 0.37 μM/s; 4000 ppm: 4.19 ± 0.11 μM/s; $F_{2,42}$ = 0.86, P = 0.44). There was a significant main effect of repeated toluene exposure on DA uptake in both the NAc core ($F_{2,72}$ = 8.37, P <

0.001) and NAc shell ($F_{2,36}$ = 6.43, P = 0.004). In the NAc core, only repeated exposures to 2000 ppm toluene decreased DA uptake (air: 2.37 ± 0.13 μM/s; 2000 ppm: 1.50 ± 0.21 μM/s; 4000 ppm; 2.19 ± 0.12 μM/s; P < 0.001), while in the NAc shell only 4000 ppm toluene increased DA uptake (air: 1.63 ± 0.23 μM/s; 2000 ppm: 1.63 ± 0.20 μM/s; 4000 ppm; 2.57 ± 0.20 μM/s; P < 0.001). These uptake alterations in the NAc induced by repeated exposure to 2000 and 4000 ppm are in contrast to our previous results where a 24 hour wait period after the last toluene inhalation (2000 and 4000 ppm) had no effect on DA uptake across all the striatal brain regions (Figure 3.6D). Collectively, the present FSCV data show that the DA dynamics in the NAc is prone to the neural action of repeated toluene exposure, which could be dose and region dependent.

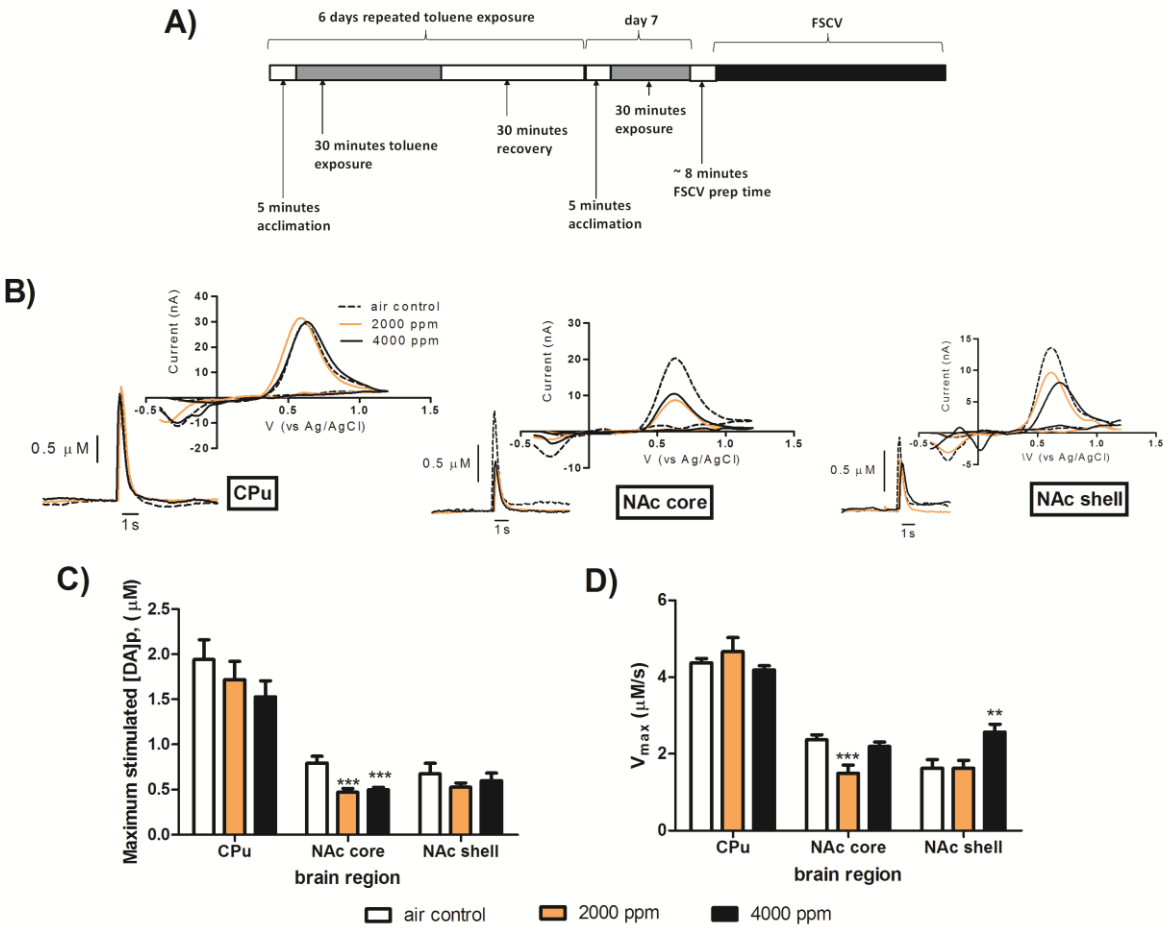

Figure 5.3: Effect of repeated toluene exposure on DA release and uptake. **A)** Repeated toluene exposure and FSCV experimental timeline which includes 5 minutes acclimation, 30 minutes toluene exposure, and 30 minutes of recovery performed every day for 6 consecutive days. The 7th day procedure excluded the recovery phase and involved ~ 8 minutes preparation before FSCV measurements. **B)** Effect of repeated toluene exposure on electrically evoked DA release across 3 sub-anatomical brain regions of the striatum (CPu, NAc core and shell) with their accompanying cyclic voltammogram indicating the detection of DA. **C)** DA release in the CPu, NAc core, and shell. **D)** DA uptake in the CPu, NAc core, and shell. Data expressed as mean ± SEM. Statistical significance was determined by one-way ANOVA with Dunnett's Multiple Comparison Test performed for each brain region (**P < 0.01, ***P < 0.001, n = 4 – 10/group).

5.3.3 Effect of repeated toluene exposure on presynaptic DA autoreceptors

There is considerable evidence that toluene may regulate DA release through DA autoreceptors. The objective of this experiment was to determine if the DA D3 agonist 7-OH-DPAT would have a shift in its dose response curve; either to the left or to the right after toluene inhalation. The agonist 7-OH-DPAT is a potent agonist of DA D3 receptors but has also been reported to activate D2 receptors in native tissue where sodium and magnesium ions are present (K_i values are D3: ~ 1 nM, and D2: 10 nM; from Tocris on-line catalog).[181, 198, 199, 213, 214] The NAc core was chosen as the target brain region because the DA release and uptake parameters in this region were significantly altered during repeated toluene exposure (Figure 5.3). However, the 7-OH-DPAT dose response curves did not significantly differ between toluene exposed animals and their air-controls. The IC_{50} values which describe the concentration at which the agonist exerts its half maximum effect, were also not significantly different between the toluene exposed mice and their air controls (air: IC_{50} = 18 ± 1 nM, toluene treated: IC_{50} = 20 ± 1 nM, P =1.00, n = 4 – 5/group, two tailed Student t-test, Figure 5.4A). However, increasing concentrations of 7-OH-DPAT (≥ 30 nM) decreased DA uptake in only the air-control mice ($F_{4,70}$ = 12.00, P < 0.0001) and not their toluene exposed littermates (F = 1.06, P = 0.386).

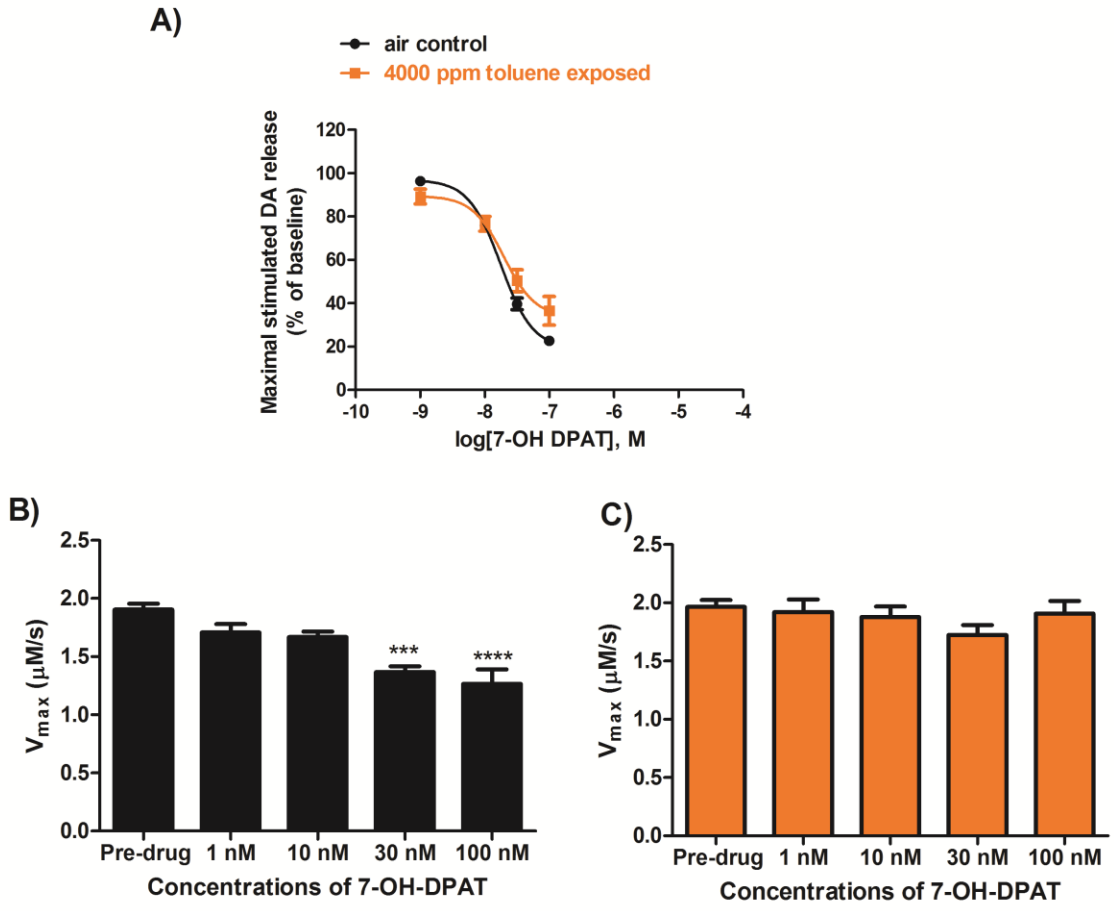

Figure 5.4: Effect of 7-OH-DPAT on presynaptic DA release and uptake in the NAc core of toluene exposed and air-control mice. A) Dose response curve showing the effect of cumulative doses (1-100 nM) of 7-OH DPAT on DA release in toluene treated mice (IC_{50} = 20 ± 1 nM) and their air-control (IC_{50} = 18 ± 1 nM). Statistical analysis was done with two tailed Student t-test ($P > 0.05$). **B)** The effect of 7-OH-DPAT on DA uptake in air-control mice, and **C)** The effect of 7-OH-DPAT on DA uptake in mice repeatedly exposed to 4000 ppm toluene vapor. Data were plotted as mean ± SEM. Statistical analysis performed with one-way ANOVA with Dunnett's Multiple Comparison Test. ***$P > 0.001$, n = 4-5/group).

5.3.4 Simultaneous monitoring of the effect of repeated toluene exposure on locomotor behavior and extracellular DA level

Following recovery from stereotaxic surgery, mice were exposed to behavior activating dose of toluene (4000 ppm) for six consecutive days in a static exposure chamber. On the 7th day, mice were exposed to the same dose of toluene vapor in a dynamic chamber fitted with a microdialysis set-up and the effect of toluene inhalation on locomotor activity and extracellular DA levels were monitored simultaneously.

The activity data for the six days toluene exposure procedure was analyzed using 3 x 6 x 10 repeated measures ANOVA with toluene treatment (0 and 4000 ppm) as the between subjects factor with days and 3-minute time blocks as the within-subjects factors. The results obtained revealed there was no main effect of the toluene treatment ($F_{1.8} = 0.98$, $P = 0.352$). However, there was a significant effect of Day ($F_{5,40} = 2.99$, $P = 0.02$), but not Day x Toluene treatment interaction ($F_{5,40} = 0.98$, $P = 0.44$) and a significant effect of Time ($F_{9,72} = 2.69$, $P = 0.009$), but not Time x Toluene treatment interaction ($F_{9,72} = 0.64$, $P = 0.76$). For the activity measurement during the recovery phase, there was no main effect of toluene treatment ($F_{1,7} = 0.16$, $P < 0.70$), day ($F_{2,14} = 0.64$, $P = 0.55$) or Day x Toluene treatment interaction ($F_{2,14} = 1.89$, $P < 0.19$). However, there was a significant main effect of Time ($F_{3,22} = 20.0$, $P < 0.0001$) and Time x Toluene treatment interaction ($F_{3,22} = 7.78$, $P = 0.001$). In all, the trends that did not reach statistical significance could be a result of low statistical power in the repeated measures design. Meanwhile, statistical analysis of the total distance traveled during toluene exposure across days (using two tailed Student's t-test) showed a significant

effect of the toluene treatment in day 1 ($P < 0.05$) and day 3 ($P < 0.01$), but not day 6 ($P > 0.05$; Figure 5.5).

The locomotor activity data for day 7 was expressed as a percentage of air-control baseline and plotted against time in 15 minutes bins. The data were graphed as a percentage of control so it would parallel the microdialysis data from baseline to post high K^+ concentration artificial cerebrospinal fluid (aCSF) infusion, which is also reported as a percent control. Statistical analysis was performed using 2 x 11 repeated measures ANOVA with toluene treatment (0 and 4000 ppm) designated as the between subjects factor, and the 15-minute time blocks as the within-subjects factors. As shown in Figure 5.6, there was a significant main effect of Time ($F_{2,13} = 4.54$, $P < 0.04$) but not Time x Toluene treatment interaction ($F_{2,13} = 2.34$, $P < 0.14$), or main effect of toluene treatment ($F_{1,8} = 3.17$, $P = 0.11$). Further analysis of locomotor activity at the first recovery point (R1) using two tailed Student t-test showed no difference between the activity of toluene exposed and air-control mice during recovery ($P > 0.05$; Figure 5.6).

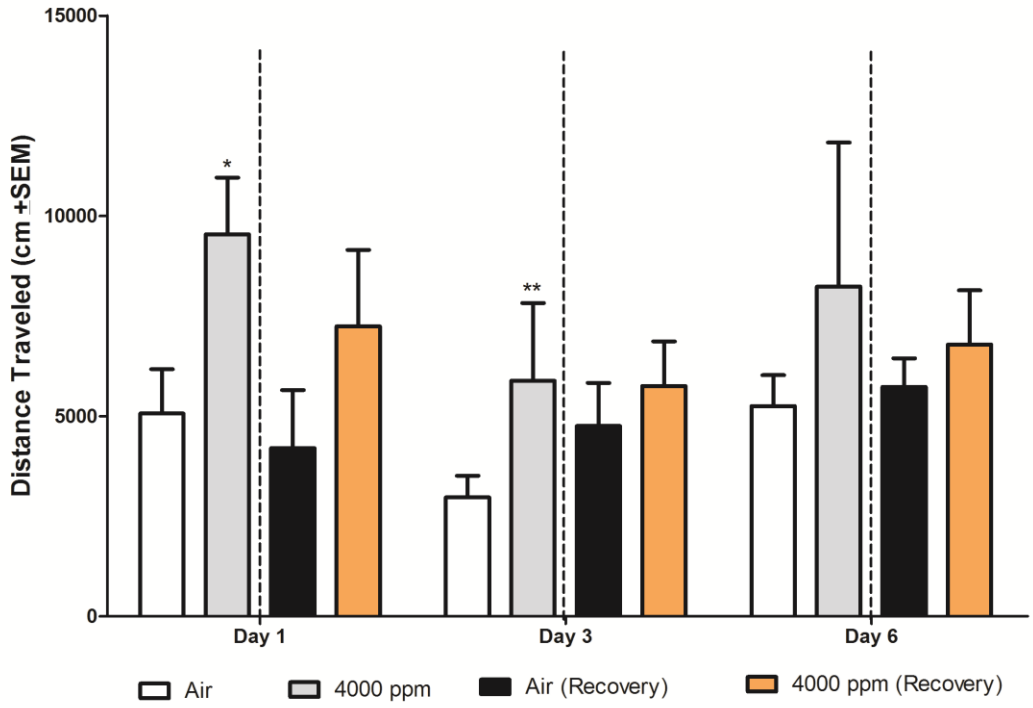

Figure 5.5: Effect of repeated toluene exposure on locomotor activity of mice. Locomotor activity expressed as distance traveled (cm ± SEM) versus days of toluene exposure. The data for each day are separated into distance traveled during air or toluene exposure and their recovery. Activity data were analyzed using repeated measures ANOVA with toluene treatment (0 and 4000 ppm) as the between subjects factor, and time and day as the within-subjects factors. Significant effect was determined using two tailed Student t-test (*$P < 0.05$, **$P < 0.01$; n = 6 - 7).

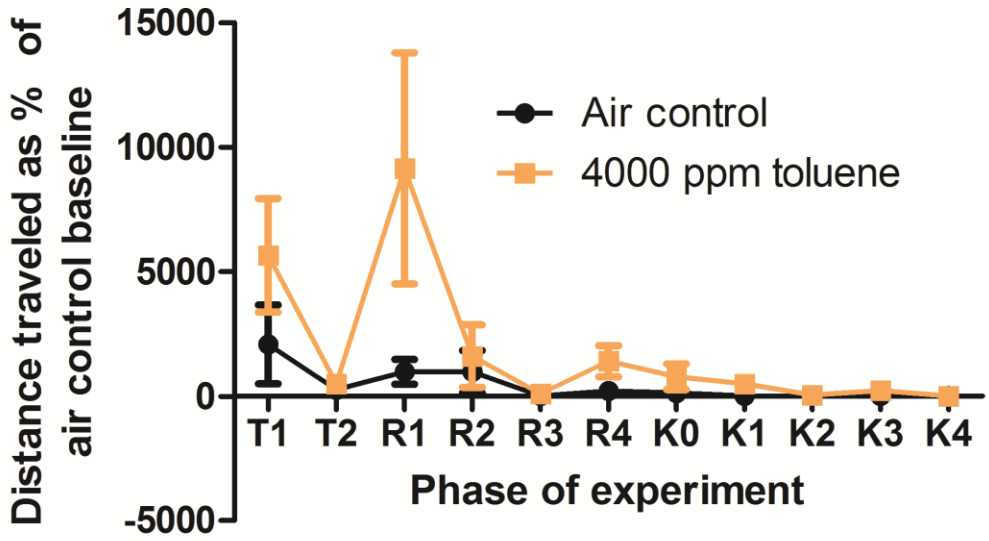

Figure 5.6: Effect of repeated toluene exposure on locomotor behavior during dialysate sample collection. Locomotor activity was expressed in 15 minutes bins. T1-T2 represents two 15 minute bins, where mice were exposed to toluene or air for 30 minutes, R1 - R4 is the 1 hour recovery phase, K0 is 15 minutes of high K^+ aCSF brain infusion, and K1 - K4 represent post high K^+ aCSF infusion. Distance traveled is expressed as a percentage of that of the air-control baseline. Statistical analysis was performed with repeated measures analysis with toluene as the between subjects factor, and 15-minute time blocks as within-subject factor. Statistical significance was determined using two tailed Student t-test (n = 5).

Microdialysis measurements were made to examine how extracellular DA levels in the NAc are altered following repeated exposure to toluene. The NAc was chosen as the brain region of interest from our earlier and present slice FSCV results that showed a decrease in DA release in the NAc following repeated toluene exposure (Figure 5.3). Dialysis samples were collected in 15 minutes fractions from toluene exposed and air-control mice during 2 hours of baseline (BL), 30 minutes of toluene exposure (T), 1 hour of toluene recovery (R), 15 minutes of high K^+ (K0), and 1 hour of post high K^+ (K). The extracellular DA levels are expressed as percentage of air-control baseline plotted with time in 15 minute bins. Statistical analysis using 2 x 11 repeated measures ANOVA with toluene treatment (0 and 4000 ppm) designated as the between subjects factor, and the 15-minute time blocks as the within-subjects factors showed a borderline significant effect of toluene treatment ($F_{1,5} = 6.37$, $P = 0.05$), a significant main effect of Time ($F_{10,50} = 4.15$, $P < 0.0001$), and a significant Time x Toluene treatment interaction ($F_{10,50} = 2.25$, $P < 0.03$). Moreover, Student's t-test revealed a significant increase in extracellular DA levels during the second half of the toluene exposure (T2; $P = 0.02$) and during recovery (R2 and R4; $P < 0.01$). An approximate 200% increase in percent baseline DA levels was seen in toluene treated mice versus the controls, that were at baseline (100%). This percent increase in DA after 60 mM K^+ aCSF infusion was significant in toluene-exposed mice compared to their air-control (K1 and K2, $P < 0.05$; K3, $P < 0.01$; Figure 5.7). Taken together, repeated toluene exposure altered the extracellular DA levels in the NAc during and following repeated toluene exposure.

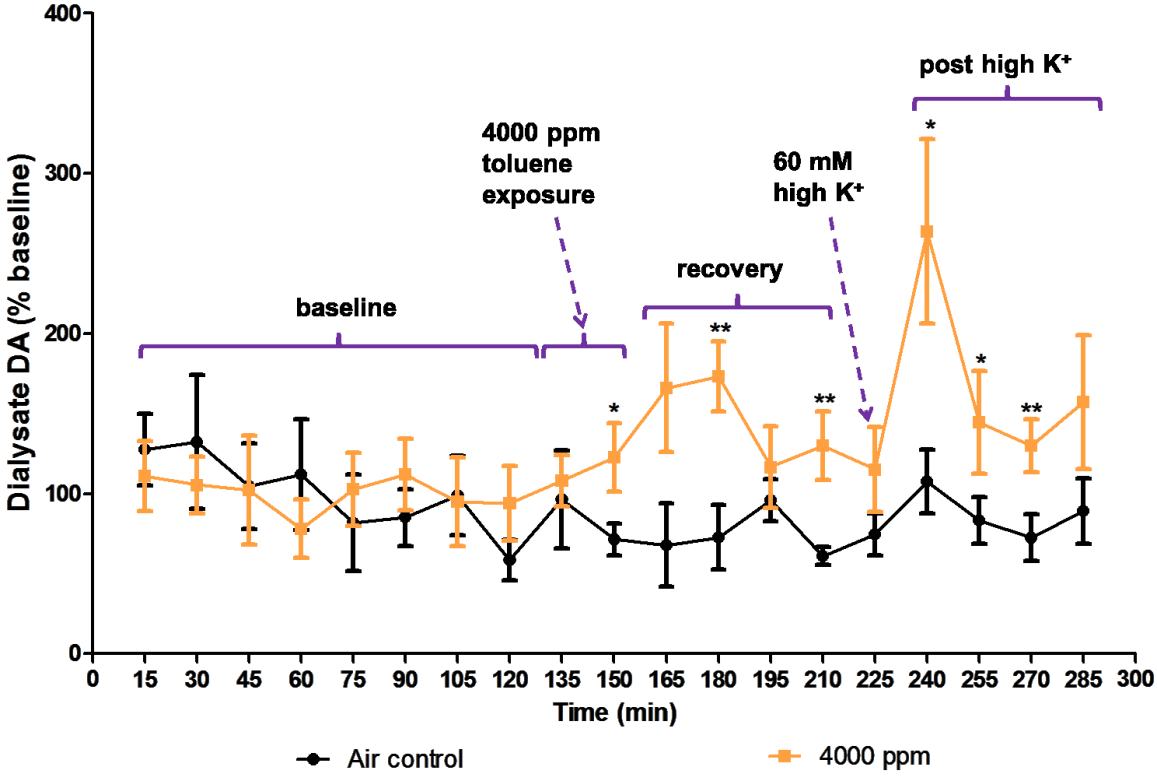

Figure 5.7: Effect of repeated toluene exposure on extracellular DA levels. Dialysis sample were collected from the NAc in 15 minute fractions throughout the experiment. The experimental time included 2 hours of baseline (15 – 120 min), 30 minutes of toluene/air exposure (135 – 150 min), 1 hour recovery (165 – 210 min), 15 minutes of high K^+ aCSF infusion (225 min), and 1 hour of post high K^+ aCSF infusion (240 – 285). Dialysate DA was expressed as a percentage of air-control baseline versus time in 15 minute block and analyzed using repeated measures ANOVA with toluene treatment (0 and 4000 ppm) as the between subjects factor, and the 15 minute time blocks as the within-subjects factors. Statistical significance was determined using a two tailed Student t-test. $*P < 0.05$, $**P < 0.01$, n = 5 – 6.

5.3.5 Effect of repeated toluene exposure on DA tissue content and its catabolism

The present experiment was performed to examine how repeated toluene exposure influences intracellular DA levels and its catabolism. Following 7 days of exposure to 4000 ppm toluene, brain tissues were taken from the CPu and the NAc and analyzed for DA, DOPAC, HVA, and 3-MT. The results obtained were expressed in terms of ng DA or metabolite per mg protein. Furthermore, the DA/DOPAC ratio was evaluated to determine if DA catabolism is altered in these specific brain regions. Statistical analysis using two tailed Student's t-test showed no difference in intracellular DA levels in the CPu (air: 839 ± 136 ng/mg protein; 4000 ppm: 984 ± 126 ng/mg protein; t = 0.78, *P* = 0.44, df: 22) between the two treatment groups, suggesting that repeated toluene exposure does not alter intracellular DA levels. There was no difference in the intracellular levels of DA metabolites following repeated exposure to 4000 ppm toluene (DOPAC: air; 202 ± 30, 4000 ppm; 168 ± 20, t = 0.97, *P* = 0.35, df = 22. HVA: air; 60 ± 8, 4000 ppm; 79 ± 9, t = 1.61, *P* = 0.12, df = 22. 3-MT: air; 33 ± 5, 4000 ppm; 44 ± 6, t = 1.45, *P* = 0.16, all means are expressed as ng/mg protein). Thus, the DA/DOPAC ratio was not different between the two groups of mice (air: 4.2 ± 0.7, 4000 ppm: 5.8 ± 0.5, t = 1.82, *P* = 0.08, df = 22, Figure 5.8C). Similar observations were made in the NAc (Figure 5.8B and C), demonstrating that repeated toluene exposure did not alter intracellular levels of DA or its metabolites in the NAc.

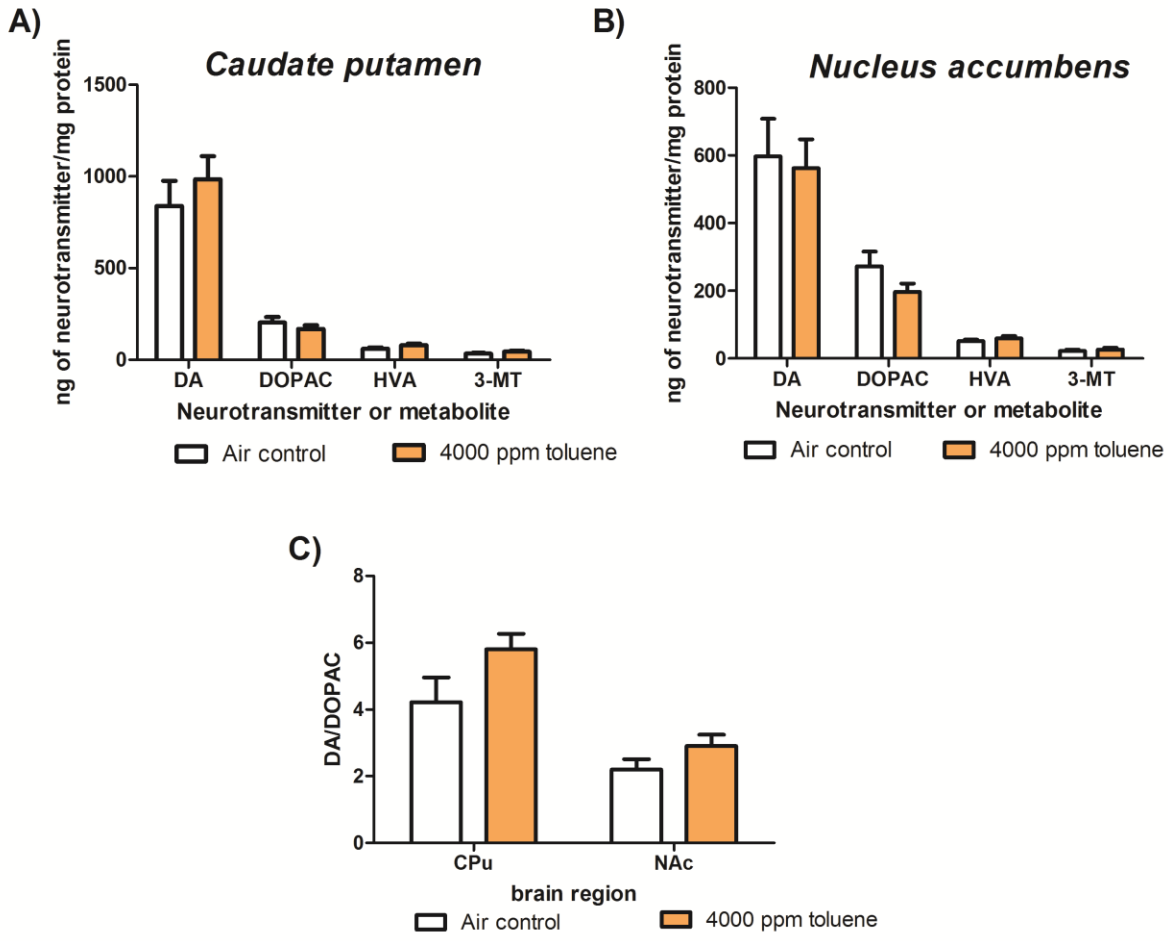

Figure 5.8: No difference in intracellular DA levels and its metabolites after repeated toluene exposure. A-B) Intracellular levels of DA, DOPAC, HVA, and 3-MT from the CPu and NAc of mice repeatedly exposed to 4000 ppm toluene vapor for 7 days and their air-control littermates. **C)** Repeated toluene exposure has no effect on DA/DOPAC ratio in the CPu and the NAc. Data shown as mean ± SEM. Statistical significance determined using two tailed Student t-test (n = 6).

5.4 Discussion

Repeated toluene administration alters striatal DA neurotransmission leading to neuroadaptations that may underlie its compulsive and repetitive use.[34, 84, 171, 215] Nevertheless, the exact neural mechanisms behind these toluene induced neuroadaptations are not well understood. The primary goal of the present study was to examine how repeated toluene exposure immediately alters DA neurotransmission in the NAc and the CPu. Evidence from our initial characterization of the effect of toluene inhalation followed by a 24-hour recovery period (Chapter 3) suggested that 7 days of repeated inhalation of 2000 or 4000 ppm of toluene impaired DA release in the NAc, but not in the CPu. In the present work, neurochemical measurements were made immediately after toluene exposure on the 7th day, without recovery period. In this case, similar impairment in DA release was observed exclusively in the NAc. Taking our two studies together, the results suggest that repeated exposure to toluene exerts a lasting effect on DA neurons in the NA, thus implicating the NAc as an important neural site for toluene abuse.[36, 216] This observation was not surprising because DA in the NAc is associated with the abuse liability for most drugs.[34, 217, 218] Repeated administration of drugs such as amphetamine, cocaine, nicotine, and morphine induced differential changes in DA neurotransmission in the core and shell of the NAc.[219-221] The present work is consistent with these reports; where slice voltammetry displayed decreased DA release in the core, but not the shell of the NAc after repeated exposure to 2000 or 4000 ppm toluene. Meanwhile, 2000 ppm of toluene decreased DA uptake exclusively in the NAc core, while 4000 ppm toluene increased DA uptake in the NAc shell. This regional specificity of was also identified in the acute toluene study (*see* Figure 4.3) where acute

toluene inhalation potentiated DA uptake only in the NAc shell. Taken together, the present observations suggest that repeated inhalation of toluene vapor preferentially decreases DA release in the NAc core while increasing DA uptake in the shell.

Throughout our numerous studies, a common observation was that DA release and uptake were decreased in the NAc core. Therefore, we hypothesized that repeated toluene inhalation would increase extracellular DA levels. We believed that elevated extracellular DA levels would lead to the compensatory down-regulation of DA release and uptake observed with slice FSCV in the core. Using *in vivo* microdialysis, increases in the extracellular DA levels were observed in the NAc during the 7th toluene treatment, although there was no difference in extracellular DA levels prior to toluene inhalation, which suggests that baseline DA levels are approximately the same between the two treatment groups. However, an increase in extracellular DA levels occurred during the exposure period and persisted through the 30-min recovery phase. There was also a potentiated response in toluene treated animals following high K^+ stimulation. With the increases in extracellular DA levels as determined by *in vivo* microdialysis, we anticipated that there would be a concomitant increase in locomotor activity since there is a strong correlation between drug induced elevations in extracellular DA levels in the NAc and heightened behavioral stimulating effects.[34, 171, 217] Although increase locomotor activity was not observed in the toluene-treated mice, the locomotor activity results suggest a trend towards increased locomotor activity in the toluene treated mice. However, the locomotor activity results did not reach statistical significance presumably because of low statistical power. We also hypothesis that, because the locomotor activity was measured in their microdialysis cage modified to record locomotor behavior,

this confound could have led to not observing the statistical significance in locomotor behavior. Future studies are aimed to address this concern. Although no difference was observed in locomotor behavior, our neurochemical measurements did highlight that toluene exposure elevated extracellular DA levels during and after the exposure, as well as after a high K^+ stimulation.

The neurochemical results thus far suggest that daily intermittent toluene exposure for 7 days increases extracellular DA levels in the NAc, with a concomitant decrease in DA release and uptake in the NAc core. Therefore, there is the possibility that toluene influences presynaptic DA autoreceptors, which are contributing to the significant alterations observed in the dopaminergic system in the NAc. DA autoreceptors play an integral role in regulating DA synthesis and release. To determine if DA autoreceptors directly mediate the action of repeated toluene inhalation on DA dynamics in the NAc; slice FSCV was used to determine the effect of the DA D3 autoreceptor agonist, 7-OH-DPAT on DA release and uptake. There was no difference between the 7-OH-DPAT dose response curves of DA release generated from toluene treated and air-control mice, suggesting no involvement of presynaptic DA D3 autoreceptors in the alterations induced by repeated toluene exposure on DA release in the NAc. This observation appears contrary to our hypothesis, where we anticipated that the reduction in stimulated DA release observed in the NAc was a compensatory down regulation of the DA D3 receptors. However, only DA D3 autoreceptor subtype was examined; future studies could evaluate the D2 autoreceptor also found in the NAc or examine heteroreceptors such as a GABA or glutamate receptor that may be influencing DA release in the NAc.[191] Although there was no difference in the 7-OH-

DPAT dose response curve, a significant decrease in DA uptake was seen between toluene exposed mice and their air-controls. The decrease in DA uptake was only observed at the highest dose of 7-OH-DPAT, which is consistent with what has been shown in other studies suggesting that higher doses of the autoreceptor agonists are non-specific and have the ability to either directly or indirectly interact with the DA transporter.[222]

To round up the neurochemical investigations with the toluene treated mice, our last investigation was to evaluate intracellular DA levels. Since our initial work in this study showed an increase in extracellular DA levels and impairment in DA release and uptake in the NAc core, a final goal was to determine if toluene has the ability to influence intracellular DA levels or its metabolites. However, repeated toluene treatment did not influence the intracellular levels of DA and its metabolites in the NAc. Furthermore, the DA/DOPAC ratio was also unaffected suggesting there was no difference in DA catabolism. It is interesting that daily, intermittent toluene exposure had no effect on DA intracellular levels, since our acute studies showed a significant increase in intracellular DA catabolism (see Figure 4.8). These current observations from the 7 daily, intermittent toluene exposure suggests tolerance to toluene inhalation, but only with a sustained amount of toluene exposure. Taken together, the neurochemical measurements made with slice FSCV, *in vivo* microdialysis, and tissue content underscore the complexity of toluene's neural action, which may involve not only the DA, but other neurotransmitters and neuromodulators.[37, 79, 84, 223, 224]

5.5 Conclusions

In conclusion, the present work demonstrated that repeated exposure to locomotor activating dose of toluene preferentially impairs DA release and uptake in the NAc core in a dose dependent fashion. The alterations in DA release were not directly mediated by DA D3 autoreceptors. Furthermore, repeated exposure to 4000 ppm toluene potentiated extracellular DA levels in the NAc, but there was no effect on intracellular levels of DA and its metabolites across the striatum. Taken together, we have proposed that toluene is most likely influencing the accumbal DA system through a heteroreceptor, possibly the GABA or glutamate receptor.

.

CHAPTER 6

Probing the Ability of Presynaptic Tyrosine Kinase Receptors to Regulate Striatal Dopamine (DA) Dynamics

Adapted and Updated with permission from:
Apawu, A. K., Maina, F. K., Mathews, T.A., "Probing the ability of presynaptic tyrosine kinase receptors to regulate striatal dopamine dynamics" ACS Chem Neurosci., 2013, 4(5): 895 – 905

6.1 Introduction

Brain derived neurotrophic factor (BDNF) belongs to a specialized class of proteins called neurotrophins that play a vital role in neuronal growth, differentiation, synaptic plasticity, and survival of neurons.[145-147] Other members of the family include nerve growth factor (NGF), neurotrophin-3, (NT-3), and neurotrophin – 4/5 (NT-4/5).[2, 15] These neurotrophins execute their functions by binding to specific isoform of tyrosine kinase receptors called tropomyosin-related kinase (Trk) receptors which are TrkA, TrkB and TrkC.[18, 225] BDNF propagates its effect by specifically binding to TrkB receptors, which causes dimerization of the receptors and phosphorylation of its tyrosine residue and subsequent activation of kinases.[16] These actions lead to activation of a number of small signaling proteins such as GRB2, SHC, and SOS that mediate various signaling cascades through phosphorylation to regulate neuronal events including cell survival, synaptic plasticity, synaptic transmission, and neurotransmitter release.[2, 16, 18, 19]

The interaction between BDNF and the DA system is well known. For example, the mesencephalic dopaminergic neurons have been shown to express TrkB receptors.[226] In addition, *in vitro* data has revealed that BDNF augments survival and differentiation of cultured nigral DA neuron whereas chronic infusion of BDNF directly

into rat's brain has been shown to enhance DA release, DA turnover and metabolism, DA neuronal activity, and survival.[150, 226-228] Moreover, BDNF has been reported to up-regulate DA transporter activity in striatal synaptosomes of rat brain.[149] Existing data also shows that BDNF heterozygous ($BDNF^{+/-}$) mice (with 50% reduction in BDNF protein levels) have higher intracellular DA concentrations in the striatum, while exhibiting decrease DA release in the striatum.[229, 230] $BDNF^{+/-}$ mice have reduced expression and function of the DA D3 receptors in the caudate-putamen (CPu) and nucleus accumbens (NAc) compared to their wildtype littermates.[183, 231] Our laboratory has shown that $BDNF^{+/-}$ mice have an ~ 2.5-fold increase in extracellular DA levels in the CPu compared to wildtype mice as measured by zero net flux, with fast scan cyclic voltammetry (FSCV) data showing a decrease in electrically evoked DA release and uptake.[232] Our initial neurochemical analysis on CPu DA dynamics suggests that endogenous BDNF influences DA system homeostasis primarily by regulating release leading to adaptions in the DA uptake function.[232] All these data together with many more provide overwhelming evidence of the ability of BDNF to modulate DA function across different brain regions including the striatum. Nevertheless, the mechanism of how BDNF influences the DA function is still not well understood.

To examine the mechanism underlining the influence of BDNF on presynaptic DA release and uptake processes, the experiments herein explores FSCV's utility to characterize the functional effect of Trk receptors on the presynaptic DA release and uptake dynamics in the striatum. The functional effect of Trk receptors has been examined previously using classic radiochemical methods in synaptosomes and brain slices.[149, 233, 234] These existing radiochemical methods provide high selectivity to

examine each of the DA parameters. For example the DA transporter function can be studied devoid of contributions from the DA release and diffusion.[235] However, the strength that FSCV brings to the field would be its high temporal resolution (up to 100 ms) and ability to assess DA release and uptake rate simultaneously. By using FSCV on striatal brain slices, it eliminates contributions from post-synaptic TrkB receptors allowing us to better understand how presynaptic TrkB receptors contribute to modulating DA dynamics. In the present work, DA release and uptake dynamics have been evaluated in the striatum by using the endogenous ligand BDNF, commercially available TrkB agonist 7,8-dihydroxyflavone (7,8-DHF), and inhibitors such as genistein, tyrphostin 23 (AG 18), and K252a. Herein, we demonstrate the ability of FSCV to assess the effect of non-DA receptors like the TrkB on striatal DA dynamics, and will be useful to provide a better understanding of how other systems contribute to the strength of synaptic DA transmission.

6.2 Hypothesis

We hypothesize that life-long reduction in BDNF results in compensatory alteration in DA release and uptake dynamics, which we believe are being modulated by presynaptic TrkB receptor activation.

6.3 Materials and Methods

6.3.1 Animals

Wildtype and $BDNF^{+/-}$ mice were purchased from Jackson Laboratories (Bar Harbor, ME) and offspring were raised as a colony in-house in a certified vivarium (Association for Assessment and Accreditation of Laboratory Animal Care; AAALAC) at

Wayne State University. Genotype identification was performed using PCR analysis of tail DNA as already described by Bosse *et al.*[94]

6.3.2 Chemicals

Chemicals used in the preparation of artificial cerebrospinal fluid (aCSF) for voltammetric solutions were purchased either from Sigma-Aldrich (St. Louis, MO), Fisher Scientific Co. (Fairlawn, NJ), or EMD Chemicals, Inc. (Gibbstown, NJ) unless otherwise noted. The following compounds were purchased from specific vendors: 7,8-DHF from Tokyo Chemical Industry Co. LTD. (Portland, OR), BDNF from PeproTech (Rocky Hill, NJ), and K252a from LC Laboratories (A Division of PKC Pharmaceuticals Inc., Woburn, MA). In all slice experiments, the pharmacological agents were dissolved in ultrapure (18 MΩ cm) water or dimethyl sulfoxide (DMSO), unless otherwise stated and then diluted in oxygenated aCSF (composition in mM: 0.4 ascorbic acid, 126 NaCl, 2.5 KCl, 1.2 $MgCl_2$, 2.4 $CaCl_2$, 25 $NaHCO_3$, 1.2 NaH_2PO_4, 11 D-glucose, and pH 7.4). All chemicals used in calibration experiments, including the verification of the redox capability of the drugs, were dissolved in DMSO and then diluted in a modified calibration aCSF buffer (composition in mM: 126 NaCl, 2.5 KCl, 1.2 $MgCl_2$, 2.4 $CaCl_2$, 25 $NaHCO_3$, 1.2 NaH_2PO_4, and pH 7.4).

TrkB receptor agonist

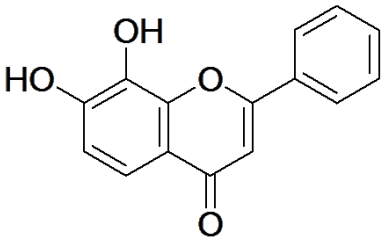

7,8-Dihydroxyflavone

Trk receptor antagonists

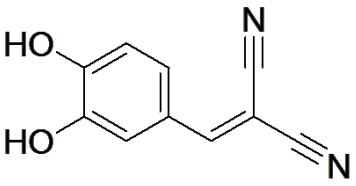

Tyrphostine 23 (AG 18)

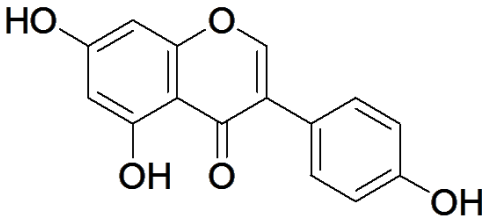

Genistein

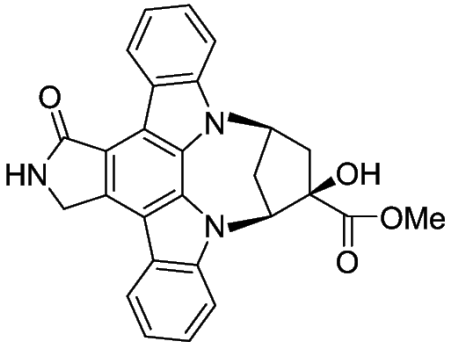

K252a

Figure 6.1: Chemical structures of TrkB receptor agonist and antagonists

6.3.3 Slice FSCV

Mouse brain slices were obtained and voltammetric recordings were made as described in Chapter 2.5. Briefly, 400 µm coronal brain slices obtained from $BDNF^{+/-}$ and Wildtype mice were stimulated every 5 minutes using a one pulse electrical stimulation (monophasic, 350 µA, 60 Hz, and 4 ms pulse width) to elicit DA which was measured using a homemade carbon fiber microelectrode (with a length between 50 - 200 µm and a 7 µm diameter held at initial potential of -0.4 V, ramped up to +1.2 V and back to -0.4 V at a scan rate of 400 V/s at 10 Hz). Current generated at the microelectrode surface as a result of the redox reaction of DA was subtracted from the background current to obtain peak oxidation current for DA. The peak oxidation current for DA was converted into concentration based on a post-calibration using 3 µM DA. Following three stable DA release profiles (within 10% of each other), the effect of cumulative concentrations of pharmacological agents; exogenous BDNF, 7,8-dihydroxyflavone (7,8-DHF), gensitein, tyrphostin 23 (AG18), K252a, or a single dose of BDNF-K252a, or 7,8-DHF- K252a cocktail was evaluated. To verify the redox capability of the pharmacological agents, flow injection analysis as described in Chapter 2.5.3 was used to measure the response of these pharmacological agents at a carbon fiber microelectrode surface. Three different concentrations (3, 10, and 20µM) of each pharmacological agent were made by dissolving the respective stock solutions in 20 mL of aCSF (calibration buffer) with physiological pH of 7.40. Each concentration was run in triplicates during which the microelectrode was held at initial potential of -0.4 V, ramped up to 1.2 V and back down to -0.4 V at a scan rate of 400 V/s.

6.3.4 Data Analysis

All voltammetric data were analyzed using LabVIEW National Instruments software (National Instruments, Austin, TX). Current versus time traces were fitted to a non-linear regression.[154, 163] A Michaelis-Menten based kinetic model was used to evaluate stimulated presynaptic DA release ([DA]*p*) and DA uptake kinetics (maximum velocity, V_{max}) and affinity of DA to its transporter (apparent K_m) by fitting DA current versus time traces.[94, 163] In all voltammetric analysis, K_m values were set to 0.16 μM, which permits a non-linear fit of DA release and uptake. Statistical analysis was performed using GraphPad Prism (GraphPad Software, Inc., San Diego, CA) during which statistical significance was determined by one-way ANOVA with Dunnett's Multiple Comparison Test. The criterion for the statistical significance of DA analysis was set to $P < 0.05$. All data are reported as mean ± standard errors of the means (SEMs).

6.4 Results and Discussion

6.4.1 Characterization of the electrochemical properties of 7,8-dihydroxyflavone, K252a gensitein, and tyrphostin 23

The main goal of the experiments described in this section was to examine if the pharmacological agents used have electrochemical properties that could directly interfere with DA signals instead of their cellular action on the DA system during the brain slice drug perfusion experiments. This goal stems from the fact that the structures of 7,8-DHF and tyrphostin 23 are similar to that of DA insofar as the molecules contain the catechol moiety, Thus, we expected these two molecules to have similar redox reaction as that of DA at the electrode surface. Furthermore, although K252a does not

contain a catechol moiety, it does have a single hydroxyl group that could be easily oxidized like tyramine and octopamine.[236] while genistein on the other hand, is a polyphenol with three hydroxyl groups (Figure 6.1) which can undergo electron transfer oxidation reaction like quercetin.[237] To delineate the electrochemical properties of these molecules, we used a flow cell apparatus to evaluate their oxidation and reduction potentials. The results obtained have been expressed in terms of background subtracted cyclic voltammograms. As expected, 7,8-DHF showed a single oxidation and reduction peak at ~ 0.4 V and at -0.2 V respectively (Figure 6.2C). The single oxidation and reduction peak for 7,8-DHF suggests that it is a reversible electrochemical reaction. It is our hypothesis that the hydroxyl groups on the catechol are oxidized in much the same way as it is in DA (Figure 6.2A) and other catecholamine molecules. A notable difference in 7,8-DHF and DA cyclic voltammograms is that 7,8-DHF oxidizes at ~ +0.2 V less than DA. We believe this difference is due to the second ring structure attached to the catechol moiety providing additional stability/resonance to the molecule. Similarly, the background subtracted voltammograms of tyrphostin 23 showed oxidation and reduction peaks at ~ 0.6 and ~ 0.02 V respectively (Figure 6.3C). Interestingly, these oxidation-reduction peaks of tyrphostin 23 were suppressed in presence of DA (Figure 6.3D). K252a gave a very distinct cyclic voltammogram with oxidation peaks at ~ +0.4 and +1.1 V, and a reduction peak at ~ +0.9 V (Figure 6.2E). When DA and K252a were combined, there appeared to be no overlap with oxidation peaks of the two components (Figure. 6.2F). Genistein showed three oxidation peaks at 0.2, 0.8 and 1.0 V respectively (Figure 6.3A; a-c) which appeared to be irreversible at physiological pH. The genistein voltammogram could suggest oxidation of the para-substituted phenol

and the resorcinol moiety.[238] The DA-genistein mixture showed peaks characteristic of the two constituents with DA masking the first peak of gensitein. Taken together, the present background subtracted voltammograms demonstrated that each of the drugs examined is electrochemically active at pH of 7.40 with most of them exhibiting reversible oxidation reactions. However, the DA signals (current) and oxidation potential are no different in the presence of these compounds which strongly support the notion that background subtraction eliminates any possible electrochemical confounds associated with the perfusion of the drugs. This assertion is further supported by the voltammograms for the slice FSCV data as no interfering peaks were observed during drug perfusion experiments (Figures 6.4-6.5).

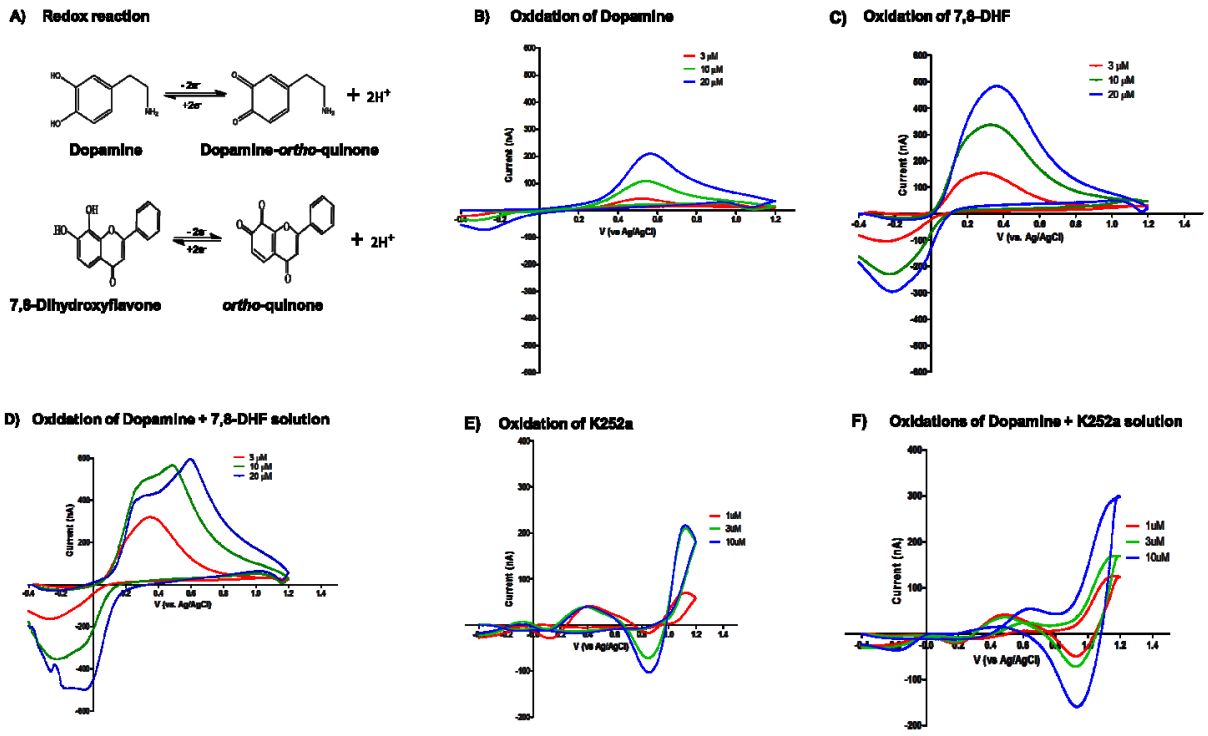

Figure 6.2: Background subtracted cyclic voltammograms and redox reactions showing electrochemical properties of DA, 7,8-dihydroxyflavone and K252a. Data was obtained using flow injection analysis of varying concentrations of each molecule. **A)** Oxidation-reduction reactions of DA and 7,8-DHF respectively. Both molecules oxidize in a similar electron transfer reaction to form ortho-quinones during the forward scan of the applied voltage. In the reverse scan, the quinones are reduced back to DA and 7,8-DHF respectively. **B)** Cyclic voltammogram shows oxidation peak of DA at ~ 0.6 V and reduction peak at ~ -0.2 V. **C)** Cyclic voltammogram of 7,8-DHF. Oxidation peak of 7,8-DHF occurs at ~ 0.4 V whereas the reduction peak appears at ~ -0.2 V. **D)** A solution of both DA and 7,8-DHF demonstrates the characteristic oxidation peaks of the two compounds only at higher concentrations as depicted by their voltammograms. **E)** Cyclic voltammogram showing oxidation and reduction peaks of K252a. F) Cyclic voltammograms showing oxidation and reduction of DA-K252a solution.

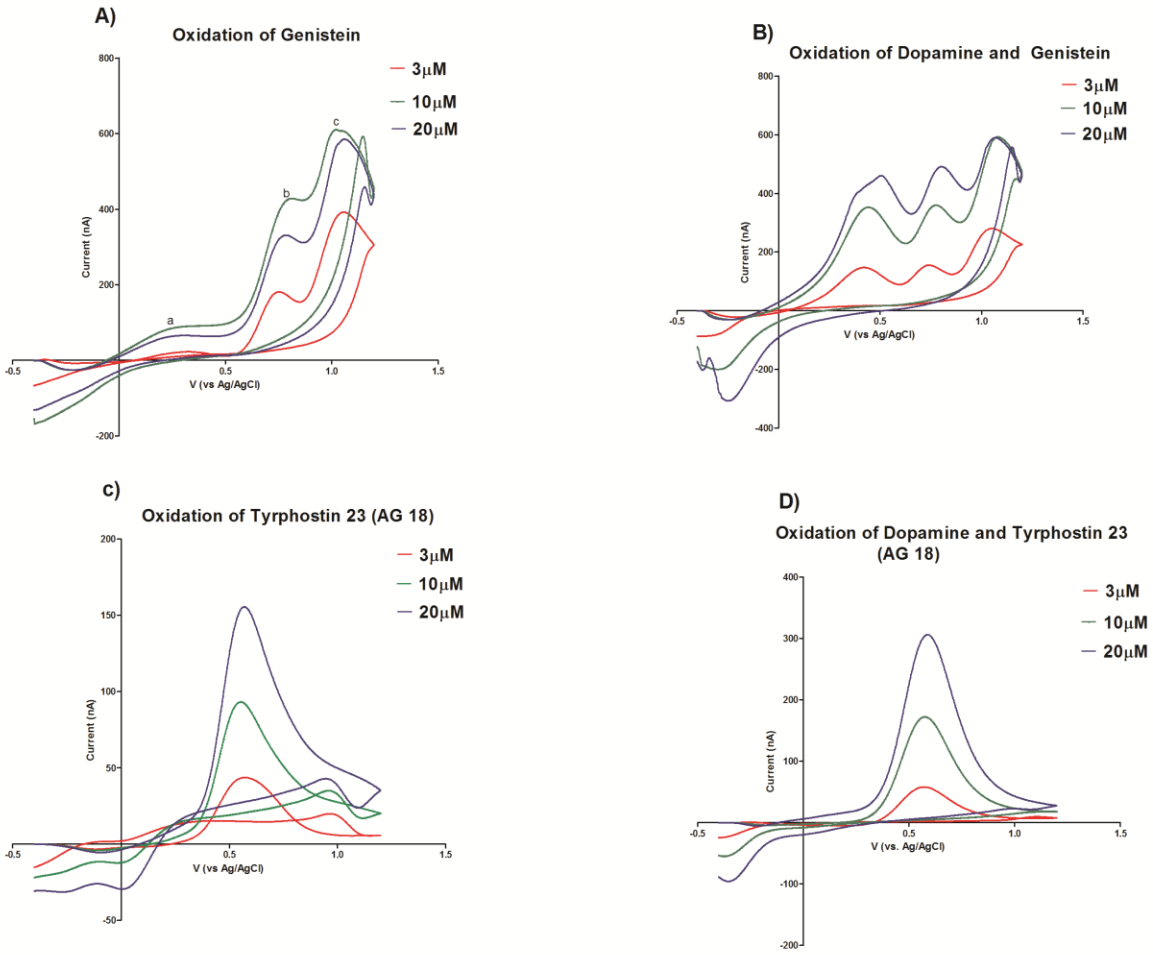

Figure 6.3: Background subtracted cyclic voltammograms showing electrochemical properties of genistein and tyrphostin 23. A) Cyclic voltammograms of gensitein showed non-reversible three oxidation peaks of the compound occurring at 0.2, 0.8 and 1.0 V respectively. **B)** In dopamine-genistein mixture, cyclic voltammograms showed both oxidation-reduction profile of DA and two non-reversible oxidation peaks of gensitein. **C)** tyrphostin 23 oxidizes at ~ 0.6 and reduces at ~ 0.02 V. **D)** The voltammogram showed the presence of DA suppressed the oxidation property of tyrphostin 23.

6.4.2 Effect of exogenous BDNF on electrically evoked DA release in BDNF$^{+/-}$ mice

Numerous reports suggest that exogenously applied BDNF enhances both DA release and uptake.[21, 149, 150, 239] To date, no one method has been used to simultaneously analyze both release and uptake parameters. To evaluate the functional effects of how exogenous BDNF influences presynaptic DA dynamics directly in the CPu, electrically evoked DA release (Figure 6.4), and uptake rates (Table 1) were monitored every 5 minutes in BDNF$^{+/-}$ mice. Direct application of cumulative concentrations of exogenous BDNF (50, 100, and 200 ng/mL) was applied to brain slices for 30 minutes. BDNF$^{+/-}$ mice were only evaluated with BDNF perfusion because we have previously shown that DA release and uptake rates are not different in wildtype mice.[94] BDNF$^{+/-}$ mice showed a concentration-dependent increase in electrically stimulated DA release after BDNF was applied to striatal brain slices compared to their pre-drug controls (50 ng/mL BDNF: ~ 12%, 100 ng/mL BDNF: ~ 17%, and 200 ng/mL BDNF: ~ 18%, Figure 6.4A). However, no difference in V_{max} was observed after BDNF perfusion (Table 1). We have extended and confirmed our previous findings,[94] that exogenous application of BDNF from 50 to 200 ng/mL elevates evoked-DA release with no effect on DA uptake rates in BDNF$^{+/-}$ mice.

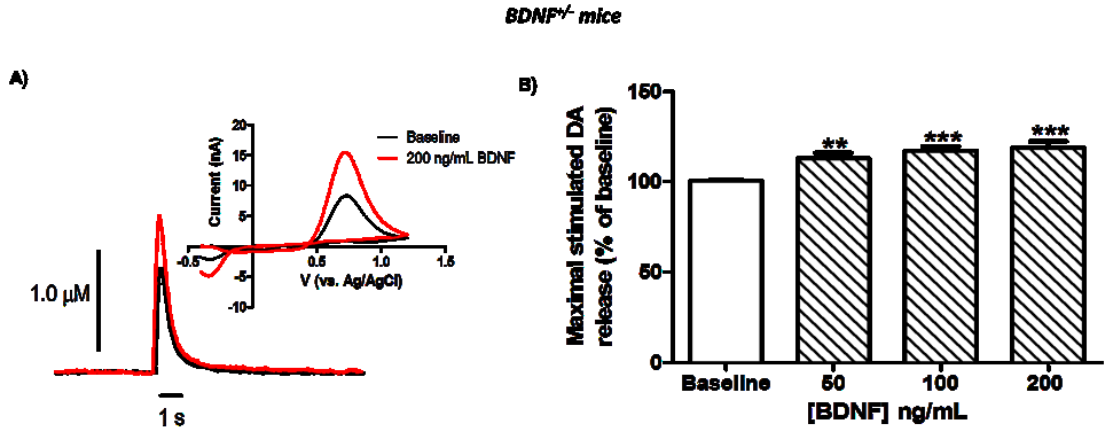

Figure 6.4: Infusion of BDNF dose dependently increases electrically stimulated DA release in the caudate-putamen of BDNF$^{+/-}$ mice. A) Current versus time trace of baseline DA signal with corresponding cyclic voltammogram (inset) compared to current versus time trace of electrically evoked DA release after a 30 minute perfusion of 200 ng/mL BDNF (red line) with corresponding cyclic voltammogram (red line, inset). **B)** Effect of varying concentrations of exogenous BDNF on DA release expressed as a percentage of pre-drug DA concentration. Data are means ± SEMs (n = 5 mice). One-way ANOVA ($F_{3,36}$ = 9.42; P < 0.0001, n = 5) followed by Dunnett's post-test revealed that each concentration of BDNF increased DA release significantly. **P < 0.01, ***P < 0.0001.

6.4.3 Effect of genistein and tyrphostin 23 (AG 18) on presynaptic DA dynamics

To examine the mechanism underlining the influence of BDNF on presynaptic DA dynamics, the experiments herein explores FSCV's utility to characterize the functional effect of Trk receptors by measuring the effect of Trk receptor antagonist; genistein and tyrphostin 23 on electrically stimulated DA release and uptake in the CPu. Genistein and tyrphostin 23 have been extensively studied as potent Trk receptor inhibitors.[149, 240-242] For example, using these two Trk receptor inhibitors, Hoover *et al.* successfully demonstrated that tyrosine kinases modulate the DA transporter function in rat brain preparations.[149] In the present work, we first obtained stable electrically evoked DA signal before perfusion of genistein or tyrphostin 23. The results obtained showed that, $BDNF^{+/-}$ mice have significantly lower pre-drug electrically evoked DA release compared to their wildtype counterpart (Figure 6.5A versus B, Figure 6.6A versus B, open bars, $^{\#}P < 0.05$, Student t-test). Furthermore, the DA uptake in the $BDNF^{+/-}$ mice was lower compared to their wildtype littermates (Figure 6.5C versus D, Figure 6.6C versus D, open bars, $^{\#\#\#}P < 0.001$, Student t-test). This low stimulated pre-drug DA release and uptake is in agreement with earlier work that has suggested that endogenous BDNF affects the homeostasis of the DA system by regulating the release and uptake processes.[94] Following stable DA signal (successive peaks with peak height within 10% of each other), cumulative concentrations of genistein (10, 50, and 100 μM) or tyrphostin 23 (10, 20, and 50 μM) were perfused on brain slice during which measurements were made every 5 minutes and the effect of each dose was monitored for 30 minutes. These concentrations of the drugs have been chosen based on preliminary experiments. When genistein was applied to the striatal brain slice, no

significant alteration in electrically stimulated DA release was observed in wildtype mice (P = 0.094, one-way ANOVA; Figure 6.5A) and BDNF$^{+/-}$ mice (P = 0.602; one-way ANOVA; Figure 6.5B) compared to their respective pre-drug controls. However, perfusing high concentrations of the inhibitor (≥ 50 μM in wildtype mice and 100 μM in BDNF$^{+/-}$ mice) decreased DA uptake rate in the two groups of mice. This observation suggests that tyrosine kinase receptors are involved in regulating the DA transporter function at the presynaptic level. While inhibition of Trk receptors with genistein did not seem to alter presynaptic DA release, we suspect that the drug could also be involved in other non-tyrosine kinase effects.[149, 241, 243-246] To verify that inhibition of Trk receptors could alter both presynaptic DA release and uptake dynamics, stimulated DA release and uptake in presence of tryphostin 23, a more selective Trk receptor inhibitor [149] was measured in both wildtype and BDNF$^{+/-}$ mice. The data obtained showed that when tyrphostin 23 was applied to the striatal slice, there was a significant decrease in electrically stimulated DA release in both genotypes. The uptake rate in the two genotypes (Figure 6.6C and D) was also decreased with increasing concentration of tyrphostin 23. Altogether, the decrease in stimulated DA release and uptake rate observed in the two groups of mice is consistent with our expectation of Trk receptor inhibitor and also with earlier report that that has shown that pre-incubation of rat dorsal striatal synaptosomes with tyrphostin 23 reduces specific uptake of radiolabeled DA into the synaptosomes in a concentration dependent fashion.[149] The present results thus, suggest that FSCV is an important tool to tease apart the effect of Trk receptors on presynaptic DA release and uptake dynamics.

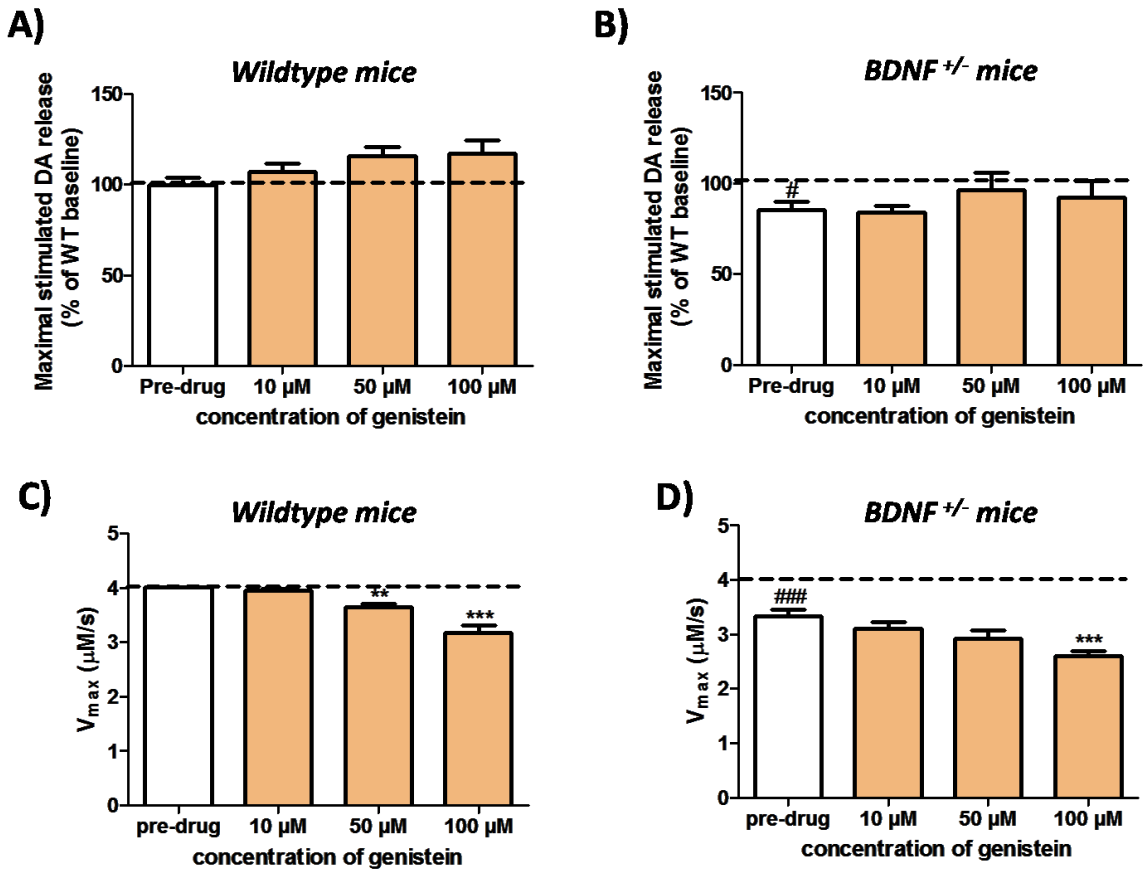

Figure 6.5: Effect of genistein on electrically evoked DA release and uptake in the CPu of wildtype (WT) and BDNF$^{+/-}$ mice. Evoked DA release in presence of perfused genistein was expressed as percentage of WT baseline for A) WT mice and B) BDNF$^{+/-}$ mice. DA uptake rate (V_{max}) was attenuated in presence of high concentrations of genistein for C) WT mice and D) BDNF$^{+/-}$ mice**.** $^{**}P < 0.01$ and $^{***}P < 0.001$ compare to respective pre-drug concentration (one way ANOVA with Dunnette Multiple comparison test), $^{\#\#\#}P < 0.001$ versus WT baseline (Student t-test), n = 5-7/group.

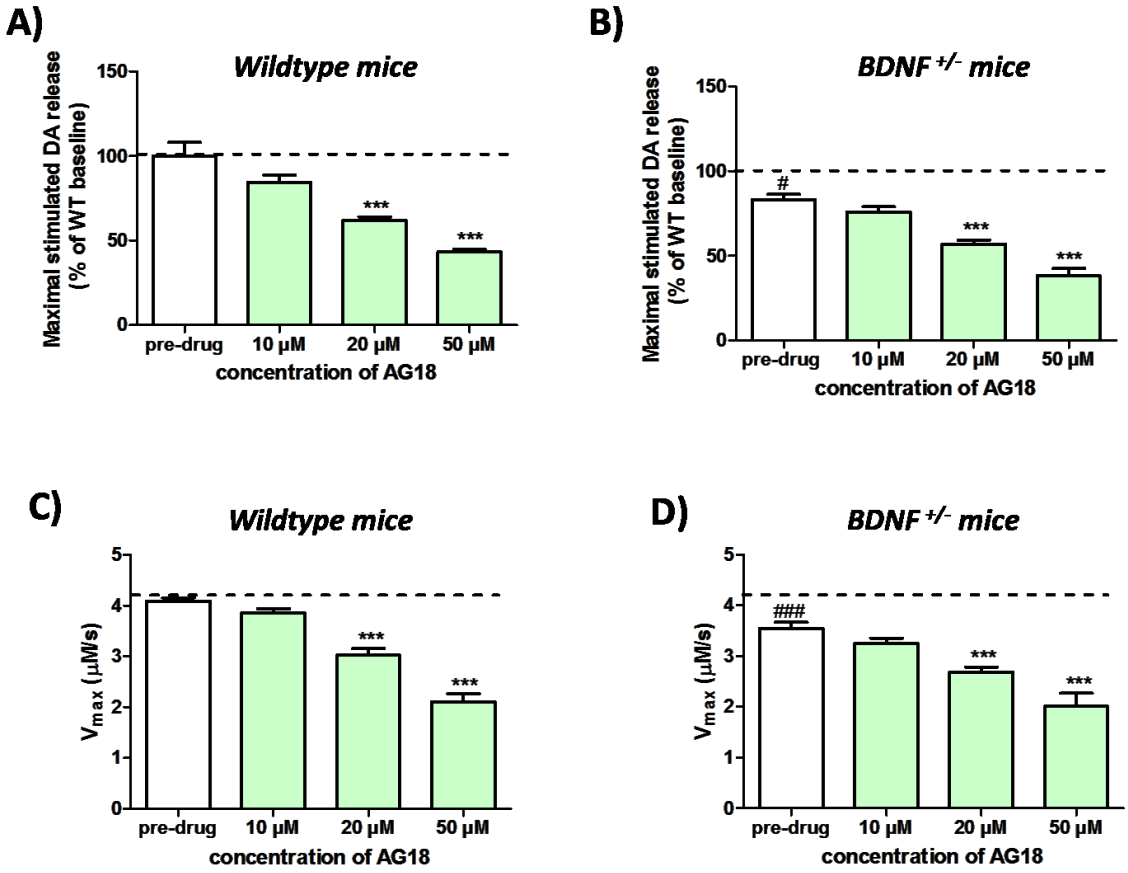

Figure 6.6: Effect of tyrphostin 23 (AG 18) on evoked DA release and uptake in the CPu of wildtype (WT) and BDNF$^{+/-}$ mice. High concentrations of tyrphostin 23 decreased electrically evoked DA release (expressed as percentage of WT baseline) in A) WT mice and B) their BDNF$^{+/-}$ littermates. DA uptake rate (as V_{max}) was decreased in the presence of high concentrations of the inhibitor in C) WT mice D) the mutant mice. ***$P < 0.001$ compare to respective pre-drug concentration (one way ANOVA with Dunnette Multiple comparison test), $^{\#}P < 0.05$ and $^{\#\#\#}P < 0.001$ versus WT baseline (Student -test), n = 4-5/group.

6.4.4 Effect of K252a on presynaptic DA dynamics in wildtype mice

BDNF signaling is mediated by the TrkB receptor.[2, 247] However, it is unclear whether the TrkB receptor activation affects DA release and uptake. To find the answer, we used potent Trk receptor inhibitor, K252a.[248, 249] K252a was perfused over a brain slice for 30 minutes per dose, and its effects were monitored every 5 minutes (Figure 6.7A). Dunnett's post-test revealed a significant ($P < 0.05$) reduction in stimulated DA release only at the highest K252a concentration (3 μM). Increasing the concentration of K252a from 0.01 to 3 μM reduced V_{max} in a concentration-dependent manner (Figure 6.7B and D).

Our results from the CPu of wildtype mouse brain slices show that concentrations less than 3 μM of K252a alone has no effect on electrically stimulated DA release. These results agree with previous studies showing that concentrations of K252a less than 1 μM have no effect on stimulated DA release.[250, 251] Only the highest concentration of K252a applied to brain slices reduced electrically stimulated DA release. We cannot rule out the possibility that K252a reduced the amount of stimulated DA release by acting at other Trk receptors. Although K252a is used to selectively block BDNF-TrkB signaling, it is also a non-specific inhibitor of tyrosine kinase protein activity including the TrkA and TrkC receptor sub-types.[252] Such actions could contribute to the decrease in electrically evoked DA when K252a is applied at the highest concentration.

This is the first report demonstrating the rapid reduction in DA transporter kinetics in the CPu of wildtype mice when K252a concentrations are greater than 0.1 μM and is in agreement with the previous work by Hoover *et al*., where inhibition of tyrosine kinases by genistein (a non-specific Trk inhibitor) or tyrphostin 23 (a selective Trk

inhibitor) resulted in rapid (5 – 15 minute), dose-dependent decreases in [^{3}H]DA uptake rates in a dorsal striatal synaptosomal preparation.[149] It may appear inconsistent that activation of TrkB with BDNF increases stimulated DA release, while inhibition of this receptor reduces DA uptake, but Trk receptors activate multiple signaling pathways. Considerable evidence in the literature suggests a divergent role for TrkB where BDNF activation increases neurotransmission,[94, 233, 239, 251] while Trk inhibitors reduce DA uptake.[149] The exact mechanism causing this divergent response is unknown, but it is hypothesized that inhibition of the Trk receptor blocks autophosphorylation, which reduces activity in numerous signaling cascades such as phosphatidylinositol-3 kinase (PI3K), mitogen-activated protein kinase (MAPK), and extracellular signal-regulated kinase (ERK1/2) reaction pathways, all of which have been linked to decreases in DA transporter activity by decreasing V_{max}.[149, 253-257] The results of this study suggest that inhibition of the TrkB receptor reduces the DA transporter function, but more studies are required to determine the specific Trk-signaling pathways that may be involved in regulating DA transporter kinetics.

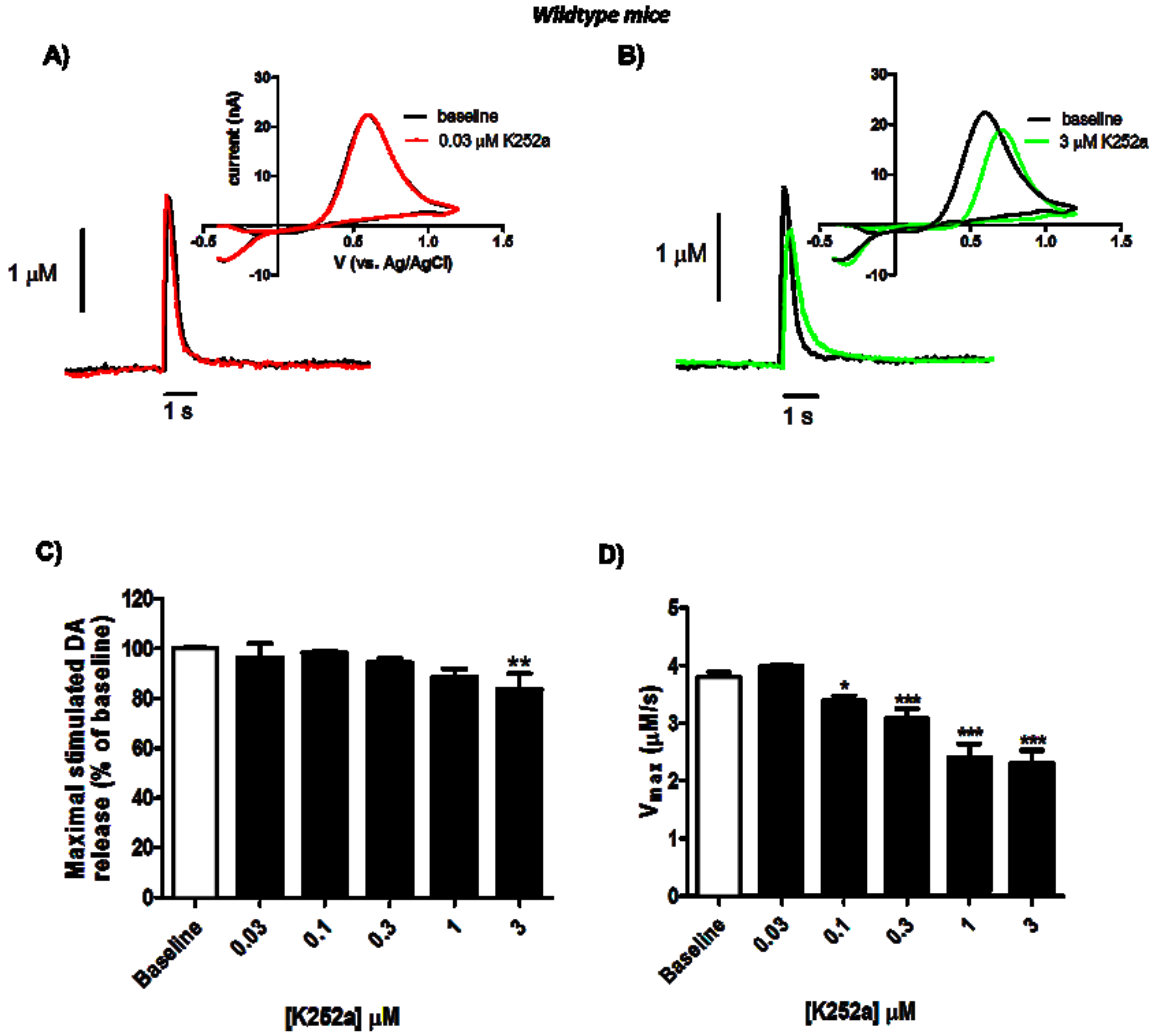

Figure 6.7: Effect of TrkB inhibitor, K252a on stimulated DA release and uptake in the CPu of WT mice. A) Representative DA release and uptake after a 30 minutes perfusion of 0.03 µM K252a compared to pre-drug DA signal shown by their representative current versus times traces with corresponding cyclic voltammograms (inset). B) Effect of 3 µM K252a on DA release and uptake represented in terms of concentration versus time trace and cyclic voltammogram (inset). C) K252a produced a significant effect on stimulated DA release as determined by a one-way ANOVA ($F_{5,61} = 3.05$; $P < 0.05$, n = 4-7). A Dunnett's post-hoc test confirmed that only 3 µM K252a perfusion attenuated stimulated DA release. D) One-way ANOVA ($F_{4,25} = 14.93$; $P < 0.0001$, n = 4 - 7) followed by Dunnett's post-test revealed that K252a concentrations greater than 0.01 µM K252a significantly decreased V_{max}. Data are means ± SEMs (n = 4 - 7 mice). *$P < 0.05$, **$P < 0.01$, ***$P < 0.001$.

6.4.5 K252a inhibits BDNF's ability to acutely modulate striatal DA release in BDNF$^{+/-}$ mice

To demonstrate that exogenously applied BDNF modulates presynaptic DA dynamics via the TrkB receptor electrically evoked DA release, and uptake rates were monitored every 5 minutes following direct application of BDNF (100 ng/mL) only, K252a (1 μM) only, or pre-treatment with K252a prior to BDNF administration to a slice for 30 minutes. In the absence of exogenous applications of BDNF or K252a, electrically evoked DA from the CPu of BDNF$^{+/-}$ mice (referred to as 'baseline' in Figure 6.8) was reduced by ~ 40% compared to their wildtype littermates, which is delineated as the dashed line at 100% (Figure 6.8). Exogenous application of BDNF significantly potentiated stimulated DA release by ~ 16% in BDNF$^{+/-}$ mice ($P < 0.001$), while there was no difference in that of the wildtype mice. Pretreatment of the striatal BDNF$^{+/-}$ slice with K252a abolished this modulatory effect of BDNF, suggesting that the increased DA release may be mediated by presynaptic TrkB receptors. There was no difference in electrically evoked DA release in wildtype mice in the presence of BDNF, K252a or the combination of the two.

The ability of K252a to block the BDNF-induced increase in DA release in the CPu of BDNF$^{+/-}$ mice suggests that the TrkB receptor can mediate DA release. Our findings are in agreement with previous results that have shown BDNF-induced stimulated DA release is blocked in the presence of K252a.[230, 239] An issue with examining monoamine output after BDNF infusion is identifying the specific signal transduction cascade(s) involved. For example, the acute BDNF-potentiation of DA release is suggested to be dependent on PI3 kinase and Ras-MEK activation only.[239]

However, the exact mechanism of how BDNF mediates DA release has remained elusive.

6.4.6 Exogenous BDNF application has no effect on DA dynamics in wildtype mice

Neurotrophic factors, like BDNF are typicallythought of as promoting long-term effects on neurons such as synaptic plasticity, neuronal survival, and differentiation. Our results demonstrate that the acute effects of TrkB activation via BDNF leads to a rapid increase in DA release in the CPu of $BDNF^{+/-}$ mice, while there is no difference in stimulated DA release with BDNF perfusion in our wildtype mice (Figure 6.8C). Previous reports using wildtype mice/rats established that acutely, exogenously applied BDNF enhances synaptic events such as DA release both *in vivo* and *in vitro.*[21, 150, 233] We hypothesize that this difference in BDNF-induced DA release between our wildtype mice and those from previous studies is a result of methodological differences between slices and synpatosomes. For example, all synaptosomal preparations required the co-incubation of BDNF and high K^+ artificial cerebral spinal fluid (aCSF) over a time course of minutes to observe BDNF-potentiated DA release.[21, 150, 233, 239] Furthermore, DA release was measured as an accumulation of exogenously applied ^{3}[H]-DA, while our wildtype slices received a one-millisecond electrical stimulation that recruited endogenous DA. Taken together, an acute perfusion of BDNF can rapidly potentiate DA release in a system with low endogenous BDNF levels, but in a normal system, like that of wildtype mice, stronger stimulation parameters may be required.

6.4.7 K252a does not modulate striatal DA transporter kinetics in $BDNF^{+/-}$ mice

Studies have also suggested a role for Trk receptors in modulation of DA uptake

evidenced by the use of Trk inhibitors, which have been shown to alter DA transporter function, expression and/or kinetics.[149] An advantage of slice FSCV is that both presynaptic DA release and uptake are simultaneously evaluated. The objective was to use FSCV to determine if an exogenous application of BDNF influences DA transporter kinetics as it does with DA release. Exogenous BDNF applications only potentiate evoked DA release with no difference in DA uptake rates in $BDNF^{+/-}$ mice (Figure 6.8D). Therefore, we have hypothesized that the 50% reduction in DA transporter function is the compensatory response to having a life-long reduction in BDNF levels since this parameter was unaltered.[94] There was no effect of K252a on DA V_{max} in $BDNF^{+/-}$ mice. With respect to DA transporter expression in $BDNF^{+/-}$ mice, when the mice are less than 6 months of age, there is no difference in DA transporter expression or activity.[258, 259] But little research has focused on evaluating whether TrkB inhibition influences DA transporter function or expression in $BDNF^{+/-}$ mice. There is no difference in striatal TrkB and phosphorylated TrkB (pTrkB) levels between the genotypes.[108] However, $BDNF^{+/-}$ mice show an increase in the ratio of striatal pTrkB/TrkB with a concomitant potentiation in striatal pERK/tERK2 levels.[108] In order to better understand *if and how* tyrosine kinase receptors modulate DA transporter expression or activity, future studies should evaluate specific intracellular cascades that may mediate the interactions between TrkB and the DA transporter.

6.4.8 K252a modulates striatal DA transporter kinetics in the presence or absence of exogenous BDNF in wildtype mice

Interestingly, perfusion of K252a in the presence or absence of BDNF significantly attenuated DA uptake rates in wildtype mice (analyzed by Dunnett's post-

test $P < 0.05$). These results show that Trk inhibition in wildtype slices has the ability to modify/regulate DA transporter kinetics given the reduction seen upon application of K252a alone. Although K252a has been shown to have no effect on DA V_{max} when applied to rat dorsal striatal synpatosomes, the same cannot be said about non-selective tyrosine kinase inhibitors.[149] When the non-selective tyrosine kinase inhibitors genistein and tyrphostin-23 were acutely applied, a significant decrease of striatal DA transporter surface expression and V_{max} were observed, but K_m was not different.[149] Western blotting suggested that this mechanism of decreasing DA transporter V_{max} and surface expression was mediated via MAPK p42 and p44 isoforms as these phosphorylated levels were decreased after inhibition.[149] The difference between the present results and those obtained by Hoover *et al.* with respect to K252a, could be due to the 10-fold less concentration of K252a (10 vs. 1000 nM, respectively) than what we used. In the present study, the high concentration of K252a could be non-selectively binding to other tyrosine kinase receptors such as the TrkA and TrkC sub-types, which, in turn, could be inducing a reduction of striatal DA uptake rates. Furthermore, there are numerous methodological differences between our FSCV results and the results obtained via the synpatosome preparations that Hoover *et al*. used. First, there is the species difference, rat versus mouse. Second, different methods were used to analyze uptake rates and their respective temporal resolution. Slice FSCV measures millisecond stimulated endogenous DA to evaluate DA release and uptake rates (V_{max}), where K_m is fixed, while synpatosome preparations require minutes to collect enough DA to analyze uptake parameters.

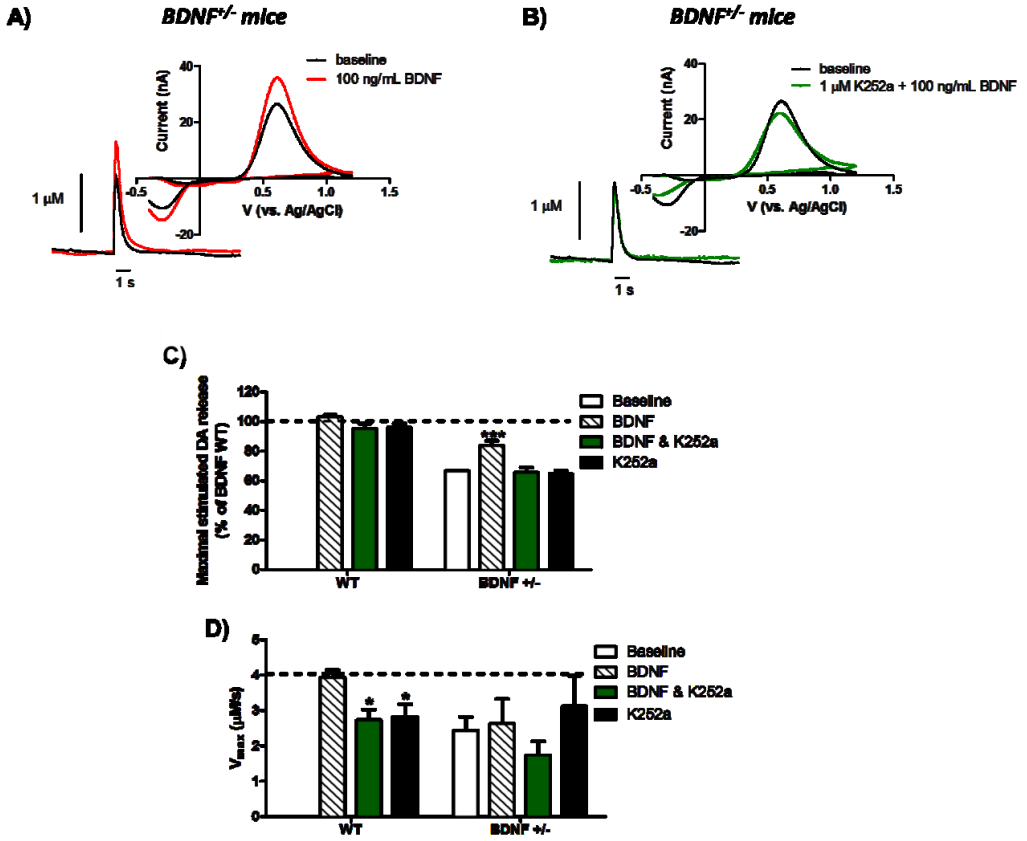

Figure 6.8: Effect of exogenous application of BDNF (100 ng/mL) on DA release and uptake rates in the CPu of WT and BDNF$^{+/-}$ mice. A) Representative current versus times traces with corresponding cyclic voltammograms (inset) from BDNF$^{+/-}$ mice before and after BDNF infusion. B) K252a blocked the ability of BDNF to potentiate DA release in the CPu of BDNF$^{+/-}$ mice as shown in representative current versus times traces with corresponding cyclic voltammograms (inset). C) Normalized single pulse, electrically evoked DA release represented as % of WT baseline, wildtype mice are represented by the dashed line. Two-way ANOVA of electrically stimulated DA release in response to drug application showed a main effect of treatment ($F_{3,74}$ = 10.37, P < 0.001), genotype ($F_{1,74}$ = 216.9, P < 0.001), while there was no treatment X genotype interaction ($F_{3,74}$= 2.612, P = 0.056). D) DA uptake rates in WT and BDNF$^{+/-}$ mice before and after 30 minute perfusion of either 100 ng/mL BDNF, 1 µM K252a, or both in the caudate putamen. A two-way ANOVA evaluating DA uptake kinetics indicated there was no difference in the main effect of treatment ($F_{3,82}$ = 2.09, P = 0.11) and treatment X genotype interaction ($F_{3,82}$ =1.45, P = 0.23). There was a significant main effect for genotype ($F_{1,82}$ = 7.38, P < 0.01), corroborating that the kinetics of the DA transporter are reduced in BDNF$^{+/-}$ mice versus wildtype mice (P < 0.01). Data are means ± SEMs (n = 4 – 5 mice per treatment group). ***P < 0.001 compared to untreated BDNF$^{+/-}$ mice (two-way ANOVA). *P < 0.05 as compared to WT mice baseline (one-way ANOVA).

6.4.9 TrkB agonist, 7,8-DHF potentiates electrically evoked DA release in the CPu of only wildtype mice

The TrkB agonist, 7,8-DHF has been reported to be neuro-protective when administered prior to a DA-neurotoxic treatment using 1-methyl-4-phenyl-1,2,3,6-tetrahydropyridine (MPTP).[260] To examine the ability of 7,8-DHF to modulate presynaptic DA dynamics, a cumulative dose (0.01, 0.03, 0.1, 0.3, 1.0, 3.0, 10, and 30 μM) of 7,8-DHF was applied to striatal brain slices following a stable, electrically evoked DA signal. The effect of 7,8-DHF on DA release and uptake processes was measured every 5 minutes for 30 minutes per dose in both wildtype and $BDNF^{+/-}$ mice. A dose response curve for the effect of cumulative dose of 7,8-DHF on electrically evoked DA release in wildtype mice was normalized to percent of baseline stimulated DA. In the wildtype mice 10 μM 7,8-DHF significantly increased stimulated DA release, where the half maximal effect (EC_{50} value) of 7,8-DHF is at ~ 150 ± 12 nM (n = 8, Figure 6.9C). With respect to $BDNF^{+/-}$ mice, there was no difference in DA release after perfusion of 7,8-DHF ($F_{8,90}$ = 0.014, P = 0.89). Stimulated DA release data from $BDNF^{+/-}$ mice was normalized with respect to wildtype mice since stimulated DA release levels are different under basal conditions (Figure 6.9C). Concentrations of 7,8-DHF greater than 1 μM show an ~ 10% further reduction in stimulated DA release levels in $BDNF^{+/-}$ mice. These results in the $BDNF^{+/-}$ mice are surprising since we initially predicted that $BDNF^{+/-}$ mice would have a leftward shift in their dose response curve based on their results with BDNF perfusion. However, future studies are required to better understand how 7,8-DHF induces DA release.

6.4.10 TrkB agonist, 7,8-DHF has no effect on DA transporter kinetics in the CPu across the genotypes

There was no difference in DA transporter V_{max} rates in wildtype mice ($F_{8,207}$ = 0.32, P = 0.99, Table 1). While a one-way ANOVA revealed a significant main effect of 7,8-DHF on the DA uptake rate in $BDNF^{+/-}$ mice ($F_{8,89}$ = 3.19; P < 0.01, Table 1). Only concentrations 3.0 and 30 μM 7,8-DHF had a significantly decreased DA V_{max} rates in $BDNF^{+/-}$ mice as analyzed by a Dunnett's post-test analysis (P < 0.05).

Similar to BDNF, acutely applied 7,8-DHF does not affect striatal DA transporter kinetics in the wildtype mice. However, it is unknown what higher BDNF concentrations (> 200 ng/mL) will do given its prohibitive cost. Thus, it is difficult to know if higher concentrations of BDNF would have a similar effect on DA transporter kinetics as 7,8-DHF. Although it is possible that these high concentrations of 7,8-DHF (> 3.0 μM) are non-specific and activating other Trk receptor subtypes like TrkA and TrkC, we have not evaluated these receptor subtypes nor their ability to regulate presynaptic DA dynamics, and cannot rule out their contribution to presynaptic DA dynamics especially at these higher doses. Overall, the primary acute effect of 7,8-DHF does not appear to regulate striatal DA transporter kinetics in wildtype mice.

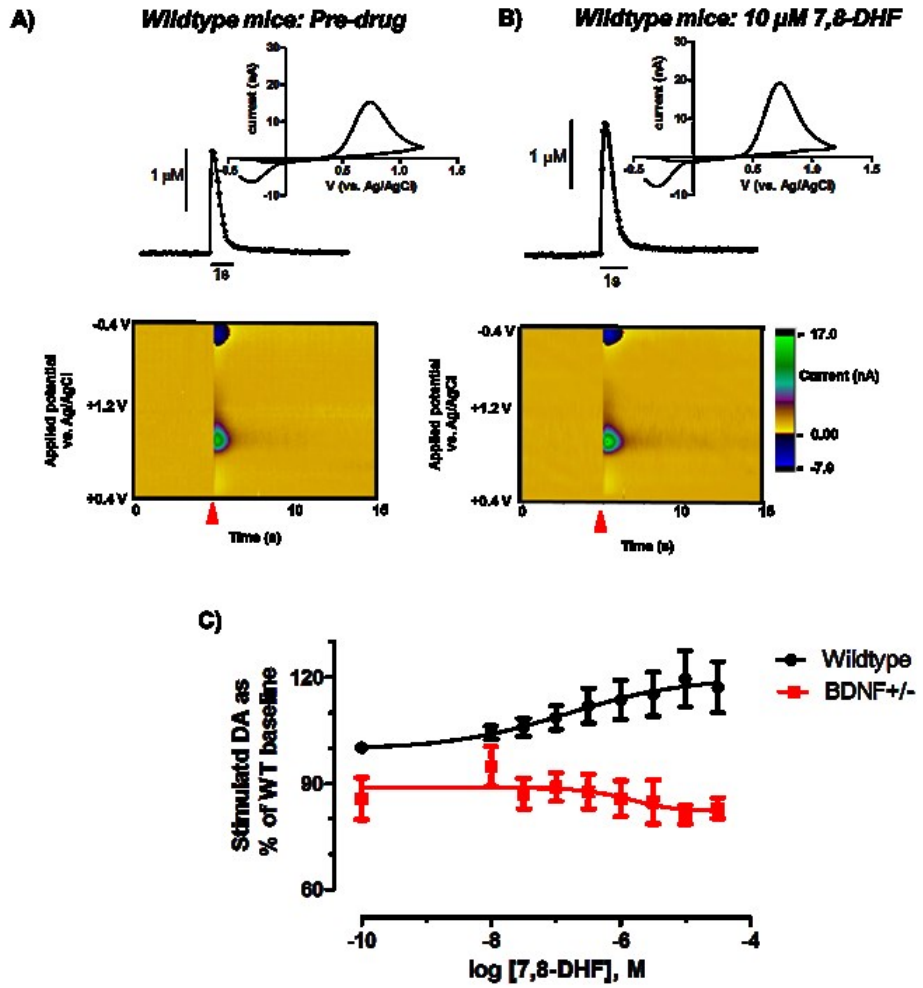

Figure 6.9: Effect of cumulative dose of TrkB agonist, 7,8-DHF on electrically evoked DA release in the CPu of WT and BDNF$^{+/-}$ mice. A) Current versus time trace of pre-drug DA signal with corresponding false color plot and cyclic voltammogram (inset). The false color plots present data in terms of time (x-axis) versus voltage (y-axis) versus current (color), where the green and blue colors denote oxidation and reduction current, respectively. The red triangle represents the point of electrical stimulation. B) Current versus time trace of electrically evoked DA release after a 30 minute perfusion of 10 µM 7,8-DHF with corresponding false color plot and cyclic voltammogram (inset). C) Dose response curve of the effect of cumulative dose of 7,8-DHF on electrically evoked DA release in WT and BDNF$^{+/-}$ mice, which is normalized to percent of wildtype baseline stimulated DA. In the wildtype mice, there was a significant main effect of 7,8-DHF on stimulated DA release ($F_{8,204}$ = 0.18, P < 0.05) as determined by one-way ANOVA. A Dunnett's post-test analysis indicated that 10 µM 7,8-DHF significantly increased stimulated DA release (P < 0.05) in wildtype mice. The cumulative dose of 7,8-DHF did not alter electrically evoked DA release in BDNF$^{+/-}$ mice (n = 3 - 4). Data are means ± SEMs.

6.4.11 K252a blocks the ability of 7,8-DHF to increases DA release in wildtype mice

To demonstrate that 7,8-DHF is mediating its effect through the TrkB receptor, K252a (30 nM) was applied to the brain slice prior to agonist application. The objective was to block the 7,8-DHF mediated increases in electrically evoked DA in wildtype mice. A concentration of 10 μM 7,8-DHF was applied to the slices; this dose was chosen because it potentiated stimulated DA release in wildtype mice with no effect on DA transporter kinetics. A one-way ANOVA showed a main effect that wildtype mice respond differently depending on TrkB treatment ($F_{3,68} = 3.29$; $P < 0.05$, Figure 6.10C). Wildtype mice showed an approximate 20% increase in stimulated DA release after 7,8-DHF ($P < 0.05$) only. While there was no difference in stimulated DA release after K252a only. When wildtype striatal slices were pretreated with K252a followed by 7,8-DHF applications, stimulated DA release was blocked. These results with K252a and 7,8-DHF demonstrate that the potentiated stimulated DA release in wildtype mice is mediated via the TrkB receptor. Numerous reports have indicated that 7,8-DHF is an agonist for the TrkB receptor [261-268] and our results further confirm these previous findings. 7,8-DHF, like exogenous BDNF applications can quickly regulate trophic factor pathways leading to activation, and/or recruitment of DA release mechanisms. These results further highlight the hypothesis that enhancement of trophic factors or their agonist not only regulate long-term synaptic events such as synaptic plasticity, neuronal differentiation, or survival, but that there is an immediate response to trophic factors. Although with FSCV we have only evaluated DA in the CPu after 7,8-DHF, others have shown that this acute TrkB activation via BDNF is not exclusive to DA or monoamines

like serotonin, but influences other systems like GABA and glutamate.[233, 239, 251]

6.4.12 K252a and 7,8-DHF have no effect on DA transporter kinetics in wildtype mice

To confirm that 7,8-DHF applications is exclusive to DA release dynamics, DA uptake rates were evaluated. A one-way ANOVA showed no effect of TrkB treatment on V_{max} ($F_{3,80}$ = 1.18, P = 0.32, Fig. 6B) in wildtype mice. By decreasing the amount of K252a that is bathed over the slice, we demonstrated that this lower dose could still inhibit TrkB release without effecting DA transporter kinetics in wildtype mice. Together, these results from wildtype mice confirm the hypothesis that 7,8-DHF is mediating DA release via the TrkB receptor in wildtype mice with no effect on DA uptake kinetics.

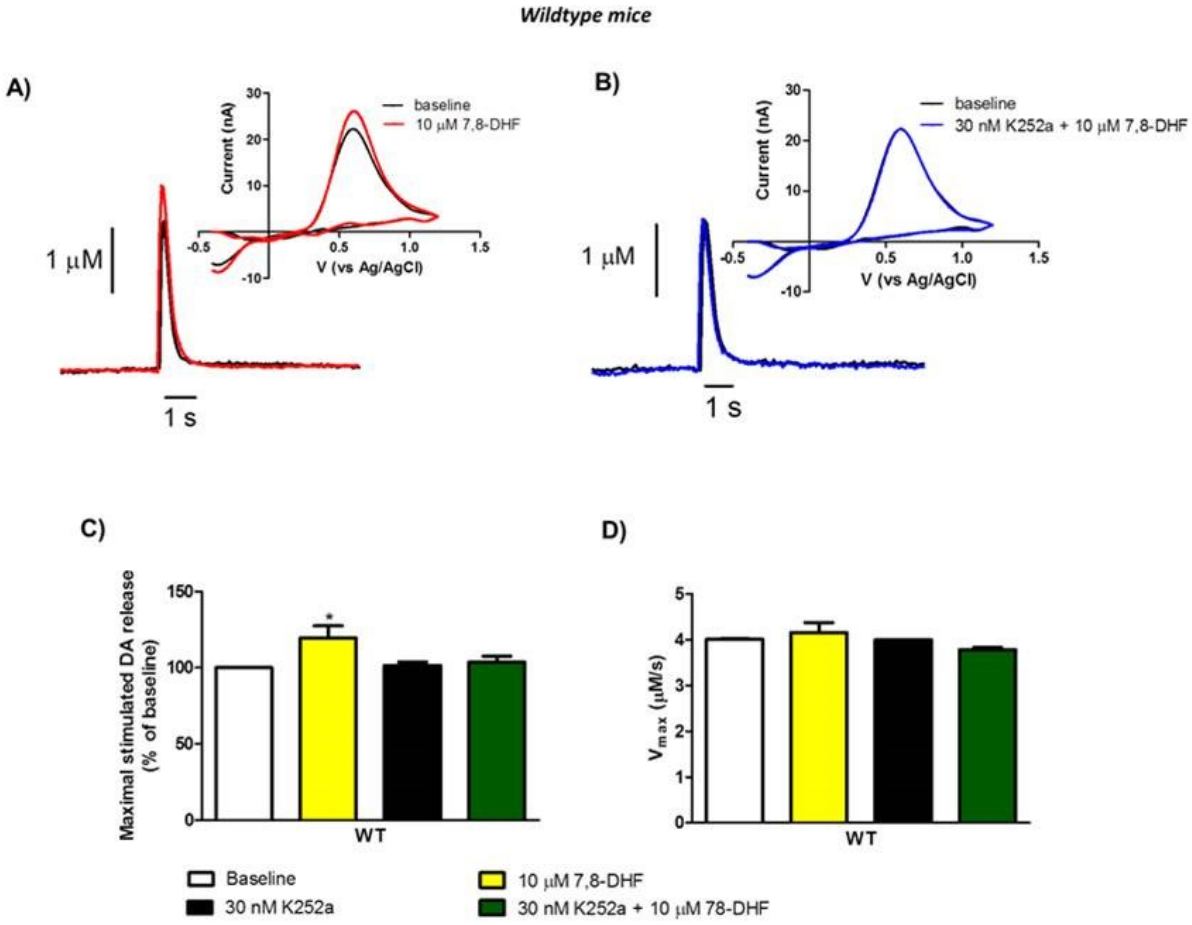

Figure 6.10: K252a blocks the effect of 7,8-DHF in the CPu of WT mice. A) Representative current verse time traces with corresponding cyclic voltammograms (inset) showing perfusion of 7,8-DHF potentiates DA release in the wildtype mice. B) Blocking the TrkB receptor with K252a inhibits the 7,8-DHF mediated increase in DA release shown by representative current versus time traces and cyclic voltamograms (inset) C) Perfusion of 10 μM 7,8-DHF significantly increases electrically stimulated DA release in the wildtype mice. Evoked DA release mediated by the TrkB agonist 7,8-DHF is blocked in presence of 30 nM K252a. D) Neither 30 nM K252a nor 10 μM 7,8-DHF altered DA uptake rate in wildtype mice. Data are means ± SEMs (n = 4 - 8 mice). Statistical significance was determined by one-way ANOVA with Dunnett's Multiple Comparison Test; **P* < 0.05.

Table 6.1. The effect of TrkB agonist on dopamine uptake rates

Agonist table			
Genotype	**Agonist**	**[Agonist]**	**V_{max} (μM/s) (Mean ± SEM)**
$BDNF^{+/-}$	BDNF (ng/mL)	Pre-drug	2.2 ± 0.2
		50	2.2 ± 0.2
		100	2.2± 0.2
		200	2.3 ± 0.2
	7,8-DHF (μM)	Pre-drug	3.0 ± 0.03
		0.010	3.0 ± 0.02
		1.00	2.7 ± 0.1
		30.0	2.4 ± 0.2**
Wildtype		Pre-drug	4.0 ± 0.01
		0.010	4.1 ± 0.12
		1.00	4.0 ± 0.1
		30.0	3.9 ± 0.2

*Significantly different from pre-drug control, **P < 0.01.*

6.5 Conclusions

A long-term goal in neuropharmacology has been to find small molecules that could mimic trophic factors and be easily administered where the small molecules could pass through the blood-brain barrier. With the recent discovery that 7,8-DHF is an agonist for TrkB receptors, numerous *in vivo* studies have shown that sub-acute applications of 7,8-DHF lead to many of the same benefits as that of a direct application of BDNF.[260, 263, 265, 266] The results from this study highlight the utility of FSCV to probe acute, striatal BDNF/TrkB receptor mediated DA release and uptake. An advantage of using FSCV versus traditional synaptosomal models is that we can quickly measure both DA release and uptake in a close to normal physiological state. FSCV has shown that a more "physiological" stimulation (1 ms) potentiates stimulated DA release in the presence of 7,8-DHF and BDNF in wildtype and $BDNF^{+/-}$ mice, respectively. This divergent role between 7,8-DHF and BDNF activating DA release may be a result of using a mouse model with a 50% reduction in BDNF protein levels, where there are not only intrinsic alterations in the BDNF/TrkB system but other neuroadaptions throughout the brain that are still unaccounted for. Our FSCV results are not limited to the evaluation of a TrkB agonist, but we also examined tyrosine kinase inhibitors. K252a did not have any effect on stimulated DA release except at the highest dose (3 μM), while concentrations greater than 1 μM altered DA transporter kinetics. Since DA uptake V_{max} was altered in both genotypes at concentrations greater than 1 μM of K252a, this suggests a promiscuous response. Although K252a is often described as a TrkB inhibitor, it is a non-selective protein kinase inhibitor that inhibits PKC, Ca^{2+}/calmodulin-stimulated phosphodiesterases (IC_{50} = 1.3 - 2.9 μM from Tocris on-line catalog), MLCK

(K_i = 20 nM from Tocris on-line catalog) and receptor tyrosine kinases, suggesting that TrkB or some other signaling system that K252a inhibits is influencing DA transporter uptake rates. Genistein did not have any effect of stimulated DA release but at high concentrations, it did significantly attenuated DA uptake. Tryphostin 23, on the other hand, decreased both DA release and uptake in both genotypes of mice examined. By using FSCV, we were able to delineate a more comprehensive understanding of how TrkB receptor activation can modulate presynaptic DA dynamics using BDNF, a TrkB receptor agonist, or inhibitors.

CHAPTER 7

Summary and Conclusions

The striatal dopamine (DA) system is a key player in learning, memory, motor functions, and reward related behaviors, and has been implicated in neurological disorders including addition.[2, 3, 14] Thus, understanding the DA system is crucial to provide the opportunity for new and improved therapeutic options for addiction as well as other neurological disorders. The present study was undertaken to: 1) provide insight into how toluene exposure modulates the striatal DA system, and 2) understand how the protein; brain-derived neurotrophic factor (BDNF), modulates striatal DA dynamics. The present chapter highlights the findings from these two main projects discussed in this dissertation and suggests future studies that will provide further insight to the present work.

7.1 Understanding how toluene modulates the DA system

Toluene inhalation has debilitating consequences on mental health.[47, 49, 192] However, not much is known about toluene's exact neural target. Although existing evidence has shown that toluene abuse influences the DA system, the mechanism underlying toluene's effect on the DA system remains elusive.[36, 38] In the present study, behavioral assays and neurochemical techniques were employed to better understand the effect of toluene inhalation on the DA system. Behavioral assays serve as a complimentary tool to neurochemical assays, since changes in behavior predict possible neurochemical effects of toluene.[34, 138, 141] The behavioral assays also provide the opportunity to identify possible similarities between abused toluene and other drugs of abuse whose neurobehavioral profiles have been well characterized in animal

models.[56] Neurochemical technique such as slice fast scan cyclic voltammetry (FSCV) provides the ability to monitor the fast DA dynamics such as release and uptake and to assess toluene's effect on the functionality of the DA autoreceptors. *In vivo* microdialysis provides the ability to monitor extracellular DA levels, whereas tissue content analysis enables evaluation of toluene's effect on intracellular DA levels and its catabolism. In all, two main exposure models were used: an acute toluene exposure model, which allowed evaluation of how brief exposure to toluene modulates the striatal DA system and a repeated toluene model which enabled the impact of chronic toluene inhalation on the DA system to be examined.

Using behavioral testing, we characterized the effect of acute and repeated toluene exposure on locomotor activity in mouse models. The results suggest a biphasic response where acute toluene exposure increased locomotor activity, while repeated toluene exposure caused sensitization to toluene induced locomotor activity. Our working hypothesis was that these differences in locomotor activity were linked to alterations in the striatal DA system. To test this hypothesis, the first objective was to characterize the effect of toluene inhalation on DA dynamics using FSCV. For the acute experiment, mice were exposed to 30 minutes of toluene inhalation followed by 30 minutes of recovery before FSCV measurements were made. In the repeated model, mice were treated to the same routine for seven consecutive days and neurochemical measurements were obtained on the eighth day to evaluate the long-term effect of chronic toluene inhalation. FSCV data revealed that acute toluene exposure potentiates electrically evoked DA release across the striatum (caudate putamen, CPu; nucleus accumbens, NAc core and shell), while repeated toluene inhalation attenuates

electrically evoked DA release in the NAc core and shell but not in the CPu. Acute or repeated toluene exposure does not affect DA uptake rate in the striatum. Taken together, these acute and repeated toluene measurements suggest that repeated toluene exposure has the opposite effects on DA dynamics compared to acute exposure. On the basis of these initial data, our hypothesis was that repeated toluene exposure would lead to downward regulation of DA release in the NAc, which may be mediated by DA autoreceptors. DA autoreceptors play an important role in regulating extracellular DA levels by modulating DA release and synthesis.[182, 194-197] Across the striatum, DA D3 autoreceptors are predominantly expressed in the NAc than in CPu while DA D2 autoreceptors are homogenously expressed across the striatum.[182-186] Since the attenuation in DA release caused by repeated toluene exposure was exclusive to the NAc, we suspected that DA D3 autoreceptors would be involved in toluene's mechanism of action.

Building on our initial neurochemical characterization, the acute toluene exposure model was modified by excluding the recovery phase from the regimen whereas in the repeated model, neurochemical measurements were made on the seventh day immediately after the seventh toluene exposure. The changes made to these exposure protocols were to gain a better understanding of the immediate effects of toluene treatment on the DA system. Using FSCV, we confirmed that acute toluene inhalation potentiates DA release across the striatum, while repeated toluene exposure decreases DA release in the NAc core. Overall, acute toluene exposure had no effect on DA uptake in the striatum, but the only exception was the NAc shell, which showed an elevation in DA uptake only at a low toluene dose. For repeated toluene exposure, there

was no difference in DA uptake rates in the CPu, but DA uptake appeared altered in the NAc. Furthermore, the follow up experiments extended the preliminary work by showing that these toluene-induced alterations in the striatum are not mediated by DA D3 autoreceptors as previously proposed. To examine the influence of toluene exposure on extracellular DA levels, a toluene exposure set-up that allowed toluene exposure and *in vivo* microdialysis measurements to be made simultaneously was constructed. This set-up also allowed monitoring of locomotor behavior of the mice during microdialysis measurement. Microdialysis data showed that the potentiation in DA release induced by acute toluene exposure (as measured by FSCV) does not lead to increased extracellular DA level in the CPu, even though the behavior data taken simultaneously showed increased locomotor activity. Thus, it appears that the increase in locomotor activity was not mediated by extracellular DA levels in the CPu. Furthermore, acute toluene exposure did not alter intracellular DA levels as measured by tissue content analysis, suggesting that the increase in stimulated DA release induced by acute toluene exposure (as measured by FSCV) was not a result of elevated intracellular DA levels or excess DA accumulation in vesicles. However, there were decreases in DA catabolism in both the CPu and NAc as measured by tissue content (Figure 7.1). Meanwhile, repeated toluene exposure elevated extracellular DA levels in the NAc, which we believe may be the alteration underlying the sensitization effect on locomotor activity observed previously in our behavior characterization. On the other hand, repeated toluene exposure did not alter intracellular DA levels or DA catabolism across the striatum as shown by the tissue content data (Figure 7.1).

Overall, with no effect of acute toluene exposure on DA uptake, DA D3 autoreceptors, extracellular and intracellular DA levels, it is most likely that toluene's action on stimulated DA release is mediated through an indirect mechanism rather than a direct action on DA autoreceptors or synthesis. However, exactly how toluene is influencing DA release is not known. Significant evidence has shown that toluene influences glutamate receptors and gamma-aminobutyric acid (GABA) receptor $GABA_{A,}$[78-80] as well as toluene's influence on voltage-gated calcium, potassium, and sodium channels.[37, 269-271] In addition, there are reports that have shown that both acute and chronic toluene treatment can stimulate the generation of reactive oxygen (ROS) and reactive nitrogen species (RNS) in the brain, which can interfere with the functions of enzymes, receptors, and ion channels.[272, 273] It is therefore possible that toluene could be influencing the DA system through these non-DA receptors and ion channels that have been implicated in toluene's neural action. In the work done by Avshalumov and colleagues, a mechanism underlining normal striatal DA release process was presented.[274] In their work, slice FSCV was used to demonstrate that striatal DA release can be modulated by glutamate and GABA receptors through a ROS; hydrogen peroxide (H_2O_2).[274] Since there are no glutamate and GABA receptors on the DA terminal, this modulatory effect has been described as an indirect mechanism, where the H_2O_2 mediating the effect is produced in a non-DA cell.[274-276] Interestingly, the actions of glutamate and GABA in this mechanism are independent of their conventional roles in excitatory and inhibitory circuitries, respectively.[274] In this mechanism, activation of glutamate receptor; alpha-amino-3-hydroxy-5-methyl-4-isoxazole propionic acid (AMPA) receptors, generates H_2O_2 that diffuses to the DA terminal where it opens

potassium channels causing hyperpolarization of the DA neuron and in turn decreases DA release.[274] However, activation of $GABA_A$ receptors is proven to inhibit this H_2O_2 mediating effect causing an increase in DA release.[274] Since the key mediators in this proposed pathway have been implicated in toluene's action, it is possible that their perturbation by acute or repeated toluene inhalation could lead to these alterations in DA release.[274] However, future studies will be necessary to validate this assertion.

7.1.1 Overall conclusion and future direction

Taken together, the present work has utilized behavior and neurochemical techniques as complementary tools to provide useful insight into how the abuse solvent toluene modulates the striatal DA system. The findings from the present work have led us to propose that toluene's action on the striatal DA release process may be mediated through an indirect mechanism that involves other neurotransmitters such as glutamate or GABA as well as the neuromodulator H_2O_2. Future studies are recommended to examine this hypothesis by examining how inhibition or activation of these non-DA receptors and ROS would influence toluene-induced alterations in the DA system, particularly DA release.

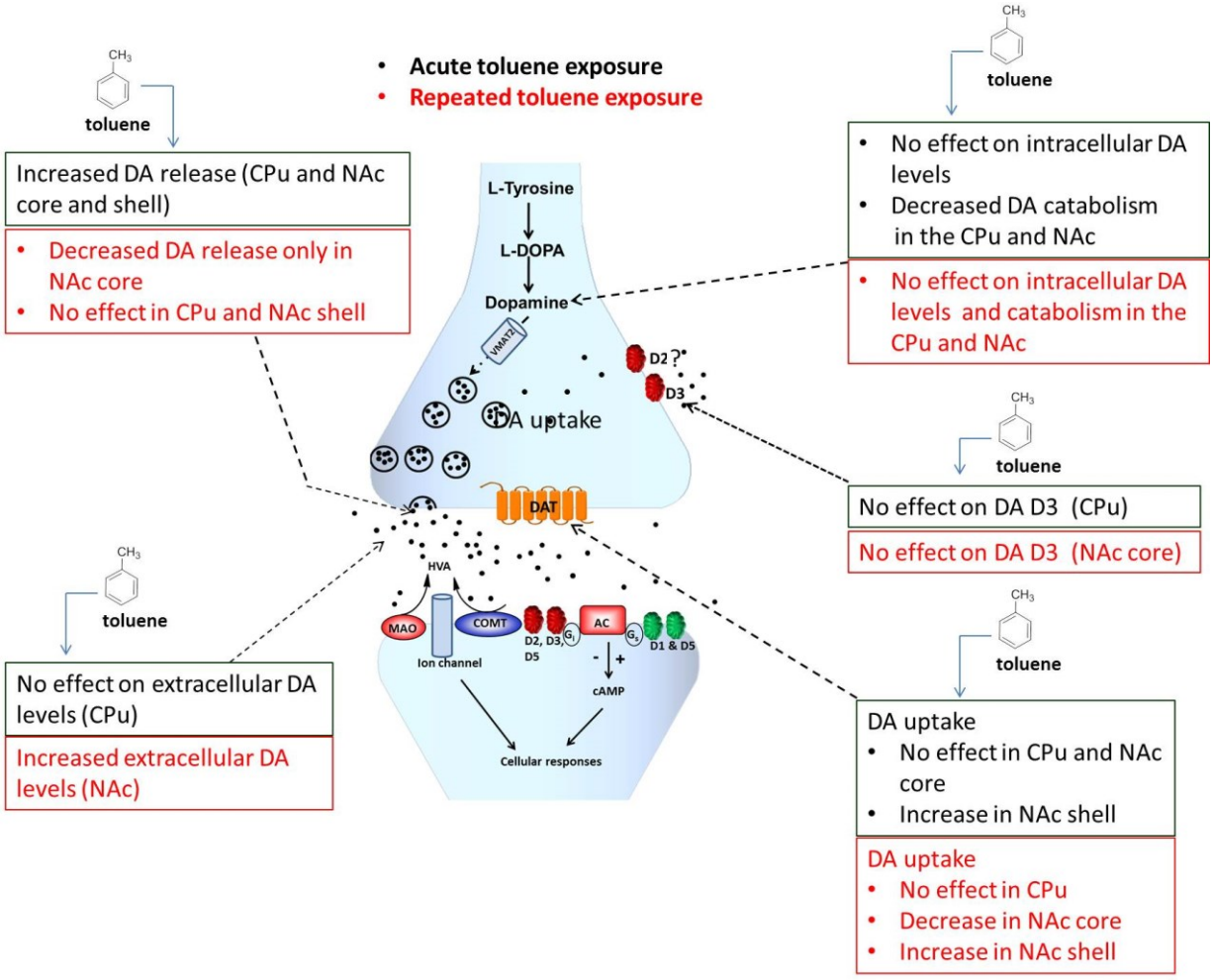

Figure 7.1: Schematic diagram summarizing the effects of toluene exposure on striatal DA system. Acute toluene treatment involved 30 minutes toluene inhalation followed by neurochemical measurements. Repeated toluene exposure involved 30 minutes toluene treatment for 7 consecutive days followed by neurochemical measurements. Striatal regions examined were caudate putamen (CPu), nucleus accumbens (NAc) core and shell. DA parameters examined include release and uptake as well as autoreceptor functionality measured by slice fast scan cyclic voltammetry (FSCV); extracellular DA levels measured by *in vivo* microdialysis; intracellular DA and metabolites measured by tissue content analysis. Definitions from the diagram: L-DOPA, L-3,4-dihydroxyphenylalanine; VMAT, vesicular monoamine transporter; DAT, dopamine transporter; MAO, monoamine oxidase, COMT, catechol-O-methyltransferase; HVA, homovanillic acid; G_i and G_s,

7.2 Probing the ability of presynaptic tyrosine kinase receptors to regulate striatal DA dynamics

Overall, the second objective of the present work seeks to understand how BDNF modulates striatal DA dynamics. Since BDNF executes its neurotrophic functions via activation of TrkB receptors, the main goal was to examine how these TrkB receptors mediate the effect of BDNF on striatal DA dynamics. To achieve this goal, slice FSCV's ability to monitor the action of tyrosine kinase (Trk) receptors on DA release and uptake was first assessed in the CPu of BDNF-deficient mice and their wildtype counterparts. Previously, it was shown that activation of TrkB receptors by exogenous BDNF increased electrically stimulated DA release, so we expected that application of a Trk antagonists would decrease electrically stimulated DA release.[94] Herein, we demonstrated FSCV's ability to measure Trk receptor mediated changes in the DA dynamics by showing that the presence of Trk antagonist, genistein decreases only DA uptake while a more potent antagonist; Tyrphostin 23, decreases DA release and uptake in both groups of mice examined. In subsequent experiments, we characterized the functional effect of TrkB receptors on DA release and uptake using BDNF, 7,8-dihydroxyflavone (7,8-DHF) and K252a (Figure 7.2). 7,8-DHF is a recently discovered TrkB agonist shown to have similar ability to influence presynaptic DA dynamics like BDNF.[260] The abilities of BDNF and 7,8-DHF to increase striatal DA release were demonstrated. The ability of BDNF and 7,8-DHF to elevate stimulated DA release were abolished by the TrkB receptor antagonist, K252a. Hence BDNF and 7,8-DHF modulate striatal DA release through activation of TrkB receptors.

7.2.1 Overall conclusion and future direction

Taken together, our findings demonstrated FSCV's ability to measure Trk mediated alterations in the presynaptic DA dynamics. The unique advantage that FSCV brings to studying the protein BDNF is its high temporal resolution of up to 100 ms that allows monitoring of BDNF's influence on DA dynamics in real time. Additionally, FSCV allows monitoring of DA release and uptake simultaneously.

Overall, the results from the present work support the assertion that BDNF modulates striatal presynaptic DA release through activation of TrkB receptors. However, the intracellular signaling cascades that mediate this action of TrkB receptors on presynaptic DA release are not well understood. The intracellular signaling cascades that are evoked upon Trk activation are categorized into three main pathways: phospholipase Cγ (PLCγ), the Ras/mitogen activated protein kinase (MAPK), and phosphatidylinositol-3-kinase (PI3K).[2, 19, 29] These intracellular signaling cascades are known to mediate several biological functions including neurotransmitter release (Figure 7.2).[2, 19-21, 29, 277] Future studies should further the present work by using FSCV to probe how TrkB receptors and their intracellular signaling components modulate presynaptic DA release and uptake in the striatum.

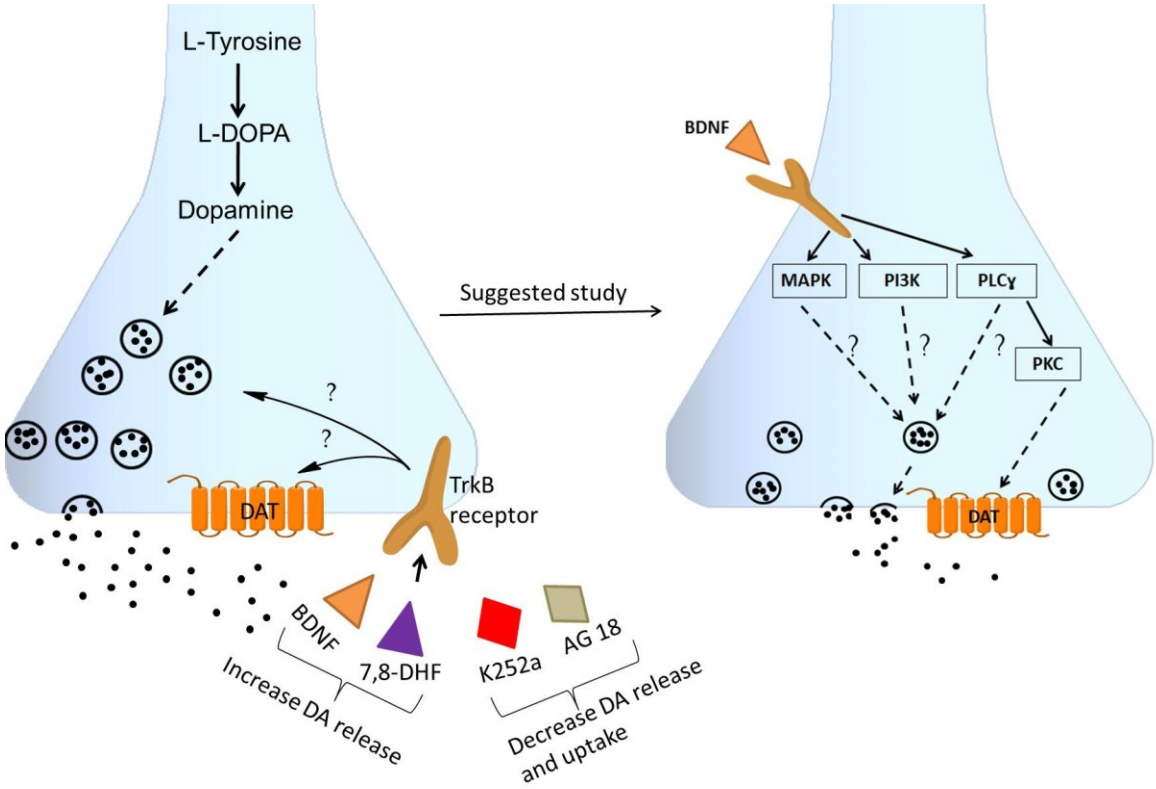

Figure 7.2: Schematic diagram showing a summary of the present work and recommended studies to understand how TrkB modulates DA dynamics. The functional effect of TrkB was examined using exogenous brain derived neurotrophic factor (BDNF); TrkB agonist, 7,8-dihydroxyflavone (7,8-DHF), and TrkB antagonist including tyrphostin 23 (AG18) and K252a. Present work demonstrated that BDNF modulate striatal DA release through activation of TrkB. The suggested study focuses on the mechanism underlining how TrkB activation influences the striatal DA dynamics by probing intracellular signaling cascade: Ras/mitogen activated protein kinase (MAPK) pathway, Phosphatidylinositol-3-kinase (PI3K) pathway and phospholipase Cγ (PLCγ) pathway.

REFERENCES

1. Paxinos G. and Franklin, K. J. B. (2001) *The mouse brain: In stereotaxic coordinates*, Second edition, Academic Press, San Diego, CA.
2. Nestler, E. J., Hyman, S. E., Malenka, R. C (2009) *Molecular neuropharmacology: A foundation for clinical neuroscience*, Second edition, McGraw-Hill Companies.
3. Cooper, J. R., Bloom, F. E., Roth, R. H. (1996) *The biochemical basis of neuropharmacology*, Seventh edition, Oxford University Press, New York.
4. Rhoades, R. A., Bell, D. R., (2013) *Medical physiology, principles for clinical medicine*, Fourth Edition, Lippincott William & Wilkins, Philadelphia, Pennsylvania.
5. Lama, R. D., Charlson, K., Anantharam, A., and Hashemi, P. (2012) Ultrafast detection and quantification of brain signaling molecules with carbon fiber microelectrodes, *Analytical Chemistry 84*, 8096-8101.
6. McGough, N. N., He, D. Y., Logrip, M. L., Jeanblanc, J., Phamluong, K., Luong, K., Kharazia, V., Janak, P. H., and Ron, D. (2004) RACK1 and brain-derived neurotrophic factor: a homeostatic pathway that regulates alcohol addiction, *J Neurosci 24*, 10542-10552.
7. Arias-Carrion, O., Stamelou, M., Murillo-Rodriguez, E., Menendez-Gonzalez, M., and Poppel, E. (2010) Dopaminergic reward system: a short integrative review, *International Archives of Medicine 3*, 24.
8. Smith, Y. and Villalba, R. (2008) Striatal and extrastriatal dopamine in the basal ganglia: an overview of its anatomical organization in normal and Parkinsonian

brains, *Movement Disorders: official journal of the Movement Disorder Society 23 Suppl 3*, S534-547.

9. Barbeau, A. (1974) High-level levodopa therapy in Parkinson's disease: five years later, *Transactions of the American Neurological Association 99*, 160-163.
10. Chinaglia, G., Alvarez, F. J., Probst, A., and Palacios, J. M. (1992) Mesostriatal and mesolimbic dopamine uptake binding sites are reduced in Parkinson's disease and progressive supranuclear palsy: a quantitative autoradiographic study using [3H]mazindol, *Neuroscience 49*, 317-327.
11. Pierce, R. C. and Kumaresan, V. (2006) The mesolimbic dopamine system: The final common pathway for the reinforcing effect of drugs of abuse?, *Neuroscience & amp; Biobehavioral Reviews 30*, 215-238.
12. Wise, R. A. (2005) Forebrain substrates of reward and motivation, *The Journal of Comparative Neurology 493*, 115-121.
13. Wise, R. A. (2004) Dopamine, learning and motivation, *Nat Rev Neurosci 5*, 483-494.
14. Siegel, G. J., Agranoff, B. W., Albers, R. W., Fisher, S. K., Uhler, M. D. (1999) *Basic neurochemistry: Molecular, cellular and medical aspects,* Sixth edition, Lippincott - Raven, New York.
15. Binder, D. K. and Scharfman, H. E. (2004) Brain-derived neurotrophic factor, *Growth factors (Chur, Switzerland) 22*, 123-131.
16. Poo, M. M. (2001) Neurotrophins as synaptic modulators, *Nat Rev Neurosci 2*, 24-32.

17. Barker, P. A. and Shooter, E. M. (1994) Disruption of NGF binding to the low affinity neurotrophin receptor p75LNTR reduces NGF binding to TrkA on PC12 cells, *Neuron 13*, 203-215.

18. Huang, E. J. and Reichardt, L. F. (2003) Trk receptors: roles in neuronal signal transduction, *Annual Review of Biochemistry 72*, 609-642.

19. Kaplan, D. R. and Miller, F. D. (2000) Neurotrophin signal transduction in the nervous system, *Curr Opin Neurobiol 10*, 381-391.

20. Altar, C. A., Boylan, C. B., Fritsche, M., Jackson, C., Hyman, C., and Lindsay, R. M. (1994) The neurotrophins NT-4/5 and BDNF augment serotonin, dopamine, and GABAergic systems during behaviorally effective infusions to the substantia nigra, *Exp Neurol 130*, 31-40.

21. Siuciak, J. A., Boylan, C., Fritsche, M., Altar, C. A., and Lindsay, R. M. (1996) BDNF increases monoaminergic activity in rat brain following intracerebroventricular or intraparenchymal administration, *Brain Research 710*, 11-20.

22. Warby, S. C., Graham, R. K., and Hayden, M. R. (1993) *Huntington Disease*.

23. Mogi, M., Togari, A., Kondo, T., Mizuno, Y., Komure, O., Kuno, S., Ichinose, H., and Nagatsu, T. (1999) Brain-derived growth factor and nerve growth factor concentrations are decreased in the substantia nigra in Parkinson's disease, *Neurosci Lett 270*, 45-48.

24. Howells, D. W., Porritt, M. J., Wong, J. Y., Batchelor, P. E., Kalnins, R., Hughes, A. J., and Donnan, G. A. (2000) Reduced BDNF mRNA expression in the Parkinson's disease substantia nigra, *Exp Neurol 166*, 127-135.

25. Zuccato, C. and Cattaneo, E. (2009) Brain-derived neurotrophic factor in neurodegenerative diseases, *Nat Rev Neurol 5*, 311-322.

26. Bolaños, C. and Nestler, E. (2004) Neurotrophic mechanisms in drug addiction, *Neuromolecular Medicine 5*, 69-83.

27. McGough, N. N. H., He, D.-Y., Logrip, M. L., Jeanblanc, J., Phamluong, K., Luong, K., Kharazia, V., Janak, P. H., and Ron, D. (2004) RACK1 and brain-derived neurotrophic factor: A Homeostatic pathway that regulates alcohol addiction, *The Journal of Neuroscience 24*, 10542-10552.

28. Willuhn, I., Wanat, M. J., Clark, J. J., and Phillips, P. E. (2010) Dopamine signaling in the nucleus accumbens of animals self-administering drugs of abuse, *Current topics in behavioral neurosciences 3*, 29-71.

29. Nestler, E. J. (2001) Molecular basis of long-term plasticity underlying addiction, *Nat Rev Neurosci 2*, 119-128.

30. Hyman, S. E., Malenka, R. C., and Nestler, E. J. (2006) Neural mechanisms of addiction: the role of reward-related learning and memory, *Annu Rev Neurosci 29*, 565-598.

31. Sulzer, D. (2011) How addictive drugs disrupt presynaptic dopamine neurotransmission, *Neuron 69*, 628-649.

32. Gardner, E. L. (2002) Addictive potential of cannabinoids: the underlying neurobiology, *Chem Phys Lipids 121*, 267-290.

33. Gupta, S. and Kulhara, P. (2007) Cellular and molecular mechanisms of drug dependence: An overview and update, *Indian Journal of Psychiatry 49*, 85-90.

34. Di Chiara, G. and Imperato, A. (1988) Drugs abused by humans preferentially increase synaptic dopamine concentrations in the mesolimbic system of freely moving rats, *Proceedings of the National Academy of Sciences 85*, 5274-5278.

35. Camí, J. and Farré, M. (2003) Drug addiction, *New England Journal of Medicine 349*, 975-986.

36. Riegel, A. C., Zapata, A., Shippenberg, T. S., and French, E. D. (2007) The abused inhalant toluene increases dopamine release in the nucleus accumbens by directly stimulating ventral tegmental area neurons, *Neuropsychopharmacology 32*, 1558-1569.

37. Bowen, S. E., Batis, J. C., Paez-Martinez, N., and Cruz, S. L. (2006) The last decade of solvent research in animal models of abuse: mechanistic and behavioral studies, *Neurotoxicol Teratol 28*, 636-647.

38. Riegel, A. C. and French, E. D. (2002) Abused inhalants and central reward pathways: electrophysiological and behavioral studies in the rat, *Annals of the New York Academy of Sciences 965*, 281-291.

39. Koob, G. F. and Volkow, N. D. (2010) Neurocircuitry of addiction, *Neuropsychopharmacology 35*, 217-238.

40. International Agency for Research on Cancer (IARC), (1989) *IARC Monographs on the evaluation of carcinogenic risks to humans: Some organic solvents, resin monomers and related compounds, pigment and occupational exposures in paint manufacturing and painting.*, Vol. 47, World Health Organization, Lyon, France.

41. Howard, M. O., Bowen, S. E., Garland, E. L., Perron, B. E., and Vaughn, M. G. (2011) Inhalant use and inhalant use disorders in the United States, *Addiction Science & Clinical Practice 6*, 18-31.

42. Cruz, S. L. and Bowen, S. E. (2008) Inhalant Abuse, *Neural mechanisms of action of drugs of abuse and natural reinforcers* (Ubach, M. M., R. Mondragon-Ceballos, Ed.), pp 61-87, Research Signpost, Kerala, India.

43. Bowen, S. E. (2011) Two serious and challenging medical complications associated with volatile substance misuse: sudden sniffing death and fetal solvent syndrome, *Subst Use Misuse 46 Suppl 1*, 68-72.

44. Flanagan, R. J., Ruprah, M., Meredith, T. J., and Ramsey, J. D. (1990) An introduction to the clinical toxicology of volatile substances, *Drug Saf 5*, 359-383.

45. Kurtzman, T. L., Otsuka, K. N., and Wahl, R. A. (2001) Inhalant abuse by adolescents, *J Adolesc Health 28*, 170-180.

46. SAMHSA. (2011) Results from the 2012 National Survey on Drug Use and Health: National findings (HTML), (Substance Abuse and Mental Health Services Administration, DHHS Publication No. SMA 033836), Department of Health and Human Services., Ed.), Rockville, MD.

47. APA, (2000) *Diagnostic and Statistical Manual of Mental Disorders*, American Psychiatric Press, Washington, D.C.

48. Flanagan, R. J. and Ives, R. J. (1994) Volatile substance abuse, *Bull Narc 46*, 49-78.

49. Howard, M. O. (2011) Inhalant use and inhalant use disorders in the United States, *Addiction science & clinical practice 6*, 18.

50. Miyake, K., Misawa, T., Aikawa, H., Yoshida, T., and Shigeta, S. (1989) The effects of prenatal trimethyltin exposure on development and learning in the rat, *Sangyo Igaku 31*, 363-371.

51. Bowen, S. E. and Cruz, S. L. (2012) Inhalants: addiction and toxic effects in the human, *In the effects of drug abuse on the human nervous system* (Madras, B., and Kuhar, M., Eds.).

52. Bowen, S. E. and McDonald, P. (2009) Abuse pattern of toluene exposure alters mouse behavior in a waiting for-reward operant task, *Neurotoxicol Teratol 31*, 18-25.

53. O'Brien, E. T., Yeoman, W. B., and Hobby, J. A. (1971) Hepatorenal damage from toluene in a "glue sniffer", *BMJ 2*, 29-30.

54. Twardowschy, C. A., Teive, H. A. G., Siquineli, F., Fernandes, A. F., Búrigo, I. P., Carvalho-Neto, A., and Werneck, L. C. (2008) Optic neuritis due to solvent abuse, *Arquivos de Neuro-Psiquiatria 66*, 108-110.

55. Pearson, M. A., Hoyme, H. E., Seaver, L. H., and Rimsza, M. E. (1994) Toluene embryopathy: delineation of the phenotype and comparison with fetal alcohol syndrome, *Pediatrics 93*, 211-215.

56. Evans, E. B. and Balster, R. L. (1991) CNS depressant effects of volatile organic solvents, *Neuroscience and biobehavioral reviews 15*, 233-241.

57. Blokhina, E. A., Dravolina, O. A., Bespalov, A. Y., Balster, R. L., and Zvartau, E. E. (2004) Intravenous self-administration of abused solvents and anesthetics in mice, *European journal of pharmacology 485*, 211-218.

58. Weiss, B., Wood, R. W., and Macys, D. A. (1979) Behavioral toxicology of carbon disulfide and toluene, *Environ Health Perspect 30*, 39-45.

59. Gerasimov, M. R., Collier, L., Ferrieri, A., Alexoff, D., Lee, D., Gifford, A. N., and Balster, R. L. (2003) Toluene inhalation produces a conditioned place preference in rats, *European Journal of Pharmacology 477*, 45-52.

60. Lee, D. E., Gerasimov, M. R., Schiffer, W. K., and Gifford, A. N. (2006) Concentration-dependent conditioned place preference to inhaled toluene vapors in rats, *Drug and Alcohol Dependence 85*, 87-90.

61. Funada, M., Sato, M., Makino, Y., and Wada, K. (2002) Evaluation of rewarding effect of toluene by the conditioned place preference procedure in mice, *Brain Res Brain Res Protoc 10*, 47-54.

62. Castilla-Serna, L., Barragan-Mejia, M. G., Rodriguez-Perez, R. A., Garcia Rillo, A., and Reyes-Vazquez, C. (1993) Effects of acute and chronic toluene inhalation on behavior, monoamine metabolism and specific binding (3H-serotonin and 3H-norepinephrine) of rat brain, *Archives of Medical Research 24*, 169-176.

63. Oshiro, W. M., Krantz, Q. T., and Bushnell, P. J. (2007) Repeated inhalation of toluene by rats performing a signal detection task leads to behavioral tolerance on some performance measures, *Neurotoxicol Teratol 29*, 247-254.

64. Himnan, D. J. (1984) Tolerance and reverse tolerance to toluene inhalation: effects on open-field behavior, *Pharmacology, Biochemistry, and Behavior 21*, 625-631.

65. Taylor, J. D. and Evans, H. L. (1985) Effects of toluene inhalation on behavior and expired carbon dioxide in macaque monkeys, *Toxicology and Applied Pharmacology 80*, 487-495.

66. Rees, D. C., Knisely, J. S., Breen, T. J., and Balster, R. L. (1987) Toluene, halothane, 1,1,1-trichloroethane and oxazepam produce ethanol-like discriminative stimulus effects in mice, *The Journal of Pharmacology and Experimental Therapeutics 243*, 931-937.

67. Rees, D. C., Knisely, J. S., Jordan, S., and Balster, R. L. (1987) Discriminative stimulus properties of toluene in the mouse, *Toxicology and applied Pharmacology 88*, 97-104.

68. Bowen, S. E. and Balster, R. L. (1998) A direct comparison of inhalant effects on locomotor activity and schedule-controlled behavior in mice, *Experimental and Clinical Psychopharmacology 6*, 235-247.

69. Moser, V. C. and Balster, R. L. (1981) The effects of acute and repeated toluene exposure on operant behavior in mice, *Neurobehavioral Toxicology and Teratology 3*, 471-475.

70. Moser, V. C. and Balster, R. L. (1985) Effects of toluene, halothane and ethanol vapor on fixed-ratio performance in mice, *Pharmacology, Biochemistry, and Behavior 22*, 797-802.

71. Gerasimov, M. R., Schiffer, W. K., Marstellar, D., Ferrieri, R., Alexoff, D., and Dewey, S. L. (2002) Toluene inhalation produces regionally specific changes in extracellular dopamine, *Drug and Alcohol Dependence 65*, 243-251.

72. Wiaderna, D., and Tomas, T. (2000) Effects of repeated exposure to toluene or amphetamine on locomotor activity in rats, *International Journal of Occupational Medicine and Environmental health 13*, 317-324.

73. Wiley, J. L., Bale, A. S., and Balster, R. L. (2003) Evaluation of toluene dependence and cross-sensitization to diazepam, *Life Sciences 72*, 3023-3033.

74. Bowen, S. E., Kimar, S., and Irtenkauf, S. (2010) Comparison of toluene-induced locomotor activity in four mouse strains, *Pharmacology, Biochemistry, and Behavior 95*, 249-257.

75. Beyer, C. E., Stafford, D., LeSage, M. G., Glowa, J. R., and Steketee, J. D. (2001) Repeated exposure to inhaled toluene induces behavioral and neurochemical cross-sensitization to cocaine in rats, *Psychopharmacology 154*, 198-204.

76. Cruz, S. L., Gauthereau, M. Y., Camacho-Munoz, C., Lopez-Rubalcava, C., and Balster, R. L. (2003) Effects of inhaled toluene and 1,1,1-trichloroethane on seizures and death produced by N-methyl-D-aspartic acid in mice, *Behavioural Brain Research 140*, 195-202.

77. Beckstead, M. J., Weiner, J. L., Eger, E. I., 2nd, Gong, D. H., and Mihic, S. J. (2000) Glycine and gamma-aminobutyric acid(A) receptor function is enhanced by inhaled drugs of abuse, *Molecular Pharmacology 57*, 1199-1205.

78. O'Leary-Moore, S. K., Galloway, M. P., McMechan, A. P., Hannigan, J. H., and Bowen, S. E. (2007) Region-dependent alterations in glutamate and GABA measured by high-resolution magnetic resonance spectroscopy following acute binge inhalation of toluene in juvenile rats, *Neurotoxicol Teratol 29*, 466-475.

79. Cruz, S. L., Mirshahi, T., Thomas, B., Balster, R. L., and Woodward, J. J. (1998) Effects of the abused solvent toluene on recombinant N-methyl-D-aspartate and non-N-methyl-D-aspartate receptors expressed in Xenopus oocytes, *The Journal of Pharmacology and Experimental Therapeutics 286*, 334-340.

80. Bale, A. S., Tu, Y., Carpenter-Hyland, E. P., Chandler, L. J., and Woodward, J. J. (2005) Alterations in glutamatergic and gabaergic ion channel activity in hippocampal neurons following exposure to the abused inhalant toluene, *Neuroscience 130*, 197-206.

81. Lopreato, G. F., Phelan, R., Borghese, C. M., Beckstead, M. J., and Mihic, S. J. (2003) Inhaled drugs of abuse enhance serotonin-3 receptor function, *Drug and Alcohol Dependence 70*, 11-15.

82. Bale, A. S., Smothers, C. T., and Woodward, J. J. (2002) Inhibition of neuronal nicotinic acetylcholine receptors by the abused solvent, toluene, *Br J Pharmacol 137*, 375-383.

83. Riegel, A. C. and French, E. D. (1999) An electrophysiological analysis of rat ventral tegmental dopamine neuronal activity during acute toluene exposure, *Pharmacology & Toxicology 85*, 37-43.

84. Riegel, A. C., Ali, S. F., Torinese, S., and French, E. D. (2004) Repeated exposure to the abused inhalant toluene alters levels of neurotransmitters and generates peroxynitrite in nigrostriatal and mesolimbic nuclei in rat, *Annals of the New York Academy of Sciences 1025*, 543-551.

85. Signore, A. P. and Yeh, H. H. (2000) Chronic exposure to ethanol alters GABA(A) receptor-mediated responses of layer II pyramidal cells in adult rat piriform cortex, *J Neurophysiol 84*, 247-254.

86. Weiss, F., Paulus, M. P., Lorang, M. T., and Koob, G. F. (1992) Increases in extracellular dopamine in the nucleus accumbens by cocaine are inversely related to basal levels: effects of acute and repeated administration, *J Neurosci 12*, 4372-4380.

87. Sziráki, I., Sershen, H., Hashim, A., and Lajtha, A. (2002) Receptors in the Ventral Tegmental Area Mediating Nicotine-Induced Dopamine Release in the Nucleus Accumbens, *Neurochemical Research 27*, 253-261.

88. Earle, M. L. and Davies, J. A. (1991) The effect of methamphetamine on the release of glutamate from striatal slices, *Journal of Neural Transmission. General section 86*, 217-222.

89. Burrows, K. B. and Meshul, C. K. (1999) High-dose methamphetamine treatment alters presynaptic GABA and glutamate immunoreactivity, *Neuroscience 90*, 833-850.

90. Chefer, V. I., Thompson, A. C., Zapata, A., and Shippenberg, T. S. (2009) Overview of brain microdialysis, *Current protocols in neuroscience/editorial board, Jacqueline N. Crawley [et al.] Chapter 7*, Unit7 1.

91. Davies, M. I., Cooper, J. D., Desmond, S. S., Lunte, C. E., and Lunte, S. M. (2000) Analytical considerations for microdialysis sampling, *Advanced drug delivery reviews 45*, 169-188.

92. Kennedy, R. T., Thompson, J. E., and Vickroy, T. W. (2002) In vivo monitoring of amino acids by direct sampling of brain extracellular fluid at ultralow flow rates and capillary electrophoresis, *Journal of Neuroscience Methods 114*, 39-49.

93. Watson, C. J., Venton, B. J., and Kennedy, R. T. (2006) In Vivo Measurements of Neurotransmitters by Microdialysis Sampling, *Analytical Chemistry 78*, 1391-1399.

94. Bosse, K. E., Maina, F. K., Birbeck, J. A., France, M. M., Roberts, J. J., Colombo, M. L., and Mathews, T. A. (2012) Aberrant striatal dopamine transmitter dynamics in brain-derived neurotrophic factor-deficient mice, *J Neurochem 120*, 385-395.

95. Bosse, K. E. and Mathews, T. A. (2011) Ethanol-induced increases in extracellular dopamine are blunted in brain-derived neurotrophic factor heterozygous mice, *Neurosci Lett 489*, 172-176.

96. Schultz, K. N. and Kennedy, R. T. (2008) Time-resolved microdialysis for in vivo neurochemical measurements and other applications, *Annual Review of Analytical Chemistry (Palo Alto, Calif.) 1*, 627-661.

97. Sharp, T., Carlsson, A., Zetterström, T., Lundstrom, K., and Ungerstedt, U. (1986) Rapid Measurement of Dopamine Release using Brain Dialysis Combined with Microbore HPLCa, *Annals of the New York Academy of Sciences 473*, 512-515.

98. McLaughlin, K. J., Faibushevich, A. A., and Lunte, C. E. (2000) Microdialysis sampling with on-line microbore HPLC for the determination of tirapazamine and its reduced metabolites in rats, *The Analyst 125*, 105-110.

99. Weber, S. G. and Purdy, W. C. (1981) Electrochemical detectors in liquid chromatography. A short review of detector design, *Industrial & Engineering Chemistry Product Research and Development 20*, 593-598.

100. Zapata, A., Chefer, V. I., Shippenberg, T. S., and Denoroy, L. (2009) Detection and quantification of neurotransmitters in dialysates, *Current protocols in neuroscience/editorial board, Jacqueline N. Crawley [et al.] Chapter 7*, Unit 7 4 1-30.

101. Robinson, D. L., Hermans, A., Seipel, A. T., and Wightman, R. M. (2008) Monitoring rapid chemical communication in the brain, *Chemical Reviews 108*, 2554-2584.

102. Keithley, R. B., Takmakov, P., Bucher, E. S., Belle, A. M., Owesson-White, C. A., Park, J., and Wightman, R. M. (2011) Higher sensitivity dopamine measurements with faster-scan cyclic voltammetry, *Analytical Chemistry 83*, 3563-3571.

103. Robinson D. L. and Wightman. R. M. (2007) Rapid dopamine release in freely moving rats, In *Electrochemical Methods for Neuroscience* (Michael, A. C., Borland, L. M., Ed.), pp 17-34, CRC Press, Boca Raton (FL).

104. Clark, J. J., Sandberg, S. G., Wanat, M. J., Gan, J. O., Horne, E. A., Hart, A. S., Akers, C. A., Parker, J. G., Willuhn, I., Martinez, V., Evans, S. B., Stella, N., and Phillips, P. E. (2010) Chronic microsensors for longitudinal, subsecond dopamine detection in behaving animals, *Nature Methods 7*, 126-129.

105. Peters, J. L., Miner, L. H., Michael, A. C., and Sesack, S. R. (2004) Ultrastructure at carbon fiber microelectrode implantation sites after acute voltammetric

measurements in the striatum of anesthetized rats, *Journal of Neuroscience methods 137*, 9-23.

106. Maina, F. K., Khalid, M., Apawu, A. K., and Mathews, T. A. (2012) Presynaptic dopamine dynamics in striatal brain slices with fast-scan cyclic voltammetry, *J Vis Exp, 59, pii: 3464. doi: 10.3791/3464*

107. Sanford, A. L., Morton, S. W., Whitehouse, K. L., Oara, H. M., Lugo-Morales, L. Z., Roberts, J. G., and Sombers, L. A. (2010) Voltammetric Detection of Hydrogen Peroxide at Carbon Fiber Microelectrodes, *Analytical Chemistry 82*, 5205-5210.

108. Hashemi, P., Dankoski, E. C., Wood, K. M., Ambrose, R. E., and Wightman, R. M. (2011) *In vivo* electrochemical evidence for simultaneous 5-HT and histamine release in the rat substantia nigra pars reticulata following medial forebrain bundle stimulation, *J Neurochem 118*, 749-759.

109. Pihel, K., Schroeder, T. J., and Wightman, R. M. (1994) Rapid and Selective Cyclic Voltammetric Measurements of Epinephrine and Norepinephrine as a Method To Measure Secretion from Single Bovine Adrenal Medullary Cells, *Analytical Chemistry 66*, 4532-4537.

110. Maina, F. K. and Mathews, T. A. (2010) Functional Fast Scan Cyclic Voltammetry Assay to Characterize Dopamine D2 and D3 Autoreceptors in the Mouse Striatum, *ACS Chemical Neuroscience 1*, 450-462.

111. Chang, S. Y., Jay, T., Munoz, J., Kim, I., and Lee, K. H. (2012) Wireless fast-scan cyclic voltammetry measurement of histamine using WINCS, a proof-of-principle study, *The Analyst 137*, 2158-2165.

112. Hashemi, P., Dankoski, E. C., Lama, R., Wood, K. M., Takmakov, P., and Wightman, R. M. (2012) Brain dopamine and serotonin differ in regulation and its consequences, *Proc Natl Acad Sci U S A 109*, 11510-11515.

113. Cooper, S. E. and Venton, B. J. (2009) Fast-scan cyclic voltammetry for the detection of tyramine and octopamine, *Analytical and Bioanalytical Chemistry 394*, 329-336.

114. Swamy, B. E. and Venton, B. J. (2007) Subsecond detection of physiological adenosine concentrations using fast-scan cyclic voltammetry, *Anal Chem 79*, 744-750.

115. Hashemi, P., Dankoski, E. C., Petrovic, J., Keithley, R. B., and Wightman, R. M. (2009) voltammetric detection of 5-Hydroxytryptamine release in the rat brain, *Analytical Chemistry 81*, 9462-9471.

116. Ross, A. E. and Venton, B. J. (2012) Nafion-CNT coated carbon-fiber microelectrodes for enhanced detection of adenosine, *The Analyst 137*, 3045-3051.

117. Zachek, M. K., Park, J., Takmakov, P., Wightman, R. M., and McCarty, G. S. (2010) Microfabricated FSCV-compatible microelectrode array for real-time monitoring of heterogeneous dopamine release, *The Analyst 135*, 1556-1563.

118. Zachek, M. K., Takmakov, P., Moody, B., Wightman, R. M., and McCarty, G. S. (2009) Simultaneous decoupled detection of dopamine and oxygen using pyrolyzed carbon microarrays and fast-scan cyclic voltammetry, *Anal Chem 81*, 6258-6265.

119. Wilson, G. S. and Johnson, M. A. (2008) *In vivo* electrochemistry: what can we learn about living systems? *Chem Rev 108*, 2462-2481.

120. Kruk, Z. L., Cheeta, S., Milla, J., Muscat, R., Williams, J. E., and Willner, P. (1998) Real time measurement of stimulated dopamine release in the conscious rat using fast cyclic voltammetry: dopamine release is not observed during intracranial self stimulation, *Journal of Neuroscience Methods 79*, 9-19.

121. Duff, A. and O'Neill, R. D. (1994) Effect of probe size on the concentration of brain extracellular uric acid monitored with carbon paste electrodes, *J Neurochem 62*, 1496-1502.

122. Garris, P. A., Ensman, R., Poehlman, J., Alexander, A., Langley, P. E., Sandberg, S. G., Greco, P. G., Wightman, R. M., and Rebec, G. V. (2004) Wireless transmission of fast-scan cyclic voltammetry at a carbon-fiber microelectrode: proof of principle, *Journal of Neuroscience Methods 140*, 103-115.

123. Griessenauer, C. J., Chang, S. Y., Tye, S. J., Kimble, C. J., Bennet, K. E., Garris, P. A., and Lee, K. H. (2010) Wireless Instantaneous Neurotransmitter Concentration System: electrochemical monitoring of serotonin using fast-scan cyclic voltammetry--a proof-of-principle study, *Journal of Neurosurgery 113*, 656-665.

124. Shon, Y. M., Chang, S. Y., Tye, S. J., Kimble, C. J., Bennet, K. E., Blaha, C. D., and Lee, K. H. (2010) Comonitoring of adenosine and dopamine using the Wireless Instantaneous Neurotransmitter Concentration System: proof of principle, *Journal of Neurosurgery 112*, 539-548.

125. Van Gompel, J. J., Chang, S. Y., Goerss, S. J., Kim, I. Y., Kimble, C., Bennet, K. E., and Lee, K. H. (2010) Development of intraoperative electrochemical detection: wireless instantaneous neurochemical concentration sensor for deep brain stimulation feedback, *Neurosurg Focus 29*, E6.

126. Khalid, M., Aoun, R. A., and Mathews, T. A. (2011) Altered striatal dopamine release following a sub-acute exposure to manganese, *Journal of Neuroscience Methods 202*, 182-191.

127. Budygin, E. A., Mathews, T. A., Lapa, G. B., and Jones, S. R. (2005) Local effects of acute ethanol on dopamine neurotransmission in the ventral striatum in C57BL/6 mice, *European Journal of Pharmacology 523*, 40-45.

128. Hellweg, R., Zueger, M., Fink, K., Hortnagl, H., and Gass, P. (2007) Olfactory bulbectomy in mice leads to increased BDNF levels and decreased serotonin turnover in depression-related brain areas, *Neurobiology of Disease 25*, 1-7.

129. Drugan, R. C., Leslie M. A., Weizman, R., Weizman, A., Deutsch, S. I., Crawley, J. N., and Paul, S. M. (1989) Stress-induced behavioral depression in the rat is associated with a decrease in GABA receptor-mediated chloride ion flux and brain benzodiazepine receptor occupancy, *Brain Research 487*, 45-51.

130. Mikkola, J. A. V., Honkanen, A., Piepponen, T. P., Kiianmaa, K., and Ahtee, L. (2001) Effects of repeated morphine treatment on metabolism of cerebral dopamine and serotonin in alcohol-preferring AA and alcohol-avoiding ANA rats, *Alcohol and Alcoholism 36*, 286-291.

131. Agardh, C. D., Carlsson, A., Linqvist, M., and Siesjo, B. K. (1979) The effect of pronounced hypoglycemia on monoamine metabolism in rat brain, *Diabetes 28*, 804-809.

132. Kelly, M. A., Rubinstein, M., Phillips, T. J., Lessov, C. N., Burkhart-Kasch, S., Zhang, G., Bunzow, J. R., Fang, Y., Gerhardt, G. A., Grandy, D. K., and Low, M. J. (1998) Locomotor Activity in D2 Dopamine Receptor-Deficient Mice Is Determined by Gene Dosage, Genetic Background, and Developmental Adaptations, *The Journal of Neuroscience 18*, 3470-3479.

133. Dumont, M. (2011) Behavioral phenotyping of mouse models of neurodegeneration, *Methods Mol Biol 793*, 229-237.

134. Taylor, T. N., Greene, J. G., and Miller, G. W. (2010) Behavioral phenotyping of mouse models of Parkinson's disease, *Behavioural Brain Research 211*, 1-10.

135. Jung, E. S., Lee, H. J., Sim, H. R., and Baik, J. H. (2013) Cocaine-induced behavioral sensitization in mice: effects of microinjection of dopamine d2 receptor antagonist into the nucleus accumbens, *Experimental Neurobiology 22*, 224-231.

136. Bowen, S. E. and Balster, R. L. (1997) A comparison of the acute behavioral effects of inhaled amyl, ethyl, and butyl acetate in mice, *Fundam Appl Toxicol 35*, 189-196.

137. Heyser, C. J., McDonald, J. S., Beauchamp, V., Koob, G. F., and Gold, L. H. (1997) The effects of cocaine on operant responding for food in several strains of mice, *Psychopharmacology 132*, 202-208.

138. Pijnenburg, A. J. J. and van Rossum, J. M. (1973) Stimulation of locomotor activity following injection of dopamine into the nucleus accumbens, *Journal of Pharmacy and Pharmacology 25*, 1003-1005.

139. Kelly, P. H. and Iversen, S. D. (1976) Selective 6OHDA-induced destruction of mesolimbic dopamine neurons: abolition of psychostimulant-induced locomotor activity in rats, *European Journal of Pharmacology 40*, 45-56.

140. Kelly, P. H., Seviour, P. W., and Iversen, S. D. (1975) Amphetamine and apomorphine responses in the rat following 6-OHDA lesions of the nucleus accumbens septi and corpus striatum, *Brain Res 94*, 507-522.

141. Wise, R. A. (2002) Brain reward circuitry: insights from unsensed incentives, *Neuron 36*, 229-240.

142. Lubman, D. I., Yucel, M., and Lawrence, A. J. (2008) Inhalant abuse among adolescents: neurobiological considerations, *Br J Pharmacol 154*, 316-326.

143. Stengard, K., Hoglund, G., and Ungerstedt, U. (1994) Extracellular dopamine levels within the striatum increase during inhalation exposure to toluene: a microdialysis study in awake, freely moving rats, *Toxicology letters 71*, 245-255.

144. McAllister, A. K., Katz, L. C., and Lo, D. C. (1999) Neurotrophins and synaptic plasticity, *Annu Rev Neurosci 22*, 295-318.

145. Tyler, W. J., Alonso, M., Bramham, C. R., and Pozzo-Miller, L. D. (2002) From acquisition to consolidation: on the role of brain-derived neurotrophic factor signaling in hippocampal-dependent learning, *Learning & Memory 9*, 224-237.

146. Pang, P. T. and Lu, B. (2004) Regulation of late-phase LTP and long-term memory in normal and aging hippocampus: role of secreted proteins tPA and BDNF, *Ageing Research Reviews 3*, 407-430.

147. Berton, O., McClung, C. A., DiLeone, R. J., Krishnan, V., Renthal, W., Russo, S. J., Graham, D., Tsankova, N. M., Bolanos, C. A., Rios, M., Monteggia, L. M., Self, D. W., and Nestler, E. J. (2006) Essential role of BDNF in the mesolimbic dopamine pathway in social defeat stress, *Science 311*, 864-868.

148. Neal, M., Cunningham, J., Lever, I., Pezet, S., and Malcangio, M. (2003) Mechanism by which brain-derived neurotrophic factor increases dopamine release from the rabbit retina, *Invest Ophthalmol Vis Sci 44*, 791-798.

149. Hoover, B. R., Everett, C. V., Sorkin, A., and Zahniser, N. R. (2007) Rapid regulation of dopamine transporters by tyrosine kinases in rat neuronal preparations, *J Neurochem 101*, 1258-1271.

150. Altar, C. A., Fritsche, M., and Lindsay, R. M. (1998) Cell body infusions of brain-derived neurotrophic factor increase forebrain dopamine release and serotonin metabolism determined with in vivo microdialysis, *Adv Pharmacol 42*, 915-921.

151. Nelson, G. O. (1971) *Controlled test atmospheres. principles and techniques*, Ann Arbor Science Publishers, Ann Arbor.

152. Jones, S. R., Garris, P. A., Kilts, C. D., and Wightman, R. M. (1995) Comparison of dopamine uptake in the basolateral amygdaloid nucleus, caudate-putamen, and nucleus accumbens of the rat, *Journal of Neurochemistry 64*, 2581-2589.

153. Jones, S. R., Gainetdinov, R. R., Wightman, R. M., and Caron, M. G. (1998) Mechanisms of amphetamine action revealed in mice lacking the dopamine transporter, *The Journal of Neuroscience 18*, 1979-1986.

154. Wightman, R. M. and Zimmerman, J. B. (1990) Control of dopamine extracellular concentration in rat striatum by impulse flow and uptake, *Brain Research 15*, 135-144.

155. Tomaszycki, M. L., Aulerich, K. E., and Bowen, S. E. (2013) Repeated toluene exposure increases c-Fos in catecholaminergic cells of the nucleus accumbens shell, *Neurotoxicol Teratol 40*, 28-34.

156. Conti, A. C., Lowing, J. L., Susick, L. L., and Bowen, S. E. (2012) Investigation of calcium-stimulated adenylyl cyclases 1 and 8 on toluene and ethanol neurobehavioral actions, *Neurotoxicol Teratol 34*, 481-488.

157. Batis, J. C., Hannigan, J. H., and Bowen, S. E. (2010) Differential effects of inhaled toluene on locomotor activity in adolescent and adult rats, *Pharmacology, Biochemistry, and Behavior 96*, 438-448.

158. Zapata, A., Gonzales, R. A., and Shippenberg, T. S. (2006) Repeated ethanol intoxication induces behavioral sensitization in the absence of a sensitized accumbens dopamine response in C57BL/6J and DBA/2J mice, *Neuropsychopharmacology 31*, 396-405.

159. Mateo, Y., Lack, C. M., Morgan, D., Roberts, D. C., and Jones, S. R. (2005) Reduced dopamine terminal function and insensitivity to cocaine following cocaine binge self-administration and deprivation, *Neuropsychopharmacology 30*, 1455-1463.

160. Cragg, S. J. (2003) Variable dopamine release probability and short-term plasticity between functional domains of the primate striatum, *The Journal of Neuroscience 23*, 4378-4385.

161. Cragg, S. J., Hille, C. J., and Greenfield, S. A. (2002) Functional domains in dorsal striatum of the nonhuman primate are defined by the dynamic behavior of dopamine, *The Journal of Neuroscience 22*, 5705-5712.

162. Cragg, S. J., Hille, C. J., and Greenfield, S. A. (2000) Dopamine Release and Uptake Dynamics within Nonhuman Primate Striatum In Vitro, *The Journal of Neuroscience 20*, 8209-8217.

163. Morse, A. C., Erwin, V. G., and Jones, B. C. (1995) Behavioral responses to low doses of cocaine are affected by genetics and experimental history, *Physiology & behavior 58*, 891-897.

164. Jones, S. R., O'Dell, S. J., Marshall, J. F., and Wightman, R. M. (1996) Functional and anatomical evidence for different dopamine dynamics in the core and shell of the nucleus accumbens in slices of rat brain, *Synapse 23*, 224-231.

165. Hinman, D. J. (1987) Biphasic dose-response relationship for effects of toluene inhalation on locomotor activity, *Pharmacology, Biochemistry, and Behavior 26*, 65-69.

166. Riegel, A. C., and French, E. D. (1999) Acute toluene induces biphasic changes in rat spontaneous locomotor activity which are blocked by remoxipride, *Pharmacology, Biochemistry, and Behavior 62*, 399-402.

167. Jones, H. E., Kunko, P. M., Robinson, S. E., and Balster, R. L. (1996) Developmental consequences of intermittent and continuous prenatal exposure

to 1,1,1-trichloroethane in mice, *Pharmacology, Biochemistry, and Behavior 55*, 635-646.

168. Jones, H. E. and Balster, R. L. (1998) Inhalant abuse in pregnancy, *Obstetrics and Gynecology Clinics of North America 25*, 153-167.

169. Bowen, S. E. and Balster, R. L. (2006) Tolerance and sensitization to inhaled 1,1,1-trichloroethane in mice: results from open-field behavior and a functional observational battery, *Psychopharmacology 185*, 405-415.

170. Bowen, S. E., Charlesworth, J. D., Tokarz, M. E., Wright, M. J., Jr., and Wiley, J. L. (2007) Decreased sensitivity in adolescent vs. adult rats to the locomotor activating effects of toluene, *Neurotoxicol Teratol 29*, 599-606.

171. Riegel, A. C., Ali, S. F., and French, E. D. (2003) Toluene-induced locomotor activity is blocked by 6-hydroxydopamine lesions of the nucleus accumbens and the mGluR2/3 agonist LY379268, *Neuropsychopharmacology 28*, 1440-1447.

172. McCarthy, M. I., Hitman, G. A., Hitchins, M., Riikonen, A., Stengard, J., Nissinen, A., Tuomilehto-Wolf, E., and Tuomilehto, J. (1994) Glucokinase gene polymorphisms: a genetic marker for glucose intolerance in a cohort of elderly Finnish men, *Diabet Med 11*, 198-204.

173. Hillefors-Berglund, M., Liu, Y., and von Euler, G. (1995) Persistent, specific and dose-dependent effects of toluene exposure on dopamine D2 agonist binding in the rat caudate-putamen, *Toxicology 100*, 185-194.

174. Wise, R. A. and Rompre, P. P. (1989) Brain dopamine and reward, *Annual Review of Psychology 40*, 191-225.

175. Volkow, N. D., Fowler, J. S., Wang, G. J., and Swanson, J. M. (2004) Dopamine in drug abuse and addiction: results from imaging studies and treatment implications, *Mol Psychiatry 9*, 557-569.

176. Volkow, N. D., Fowler, J. S., and Wang, G.-J. (2003) The addicted human brain: insights from imaging studies, *The Journal of Clinical Investigation 111*, 1444-1451.

177. Volkow, N. D., Fowler, J. S., Wang, G. J., Baler, R., and Telang, F. (2009) Imaging dopamine's role in drug abuse and addiction, *Neuropharmacology 56 Suppl 1*, 3-8.

178. Stengård, K., Höglund, G., and Ungerstedt, U. (1994) Extracellular dopamine levels within the striatum increase during inhalation exposure to toluene: a microdialysis study in awake, freely moving rats, *Toxicology Letters 71*, 245-255.

179. Lo, P. S., Wu, C. Y., Sue, H. Z., and Chen, H. H. (2009) Acute neurobehavioral effects of toluene: involvement of dopamine and NMDA receptors, *Toxicology 265*, 34-40.

180. Levant, B. (1997) The D3 dopamine receptor: neurobiology and potential clinical relevance, *Pharmacological Reviews 49*, 231-252.

181. Lévesque, D., Diaz, J., Pilon, C., Martres, M. P., Giros, B., Souil, E., Schott, D., Morgat, J. L., Schwartz, J. C., and Sokoloff, P. (1992) Identification, characterization, and localization of the dopamine D3 receptor in rat brain using 7-[3H]hydroxy-N,N-di-n-propyl-2-aminotetralin, *Proceedings of the National Academy of Sciences 89*, 8155-8159.

182. Sokoloff, P., Giros, B., Martres, M. P., Bouthenet, M. L., and Schwartz, J. C. (1990) Molecular cloning and characterization of a novel dopamine receptor (D3) as a target for neuroleptics, *Nature 347*, 146-151.

183. Guillin, O., Diaz, J., Carroll, P., Griffon, N., Schwartz, J. C., and Sokoloff, P. (2001) BDNF controls dopamine D3 receptor expression and triggers behavioural sensitization, *Nature 411*, 86-89.

184. Sokoloff, P., Diaz, J., Le Foll, B., Guillin, O., Leriche, L., Bezard, E., and Gross, C. (2006) The dopamine D3 receptor: a therapeutic target for the treatment of neuropsychiatric disorders, *CNS & neurological disorders drug targets 5*, 25-43.

185. Sokoloff, P., Guillin, O., Diaz, J., Carroll, P., and Griffon, N. (2002) Brain-derived neurotrophic factor controls dopamine D3 receptor expression: implications for neurodevelopmental psychiatric disorders, *neurotox res 4*, 671-678.

186. Bouthenet, M. L., Souil, E., Martres, M. P., Sokoloff, P., Giros, B., and Schwartz, J. C. (1991) Localization of dopamine D3 receptor mRNA in the rat brain using in situ hybridization histochemistry: comparison with dopamine D2 receptor mRNA, *Brain Res 564*, 203-219.

187. Staley, J. K. and Mash, D. C. (1996) Adaptive increase in D3 dopamine receptors in the brain reward circuits of human cocaine fatalities, *J Neurosci 16*, 6100-6106.

188. Segal, D. M., Moraes, C. T., and Mash, D. C. (1997) Up-regulation of D3 dopamine receptor mRNA in the nucleus accumbens of human cocaine fatalities, *Brain Res Mol Brain Res 45*, 335-339.

189. Le Foll, B., Frances, H., Diaz, J., Schwartz, J. C., and Sokoloff, P. (2002) Role of the dopamine D3 receptor in reactivity to cocaine-associated cues in mice, *Eur J Neurosci 15*, 2016-2026.

190. Le Foll, B., Schwartz, J. C., and Sokoloff, P. (2003) Disruption of nicotine conditioning by dopamine D(3) receptor ligands, *Mol Psychiatry 8*, 225-230.

191. von Euler, G., Ogren, S. O., Li, X. M., Fuxe, K., and Gustafsson, J. A. (1993) Persistent effects of subchronic toluene exposure on spatial learning and memory, dopamine-mediated locomotor activity and dopamine D2 agonist binding in the rat, *Toxicology 77*, 223-232.

192. von Euler, M., Pham, T. M., Hillefors, M., Bjelke, B., Henriksson, B., and von Euler, G. (2000) Inhalation of Low Concentrations of Toluene Induces Persistent Effects on a Learning Retention Task, Beam-Walk Performance, and Cerebrocortical Size in the Rat, *Experimental Neurology 163*, 1-8.

193. Bello, E. P., Mateo, Y., Gelman, D. M., Noain, D., Shin, J. H., Low, M. J., Alvarez, V. A., Lovinger, D. M., and Rubinstein, M. (2011) Cocaine supersensitivity and enhanced motivation for reward in mice lacking dopamine D2 autoreceptors, *Nat Neurosci 14*, 1033-1038.

194. Benkert, O., Grunder, G., and Wetzel, H. (1992) Dopamine autoreceptor agonists in the treatment of schizophrenia and major depression, *Pharmacopsychiatry 25*, 254-260.

195. Freedman, S. B., Patel, S., Marwood, R., Emms, F., Seabrook, G. R., Knowles, M. R., and McAllister, G. (1994) Expression and pharmacological

characterization of the human D3 dopamine receptor, *The Journal of Pharmacology and Experimental Therapeutics 268*, 417-426.

196. Ford, C. P., Gantz, S. C., Phillips, P. E., and Williams, J. T. (2010) Control of extracellular dopamine at dendrite and axon terminals, *J Neurosci 30*, 6975-6983.

197. Schmitz, Y., Benoit-Marand, M., Gonon, F., and Sulzer, D. (2003) Presynaptic regulation of dopaminergic neurotransmission, *J Neurochem 87*, 273-289.

198. Wallace, D. R., and Booze, R. M. (1995) Identification of D3 and σ Receptors in the rat striatum and nucleus accumbens using (±)-7-Hydroxy-N,N-Di-n-[3H]Propyl-2-Aminotetralin and carbetapentane, *Journal of Neurochemistry 64*, 700-710.

199. Levesque, D. (1996) Aminotetralin drugs and D3 receptor functions. What may partially selective D3 receptor ligands tell us about dopamine D3 receptor functions?, *Biochem Pharmacol 52*, 511-518.

200. Apawu, A. K., Maina, F. K., Taylor, J. R., and Mathews, T. A. (2013) Probing the ability of presynaptic tyrosine kinase receptors to regulate striatal dopamine dynamics, *ACS Chemical Neuroscience 4*, 895-904.

201. Beckley, J. T., Evins, C. E., Fedarovich, H., Gilstrap, M. J., and Woodward, J. J. (2013) medial prefrontal cortex inversely regulates toluene-induced changes in markers of synaptic plasticity of mesolimbic dopamine neurons, *The Journal of Neuroscience 33*, 804-813.

202. Alheid, G. F., and Heimer, L. (1988) New perspectives in basal forebrain organization of special relevance for neuropsychiatric disorders: The

striatopallidal, amygdaloid, and corticopetal components of substantia innominata, *Neuroscience 27*, 1-39.

203. Heimer, L., Zahm, D. S., Churchill, L., Kalivas, P. W., and Wohltmann, C. (1991) Specificity in the projection patterns of accumbal core and shell in the rat, *Neuroscience 41*, 89-125.

204. Jongen-Rêlo, A. L., Voorn, P., and Groenewegen, H. J. (1994) Immunohistochemical characterization of the shell and core territories of the nucleus accumbens in the rat, *European Journal of Neuroscience 6*, 1255-1264.

205. Zahm, D. S. and Heimer, L. (1990) Two transpallidal pathways originating in the rat nucleus accumbens, *The Journal of Comparative Neurology 302*, 437-446.

206. Ito, R., Dalley, J. W., Howes, S. R., Robbins, T. W., and Everitt, B. J. (2000) Dissociation in conditioned dopamine release in the nucleus accumbens core and shell in response to cocaine cues and during cocaine-seeking behavior in rats, *J Neurosci 20*, 7489-7495.

207. Pontieri, F. E., Tanda, G., and Di Chiara, G. (1995) Intravenous cocaine, morphine, and amphetamine preferentially increase extracellular dopamine in the "shell" as compared with the "core" of the rat nucleus accumbens, *Proc Natl Acad Sci U S A 92*, 12304-12308.

208. Miyachi, S., Hikosaka, O., Miyashita, K., Karadi, Z., and Rand, M. K. (1997) Differential roles of monkey striatum in learning of sequential hand movement, *Exp Brain Res 115*, 1-5.

209. Kondo, H., Huang, J., Ichihara, G., Kamijima, M., Saito, I., Shibata, E., Ono, Y., Hisanaga, N., Takeuchi, Y., and Nakahara, D. (1995) Toluene induces behavioral

activation without affecting striatal dopamine metabolism in the rat: Behavioral and microdialysis studies, *Pharmacology Biochemistry and Behavior 51*, 97-101.

210. Casanova, J. P., Velis, G. P., and Fuentealba, J. A. (2013) Amphetamine locomotor sensitization is accompanied with an enhanced high K(+)-stimulated Dopamine release in the rat medial prefrontal cortex, *Behavioural Brain Research 237*, 313-317.

211. Alfaro-Rodriguez, A., Bueno-Nava, A., Gonzalez-Pina, R., Arch-Tirado, E., Vargas-Sanchez, J., and Avila-Luna, A. (2011) Chronic exposure to toluene changes the sleep-wake pattern and brain monoamine content in rats, *Acta Neurobiologiae Experimentalis 71*, 183-192.

212. Berenguer, P., Soulage, C., Fautrel, A., Péquignot, J.-M., and Abraini, J. H. (2004) Behavioral and neurochemical effects induced by subchronic combined exposure to toluene at 40 ppm and noise at 80 dB-A in rats, *Physiology & Behavior 81*, 527-534.

213. Burris, K. D., Pacheco, M. A., Filtz, T. M., Kung, M. P., Kung, H. F., and Molinoff, P. B. (1995) Lack of discrimination by agonists for D2 and D3 dopamine receptors, *Neuropsychopharmacology 12*, 335-345.

214. Roberts, C., Cummins, R., Gnoffo, Z., and Kew, J. N. (2006) Dopamine D3 receptor modulation of dopamine efflux in the rat nucleus accumbens, *European Journal of Pharmacology 534*, 108-114.

215. Koob, G. F. (1992) Drugs of abuse: anatomy, pharmacology and function of reward pathways, *Trends in Pharmacological Sciences 13*, 177-184.

216. Riegel, A. C. and French, E. D. (2002) Abused Inhalants and Central Reward Pathways, *Annals of the New York Academy of Sciences 965*, 281-291.

217. Di Chiara, G., and Imperato, A. (1986) Preferential stimulation of dopamine release in the nucleus accumbens by opiates, alcohol, and barbiturates: studies with transcerebral dialysis in freely moving rats, *Annals of the New York Academy of Sciences 473*, 367-381.

218. Di Chiara, G., Bassareo, V., Fenu, S., De Luca, M. A., Spina, L., Cadoni, C., Acquas, E., Carboni, E., Valentini, V., and Lecca, D. (2004) Dopamine and drug addiction: the nucleus accumbens shell connection, *Neuropharmacology 47 Suppl 1*, 227-241.

219. Cadoni, C., and Di Chiara, G. (2000) Differential changes in accumbens shell and core dopamine in behavioral sensitization to nicotine, *European journal of pharmacology 387*, R23-R25.

220. Cadoni, C., Solinas, M., and Di Chiara, G. (2000) Psychostimulant sensitization: differential changes in accumbal shell and core dopamine, *European Journal of Pharmacology 388*, 69-76.

221. Cadoni, C., and Di Chiara, G. (1999) Reciprocal changes in dopamine responsiveness in the nucleus accumbens shell and core and in the dorsal caudate-putamen in rats sensitized to morphine, *Neuroscience 90*, 447-455.

222. Maina, F. K. (2010) Functional Fast scan cyclic voltammetry assay to characterize dopamine d2 and d3 autoreceptors in the mouse striatum, *ACS chemical neuroscience 1*, 450-462.

223. Cruz, S. L., Balster, R. L., and Woodward, J. J. (2000) Effects of volatile solvents on recombinant N-methyl-D-aspartate receptors expressed in Xenopus oocytes, *Br J Pharmacol 131*, 1303-1308.

224. Tillar, R., Shafer, T. J., and Woodward, J. J. (2002) Toluene inhibits voltage-sensitive calcium channels expressed in pheochromocytoma cells, *Neurochemistry international 41*, 391-397.

225. Reichardt, L. F. (2006) Neurotrophin-regulated signalling pathways, *Philosophical Transactions of the Royal Society of London. Series B, Biological sciences 361*, 1545-1564.

226. Numan, S., and Seroogy, K. B. (1999) Expression of trkB and trkC mRNAs by adult midbrain dopamine neurons: a double-label in situ hybridization study, *The Journal of comparative neurology 403*, 295-308.

227. Martin-Iverson, M. T., Todd, K. G., and Altar, C. A. (1994) Brain-derived neurotrophic factor and neurotrophin-3 activate striatal dopamine and serotonin metabolism and related behaviors: interactions with amphetamine, *J Neurosci 14*, 1262-1270.

228. Altar, C. A., Boylan, C. B., Jackson, C., Hershenson, S., Miller, J., Wiegand, S. J., Lindsay, R. M., and Hyman, C. (1992) Brain-derived neurotrophic factor augments rotational behavior and nigrostriatal dopamine turnover in vivo, *Proc Natl Acad Sci U S A 89*, 11347-11351.

229. Dluzen, D. E., Gao, X., Story, G. M., Anderson, L. I., Kucera, J., and Walro, J. M. (2001) Evaluation of nigrostriatal dopaminergic function in adult +/+ and +/- BDNF mutant mice, *Exp Neurol 170*, 121-128.

230. Dluzen, D. E., Anderson, L. I., McDermott, J. L., Kucera, J., and Walro, J. M. (2002) Striatal dopamine output is compromised within +/- BDNF mice, *Synapse 43*, 112-117.

231. Joyce, J. N., Renish, L., Osredkar, T., Walro, J. M., Kucera, J., and Dluzen, D. E. (2004) Methamphetamine-induced loss of striatal dopamine innervation in BDNF heterozygote mice does not further reduce D3 receptor concentrations, *Synapse 52*, 11-19.

232. Cordeira, J. W., Frank, L., Sena-Esteves, M., Pothos, E. N., and Rios, M. (2010) Brain-derived neurotrophic factor regulates hedonic feeding by acting on the mesolimbic dopamine system, *J Neurosci 30*, 2533-2541.

233. Goggi, J., Pullar, I. A., Carney, S. L., and Bradford, H. F. (2002) Modulation of neurotransmitter release induced by brain-derived neurotrophic factor in rat brain striatal slices in vitro, *Brain Res 941*, 34-42.

234. Chi, L. and Reith, M. E. (2003) Substrate-induced trafficking of the dopamine transporter in heterologously expressing cells and in rat striatal synaptosomal preparations, *The Journal of pharmacology and experimental therapeutics 307*, 729-736.

235. Borland, L. M. and Michael A. C. (2007) *Electrochemical Methods for Neuroscience*, Boca Raton (FL): CRC Press.

236. Bowen, S. E., Hannigan, J. H., and Cooper, P. B. (2009) Abuse pattern of gestational toluene exposure alters behavior in rats in a "waiting-for-reward" task, *Neurotoxicol Teratol 31*, 89-97.

237. Brett, A. M. O. and Ghica, M. E. (2003) Electrochemical Oxidation of quercetin, *Electroanalysis 15*, 1745-1750.

238. Enache, T. A. and Oliveira-Brett, A. M. (2011) Phenol and para-substituted phenols electrochemical oxidation pathways, *Journal of Electroanalytical Chemistry 655*, 9-16.

239. Goggi, J., Pullar, I. A., Carney, S. L., and Bradford, H. F. (2003) Signalling pathways involved in the short-term potentiation of dopamine release by BDNF, *Brain Research 968*, 156-161.

240. Akiyama, T., Ishida, J., Nakagawa, S., Ogawara, H., Watanabe, S., Itoh, N., Shibuya, M., and Fukami, Y. (1987) Genistein, a specific inhibitor of tyrosine-specific protein kinases, *J Biol Chem 262*, 5592-5595.

241. Polkowski, K. and Mazurek, A. P. (2000) Biological properties of genistein. A review of in vitro and in vivo data, *Acta Poloniae Pharmaceutica 57*, 135-155.

242. Cataldi, M., Taglialatela, M., Guerriero, S., Amoroso, S., Lombardi, G., di Renzo, G., and Annunziato, L. (1996) Protein-tyrosine kinases activate while protein-tyrosine phosphatases inhibit L-type calcium channel activity in pituitary GH3 cells, *J Biol Chem 271*, 9441-9446.

243. Goldberg, D. J. and Wu, D. Y. (1995) Inhibition of formation of filopodia after axotomy by inhibitors of protein tyrosine kinases, *Journal of Neurobiology 27*, 553-560.

244. Linford, N. J., Yang, Y., Cook, D. G., and Dorsa, D. M. (2001) Neuronal apoptosis resulting from high doses of the isoflavone genistein: role for calcium

and p42/44 mitogen-activated protein kinase, *The Journal of pharmacology and Experimental Therapeutics 299*, 67-75.

245. Kuiper, G. G., Lemmen, J. G., Carlsson, B., Corton, J. C., Safe, S. H., van der Saag, P. T., van der Burg, B., and Gustafsson, J. A. (1998) Interaction of estrogenic chemicals and phytoestrogens with estrogen receptor beta, *Endocrinology 139*, 4252-4263.

246. Davis, M. J., Wu, X., Nurkiewicz, T. R., Kawasaki, J., Gui, P., Hill, M. A., and Wilson, E. (2001) Regulation of ion channels by protein tyrosine phosphorylation, *American Journal of Physiology. Heart and Circulatory Physiology 281*, H1835-1862.

247. Dinwiddie, S. H. (1994) Abuse of inhalants: a review, *Addiction 89*, 925-939.

248. Knusel, B., and Hefti, F. (1992) K-252 compounds: modulators of neurotrophin signal transduction, *J Neurochem 59*, 1987-1996.

249. Tapley, P., Lamballe, F., and Barbacid, M. (1992) K252a is a selective inhibitor of the tyrosine protein kinase activity of the Trk family of oncogenes and neurotrophin receptors, *Oncogene 7*, 371-381.

250. Goggi, J., Pullar, I. A., Carney, S. L., and Bradford, H. F. (2003) Signalling pathways involved in the short-term potentiation of dopamine release by BDNF, *Brain Res 968*, 156-161.

251. Paredes, D., Granholm, A. C., and Bickford, P. C. (2007) Effects of NGF and BDNF on baseline glutamate and dopamine release in the hippocampal formation of the adult rat, *Brain Res 1141*, 56-64.

252. Nye, S. H., Squinto, S. P., Glass, D. J., Stitt, T. N., Hantzopoulos, P., Macchi, M. J., Lindsay, N. S., Ip, N. Y., and Yancopoulos, G. D. (1992) K-252a and staurosporine selectively block autophosphorylation of neurotrophin receptors and neurotrophin-mediated responses, *Molecular Biology of the Cell 3*, 677-686.

253. Carvelli, L., Moron, J. A., Kahlig, K. M., Ferrer, J. V., Sen, N., Lechleiter, J. D., Leeb-Lundberg, L. M., Merrill, G., Lafer, E. M., Ballou, L. M., Shippenberg, T. S., Javitch, J. A., Lin, R. Z., and Galli, A. (2002) PI3-kinase regulation of dopamine uptake, *J Neurochem 81*, 859-869.

254. Doolen, S. and Zahniser, N. R. (2001) Protein tyrosine kinase inhibitors alter human dopamine transporter activity in Xenopus oocytes, *The Journal of Pharmacology and Experimental Therapeutics 296*, 931-938.

255. Ramamoorthy, S., Shippenberg, T. S., and Jayanthi, L. D. (2011) Regulation of monoamine transporters: Role of transporter phosphorylation, *Pharmacology & Therapeutics 129*, 220-238.

256. Zapata, A., Kivell, B., Han, Y., Javitch, J. A., Bolan, E. A., Kuraguntla, D., Jaligam, V., Oz, M., Jayanthi, L. D., Samuvel, D. J., Ramamoorthy, S., and Shippenberg, T. S. (2007) Regulation of dopamine transporter function and cell surface expression by D3 dopamine receptors, *J Biol Chem 282*, 35842-35854.

257. Moron, J. A., Zakharova, I., Ferrer, J. V., Merrill, G. A., Hope, B., Lafer, E. M., Lin, Z. C., Wang, J. B., Javitch, J. A., Galli, A., and Shippenberg, T. S. (2003) Mitogen-activated protein kinase regulates dopamine transporter surface expression and dopamine transport capacity, *J Neurosci 23*, 8480-8488.

258. Dluzen, D. E., McDermott, J. L., Anderson, L. I., Kucera, J., Joyce, J. N., Osredkar, T., and Walro, J. M. (2004) Age-related changes in nigrostriatal dopaminergic function are accentuated in +/- brain-derived neurotrophic factor mice, *Neuroscience 128*, 201-208.

259. Boger, H. A., Mannangatti, P., Samuvel, D. J., Saylor, A. J., Bender, T. S., McGinty, J. F., Fortress, A. M., Zaman, V., Huang, P., Middaugh, L. D., Randall, P. K., Jayanthi, L. D., Rohrer, B., Helke, K. L., Granholm, A. C., and Ramamoorthy, S. (2011) Effects of brain-derived neurotrophic factor on dopaminergic function and motor behavior during aging, *Genes Brain Behav 10*, 186-198.

260. Jang, S. W., Liu, X., Yepes, M., Shepherd, K. R., Miller, G. W., Liu, Y., Wilson, W. D., Xiao, G., Blanchi, B., Sun, Y. E., and Ye, K. (2010) A selective TrkB agonist with potent neurotrophic activities by 7,8-dihydroxyflavone, *Proceedings of the National Academy of Sciences 107*, 2687-2692.

261. Jang, S. W., Liu, X., Yepes, M., Shepherd, K. R., Miller, G. W., Liu, Y., Wilson, W. D., Xiao, G., Blanchi, B., Sun, Y. E., and Ye, K. (2010) A selective TrkB agonist with potent neurotrophic activities by 7,8-dihydroxyflavone, *Proc Natl Acad Sci U S A 107*, 2687-2692.

262. Andero, R., Daviu, N., Escorihuela, R. M., Nadal, R., and Armario, A. (2012) 7,8-dihydroxyflavone, a TrkB receptor agonist, blocks long-term spatial memory impairment caused by immobilization stress in rats, *Hippocampus 22*, 399-408.

263. Andero, R., Heldt, S. A., Ye, K., Liu, X., Armario, A., and Ressler, K. J. (2011) Effect of 7,8-dihydroxyflavone, a small-molecule TrkB agonist, on emotional learning, *The American Journal of Psychiatry 168*, 163-172.

264. Devi, L. and Ohno, M. (2012) 7,8-dihydroxyflavone, a small-molecule TrkB agonist, reverses memory deficits and BACE1 elevation in a mouse model of Alzheimer's disease, *Neuropsychopharmacology 37*, 434-444.

265. Liu, X., Chan, C. B., Qi, Q., Xiao, G., Luo, H. R., He, X., and Ye, K. (2012) Optimization of a small tropomyosin-related kinase B (TrkB) agonist 7,8-dihydroxyflavone active in mouse models of depression, *J Med Chem 55*, 8524-8537.

266. Liu, X., Qi, Q., Xiao, G., Li, J., Luo, H. R., and Ye, K. (2013) O-methylated metabolite of 7,8-dihydroxyflavone activates TrkB receptor and displays antidepressant activity, *Pharmacology 91*, 185-200.

267. Ren, Q., Zhang, J. C., Fujita, Y., Ma, M., Wu, J., and Hashimoto, K. (2013) Effects of TrkB agonist 7,8-dihydroxyflavone on sensory gating deficits in mice after administration of methamphetamine, *Pharmacology, Biochemistry, and Behavior 106*, 124-127.

268. Uluc, K., Kendigelen, P., Fidan, E., Zhang, L., Chanana, V., Kintner, D., Akture, E., Song, C., Ye, K., Sun, D., Ferrazzano, P., and Cengiz, P. (2013) TrkB receptor agonist 7, 8 dihydroxyflavone triggers profound gender-dependent neuroprotection in mice after perinatal hypoxia and ischemia, *CNS & Neurological Disorders Drug Targets 12*, 360-370.

269. Cruz, S. L., Orta-Salazar, G., Gauthereau, M. Y., Millan-Perez Pena, L., and Salinas-Stefanon, E. M. (2003) Inhibition of cardiac sodium currents by toluene exposure, *British Journal of Pharmacology 140*, 653-660.

270. Tillar, R., Shafer, T. J., and Woodward, J. J. (2002) Toluene inhibits voltage-sensitive calcium channels expressed in pheochromocytoma cells, *Neurochem Int 41*, 391-397.

271. Del Re, A. M., Dopico, A. M., and Woodward, J. J. (2006) Effects of the abused inhalant toluene on ethanol-sensitive potassium channels expressed in oocytes, *Brain Res 1087*, 75-82.

272. Myhre, O. and Fonnum, F. (2001) The effect of aliphatic, naphthenic, and aromatic hydrocarbons on production of reactive oxygen species and reactive nitrogen species in rat brain synaptosome fraction: the involvement of calcium, nitric oxide synthase, mitochondria, and phospholipase A, *Biochemical Pharmacology 62*, 119-128.

273. Mattia, C., Ali, S., and Bondy, S. (1993) Toluene-induced oxidative stress in several brain regions and other organs, *Molecular and Chemical Neuropathology 18*, 313-328.

274. Avshalumov, M. V., Chen, B. T., Marshall, S. P., Pena, D. M., and Rice, M. E. (2003) Glutamate-dependent inhibition of dopamine release in striatum is mediated by a new diffusible messenger, H_2O_2, *J Neurosci 23*, 2744-2750.

275. Chen, Q., Veenman, L., Knopp, K., Yan, Z., Medina, L., Song, W. J., Surmeier, D. J., and Reiner, A. (1998) Evidence for the preferential localization of glutamate

receptor-1 subunits of AMPA receptors to the dendritic spines of medium spiny neurons in rat striatum, *Neuroscience 83*, 749-761.

276. Bernard, V. and Bolam, J. P. (1998) Subcellular and subsynaptic distribution of the NR1 subunit of the NMDA receptor in the neostriatum and globus pallidus of the rat: co-localization at synapses with the GluR2/3 subunit of the AMPA receptor, *Eur J Neurosci 10*, 3721-3736.

277. Schlessinger, J. (2000) Cell signaling by receptor tyrosine kinases, *Cell 103*, 211-225.

ABSTRACT

EVALUATION OF PRESYNAPTIC DOPAMINE DYNAMICS AFTER: TOLUENE INHALATION OR TRKB RECEPTOR ACTIVATION

by

AARON KWAKU APAWU

May 2014

Advisor: Dr. Tiffany A. Mathews

Major: Chemistry (Analytical)

Degree: Doctor of Philosophy

Dopamine (DA) neurons in the striatum mediate several functions of the brain and have been linked to a host of neurological disorders including Parkinson's disease and addiction, both of which occur as a result of dysfunction in the DA system. In the present study, our first objective was to understand how the striatal DA system adapts to acute and repeated administration of inhalant toluene. The use of toluene as inhalant, like other drugs of abuse, is known to perturb DA neurotransmission in the brain reward pathway. However, the exact mechanism underling toluene's influence on striatal DA neurotransmission is unknown. The current work utilized behavior assays and neurochemical techniques such as slice fast scan cyclic voltammetry (FSCV), *in vivo* microdialysis, and brain tissue content analysis to examine how toluene inhalation alters the striatal DA system. Overall, both behavior and neurochemical data confirmed that toluene inhalation alters stimulated DA release in striatum. Mechanistically, the neurochemical data indicated that acute toluene inhalation potentiates striatal DA release and catabolism but there is no difference on DA uptake or extracellular DA levels in the caudate putamen (CPu). Furthermore, toluene induced potentiation in DA

release is not mediated by DA D3 autoreceptors. Meanwhile, chronic toluene exposure attenuated DA release only in the nucleus accumbens (NAc). Repeated toluene exposure also increased extracellular DA levels in the NAc, which is typical of addictive drugs. However, repeated toluene inhalation had no effect on DA D3 autorecepetors, and DA catabolism. Taken together, the present data suggest that acute or repeated toluene alters the striatal DA system through indirect neuronal action.

The second objective was to understand how brain derived neurotrophic factor (BDNF) modulates striatal DA dynamics. Aside from its conventional role as a neurotrophic factor, BDNF has also been implicated in synaptic transmission and neurological disorders. Since BDNF mediates it neurotrophic functions through tyrosine kinase receptor TrkB, the functional effects of tyrosine kinase receptor TrkB on the striatal DA release and uptake rate were examined. This work utilized FSCV to evaluate the effect of exogenous BDNF, TrkB agonist; 7,8-dihydroxyflavone (7,8-DHF), and TrkB antagonists; genistein, tyrphostin 23, and K252a, on DA dynamics in the CPu of brain slices obtain from BDNF deficient ($BDNF^{+/-}$) mice and their wildtype littermates. Overall, the results obtained highlighted the utility of FSCV to probe the functional effect of Trk receptors on DA dynamics. The results also showed that activation of TrkB receptors with exogenous BDNF and 7,8-DHF potentiated presynaptic DA release in $BDNF^{+/-}$ and wildtype mice respectively, with no effect on DA uptake. However, concentrations greater than 3 μM 7,8-DHF attenuated DA uptake rates in only $BDNF^{+/-}$ mice. In the presence of K252a, the BDNF or 7,8-DHF induced potentiation of DA release was abolished, suggesting that the effect of BDNF or 7,8-DHF on presynaptic DA release is TrkB mediated.

AUTOBIOGRAPHICAL STATEMENT

Education

Wayne State University (Detroit, Michigan) **2009 – 2014**
Doctor of Philosophy (Ph.D.), Chemistry (Analytical)
Dissertation: Evaluation of Presynaptic Dopamine Dynamics After: Toluene Inhalation or TrkB Receptor Activation
(Advisor: Dr. Tiffany A. Mathews)

East Tennesse State University (Johnson City, Tennessee) **2007 – 2009**
Master of Science (M.S), (Analytical)
Thesis: Reversed – Phase HPLC Determination of Alliin in Diverse Varieties of Fresh Garlic and Commercial Garlic Products
(Dr. Advisor: Chu-Ngi Ho)

University of Cape Coast (Cape Coast, Ghana) **2001 – 2005**
Bachelor of Science (BS). Chemistry

Employment

Wayne State University (Detroit, Michigan) **2009 – 2014**
Research/Teaching Assistant

East Tennessee State University (Johnson City, Tennessee) **2007 – 2009**
Research/Teaching Assistant

University of Cape Coast (Cape Coast, Ghana) **2005 – 2007**
Research/Teaching Assistant

Publications

- **Apawu, A.K***., Maina, F.K*., Taylor, J.R., Mathews, T.A. (2013), Probing the Ability of Presynaptic Tyrosine Kinase Receptors to Regulate Striatal Dopamine Dynamics, *ACS Chem Neurosci.*, 4(5):895-904. *Co-first authors.
- Maina, F.K,* Khalid, M.,***Apawu, A.K,*** and Mathews, T.A., "Presynaptic Dopamine Dynamics in Striatal Brain Slices with Fast Scan Cyclic Voltammetry" *J Vis Exp*, **59**, pii: 3464. doi: 10.3791/3464 (2012). *Co-first authors.
- **Apawu, A.K**., Mathews, T.A., and Bowen, S.E., "Striatal Dopamine Dynamics in Mice Following Acute and Repeated Toluene Exposure", *in revision for publication in Psychopharmacology.*

Awards and Membership

- Wayne State University Summer 2013 Dissertation Fellowship Award **2013**
- WSU Chemistry Departmental Citations for Excellence in Teaching Service **2012**
- WSU Chemistry Departmental Citations for Excellence in Teaching Service **2013**

Professional Societies

- American Chemical Society (ACS) **2012 – 2014**
- Society for Neuroscience, Michigan Chapter (MiSFN) **2012 – 2014**